U.S. Department
of Commerce

Volume 107
Number 2
April 2009

Fishery Bulletin

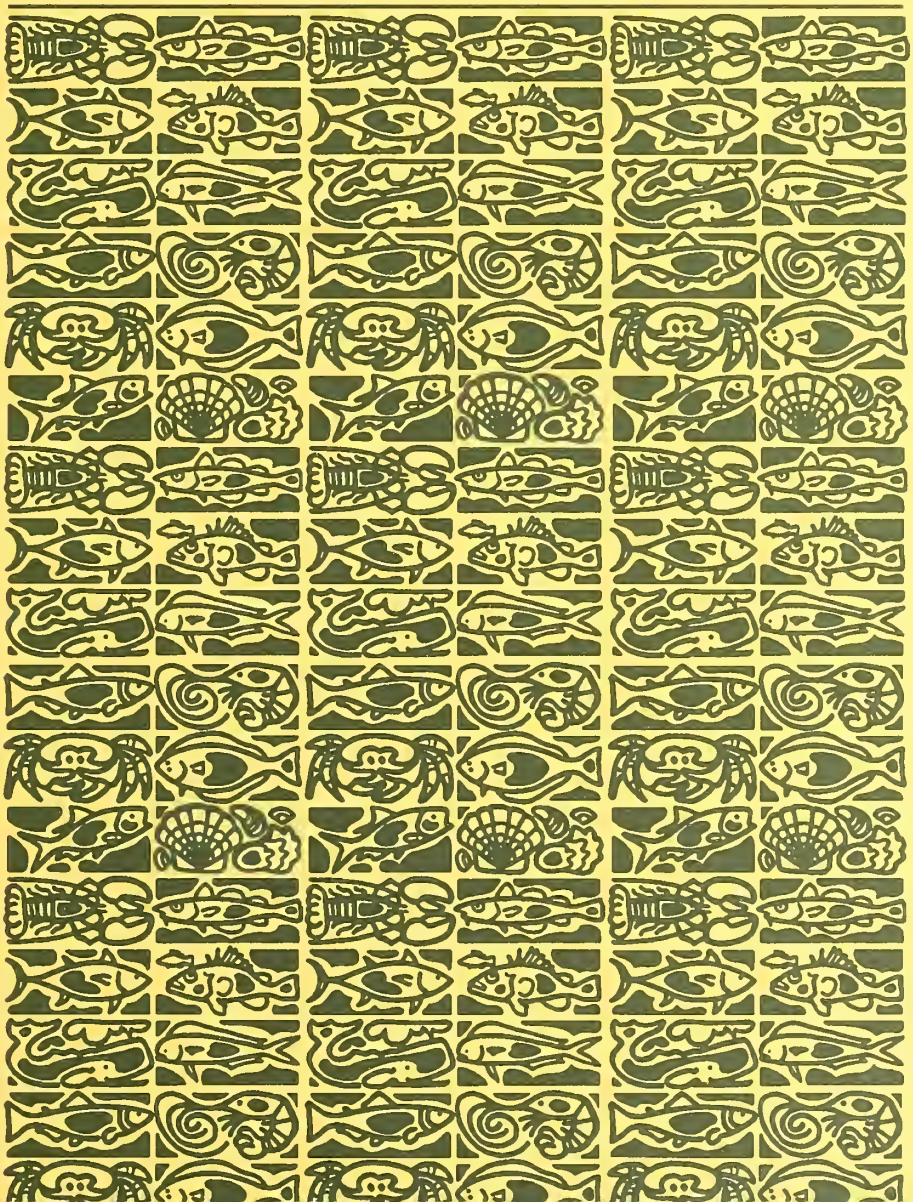

Fishery Bulletin

***Fishery Bulletin* web site: www.fishbull.noaa.gov**

The *Fishery Bulletin* (ISSN 0090-0656) is published quarterly by the Scientific Publications Office, National Marine Fisheries Service, NOAA, 7600 Sand Point Way NE, BIN C15700, Seattle, WA 98115-0070. Periodicals postage is paid at Seattle, WA. POSTMASTER: Send address changes for subscriptions to Fishery Bulletin, Superintendent of Documents, Attn.: Chief, Mail List Branch, Mail Stop SSOM, Washington, DC 20402-9373.

The Secretary of Commerce has determined that the publication of this periodical is necessary according to law for the transaction of public business of this Department. Use of funds for printing of this periodical has been approved by the Director of the Office of Management and Budget.

For sale by the Superintendent of Documents, U.S. Government Printing Office, Washington, DC 20402. Subscription price per year: $36.00 domestic and $50.40 foreign. Cost per single issue: $21.00 domestic and $29.40 foreign. See **back for order form.**

The *Fishery Bulletin* carries original research reports and technical notes on investigations in fishery science, engineering, and economics. It began as the Bulletin of the United States Fish Commission in 1881; it became the Bulletin of the Bureau of Fisheries in 1904 and the *Fishery Bulletin* of the Fish and Wildlife Service in 1941. Separates were issued as documents through volume 46; the last document was No. 1103. Beginning with volume 47 in 1931 and continuing through volume 62 in 1963, each separate appeared as a numbered bulletin. A new system began in 1963 with volume 63 in which papers are bound together in a single issue of the bulletin. Beginning with volume 70, number 1, January 1972, the *Fishery Bulletin* became a periodical, issued quarterly. In this form, it is available by subscription from the Superintendent of Documents, U.S. Government Printing Office, Washington, DC 20402. It is also available free in limited numbers to libraries, research institutions, State and Federal agencies, and in exchange for other scientific publications.

U.S. Department of Commerce
Seattle, Washington

Volume 107
Number 2
April 2009

Fishery Bulletin

Contents

Articles

Abstract—In the first of two companion papers, a 54-yr time series for the oyster population in the New Jersey waters of Delaware Bay was analyzed to develop biological relationships necessary to evaluate maximum sustainable yield (MSY) reference points and to consider how multiple stable points affect reference point-based management. The time series encompassed two regime shifts, one circa 1970 that ushered in a 15-yr period of high abundance, and a second in 1985 that ushered in a 20-yr period of low abundance. The intervening and succeeding periods have the attributes of alternate stable states. The biological relationships between abundance, recruitment, and mortality were unusual in four ways. First, the broodstock–recruitment relationship at low abundance may have been driven more by the provision of settlement sites for larvae by the adults than by fecundity. Second, the natural mortality rate was temporally unstable and bore a nonlinear relationship to abundance. Third, combined high abundance and low mortality, though likely requiring favorable environmental conditions, seemed also to be a self-reinforcing phenomenon. As a consequence, the abundance–mortality relationship exhibited both compensatory and depensatory components. Fourth, the geographic distribution of the stock was intertwined with abundance and mortality, such that interrelationships were functions both of spatial organization and inherent population processes.

Manuscript submitted 29 November 2007.
Manuscript accepted 9 September 2008.
Fish. Bull. 107:109–132 (2009).

The views and opinions expressed or implied in this article are those of the author and do not necessarily reflect the position of the National Marine Fisheries Service, NOAA.

Multiple stable reference points in oyster populations: biological relationships for the eastern oyster (*Crassostrea virginica*) in Delaware Bay

Eric N. Powell (contact author)[1]
John M. Klinck[2]
Kathryn A. Ashton-Alcox[1]
John N. Kraeuter[1]

Email address for contact author: eric@hsrl.rutgers.edu

[1] Haskin Shellfish Research Laboratory
Rutgers University
6959 Miller Avenue
Port Norris, New Jersey 08349

[2] Center for Coastal Physical Oceanography
Crittenton Hall
Old Dominion University
Norfolk, Virginia 23529

All federal fisheries, and some state fisheries, are managed under biological reference-point guidelines that implement a yearly allocation or quota, often termed TAC (total allowable catch) or TAL (total allowable landing), to constrain fishing mortality (e.g., Wallace et al., 1994). The biological reference-point approach for federal fisheries was mandated by the Magnuson-Stevens Fishery Conservation and Management Act (Anonymous, 1996) which requires management at a biomass that provides maximum sustainable yield, B_{MSY}. Under this system, sophisticated survey, analytical, and modeling procedures are used to identify selected biological reference points, such as the target biomass, B_{MSY}, and carrying capacity, K. Fishing mortality is then set in relation to these goals. As a consequence, much attention has been given to the choice and application of biological reference points in fisheries management (e.g., Sissenwine and Shepherd, 1987; Hilborn, 2002; Imeson et al., 2002; Mangel et al., 2002).

Normally, B_{MSY} is defined in relation to carrying capacity, the biomass present without fishing, where natural mortality balances recruitment (e.g., May et al., 1978; Johnson, 1994; Mangel and Tier, 1994; Rice, 2001). This stable point is characterized by a population in which most animals are adults, where natural mortality rates are low, and where recruitment is limited by compensatory processes such as resource limitation constraining fecundity. B_{MSY} is most commonly defined as $\frac{K}{2}$, based on the well-known Schaefer model which stipulates the guiding premise that surplus production is highest at $\frac{K}{2}$ (Hilborn and Walters [1992]; see Restrepo et al. [1998] for more details on the federal management system; see NEFSC [1999[1], 2000[2], 2002[3]] for examples of implementation of reference-point management).

[1] NEFSC (Northeast Fisheries Science Center). 1999. 29th Northeast regional stock assessment workshop (29th SAW): Stock Assessment Review Committee (SARC) consensus summary of assessments. NMFS NEFSC Ref. Doc. 99-14, 347 p.

[2] 2000. 30th Northeast regional stock assessment workshop (30th SAW): Stock Assessment Review Committee (SARC) consensus summary of assessments. NMFS NEFSC Ref. Doc. 00-03, 477 p.

[3] 2002. 34th Northeast regional stock assessment workshop (34th SAW): Stock Assessment Review Committee (SARC) consensus summary of assessments. NMFS NEFSC Ref. Doc. 02-06, 346 p.

Some have expressed concerns about managing at B_{MSY} (e.g., Peterman, 1977; Hilborn, 2002; Mangel et al., 2002), but only recently has the possibility been raised that carrying capacity may not be the long-term constant typically assumed under B_{MSY} management. That realization arises ineluctably from the recognition that regime shifts profoundly affect the balance between population and environment (Rothschild, 2000; Collie et al., 2004; Rothschild and Shannon, 2004; Sakuramoto, 2005). Increasingly, fisheries biologists recognize these transitions as an important long-term component of population variation (e.g., Botsford, 1981; Steele and Henderson, 1984; Ware, 2000; Jackson et al., 2001; Choi et al., 2004; Collie et al., 2004; Breitburg and Fulford, 2006). Any change in carrying capacity assuredly changes B_{MSY}.

The acceptance of regime shifts requires an acknowledgement that populations can exist in alternating stable states that are self-reinforcing for protracted periods of time. The record of oyster abundance in Delaware Bay indicates at least two regime shifts (Powell et al., 2008), circa 1970 and circa 1985, with intervening and succeeding intervals having the attributes of alternate stable population states (*sensu* Gray, 1977; Peterson, 1984; Knowlton, 2004). These periods of relative stability are multigenerational and demonstrably not of anthropogenic origin[4] (see Knowlton, 2004) because fishing mortality rates have been far below natural mortality rates over much of this time. The periods of stability are persistent over a range of climatic conditions (Soniat et al., in press). The association of unique climatic events with each of the regime shifts is consistent with models that emphasize the unique confluence of a set of forcing factors in the initiation of catastrophic events (DeAngelis and Waterhouse, 1987; Deakin, 1990; Hastings, 1991) and supports the observation of Collie et al. (2004) that large-scale changes in the population dynamics of species are commonly characterized by a poor correlation between the response variable and potential forcing factors.

Evaluation of MSY-style reference points requires an understanding of the capacity of a species to expand its biomass over a range of biomasses. In fisheries parlance, this expansion capacity is related to surplus production. Regime shifts change expansion capacity in relation to biomass. Surplus production models are well described (e.g., Sissenwine and Shepherd, 1987; Maunder, 2003), but the influence of range shifts has rarely been considered. In the first of two companion contributions, we develop relationships supporting a surplus production model for a species, the eastern oyster (*Crassostrea virginica*), and a location, Delaware Bay, characterized by distinctive and well described range shifts. We take advantage of a 54-yr time series of oyster abundance, recruitment, and mortality for this analysis.

[4] We recognize that the introduction of *Haplosporidium nelsoni* (MSX) circa 1957 (Burreson et al., 2000), which subsequently played a critical role in the 1985 regime shift, was likely anthropogenically driven.

Table 1

The bed groups (by location: upbay and downbay) and subgroups (by mortality rate) for the eastern oyster (*Crassostrea virginica*) collected on twenty beds in Delaware Bay, as shown in Figure 1. Mortality rate divides each of the primary groups, themselves being divided by location, a surrogate for up bay-downbay variations in dredge efficiency and fishery area-management regulations.

Bed group and subgroup	Bed
Upbay group	
Low mortality	Round Island, Upper Arnolds, Arnolds
Medium mortality	Upper Middle, Middle, Sea Breeze, Cohansey, Ship John
Downbay group	
Medium mortality	Shell Rock
High mortality	Bennies Sand, Bennies, New Beds, Nantuxent Point, Hog Shoal, Hawk's Nest, Strawberry, Vexton, Beadons, Egg Island, Ledge,

Materials and methods

The survey time series

The New Jersey survey began as a response to overfishing that had reduced stock abundance by the early 1950s. By 2006, this 54-yr record covered a number of unique periods, including the period of time after the onset of MSX, a disease caused by the protozoan *Haplosporidium nelsoni*, circa 1957 (Haskin and Andrews, 1988; Ford, 1997) and the period after the onset of Dermo, a disease caused by the protozoan *Perkinsus marinus*, circa 1990 (Ford, 1996; Cook et al., 1998).

In what follows, we define the population on the twenty primary oyster beds in Delaware Bay (Fig. 1) as the oyster stock in the New Jersey waters of Delaware Bay, but for simplicity we refer to it as the Delaware Bay oyster stock.[5] The analyses that follow will delineate four bed groups based on the long-term average rates of natural mortality, productivity, and survey catchability (Table 1). Analyses of the Delaware Bay oyster resource

[5] Oysters are also found on the Delaware side of the bay, although the total bed area is much less than that in the New Jersey waters (Moore, 1911; Maurer et al., 1971; Maurer and Watling, 1973), as well as in many of the river mouths; and an unknown number (but significant during certain periods of history [MacKenzie, 1996; Ford, 1997]) have been present on leased grounds, most of which are situated downbay of Egg Island (see Fig. 1 of Haskin and Ford, 1982). Inadequate survey data exist to include oysters in bay margin habitats and on leased grounds in the stock analysis. Delaware maintains an independent survey, but these data are not yet available on a per-m^2 basis. However, abundance and recruitment trends typically have been similar on both sides of the bay.

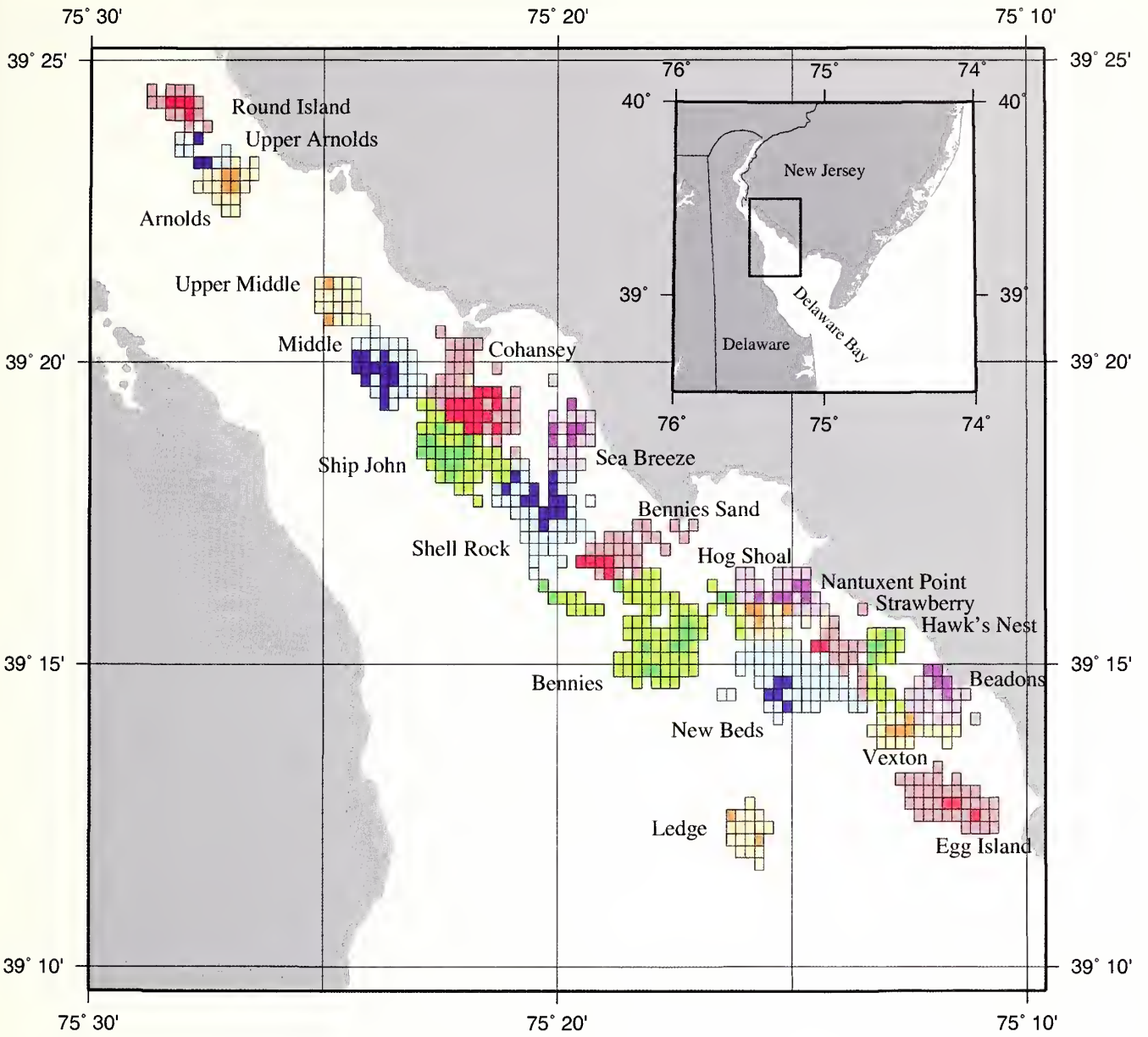

Figure 1

The twenty natural oyster beds of the eastern oyster (*Crassostrea virginica*) in the New Jersey waters of Delaware Bay may be characterized in terms of high-quality (dark shade) and medium-quality (light shade) grids, the term quality referring to a relative differential in long-term average oyster abundance (Powell et al, 2008). The footprints for the Middle bed (upper portion of figure) and the beds downbay from it, excepting New Beds, Egg Island, and Ledge, were updated with data from surveys in 2005 and 2006. The footprints for the remaining beds were based on historical definitions.

of New Jersey routinely reveal a division between an upbay group of eight beds (Round Island, Upper Arnolds, Arnolds, Upper Middle, Middle, Sea Breeze, Cohansey, and Ship John) and a downbay group of twelve beds (Shell Rock, Bennies Sand, Bennies, New Beds, Nantuxent Point, Hog Shoal, Hawk's Nest, Strawberry, Vexton, Beadons, Egg Island, and Ledge) (Fig.1). Salinity, natural mortality rate, and growth rate are higher downbay. Dredge efficiencies are significantly higher downbay (Powell et al., 2002a, 2007). Both regions can be subdivided by natural mortality rate and productivity. In the upbay group, natural mortality rates and growth rates are significantly lower for the upper three beds, Round Island, Upper Arnolds, and Arnolds, than for the remaining beds. Henceforth these two groups will be termed "the low-mortality" and "medium-mortality" beds, respectively (Table 1). In the downbay group, growth rates and mortality rates are lower for

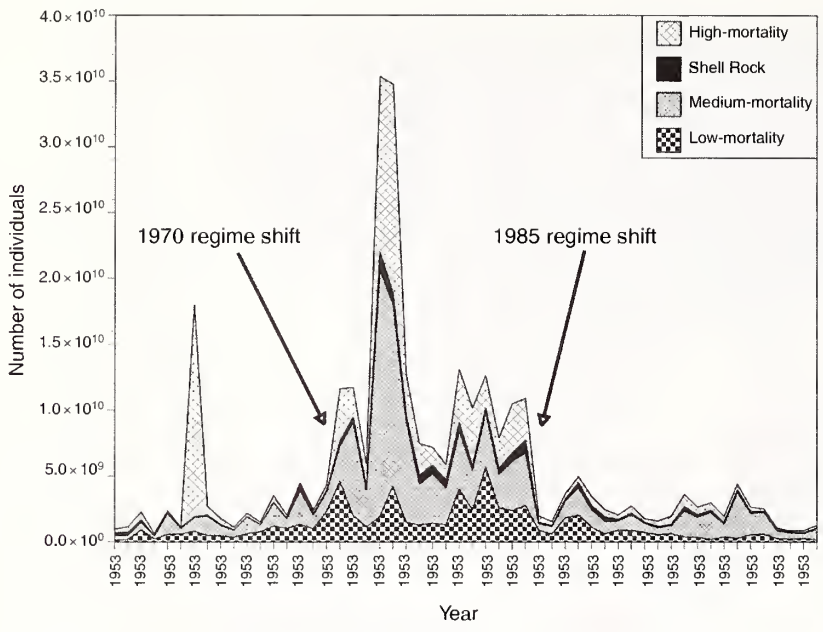

Figure 2

Time series of abundance of the eastern oyster (*Crassostrea virginica*) in Delaware Bay, showing four subgroups defined by location and natural mortality rate. Total oyster abundance for any year is the sum of abundance in the subgroups. Beds in the subgroups are listed in Table 1.

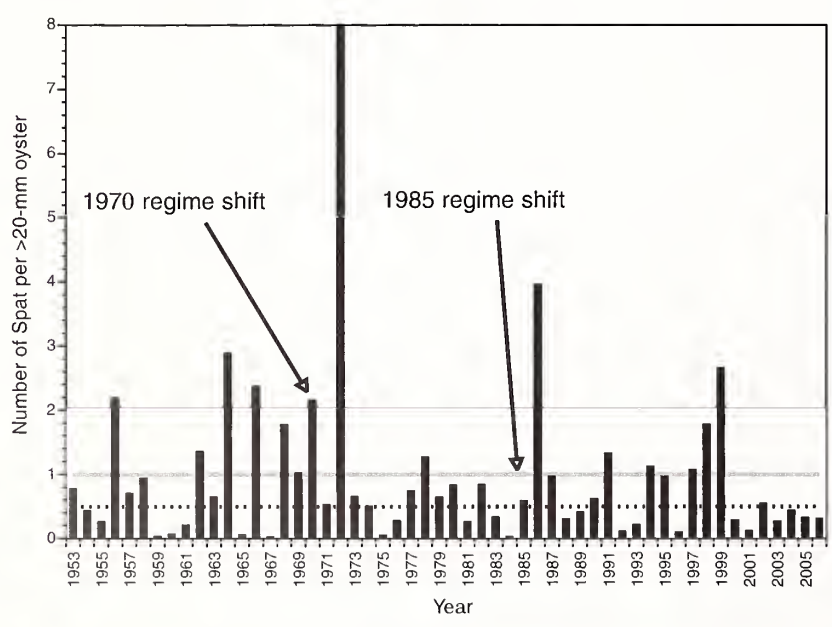

Figure 3

Time series of spat recruitment per >20-mm eastern oyster (*Crassostrea virginica*) in Delaware Bay. Solid and dashed lines mark the 1.0 and 0.5 spat-to-oyster levels, respectively.

Shell Rock, leading to its designation as a medium-mortality bed; the remainder are high-mortality beds (Table 1).

Powell et al. (2008) have described the Delaware Bay time series in detail. The pertinent findings are summarized in the following sections.

Pre-1970 period of low abundance

In the few years before 1957 when survey data were available, the Delaware Bay oyster population was characterized by relatively low abundance (Fig. 2), an unremarkable rate of recruitment (Fig. 3), relatively low natural mortality (Fig. 4), and a spatial distribution in which the fraction of the stock on the medium-mortality beds was relatively low in comparison with the 54-yr median of 0.417 (Fig. 5). The dispersion of the stock was likely maintained by overfishing because the fishery predominantly targeted the medium-mortality beds during this time (Powell et al., 2008). Given that natural mortality rates averaged below 10% during this period, and fishing rates routinely exceeded 10%, we speculate that, had fishing rates been the same as those in later years (typically <7% of the stock), the medium-mortality beds likely would have contributed a larger proportion of the stock, and stock abundance likely would have been higher than that observed.

MSX entered the picture circa 1957. Abundance was unchanged, in part because of implementation of reference point-based management that curtailed overfishing (Fegley et al., 2003; Powell et al., 2008). The early reference point referred to as "the 40% rule" limited removals from individual beds when the volume of live oysters declined below 40% of a bushel haul (Powell et al., 2008). The 40% rule successfully limited harvest from the late 1950s until the 1985 regime shift, after which changes in the fishery imposed by low abundance and Dermo required development of management alternatives and new reference points (Powell et al., 2008). Under the 40% rule,

the highest fishing mortality rate observed after 1958 was about 10% of the stock (Powell et al., 2008). By circa 1960, the effect of an increase in natural mortality, on the order of 5–10% of the stock, had been ameliorated by a decrease in fishing mortality at least that large. From 1957 through 1966, natural mortality neared 15% of the stock in most years and exceeded 20% in two years (Fig. 4). Mortality substantively increased downbay and by 1960, animals on the high-mortality beds were contributing a disproportionate share of the total mortality of the population (Fig. 6). As a consequence, during the 1960s, individuals on the medium-mortality beds contributed more than their long-term median proportion of the total stock in eight of ten years (Fig. 5). Although the fishery continued to target these beds (Powell et al., 2008), the reduction in total removals minimized the influence of the fishery on the stock.

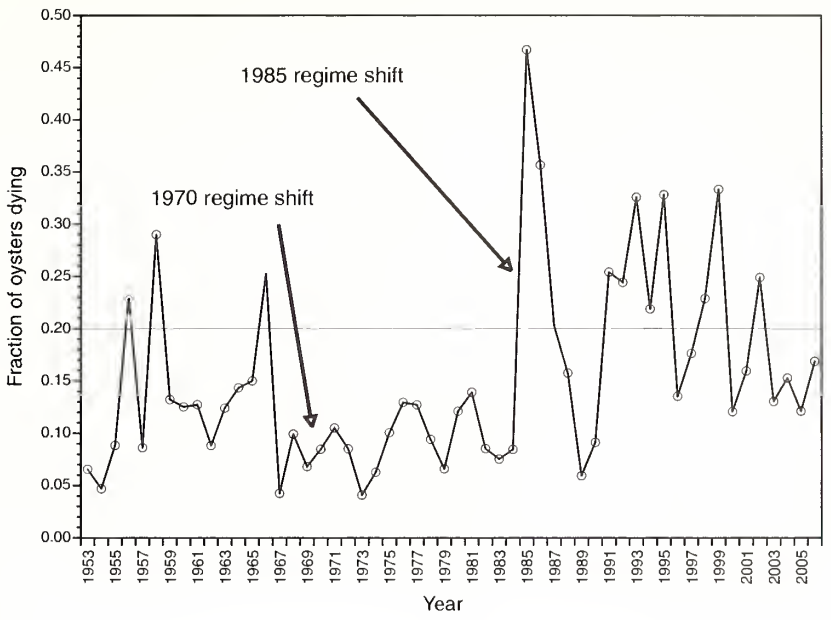

Figure 4

The fraction of eastern oyster (*Crassostrea virginica*) dying each year in the New Jersey waters of Delaware Bay, 1953–2006.. Horizontal line marks an arbitrary boundary between mortality in epizootic (above the line) and non-epizootic years.

The 1970 population expansion

In 1970, the oyster population increased by more than a factor of two, and this high level of abundance was maintained for the succeeding 15 years. This was a period of high abundance in a number of other species of commercial importance (Gabriel, 1992; Link et al., 2002), including many finfish species in the Gulf of Maine and Mid-Atlantic Bight, hard clams along the Long Island coast (Kraeuter et al., 2005; Hofmann et al., 2006), and *Illex* squid off Newfoundland (Dawe et al., 2000). In many of these cases, this abundance was rapidly impacted by overfishing (e.g., Kraeuter et al., 2008), which artificially limited its duration. A decline in population, however, did not occur for the Delaware Bay oyster stock. However, the general coincidence of abundance in bay and shelf species, both temperate and boreal, bespeaks of a large-scale climatic event that influenced much of the northeast

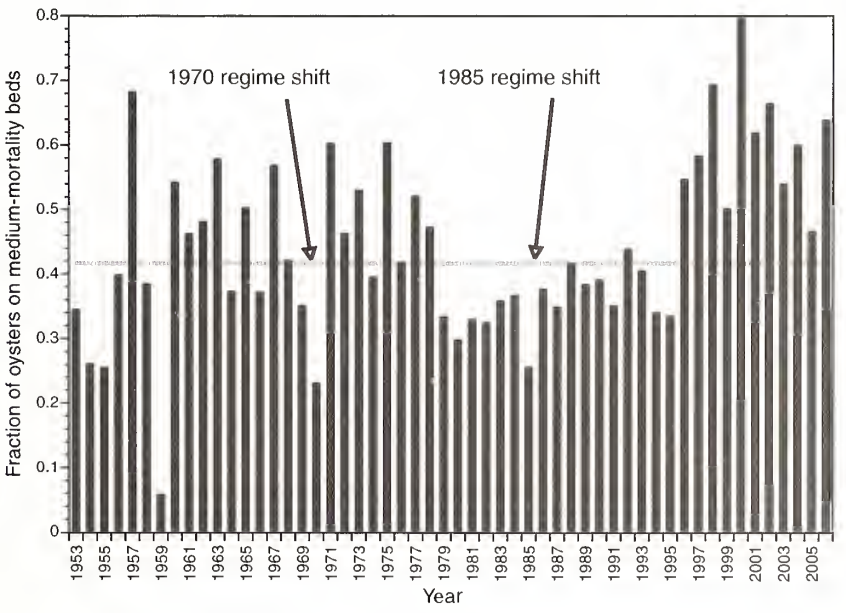

Figure 5

The fraction of the total stock of eastern oyster (*Crassostrea virginica*) in the New Jersey waters of Delaware Bay that was located on the medium-mortality beds, 1953–2006. The horizontal bar represents the 54-yr median of 0.417.

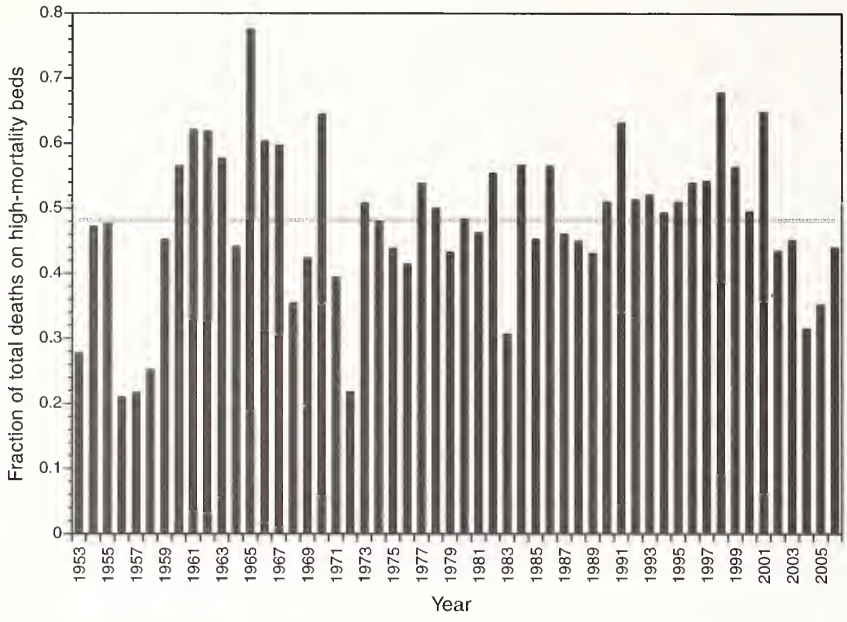

Figure 6

The fraction of total deaths in the population of eastern oyster (*Crassostrea virginica*) in the Delaware Bay contributed by the individuals on the high-mortality beds. The horizontal bar represents the 54-yr median level of 0.482.

U.S. coastline. Baines and Folland (2007) documented the climatic forcing that certainly provided the basis for the 1970 regime shift, although how climate change in the North Atlantic imposed the conditions for increased productivity on the local scale remains uncertain.

Two noteworthy events preceded population expansion in Delaware Bay. First, 1968–70 were three successive years of relatively high recruitment (Fig. 3). Only one other trio of such years, 1997–99, exists in the time series. Relatively high recruitment in these three years occurred in three of four bay subgroups (medium-mortality, Shell Rock, and high-mortality). No equivalent coincidence of years and bay coverage exists in the time series. Second, beginning in 1967, natural mortality dropped below 10% after the largest MSX epizootic event of the 1960s and remained at or below this level through 1975 (Fig. 4). The coincidence of dramatically lower natural mortality and a triplex of high recruitment years was unique in the time series and certainly provided the proximate conditions for the population expansion of 1970.

The 1970–85 high-abundance interval and its termination

The 1970–85 time period was remarkable for its persistent high level of oyster abundance (Fig. 2). The period was characterized by a lower contribution of animals on the high-mortality beds to total population mortality (Fig. 6) and by natural mortalities that rarely exceeded 13% of the stock annually (Fig. 4). During this period, the fraction of deaths on the high-mortality beds exceeded the long-term median only six times (Fig. 6). In the first half of the period, the medium-mortality beds contributed proportionately more to the stock, as they had during most of the MSX-dominated decade that preceded this period (Fig. 5). High freshwater inflow contributed to sustainable high abundance by limiting mortality from MSX. A dramatic shift in stock dispersion began in 1979, coincident with the cessation of consistently high freshwater inflows, and led, over a few years, to proportional increases in abundance in the more environmentally sensitive waters of the upbay and downbay margins. An increase in the susceptibility of the population to epizootic disease mortality consequent of the increased abundance downbay evolved from 1985 to 1986 through a coincidence of climatic events into the largest epizootic event in the recorded history of Delaware Bay (Fig. 4). Interestingly, the 1985–86 stock collapse was not obviously associated with any unusual trends in recruitment immediately before or after the collapse (Fig. 3), nor did the distribution of deaths (Fig. 6) or the dispersion of the stock (Fig. 5) change. Abundance declined in all bay regions.

The post-MSX period

The few years immediately following the 1985–86 MSX epizootic event and preceding the onset of Dermo circa 1990 were not unusual in any way, and neither was the first half-decade after Dermo became an important contributor to population mortality. Total abun-

dance remained relatively stable from 1987 through 2001 (Fig. 2). Recruitment was not unusual (Fig. 3). However, natural mortality rose dramatically, from the 10% level immediately after 1986, to often exceed 20–30% throughout the 1990s (Fig. 4). The fraction of deaths contributed by the high-mortality beds did not change markedly over the 1990s, although the fractions of deaths did rise incrementally in 1990 compared to the few preceding years (Fig. 6). The dispersal pattern of the 1980s remained through 1995 (Fig. 5), despite the increased mortality rate on the high-mortality beds.

The response of the stock to Dermo became more apparent in 1996, when the stock began a rapid contraction to its refuge on the medium-mortality beds. This contraction in dispersion occurred at the same time as increased recruitment on these beds (Fig. 5) and counterweighed the accumulating losses of individuals farther downbay (Fig. 6), so that total abundance did not change.

The post-2000 era

Although the time series is still limited in scope, a change in population dynamics is evident around 2000. Beginning in 2000, the recruitment rate declined precipitously and remained low at least through 2006 (Fig. 3). Total abundance declined with continuing high mortality on the high-mortality beds (Fig. 6), but stock consolidation continued, with an increasing proportion of animals on the medium-mortality beds. As a consequence, mortality in the population as a whole declined (Fig. 4). The fraction of total mortality contributed by the high-mortality beds declined to its lowest level since the 1950s and remained low (Fig. 6) because consolidation of the stock upbay limited the number of individuals available to die on the high-mortality beds.

Overview of fishing activities

The analysis that follows makes reference to two distinctive types of fishing on the Delaware Bay oyster beds of New Jersey. From 1953 through 1995, a "bay-season" fishery occurred, in which a portion of the beds was opened, usually for 2–6 weeks in the spring. Oysters were removed *en masse* and transplanted downbay to leased grounds. Based on recent dredge efficiency estimates (Powell et al., 2007), the method for transplanting was relatively nonselective for oyster size; oysters were moved more or less in proportion to their contribution to the size-frequency distribution of the population. In most years, the fishery was limited by the 40% rule. As a consequence, target beds varied during the program from year to year as the relative abundance of the resource varied.

Since 1996, a direct-market fishery has been prosecuted for the most part on beds from Shell Rock downbay (Fig. 1). In this fishery, market-size oysters are taken directly off the beds and marketed immediately or stored for a time on leased grounds before they are marketed. The vast majority of animals removed by this fishery have exceeded 63 mm (Powell et al., 2005).

Model formulations and statistics

Basic population dynamics Quantification of the Delaware Bay time series has been described in Powell et al. (2008). Natural mortality fractions were obtained from box counts under the assumption that

$$N_{oysters_{t-1}} = N_{boxes_t} + N_{live\ oysters_t}, \quad (1)$$

where N = the number of individuals; and
t = any given year.

Hence

$$\Phi_{bc} = \frac{N_{boxes_t}}{N_{boxes_t} + N_{live\ oysters_t}}, \quad (2)$$

where Φ_{bc} = mortality expressed as the fraction of individuals alive at the end of year t that died during the next year, based on box counts (bc).

In Delaware Bay, boxes appear to remain intact, on the average, for a little less than one year (Powell et al., 2001; Ford et al., 2006). On the other hand, dredge efficiencies indicate that some boxes may be old (Powell et al., 2007). The degree to which the two biases counterweigh is unclear; however, box counts are clearly adequate to identify significant changes in yearly mortality rates (Ford et al., 2006). We consider box counts to be the best available basis for estimating the natural mortality rate of adult oysters.

However, boxes very likely do not adequately measure the mortality of juvenile animals. Juvenile shells are taphonomically more active (Cummins et al., 1986a, 1986b; Powell et al., 1986; Glover and Kidwell, 1993) and thus can be expected to remain intact for a relatively short time. In addition, deaths of smaller animals do not leave intact boxes as often because many deaths are caused by shell-crushing predators (Powell et al., 1994; Alexander and Dietl, 2001; Milke and Kennedy, 2001). Inasmuch as the mortality rate of juvenile animals is likely to be underestimated by box counts, the fraction dying, but not recorded by box counts, Φ_0, was obtained by difference:

$$\Phi_0 = \frac{(N_t - N_{t-1}) - (R_{t-1} - \Phi_{bc} N_{t-1} - \Phi_f N_{t-1})}{N_{t-1} + R_{t-1}}, \quad (3)$$

where Φ_f = the fraction taken by the fishery;
R = the number of recruits into the population; and the first parenthetical term on the right-hand side represents the difference in abundance between two consecutive surveys.

Mortality unrecorded by box counts, Φ_0, varied randomly over the time series, with a 54-yr mean of 0.274 and a 54-yr median of 0.311 (Powell et al., 2008).

Forces modifying abundance: broodstock–recruitment relationship A linear fit to the broodstock and recruitment data returned a regression coefficient of only 0.076 (Fig. 7). The relationship was strongly compensatory. A variety of broodstock–recruitment models might be applied (e.g., May et al., 1978; Hilborn and Walters, 1992; Kraeuter et al., 2005), given the scatter of data at high abundance and the paucity of extremely high values. We used a relationship that produced declining recruitment at high abundance (overcompensation *sensu* Hancock, 1973; McCann et al., 2003), because shellfish can achieve densities sufficient to limit growth and reproduction (e.g., Fréchette and Bourget, 1985; Fréchette and Lefaivre, 1990; Powell et al., 1995). Application of the simple filtration model of Wilson-Ormond et al. (1997) indicated that present-day abundances, even on the medium-mortality beds, are below such densities, but abundances in the 1970s were very likely high enough and medium-mortality abundances circa 2002 (Fig. 2) may have been high enough to restrict growth. Thus, from Hilborn and Walters (1992):

$$\tilde{R}_t = \tilde{N}_{t-1} e^{-\alpha\left(1+\frac{\tilde{N}_{t-1}}{\beta}\right)}, \quad (4)$$

where $\tilde{R}$ = the number of spat in millions; and
$\tilde{N}_{t-1}$ = oyster abundance in millions.

Fitting this curve to the data for the high- and medium-quality strata (Fig. 1) yields $\alpha = 0.3746$, and $\beta = 5121.9$ (Figs. 7 and 8). We compared the result of Equation 4 to the result of a best-fit linear regression with zero intercept (Fig. 8). The linear relationship is

$$R_t = 0.493 N_{t-1}. \quad (5)$$

Broodstock and box-count mortality Box-count estimates of natural mortality are also related to trends in abundance (Fig. 9). At abundances greater than 4×10^9, mortality was low. The fraction dying each year averaged 9.6% for these nonepizootic years, defined for convenience as years in which the fraction dying was less than 20%. The nonepizootic death rate was relatively independent of abundance, although the lowest mortalities, less than 6%, occurred at abundances below 6×10^9.

Of the 14 epizootic years in the 54-yr record, defined in our study as deaths exceeding 20% of the stock, 13 occurred at abundances less than 3×10^9 (Fig. 9). The exception was 1985. Of the 32 years with abundances less than 3×10^9, 14 were epizootic years. Of these 32, only one had a fractional mortality between 0.15 and 0.20. Accordingly, two divergent outcomes existed over a range of low abundances. In some years, the fraction dying approximated the long-term mean for high-abundance years, about 9.6%. In other years, epizootic mortalities occurred. Epizootic events also occur rarely at very low abundances. Note on Figure 9 that no mortality fraction exceeded 0.17 at abundances below 1.5×10^9. Thus, a complex relationship exists between abundance and mortality.

We apply an admittedly *ad hoc* empirically derived equation to describe the relationship between box-count mortality and abundance depicted in Figure 9:

$$\Phi_{bc_t} = \omega + \kappa \log_e(\tilde{N}_{t-1} + \rho) - \varphi \tilde{N}_{t-1} + \chi \tilde{N}_{t-1} e^{\left(-\frac{(\tilde{N}_{t-1}-\psi)^2}{2\upsilon^2}\right)}, \quad (6)$$

where $\omega = 0.055$;
$\kappa = 0.03$;
$\rho = 1.0$;
$\varphi = 0.0025$
$\chi = 0.1$;
$\psi = 2.2$;
$\upsilon = 0.8$; and
$\tilde{N}$ is expressed as billions of animals.

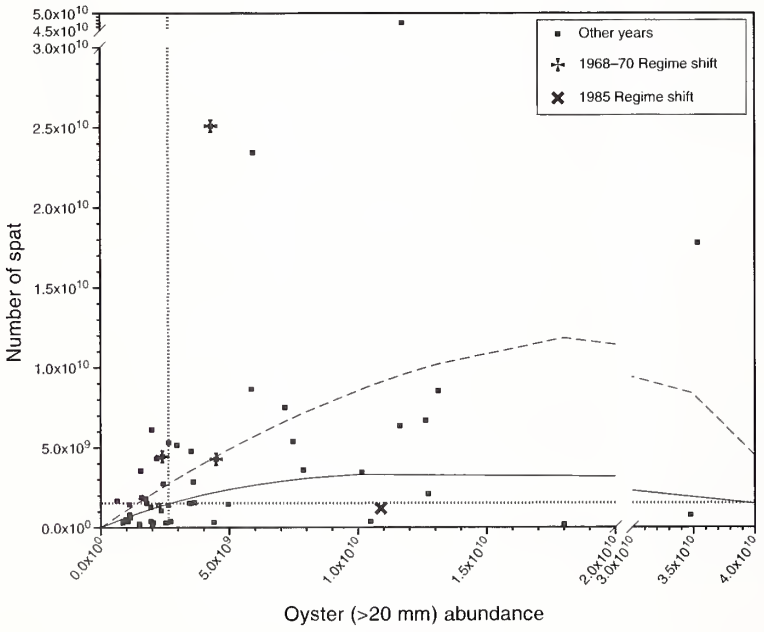

Figure 7

The broodstock–recruitment relationships for eastern oyster (*Crassostrea virginica*), 1953–2006. The solid line is the best-fitted Ricker curve (Eq. 4). The dashed line is a second-order polynomial fit (see Kraeuter et al., 2005). Note that the polynomial fit overestimates recruitment at high abundance. Dotted lines (vertical and horizontal) mark the 54-yr medians of abundance and recruitment.

Equation 6 has the unique property of eliciting both depensatory and compensatory trends at low abundance. Sissenwine (1984), Hilborn and Walters (1992), and Peterson et al. (2001) have provided examples of the well-known depensatory process in which increased predatory mortality rate is associated with increased prey population density because of increased prey preference at high prey density. Allen (1979) provided a somewhat unusual case for depensation in oysters determined by substrate availability rather than by disease. Hilborn and Walters (1992) provided an analogous example from human exploitation of declining fish stocks. The present case is unusual, however, because box-count mortality first increases with declining abundance, but this depensatory phase is then followed by compensation in the mortality rate as abundance continues to decline.

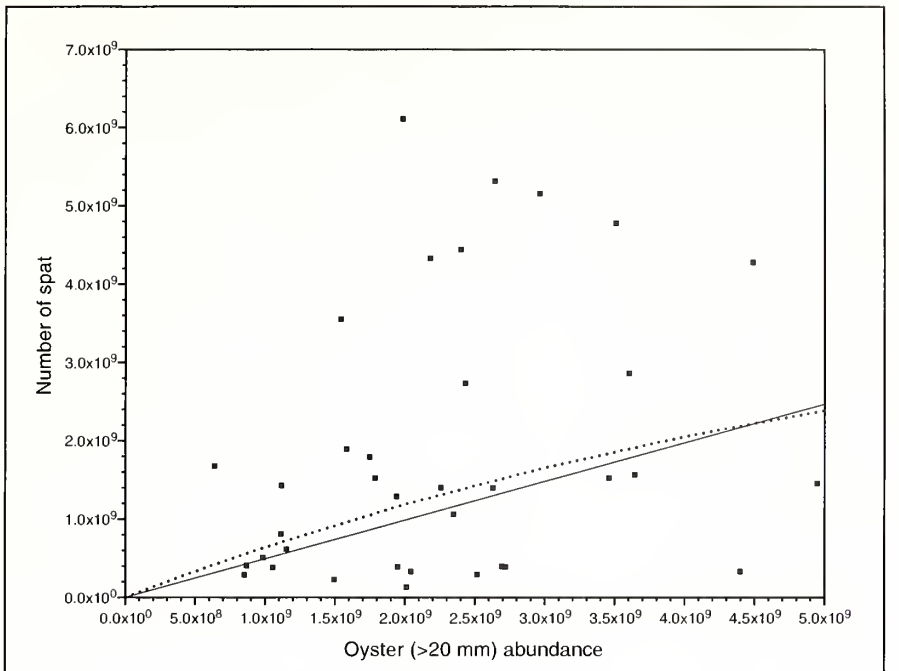

Figure 8

The low-abundance portion of the broodstock–recruitment relationship for the natural oyster beds of eastern oyster (*Crassostrea virginica*) in Delaware Bay, 1953–2006. The dotted line is the best-fitted Ricker curve (Eq. 4), also shown in Figure 7 for the entire data set. The solid line is a linear fit (Eq. 5) with zero intercept. Note that at low abundance, the linear fit travels through the recruitment values slightly below that traversed by the Ricker curve.

Calculation of first passage time

Mean first-passage times were calculated from Redner (2001), according to the methods of Rothschild et al. (2005) and Rothschild and Mullen (1985). Input data were obtained by dividing a two-dimensional data set into quadrants by the medians of the x and y variables (Fig. 10). An example frequency table for the broodstock and recruitment relationship (Table 2) shows the frequency of occurrence of the data from the 54-yr time series in each of the four quadrants, employing the quadrant numbering convention depicted in Figure 10. For instance, years characterized by low abundance and low recruitment, thus falling into quadrant 1, occurred 32% of the time. Table 2 also displays one-year transition probabilities compiled by examining the quadrant location of the x–y datum in successive years. For example, a low-recruitment+low-abundance year falling into quadrant 1, was followed one year later by a high-recruitment+high-abundance year, an occurrence falling into quadrant 4, 18.8% of the time, whereas 50% of the time, the following year was also a low-recruitment+low-abundance year. Thus, given that quadrant 1 is the starting point, the interval of time in which the population finds itself back in quadrant 1 should be a lesser number of years than the time required for the population to shift from quadrant 1 to quadrant 4. Mean first passage times (Table 3) express the number of years likely to elapse before the population with the x–y relationship characteristic of any one quadrant is again described by the relationship characteristic of that same quadrant, or obtains the relationship characteristic of one of the three other quadrants.

Results and discussion

Biological relationships that determine population dynamics

Broodstock and recruitment A relationship between broodstock and recruitment is commonly found for shellfish (Hancock, 1973; Peterson and Summerson, 1992; McGarvey et al., 1993; Lipcius and Stockhausen, 2002; Kraeuter et al., 2005), although not in every case has one been observed (Hancock, 1973; Crocos, 1991; Honkoop et al., 1998; Livingston et al., 2000). Such a relationship is commonly assumed for population dynamics models, and the adequacy of these models supports the likely importance of such a relationship in oysters (Mann and Evans, 1998, 2004; Dekshenieks et al., 2000; Powell et al., 2003). However, empirical evidence in oysters is contradictory and not well documented (e.g., Hofstetter, 1983; Mann et al., 1994; Southworth and Mann, 1998; Livingston et al., 2000), and the travails of larval life and at settlement are certainly likely to add considerable uncertainty to the success of any search for such

evidence (Osman et al., 1989; Powell et al., 2002b, 2004; Hofmann et al., 2004).

In Delaware Bay, recruitment rates below 2×10^9 spat are disproportionately associated with abundances of less than 3×10^9 oysters (Fig. 7). The distribution of years in the four quadrants of the broodstock–recruitment diagram was 17, 9, 9, and 18 for quadrants 1, 2, 3, and 4 (as defined in Fig. 10), respectively (Table 2). This distribution was unlikely by chance, given the expectation that one-quarter of the years should fall into each quadrant: P~0.10, P<0.10; P<0.10; P<0.10, for quadrants 1–4, respectively (binomial test: p=0.25, q=0.75). Twice as many high-recruitment events were associated with high abundance than with low abundance, and about twice as many low-recruitment events were associated with low abundance than with high abundance. The 54-yr average recruitment rate, expressed as the number of spat per >20-mm oyster per year, was 0.959. The median was lower, at 0.600. The long-term likelihood of a one-year population-replacement event (i.e. one spat per >20-mm oyster) was 17 in 54, and a recruitment rate half that high occurred in 27 of 54 years (Fig. 3).

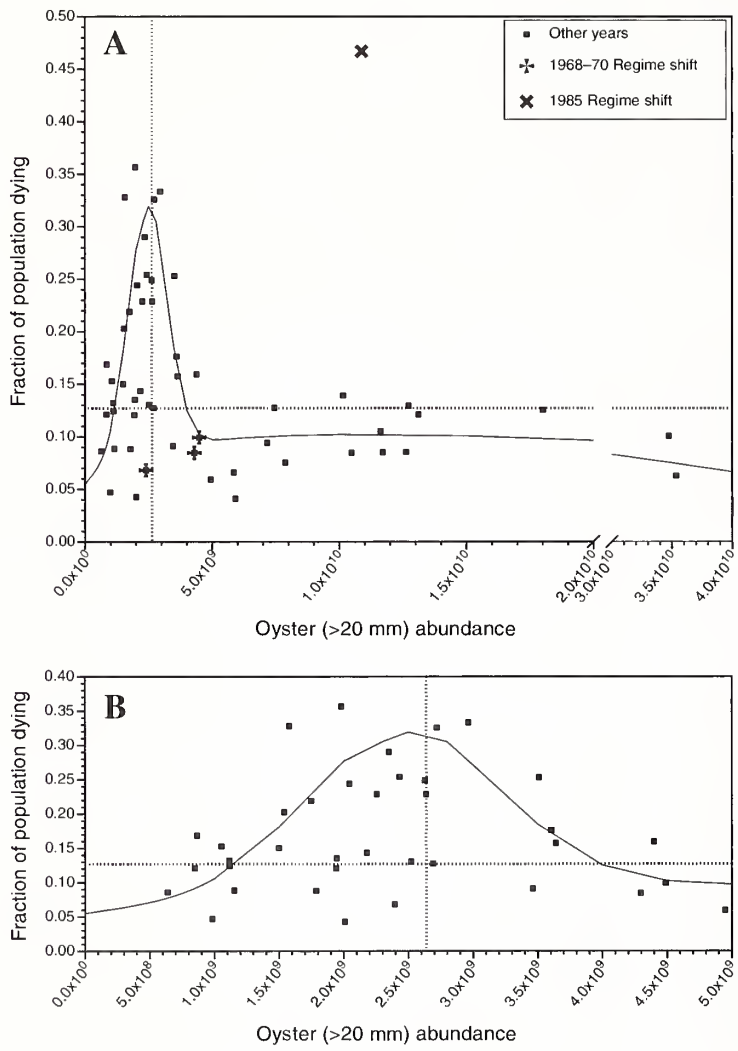

Figure 9

The relationship between oyster abundance and box-count mortality for the eastern oyster (*Crassostrea virginica*) on the natural oyster beds of Delaware Bay during 1953–2006. The solid line is the curve described by Equation 6 fitted to the data. Dotted lines mark the 54-yr medians of abundance and box-count mortality (Table 4). (**A**) represents entire data set; (**B**) focuses on the region of the diagram encompassing abundances below 5×10^9, an abundance range in which an increase in mortality frequently occurs due to epizootic events. Years characteristic of regime shifts are identified in A only.

Only four massive recruitment events (>1.7×10^9 spat) occurred over the 54 years (Fig. 7). The rarity of these occurrences is not unusual (e.g., Loosanoff, 1966; Hofstetter, 1983; Oviatt, 2004; Southworth and Mann, 2004). The events were not predicted by the broodstock–recruitment curve. In most years, however, the broodstock–recruitment relationship was relatively predictive, and the vast majority of recruits sustaining the population over the 54 years accrued from the 50 more-standard recruitment events. Nevertheless, even in average recruitment years, variability about the curve was large, about 4×10^9 spat.

Mean first-passage times calculated from one-year transition probabilities (Table 2) varied from 3 to 8 years (Table 3). Return intervals were about 3 years for a population beginning in quadrant 1 (low recruitment and low abundance) returning to quadrant 1, and for a population beginning in quadrant 4 (high recruitment and high abundance) returning to quadrant 4. The longest return intervals were associated with quadrant 3 (low recruitment and high abundance) as a destination. A population beginning in quadrant 2 or quadrant 3 was somewhat more likely to fall to quadrant 1 than to move to quadrant 4. Thus, overall, populations at low abundance were likely to remain there (quadrant 1) because of low recruitment, whereas populations at high abundance were likely to remain there because of high recruitment. Quadrants 1 and 4 have the characteristics expected of stable states.

The broodstock–recruitment relationship (Fig. 7) indicated that the number of recruits per adult declined at high abundance. Note in particular (Fig. 3) that the number of recruits per adult was not unusually high during the 1970–85 high-abundance period, with the exception of 1972. In fact the number of one-year replacement events (i.e. one spat per adult) was lower for a longer time during this

Table 2

One-year transition probabilities and the frequency of occurrences for the eastern oyster (*Crassostrea virginica*) population in each quadrant over the 54-yr time series were calculated from the Delaware Bay oyster broodstock–recruitment distribution (Fig. 7). Median abundance over 54 years was 2.64×10^9 and median recruitment was 1.53×10^9. Arrows indicate trajectories between quadrants. Quadrants are defined in Figure 10.

Quadrant	1	2	3	4
1 →	0.500	0.125	0.188	0.188
2 →	0.444	0.222	0.000	0.333
3 →	0.222	0.333	0.333	0.111
4 →	0.111	0.111	0.167	0.611
Frequency of occurrence	0.320	0.170	0.170	0.340
Number of years	17	9	9	18

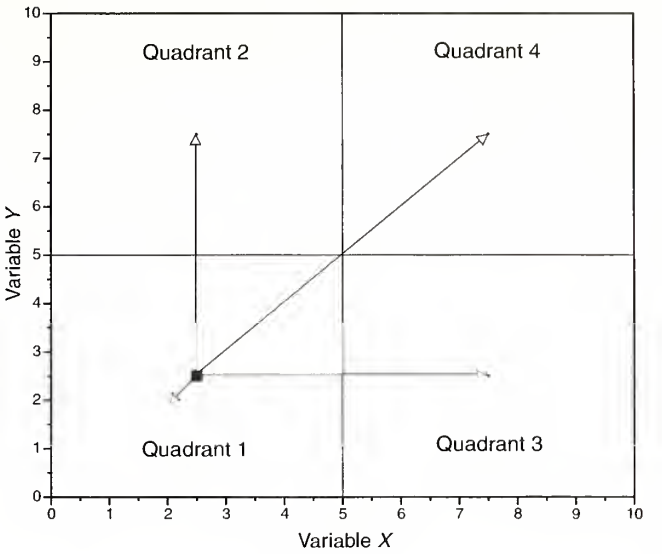

Figure 10

Mean first passage times for eastern oyster (*Crassostrea virginica*) were calculated by employing an arbitrary quadrant numbering convention. One-year transition probabilities were obtained by examining the position of consecutive x–y data pairs in quadrant space. Four transitions are possible for each starting position, the possibilities for quadrant 1 being depicted. Sixteen total trajectories are possible.

15-yr period than at any other time before 2000. Thus, high broodstock abundance was not rewarded by equivalently high recruitment. Three mechanisms seem viable. The first is that fecundity declines at high abundance as availability of food becomes limited. Food limitation by high densities of filter feeders is well described (e.g., Peterson and Black, 1987; Rheault and Rice, 1996; Wilson-Ormond et al., 1997). The second is that cannibalism of larvae occurs, but this cause of mortality is of unlikely importance (Andre et al., 1993; Tamburri et al., 2007). The third is that predation rates on juveniles increase at high abundance. Although little evidence of this effect exists (e.g., Whitlatch and Osman, 1994; Powell et al., 1995), a proportional increase in predation on juveniles at high abundance is consistent with optimal foraging theory (Hughes, 1980), under the assumption that oyster predators are optimal foragers (Powell et al., 1995; see also Pyke, 1984; Pierce and Ollason, 1987). All are standard explanations for compensation in the broodstock–recruitment relationship (e.g., Myers and Barrowman, 1996).

The broodstock–recruitment diagram (Fig. 7) indicates that low abundance limited total recruitment in some way. This relationship is clear despite the exclusion from this data series of an unknown number of adults and recruits in State of Delaware waters, along the fringes of the bay, particularly in the river mouths, and on the leased grounds downbay of the high-mortality beds. Moreover, the leased grounds likely retained substantial numbers of adult animals before the mid-1980s, although estimates of abundance are not available. Many fewer were present thereafter because of the demise of the bay-season fishery.[6] Interestingly, the decline in abundance on leased grounds after 1985 does not generate a perceptible change in the broodstock–recruitment relationship.

Table 3

Mean first passage times, as well as the distribution of occurrences of the eastern oyster (*Crassostrea virginica*) population in each quadrant, after an infinite number of steps were calculated from the Delaware Bay oyster broodstock–recruitment distribution (Fig. 7). The observed distribution of occurrences is given in Table 2. Arrows indicate trajectories between quadrants. Quadrants are defined in Figure 10.

Quadrant	1	2	3	4
Mean first passage time (yr)				
1 →	3.25	6.06	6.45	5.00
2 →	3.60	5.78	7.82	4.14
3 →	4.20	4.56	5.78	5.24
4 →	5.40	6.26	6.65	2.89
Distribution after an infinite number of steps	0.308	0.173	0.173	0.346

Oyster larvae tend to set preferentially on live oysters and boxes rather than on cultch (shell clumps, shells,

[6] Anecdotal information indicates that numbers were low in the 1960s as well.

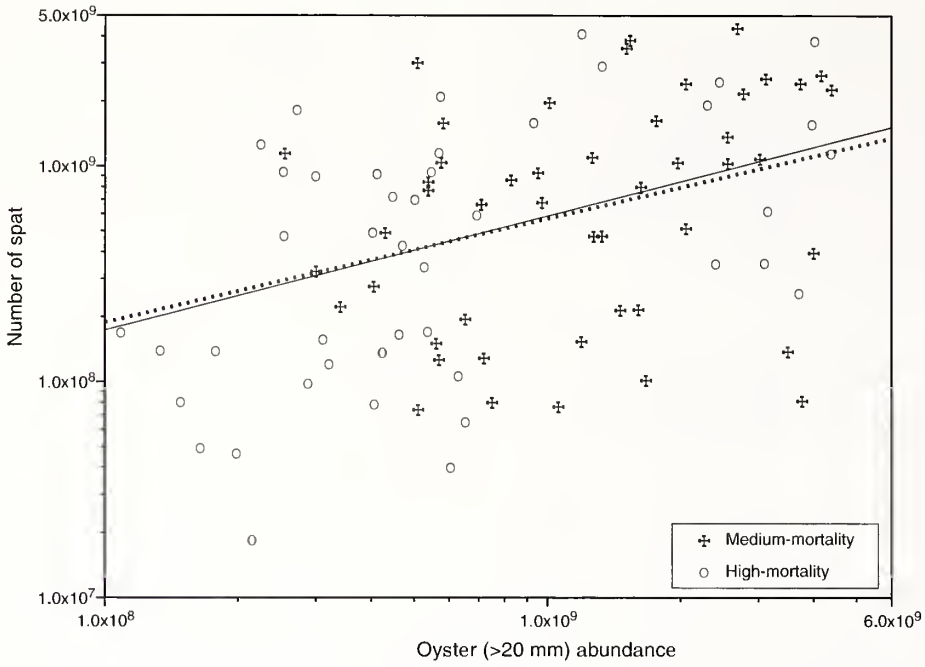

Figure 11

The broodstock–recruitment relationship for eastern oyster (*Crassostrea virginica*) was nearly identical for two key bay areas, the medium-mortality and high-mortality beds (as defined in Table 1), except for the highest abundance–recruitment pairs, where compensation occurred. The best-fitted power curves for the medium-mortality beds (solid line) and the high-mortality beds (dashed line) are shown. For clarity, a log scale was used for both axes.

and shell fragments without attached live oysters or boxes) (Powell et al., 2008); therefore, one possible explanation for the relationship between broodstock and recruitment is that adult abundance increased settlement success by providing a principal source of clean shell. Two avenues of evidence support this idea. First, a recruitment-enhancement program initiated in 2005 strongly indicated that Delaware Bay is not larvae-limited, even at low population abundance levels (unpubl. data, first author). Clean shell planted at the appropriate time consistently sustains a settlement rate 5 to 10 times that for native shell. Second, the relationship between adult numbers and recruitment held for the bay overall, even though the numbers of animals in various regions of the bay varied relatively independently, and independently of numbers for the bay as a whole. The broodstock–recruitment relationship was nearly identical for two key bay areas, the medium-mortality and high-mortality beds (Fig. 11), despite widely and independently varying abundances over the time series (Fig. 5). Different trajectories would have been expected if recruitment rate depended upon a stock-wide abundance with trends divergent from local peregrinations.

Broodstock and mortality Epizootics, here defined as bay-wide disease-induced mortality events affecting greater than 20% of the stock, occurred in about half of the years since 1989 (Figs. 4 and 9), but with much lower frequency in prior years. Deaths in nonepizootic years affected on average around 10% of the stock. All but one of the epizootics occurred at abundances between 1.5×10^9 and 4×10^9. The single outlier occurred at just over 10×10^9 animals; this is the 1985 MSX epizootic event that terminated the high-abundance period of the 1970s. The remaining events included the relatively few MSX epizootics of the 1950s and 1960s and the more frequent Dermo epizootics of the 1990s and 2000s. The distribution of data points in the four quadrants based on information in Figure 9 was 9, 17, 17, and 10 in quadrants 1, 2, 3, and 4, respectively (Table 4). This distribution is unlikely to occur by chance, but barely so: $P<0.10$, $P\sim0.10$; $P\sim0.10$; $P>0.10$, for quadrants 1–4, respectively (binomial test: $p=0.25$, $q=0.75$). Note that the use of the median mortality of 0.127 to define high- and low-mortality quadrant groups yields a number of nonepizootic years in the same quadrants as the epizootic years (those with mortalities exceeding 0.20). Thus, the high-mortality quadrants include years when mortalities were not extraordinarily high. Note also that high-abundance years, those with abundance exceeding the median of 2.64×10^9, include a few epizootic years with abundances near the median. That is, the use of

Table 4

One-year transition probabilities, as well as the frequency of occurrence, of the eastern oyster (*Crassostrea virginica*) population in each quadrant over the 54-yr time series were calculated from the Delaware Bay oyster broodstock–mortality distribution (Fig. 9). Median abundance was 2.64×10^9 and the median mortality fraction was 0.127. Arrows indicate trajectories between quadrants. Quadrants are defined in Figure 10.

Quadrant	1	2	3	4
1 →	0.222	0.444	0.222	0.111
2 →	0.125	0.500	0.063	0.313
3 →	0.059	0.059	0.647	0.233
4 →	0.300	0.400	0.300	0.000
Frequency of occurrence	0.170	0.320	0.320	0.189
Number of years	9	17	17	10

Table 5

Mean first passage times as well as the distribution of occurrences of the eastern oyster (*Crassostrea virginica*) population in each quadrant after an infinite number of steps were calculated from the Delaware Bay oyster broodstock–mortality distribution (Fig. 9). The observed distribution of occurrences is given in Table 4. Arrows indicate trajectories between quadrants. Quadrants are defined in Figure 10.

Quadrant	1	2	3	4
Mean first passage time (yr)				
1 →	6.54	3.55	6.14	4.59
2 →	6.87	3.03	7.09	3.67
3 →	8.10	6.00	3.11	4.21
4 →	6.18	3.88	5.68	5.11
Distribution after infinite steps	0.153	0.339	0.321	0.196

medians allocates most, but not all, epizootic years in the abundance range of 1.5×10^9 to 3×10^9 to a single quadrant.

Nevertheless, even with this ambiguity, high-mortality events were more likely with low abundance and some transitions were more likely to occur than others. Mean first-passage times were particularly long for transitions to quadrant 1 (low-mortality+low-abundance), always exceeding 6 years (Table 5). Mean first-passage times were also long for most transitions to quadrant 3, the low-mortality+high-abundance quadrant, with the exception of those with quadrant 3 as the initial state. By contrast, the population was likely to return to quadrant 2 (high-mortality+low-abundance) from most quadrants in about 3–4 years (Table 5). This return interval is an expression of the relative frequency of Dermo epizootics. Interestingly, the tendency to return to quadrant 2 (high-mortality+low-abundance) was distinctly less from quadrant 3 (low-mortality and high abundance) than from other quadrants. High-mortality events were unlikely to occur when abundance was high. The distribution of first-passage times again supports the presence of multiple stable states for the Delaware Bay oyster population.

The distribution of mortality with abundance is not constant, nor does it display a simple density dependency. Epizootics occurred less often at high abundance and near lowest abundance. Decreased mortality at low abundance was not unexpected for a population exposed to a disease that generates epizootic conditions (Gill, 1928; Ackerman et al., 1984; Kermack and McKendrick, 1991). Normally, transmission rates of disease decline with decreased host density because contact rates decrease (Black, 1966; Andreasen and Pugliese, 1995; Godfray and Briggs, 1995; Heesterbeek and Roberts, 1995) and this leads to lower rates of mortality. This decline in transmission rates is true for nearly all diseases but does not seem to be the case for MSX or Dermo, which are characterized by inherently high transmission rates over a wide range of abundance (Hofmann et al., 1995; Powell et al., 1996, 1999). In the Delaware Bay oyster stock, the declining frequency of epizootics at low abundance originates in the dynamics of stock dispersion. A contraction of the stock away from areas of highest disease mortality normally is associated with low abundance. Thus, epizootics are most likely to occur in a narrow window of abundance as the stock expands from its habitat of refuge on the medium-mortality beds, thereby leaving a greater proportion of the stock once again on the medium-mortality beds. This stock contraction, consequently, mitigates against a recurrence of the high-mortality event. Depensation in the mortality rate as abundance declines is, of course, an extinction scenario, were it to continue. The countervailing compensatory process of stock contraction is the dominant protective action against local extinction, rather than a decline in host density that reduces disease transmission rates.

What is unusual is the low probability of epizootics at high abundance. Mortality rates are often assumed to be invariant over a wide abundance range for marine species (e.g., Paloheimo, 1980; Hoenig, 1983; Vetter, 1987; Clark, 1999) and, contrariwise, increased mortality at high abundance is expected of most populations exposed to epizootic disease (e.g., Anderson and Gordon, 1982; Andreasen and Pugliese, 1995; Godfray and Briggs, 1995; Jaenike, 1998). Neither expectation conforms to what has been observed. Thus, one of the interesting quandaries is the maintenance of population abundance near the higher carrying capacity of the population during the 1970s–1985 high-abundance period. Some portion of this was caused by reference point-based management, which controlled fishing mortality to values normally below 5% of the stock (Powell et al., 2008). Some portion was due to higher than

average freshwater inflows for much of the 1970s, which limited the influence of MSX. However, the fact that high abundance continued for at least five years after freshwater inflows subsided to more normal conditions circa 1979, and the depensation in the abundance–mortality relationship, would indicate that high abundance may reduce the probability of epizootics. This possibility has been treated theoretically by Powell et al. (1996), who showed that simulated oyster populations undergoing significant increases in abundance were very unlikely to also generate Dermo epizootics. Simulations indicate that the oyster population can expand more rapidly than Dermo can expand and intensify, when the number of recruits is high (Fig. 7). Alternatively, or perhaps as an abetting process, the number of infective elements in the water column may be reduced below the level needed to generate an infective dose because of the volume of water filtered by the population at high abundance. An infective dose is hypothesized for MSX (Ford et al., 1999; Powell et al., 1999), and some evidence supports dose-dependency in Dermo (Bushek et al., 1997). However, insufficient information on the interaction of disease with oyster populations at high abundance is available to definitively decipher the relationship between parasite and host at high abundance because oyster populations at high abundance are now rare or nonexistent for study.

Interpretation and application of the compensatory and depensatory portions of the mortality curve described by Equation 6 (Fig. 9) come with a number of important caveats. 1) The probability of occurrence of an epizootic has increased since 1990 with the replacement of MSX by Dermo as the primary disease that produces mortality. An increase in frequency may be expected because of the greater tolerance of the parasite for low salinity (e.g., Ford, 1985; Powell et al., 1996; Ford et al., 1999; Ragone Calvo et al., 2001). Thus the ambit of oyster population dynamics may be more restricted by Dermo than by MSX. 2) The time series contains no high-abundance years since the replacement of MSX by Dermo circa 1990. Whether a return to high abundance is precluded by Dermo is unknown, but the difference in transmission dynamics between the two parasites (e.g., Ford and Tripp, 1996) and the expanded environmental range of Dermo in comparison to MSX would indicate that this may be the case. 3) Environmental conditions have not been constant over the 54 years, and environmental change significantly influences the chief agents of increased mortality, MSX and Dermo, as well as the autocorrelational dynamics of the epizootic process (e.g., Soniat et al., 1998). The mortality curve integrates environmental and biological dynamics. 4) The rise in winter temperature since the 1970s, that accelerated after 1990 (Scavia et al., 2002; Nixon et al., 2004), may have modified the interaction of disease with oyster population dynamics (e.g., Ford, 1996; Cook et al.; 1998, see also Hofmann et al., 1995; Powell et al., 1996), decreasing the applicability of the pre-1990 portion of the time series. 5) As abundance declines, a greater proportion of the oyster population is found on the medium-mortality beds (Powell et al., 2008). As a consequence, the probability of an epizootic begins to decline at abundances somewhere above 1×10^9 animals. Insufficient data are available to determine the trajectory for extrapolating this curve to lower abundances; therefore considerable uncertainty exists regarding the implementation of the abundance–mortality curve for abundances below 0.8×10^9.

Table 6

One-year transition probabilities, as well as the frequency of occurrences of the eastern oyster (*Crassostrea virginica*) population in each quadrant over the 54-yr time series were calculated from the Delaware Bay oyster recruitment–mortality distribution (Fig. 12). Median recruitment was 1.53×10^9 and the median mortality fraction was 0.127. Arrows indicate trajectories between quadrants. Quadrants are defined in Figure 10.

Quadrant	1	2	3	4
1 →	0.308	0.385	0.077	0.231
2 →	0.231	0.385	0.077	0.308
3 →	0.143	0.071	0.714	0.071
4 →	0.231	0.231	0.154	0.385
Frequency of occurrence	0.241	0.259	0.259	0.241
Number of years	13	14	14	13

Mortality and recruitment Both MSX and Dermo reduce the energy budget of a host (e.g., Hofmann et al., 1995; Ford et al., 1999) and, as a consequence, may reduce fecundity. Some empirical evidence exists that disease reduces the fecundity of individual oysters (Mackin, 1953; Barber et al., 1988; Ford and Figueras, 1988; Barber, 1996; Paynter, 1996; Dittman et al., 2001). One expectation is that fecundity may drop during epizootic years. No overall pattern is found between recruitment and box-count mortality in Delaware Bay (Ford and Figueras, 1988); however, the four massive settlement events with spat numbers above 1.5×10^{10} occurred during years when box-count mortality was very low, quadrant 3, (Fig. 12). Whether this coincidence is an independent outcome of two processes responding to common environmental and population forces, or whether it documents a causative connection, cannot yet be determined.

Data points in the recruitment and box-count mortality distribution fell into quadrants 1–4 with a frequency of 13, 14, 14, and 13 years, respectively (Table 6). Such a distribution is expected by chance. Cases of high recruitment occur equally often with low and high mortality. Despite the seeming randomness of the relationship, mean first-passage times are far from equivalent across all transitions (Table 7). The high-recruitment+low-mortality state is reached from the other three quadrants about three times less frequently

than is any other population state. Once there, the population is much more likely to remain there than move to any of the other three quadrants. High recruitment with low mortality is a relatively stable state.

Unrecorded mortality Box-count mortality is generally a measure of mortality of larger animals. Presumably, much of the mortality unrecorded by box counts is associated with predation in the first year of life and, therefore, likely would not show a discernible relationship with recruitment. Estimates of survival to one year of age indicate that mortality rates are at least a factor of three to five above the population average for older animals (Powell et al., 2009), confirming that much of the unrecorded mortality is juvenile mortality. The assumption that juvenile mortality rate varies randomly with respect to other indices of population dynamics is supported by comparisons with abundance, recruitment, and box-count mortality (Figs. 13–15).

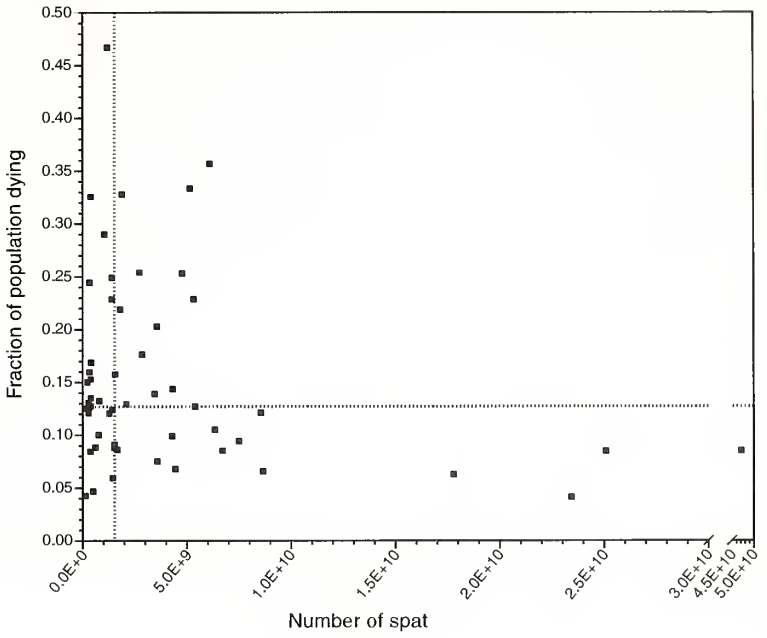

Figure 12

The relationship between box-count mortality and recruitment for the eastern oyster (*Crassostrea virginica*) in 1953–2006 for the natural oyster beds of Delaware Bay. Dotted lines indicate the 54-yr medians of box-count mortality and recruitment.

Influence of regime shifts on biological relationships

Both the broodstock abundance–recruitment (Fig. 7) and abundance–mortality (Fig. 9) curves have outlying points. These are more common in the former than in the latter. Arguably, data for years when regime shifts occur should not be used in defining such relationships because the purpose of such relationships is to understand and model the typical population dynamics of the stock. Stock dynamics during regime shifts are atypical.

The abundance–mortality relationship (Fig. 9A) shows only a single outlying point This outlier (X), the only case of epizootic mortality at stock abundances greater than 5×10^9, marks the regime shift year of 1985, when stock abundance reverted to the low-abundance state after more than a decade of high abundance. The 1968–70 period, during which time conditions supported a dramatic population expansion, did not leave an indelible imprint. All three years were characterized by low mortality, but many other such years displayed similar abundance levels.

In contrast, the abundance–recruitment scatterplot (Fig. 7) contains four clear high-recruitment outliers. In this case, the 1985 regime shift is not unusual. Other low-recruitment years show high abundance. The 1968–70 period contains one of the four outliers (Fig. 7) and the years 1972–74 contain the other three. The inference drawn from Figure 2 is that these four outliers are of two types. One outlier is the previously-mentioned outlier that occurred during the 1968–70 period and represents the unusual event that dramatically impacted the stock. The other three are associated with an unusual transit of abundance above carrying capacity (Powell et al., 2008, 2009) and represent events that had no long-term consequences for the stock, except to maintain abundance near the carrying capacity

Table 7

Mean first passage times and the distribution of occurrence of the eastern oyster (*Crassostrea virginica*) population in each quadrant after an infinite number of steps were calculated from the Delaware Bay oyster recruitment–mortality distribution (Fig. 12). The observed distribution of occurrences is given in Table 6.))Arrows indicate trajectories between quadrants. Quadrants are defined in Figure 10.

Quadrant	1	2	3	4
Mean first passage time (yr)				
1 →	4.45	3.72	9.97	4.52
2 →	4.83	3.79	9.91	4.17
3 →	5.94	6.52	3.78	6.80
4 →	4.92	4.65	9.08	4.05
Distribution of occurrence after infinite steps	0.225	0.264	0.264	0.247

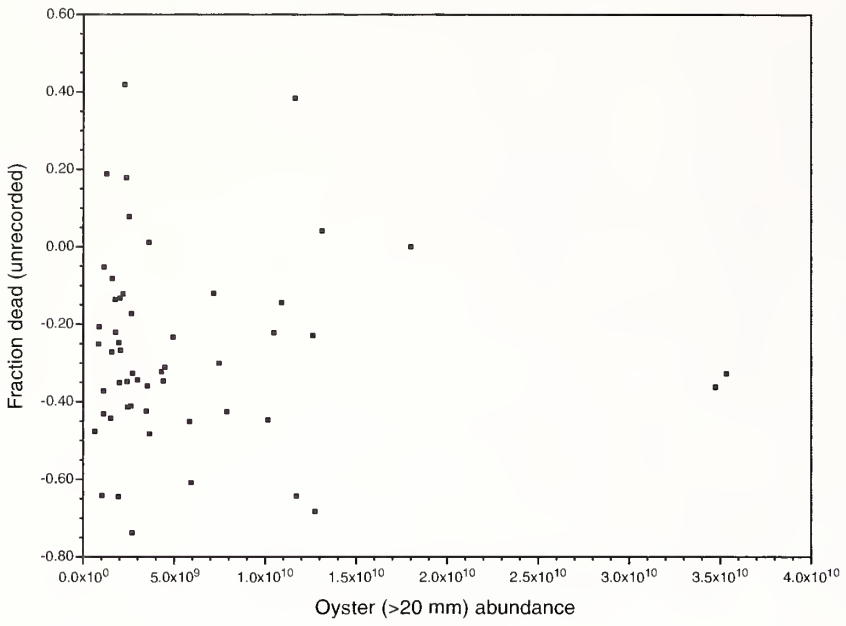

Figure 13

The relationship between oyster abundance and unrecorded mortality for the eastern oyster (*Crassostrea virginica*) in 1953–2006 for the natural oyster beds of Delaware Bay. Irrational (positive) values on the ordinate indicate survey imprecision.

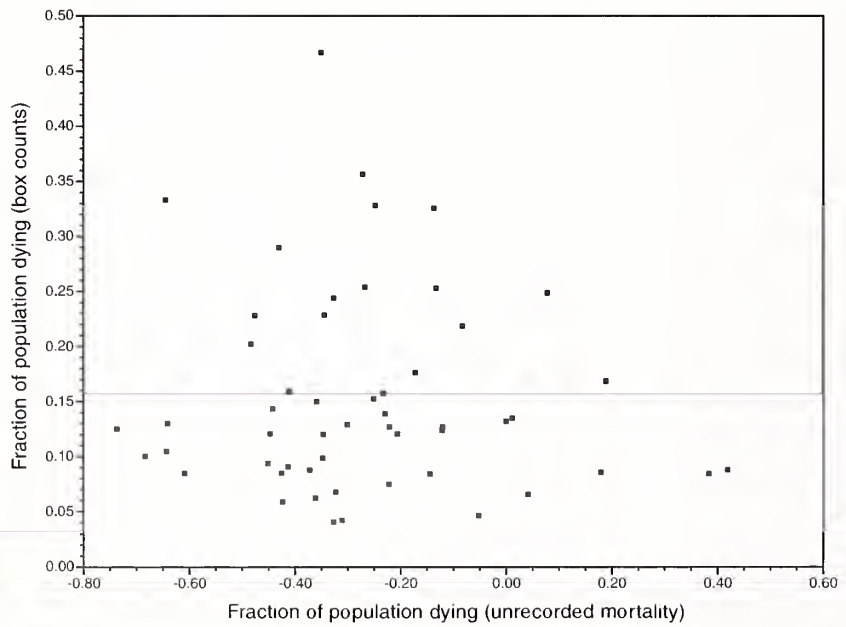

Figure 14

The relationship between box-count mortality and unrecorded mortality of the eastern oyster (*Crassostrea virginica*), 1953–2006, for the natural oyster beds of Delaware Bay. Irrational (positive) values on the abscissa indicate survey imprecision.

originally established circa 1970. In this scenario, these years were not unique. Nevertheless, for both cases, the performance of the stock was not representative of the dynamics defined by the remaining 50 years of observation. As a consequence, a mathematical relationship weighting these four observations overly much (e.g., the polynomial fit in Fig. 7) would not appropriately parameterize a model of the stock either in its high-abundance or low-abundance state.

The influence of spatial relationships on population dynamics

The relationships between broodstock, recruitment, and mortality expressed by Equations 4 and 6 and by Figures 7 and 9 attempt to portray the time series of observations in terms of the ambit of the stock's population dynamics. In fact, in one sense, this misrepresents the true range of the species' population dynamics at any particular time because the ambit of the stock in one regime differs from that of the other. First-passage times support this conclusion, as does a closer look at the distribution of abundance, recruitment, and mortality for the four bay regions over the full time series (Powell et al., 2008).

Consider first the broodstock abundance–recruitment relationship (Fig. 7). We identify two sets of points characteristic of times when the stock was relatively consolidated within its distributional range (Fig. 16). In these periods, a large proportion of the stock was found on the medium-mortality beds (Fig. 5). Such an occurrence was characteristic of the stock in both low- and high-abundance regimes and for extended periods of time, including most years between 1960 and 1963 (low-abundance regime), the 1970–77 period (high-abundance regime), and the 1997–2006 period (low-abundance regime). The 1970s occurrences all fall in quadrant 4 (high abundance+high

recruitment) (Fig. 16). Whereas other years also fall in this quadrant, when the stock is consolidated at high abundance, the likelihood that recruitment will be above the median of all years is extraordinarily high. When the stock is dispersed, the likelihood is not as great, but still, in most years, the population's performance falls into quadrant 4. Thus, stock dispersion has little influence on the outcome of recruitment events during the high-abundance regime.

In contrast, occurrences when relatively more of the stock was found on the medium-mortality beds during the low-abundance regime fall disproportionately into quadrant 1 (low abundance+low recruitment) (Fig. 16). Eight of fourteen occurrences in these years fall into this quadrant, a value significantly greater than expected by an even distribution of points among the four quadrants ($P<0.005$), and 10 of 14 display low recruitment (quadrants 1 and 3), a value significantly greater than expected by an even split ($P\sim0.05$). Thus, when the stock is consolidated within its range, and in its low-abundance regime, a high-recruitment event is unlikely. During the late 1980s and early 1990s, the stock was at relatively low abundance, but more distributed among bed regions (Fig. 5). These years are more evenly distributed among the four quadrants (Fig. 16). In particular, three occur in quadrant 3, accounting for a high percentage of all such events, and five fall above the long-term median for recruitment. Thus, although a dispersed stock can result in low recruitment during the low-abundance regime, the chance of a high-recruitment event is much improved.

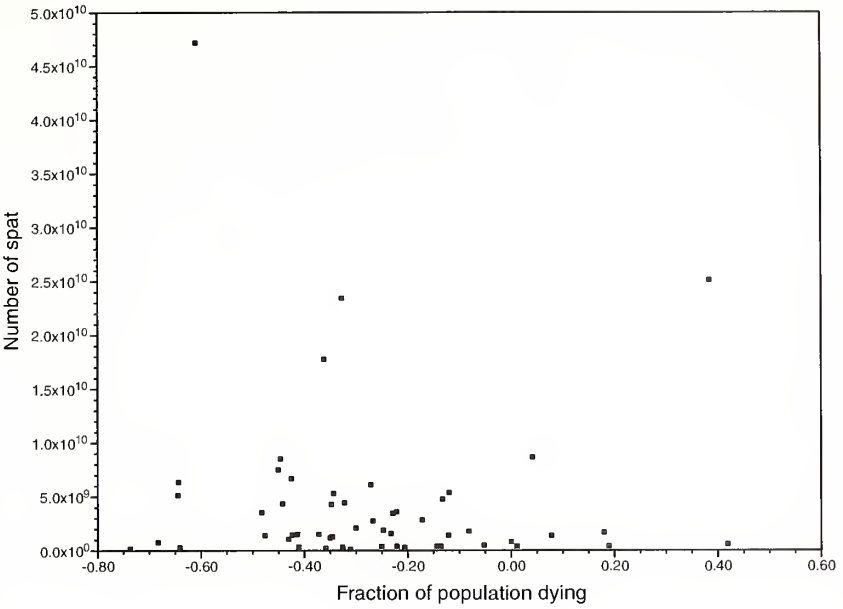

Figure 15

The relationship between unrecorded mortality and recruitment in 1953–2006 for the natural oyster beds of Delaware Bay. Irrational (positive) values on the abscissa indicate survey imprecision.

One inference from these data is that high recruitment events are the result of spawning by oysters downbay of the medium-mortality region, in waters of higher salinity. This inference is supported by the tendency for the high-mortality beds to recruit more consistently (Powell et al., 2008). The fact that quadrants 1 and 4 are primarily represented by years when a consolidated stock distribution was present indicates that spawning potential differs between the two regimes. Perhaps it is no coincidence that the 1970 stock expansion was preceded by a tendency for the stock to expand at low abundance, thereby increasing the probability of a high recruitment event at low abundance. And perhaps it is no surprise that the decrease in recruitment during the first years of the 2000s (Powell et al., 2008) was preceded by a consolidation of the stock beginning in 1996, which reduced the probability of a high-recruitment event. All of these observations would imply that a high recruitment is primarily driven by increased spawning potential on higher-salinity beds. Thus, the broodstock–recruitment relationship (Fig. 7) fails to emphasize a substantive impact from stock dispersion. The range in recruitment at a given abundance, blithely inferred to represent stochastic variation about a mean, in actuality includes a large influence from stock distribution that cannot be readily represented by a simple mathematical relationship between observed recruitment and stock size. This dispersion imprint is a dominant contributor to the dynamics of a population at low abundance, but not at high abundance, when compensatory processes begin to become important, and helps explain why the 1970 regime shift was an unlikely event.

The influence of geographic dispersion is also observed in the abundance–mortality diagram (Fig. 9). Not surprisingly, the high-abundance regime is associated with low mortality, regardless of the degree of consolidation of the stock (Fig. 17). This association conforms with the relationships observed for the broodstock–recruitment relationship (Fig. 16). By contrast, the years characterized by consolidated and dispersed stock during the low-abundance regime are divergent, and again this divergence is similar to our conclusion drawn from the broodstock–recruitment relationship. The mortality rate should be lower when more oysters are found on the medium-mortality beds, and this

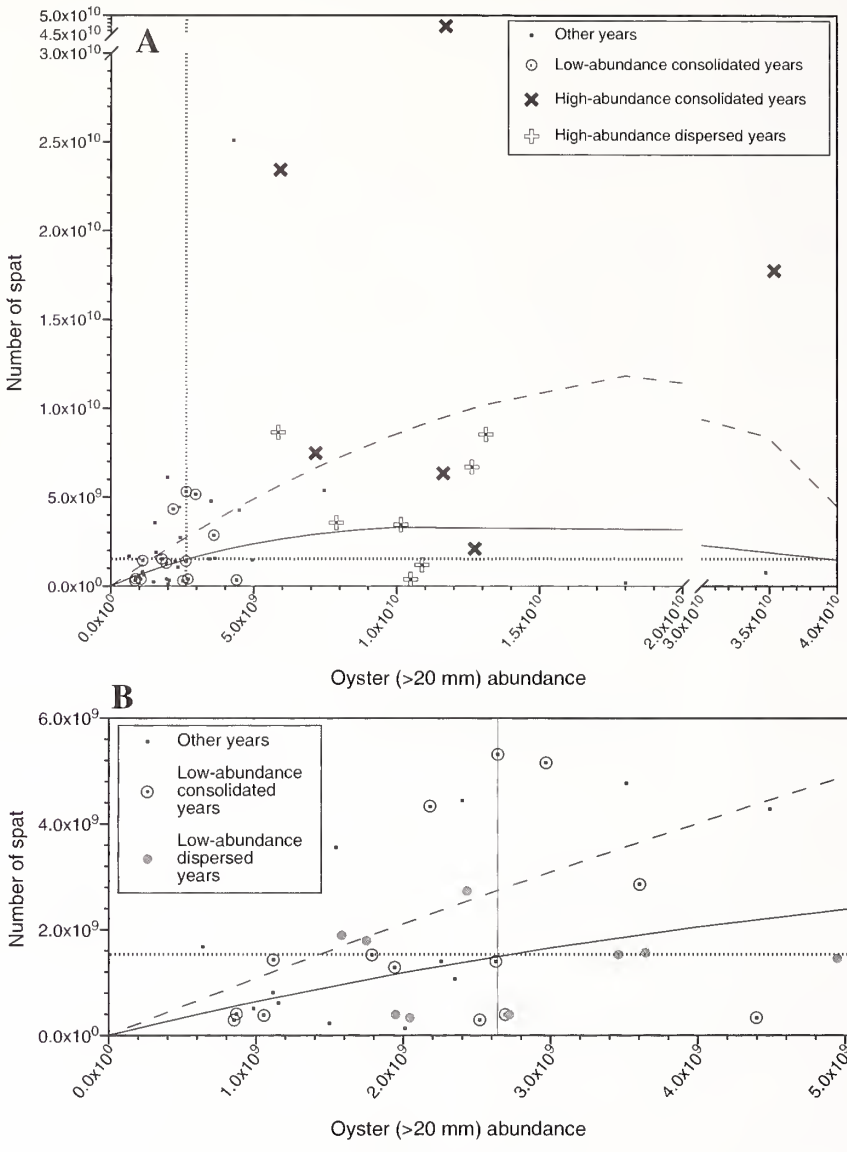

Figure 16

The broodstock–recruitment relationship of the eastern oyster (*Crassostrea virginica*), 1953–2006, for the natural oyster beds of Delaware Bay, showing low-abundance consolidated years (1960–1963 and 1996–2006), low-abundance dispersed years (1987–1995), high-abundance consolidated years (1971–1978), high-abundance dispersed years (1979–1984), and low-abundance dispersed years (1987–1995). Consolidated and dispersed refer to the proportional contribution of the medium-mortality beds to total stock abundance as defined by the median value in Figure 5. The solid line is the best-fitted Ricker curve (Eq. 4). The dashed line is a second-order polynomial fit (see Kraeuter et al., 2005). The dotted lines represent the 54-yr medians, which define the four quadrants (Fig. 10). Graph (**A**) represents the entire data set and (**B**) represents years with recruitment $\leq 6\times10^9$ and abundance $\leq 5.5\times10^9$.

is the case. Epizootic mortalities (>0.20 in Fig. 17) occurred in four of eight years when the stock was dispersed, but only in three of fourteen years when consolidated. The second proportion differs significantly from the first ($P<0.025$). Epizootics are an important mechanism leading to stock consolidation, and a consolidated stock is resistant to further epizootic challenge.

If one considers the relationships of recruitment and mortality to broodstock abundance, the high-

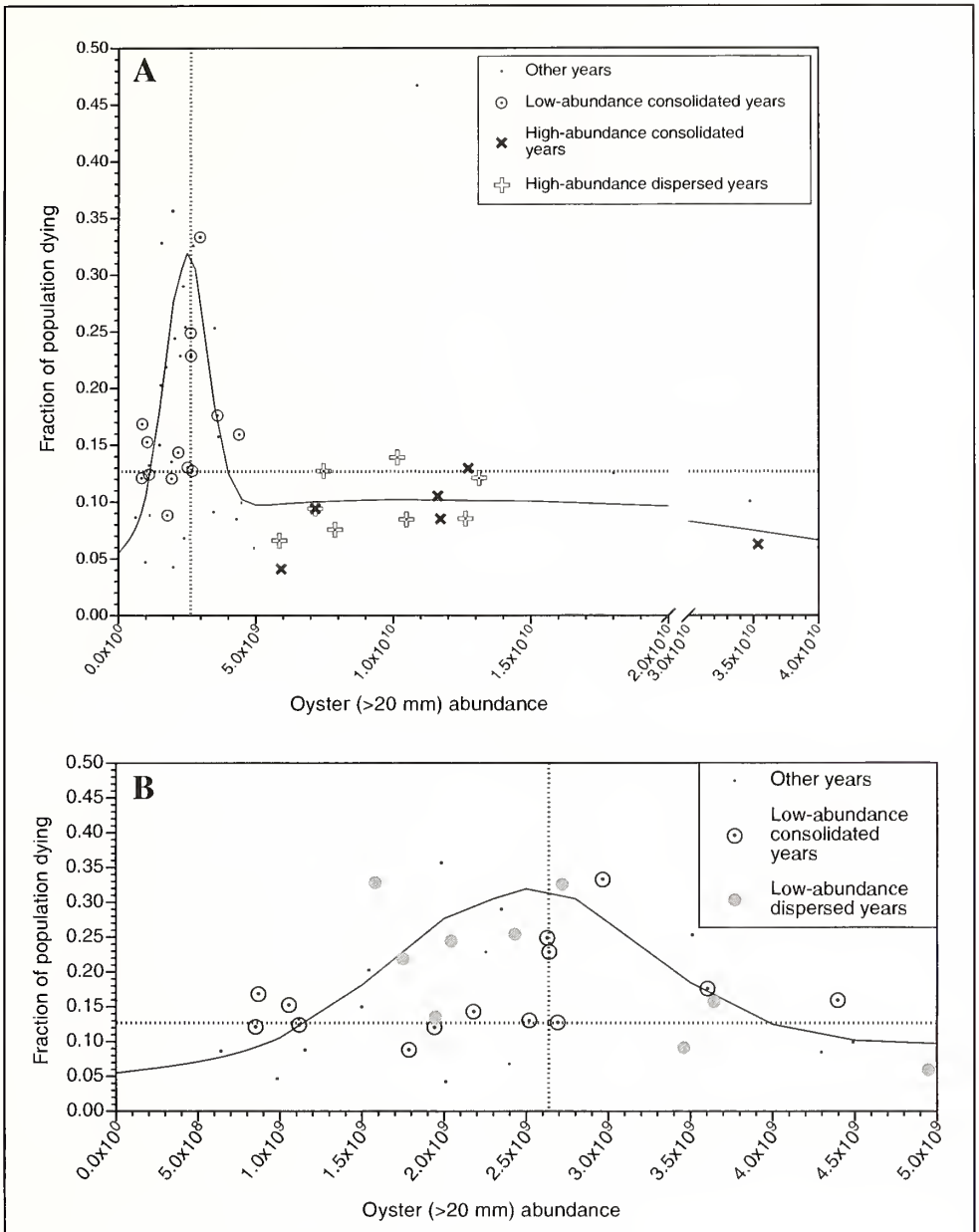

Figure 17

The broodstock–mortality relationship for the eastern oyster (*Crassostrea virginica*), 1953–2006, time period for the natural oyster beds of Delaware Bay, showing low-abundance consolidated years (1960–1963 and 1996–2006), high-abundance consolidated years (1971–1978), high-abundance dispersed years (1979–1984), and low-abundance dispersed years (1987–1995). The solid line is the curve fitted from Equation 6. The dotted lines represent the 54-yr medians which define the four quadrants (Fig. 10). Consolidated and dispersed refer to the proportion of the population on medium-mortality beds (Fig. 5) above or below the 54-yr median, respectively. The upper graph presents the entire dataset and the lower graph focuses on years of abundance $\leq 5 \times 10^9$.

abundance regime is noteworthy for low mortality and high recruitment, regardless of stock dispersion. However, during low-abundance intervals, the consolidated stock is in a relatively stable state and characterized by low mortality and low recruitment. The dispersed state is moderately less stable, characterized by higher mortality and higher recruitment. The interesting coincidence of similar trends in mortality and recruitment in both instances is noteworthy.

Conclusions

The oyster population in Delaware Bay exhibits population dynamics that are not normally described in commercial species. One reason is the presence of multiple distinct, dynamically stable states delimited by temporally rapid regime shifts. Such dynamics are becoming more widely appreciated in fished species as a whole; therefore these unique dynamics may be more apparent than real. Oyster populations display four unusual biological relationships, however, that impute greater peculiarity to their population dynamics. First, it seems likely that the broodstock–recruitment relationship, at least at low abundance, is driven more by the provision of settlement sites for larvae by the adults than by fecundity. Second, the natural mortality rate is temporally unstable and bears a nonlinear relationship with abundance (Fig. 9). This nonlinearity is driven by MSX and Dermo, both acting similarly despite the multifarious differences in their life histories, and by the environmental gradient of the habitable areas, which provide habitats of refuge from disease during epizootics. Third, high abundance and low mortality, though likely requiring favorable environmental conditions, also seem to be self-reinforcing, although the specific underpinning dynamics remain unclear. As a consequence, an increased probability of high mortality occurs over a relatively small range of total abundances. The mortality relationship exhibits both compensatory and depensatory components. Fourth, the geographic distribution of the stock is intertwined with the variables of abundance, recruitment, and mortality, such that biological relationships are functions both of spatial organization and inherent population processes. As a consequence of the imprint of geographic distribution on population dynamics, epizootic-level mortalities normally occur only when the animal has expanded its population beyond the refuge sufficiently that a significant fraction of the population is exposed to higher mortality. Consolidation limits mortality. What is equally interesting is the parallel influence on recruitment such that the consolidated stock has a lower recruitment potential, while also minimizing epizootic mortality.

One is often dismayed by the dispersion of data in plots of the relationships of broodstock to recruitment and abundance to mortality. This dispersion is normally ascribed to stochastic processes, and stochasticity is certainly a causal element. However, both governing regime and geographic distribution of the stock influence the dispersion of these data. Of note is the influence of stock dispersion, where the ambit of the population when the stock is in a contracted state is dissimilar from the ambit when the stock is in a dispersed state. This dynamic imposes a wider range in stock performance for a given stock abundance than would be observed for either distributional state alone. At least for oysters, a substantive component of apparent stochasticity observed in the relationships of recruitment and mortality to abundance originates not from simple year-to-year variation in stock performance, but from different distributions for the stock dictated by modifications in the geographic distribution of the stock, and these distributional states tend to be self-reinforcing, as evidenced by similar changes in both recruitment and mortality over half-decadal or longer intervals of time.

Acknowledgments

We recognize the many people who contributed to the collection of survey data during the 54 years surveyed for this report, with particular recognition of H. Haskin, D. Kunkle, and B. Richards for their scientific contributions. We appreciate the many suggestions on content provided by S. Ford. The study was funded by an appropriation from the State of New Jersey to the Haskin Shellfish Research Laboratory, Rutgers University, and authorized by the Oyster Industry Science Steering Committee, a standing committee of the Delaware Bay Section of the Shell Fisheries Council of New Jersey.

Literature cited

Ackerman, E., L. R. Elveback, and J. P. Fox.
1984. Simulation of infectious disease epidemics, 202 p. Charles C. Thomas, Springfield, IL.

Alexander, R. R., and G. P. Dietl.
2001. Shell repair frequencies in New Jersey bivalves: a recent baseline for tests of escalation with Tertiary, Mid-Atlantic congeners. Palaios 16:354–371.

Allen, R. L.
1979. A yield model for the Foveaux Strait oyster (*Ostrea lutaria*) fishery. Rapp. P.-V. Réun. Cons. Int. Explor. Mer 175:70–79.

Anderson, R. M., and D. M. Gordon.
1982. Processes influencing the distribution of parasite numbers within host populations with special emphasis on parasite-induced host mortalities. Parasitology 85:373–398.

Andre, C., P. R. Jonsson, and M. Lindegarth.
1993. Predation on settling bivalve larvae by benthic suspension feeders: the role of hydrodynamics and larval behavior. Mar. Ecol. Prog. Ser. 97:183–192.

Andreasen, V., and A. Pugliese.
1995. Pathogen coexistence induced by density-dependent host mortality. J. Theor. Biol. 177:159–165.

Anonymous.
1996. Magnuson–Stevens Fishery Conservation and Management Act. U.S. Dep. Commer., NOAA Tech. Memo. NMFS-F/SPO-23, 121 p.

Baines, P. G., and C. K. Folland.
2007. Evidence for a rapid global climate shift across the late 1960s. J. Climate 20:2721–2744.

Barber, B. J.
1996. Gametogenesis of eastern oysters, *Crassostrea virginica* (Gmelin, 1791), and Pacific oysters, *Crassostrea gigas* (Thunberg, 1793) in disease-endemic lower Chesapeake Bay. J. Shellfish Res. 15:285–290.

Barber, B. J., S. E. Ford, and H. H. Haskin.
1988. Effects of the parasite MSX (*Haplosporidium nelsoni*) on oyster (*Crassostrea virginica*) energy metabolism. I. Condition index and relative fecundity. J. Shellfish Res. 7:25–31.

Black, F. L.
1966. Measles endemicity in insular populations: critical community size and its evolutionary implications. J. Theor. Biol. 11:207–211.

Botsford, L. W.
1981. The effects of increased individual growth rates on depressed population size. Am. Nat. 117:38–63.

Breitburg, D. L., and R. S. Fulford.
2006. Oyster–sea nettle interdependence and altered control within the Chesapeake Bay ecosystem. Estuaries Coasts 29:776–784.

Burreson, E. M., N. A. Stokes, and C. S. Friedman.
2000. Increased virulence in an introduced pathogen: *Haplosporidium nelsoni* (MSX) in the eastern oyster *Crassostrea virginica*. J. Aquat. Anim. Health 12:1–8.

Bushek, D., S. E. Ford, K. A. Alcox, R. Gustafson, and S. K. Allen Jr.
1997. Response of the eastern oyster, *Crassostrea virginica*, to *in vitro* cultured *Perkinsus marinus* and the early fate of parasites delivered via three dosing methods. J. Shellfish Res. 16:479–485.

Choi, J. S., K. T. Frank, W. C. Leggett, and K. Drinkwater.
2004. Transition to an alternate state in a continental shelf ecosystem. Can. J. Fish. Aquat. Sci. 61:505–510.

Clark, W. G.
1999. Effects of an erroneous natural mortality rate on a simple age-structured stock assessment. Can. J. Fish. Aquat. Sci. 56:1721–1731.

Collie, J. S., K. Richardson, and J. H. Steele.
2004. Regime shifts: can ecological theory illuminate the mechanisms? Prog. Oceanogr. 60:281–302.

Cook, T., M. Folli, J. Klinck, S. Ford, and J. Miller.
1998. The relationship between increasing sea-surface temperature and the northward spread of *Perkinsus marinus* (Dermo) disease epizootics in oysters. Estuar. Coast. Shelf Sci. 46:587–597.

Crocos, P. J.
1991. Reproductive dynamics of three species of Penaeidae in tropical Australia, and the role of reproductive studies in fisheries management. *In* Crustacean egg production (A. Wenner, and A. Kuris, eds.), p. 317–331. A. A Balkema, Rotterdam, Netherlands.

Cummins, H., E. N. Powell, R. J. Stanton Jr., and G. Staff.
1986a. The rate of taphonomic loss in modern benthic habitats: how much of the potentially preservable community is preserved? Palaeogeogr. Palaeoclimatol. Palaeoecol. 52:291–320.
1986b. The size-frequency distribution in palaeoecology: the effects of taphonomic processes during formation of death assemblages in Texas bays. Palaeontology (Lond.) 29:495–518.

Dawe, E. G., E. B. Colbourne, and K. F. Drinkwater.
2000. Environmental effects on recruitment of short-finned squid (*Illex illecebrosus*). ICES J. Mar. Sci. 57:1002–1013.

Deakin, M. A. B.
1990. Catastrophe modelling in the biological sciences. Acta Biotheor. 38:3–22.

DeAngelis, D. L., and J. C. Waterhouse.
1987. Equilibrium and nonequilibrium concepts in ecological models. Ecol. Monogr. 57:1–21.

Dekshenieks, M. M., E. E. Hofmann, J. M. Klinck, and E. N. Powell.
2000. Quantifying the effects of environmental change on an oyster population: a modeling study. Estuaries 23:593–610.

Dittman, D. E., S. E. Ford, and D. K. Padilla.
2001. Effects of *Perkinsus marinus* on reproduction and condition of the eastern oyster, *Crassostrea virginica,* depend on timing. J. Shellfish Res. 20:1025–1034.

Fegley, S. R., S. E. Ford, J. N. Kraeuter, and H. H. Haskin.
2003. The persistence of New Jersey's oyster seedbeds in the presence of MSX disease and harvest: management's role. J. Shellfish Res. 22:451–464.

Ford, S.
1997. History and present status of molluscan shellfisheries from Barnegat Bay to Delaware Bay. *In* The history, present condition, and future of the molluscan fisheries of North and Central America and Europe. Vol. 1, Atlantic and Gulf Coasts (C. L. MacKenzie Jr., V. G. Burrell Jr., A. Rosenfield, and W. L. Hobart, eds.). NOAA Tech. Rep. NMFS 127:119–140.

Ford, S., E. Powell, J. Klinck, and E. Hofmann.
1999. Modeling the MSX parasite in eastern oyster (*Crassostrea virginica*) populations. I. Model development, implementation, and verification. J. Shellfish Res. 18:475–500.

Ford, S. E.
1985. Effects of salinity on survival of the MSX parasite *Haplosporidium nelsoni* (Haskin, Stauber, and Mackin) in oysters. J. Shellfish Res. 5:85–90.
1996. Range extension by the oyster parasite *Perkinsus marinus* into the northeastern United States: response to climate change. J. Shellfish Res. 15:45–56.

Ford, S .E., M. J. Cummings, and E. N. Powell.
2006. Estimating mortality in natural assemblages of oysters. Estuaries Coasts 29:361–374.

Ford, S. E., and A. J. Figueras.
1988. Effects of sublethal infection by the parasite *Haplosporidium nelsoni* (MSX) on gametogenesis, spawning, and sex ratios of oysters in Delaware Bay, USA. Diss. Aquat. Org. 4:121–133.

Ford, S. E., and M. R. Tripp.
1996. Diseases and defense mechanisms. *In* The eastern oyster: *Crassostrea virginica* (V. S. Kennedy, R. I. E. Newell, and A. F. Eble, eds.), p. 581–659. Maryland Sea Grant College Program, College Park, MD.

Fréchette, M., and E. Bourget.
1985. Food-limited growth of *Mytilus edulis* L. in relation to the benthic boundary layer. Can. J. Fish. Aquat. Sci. 42:1166–1170.

Fréchette, M., and D. Lefaivre.
1990. Discriminating between food and space limitation in benthic suspension feeders using self-thinning relationships. Mar. Ecol. Prog. Ser. 65:15–23.

Gabriel, W. L.
1992. Persistence of demersal fish assemblages between Cape Hatteras and Nova Scotia, northwest Atlantic. J. Northwest Atl. Fish. Sci. 14:29–46.

Gill, C. A.
1928. The genesis of epidemics and the natural history of disease, 550 p. William Wood, New York, NY.

Glover, C. P., and S. M. Kidwell.
1993. Influence of organic matrix on the post-mortem destruction of molluscan shells. J. Geol. 101:729–747.

Godfray, H. C. J., and C. J. Briggs.
1995. The population dynamics of pathogens that control insect outbreaks. J. Theor. Biol. 176:125–136.
Gray, J. S.
1977. The stability of benthic ecosystems. Helgol. Wiss. Meeresunters. 30:427–444.
Hancock, D. A.
1973. The relationship between stock and recruitment in exploited invertebrates. Rapp. P.-V. Réun. Cons. Int. Explor. Mer 164:113–131.
Haskin, H. H., and J. D. Andrews.
1988. Uncertainties and speculations about the life cycle of the eastern oyster pathogen *Haplosporidium nelsoni* (MSX). Am. Fish. Soc. Spec. Publ. 18:5–22.
Haskin, H. H., and S. E. Ford.
1982. *Haplosporidium nelson* (MSX) on Delaware Bay seed oyster beds: a host-parasite relationship along a salinity gradient. J. Invertebr. Pathol. 40:388–405.
Hastings, A.
1991. Structured models of metapopulation dynamics. *In* Metapopulation dynamics: empirical and theoretical investigations (M. Gilpin, and I. Hanski. eds.). Biol. J. Linn. Soc. 42:57–71.
Heesterbeek, J. A. P., and H. G. Roberts.
1995. Mathematical models for microparasites of wildlife. *In* Ecology of infectious diseases in natural populations (B. T. Grenfell, and A. P. Dobson, eds.), p. 90–122. Cambridge Univ. Press, Cambridge, UK.
Hilborn, R.
2002. The dark side of reference points. Bull. Mar. Sci. 70:403–408.
Hilborn, R., and C. J. Walters.
1992. Quantitative fisheries stock assessment: choice, dynamics and uncertainty, 570 p. Chapman and Hall, New York, NY.
Hoenig, J. M.
1983. Empirical use of longevity data to estimate mortality rates. Fish. Bull. 83:898–903.
Hofmann, E. E., J. M. Klinck, J. N. Kraeuter, E. N. Powell, R. E. Grizzle, S. C. Buckner, and V. M. Bricelj.
2006. A population dynamics model of the hard clam, *Mercenaria mercenaria*: development of the age- and length-frequency structure of the population. J. Shellfish Res. 25:417–444.
Hofmann, E. E., E .N. Powell, E. A. Bochenek, and J. M. Klinck.
2004. A modelling study of the influence of environment and food supply on survival of *Crassostrea gigas* larvae. ICES J. Mar. Sci. 61:596–616.
Hofmann, E. E., E. N. Powell, J. M. Klinck, and G. Saunders.
1995. Modeling diseased oyster populations I. Modelling *Perkinsus marinus* infections in oysters. J. Shellfish Res. 14:121–151.
Hofstetter, R. P.
1983. Oyster population trends in Galveston Bay 1973–1978. Texas Parks and Wildl. Dept. Manag. Data Ser. 51, 33 p.
Honkoop, P. J. C., J. van der Meer, J. J. Beukema, and D. Kwast.
1998. Does temperature-influenced egg production predict the recruitment in the bivalve *Macoma balthica*? Mar. Ecol. Prog. Ser. 164:229–235.
Hughes, R. N.
1980. Optimal foraging theory in the marine context. Oceanogr. Mar. Biol. Annu. Rev. 18:423–481.
Imeson, R. J., J. C. J. M. van den Bergh, and J. Hoekstra.
2002. Integrated models of fisheries management and policy. Environ. Model. Assess. 7:259–271.
Jackson, J. B. C., M. X. Kirby, W. H. Berger, K. A. Bjorndal, L. W. Botsford, B. J. Bourque, R. H. Bradbury, R. Cooke, J. Erlandson, J. A. Estes, T. P. Hughes, S. Kidwell, C. B. Lange, H. S. Lenihan, J. M. Pandolfi, C. H. Peterson, R. S. Steneck, M. J. Tegner, and R. R. Warner.
2001. Historical overfishing and the recent collapse of coastal ecosystems. Science 293:629–637.
Jaenike, J.
1998. On the capacity of macroparasites to control insect populations. Am. Nat. 151:84–96.
Johnson, L.
1994. Pattern and process in ecological systems: a step in the development of a general ecological theory. Can. J. Fish. Aquat. Sci. 51:226–246.
Kermack, W. O., and A. G. McKendrick.
1991. Contributions to the mathematical theory of epidemics I. Bull. Math. Biol. 53:33–55.
Knowlton, N.
2004. Multiple "stable states" and the conservation of marine ecosystems. Prog. Oceanogr. 60:387–396.
Kraeuter, J. N., S. Buckner, and E. N. Powell.
2005. A note on a spawner–recruit relationship for a heavily exploited bivalve: the case of northern quahog (hard clams), *Mercenaria mercenaria*, in Great South Bay, New York. J. Shellfish Res. 24:1043–1052.
Kraeuter, J. N., J. M Klinck, E. N. Powell, E. E. Hofmann, S. C. Buckner, R. E. Grizzle, and V. M. Bricelj.
2008. Effects of the fishery on the hard clam (*Mercenaria mercenaria* (L.)) population in Great South Bay, New York: a modeling study. J. Shellfish Res. 27:653–666.
Link, J. S., J. K. T. Brodziak, S. F. Edwards, W. J. Overholtz, D. Mountain, J. W. Jossi, T. D. Smith, and M. J. Fogarty.
2002. Marine ecosystem assessment in a fisheries management context. Can. J. Fish. Aquat. Sci. 59:1429–1440.
Lipcius, R. N., and W. T. Stockhausen.
2002. Concurrent decline of the spawning stock, recruitment, larval abundance, and size of the blue crab *Callinectes sapidus* in Chesapeake Bay. Mar. Ecol. Prog. Ser. 226:45–61.
Livingston, R. J., F. G. Lewis, G. C. Woodsum, X.-F. Niu, B. Galperin, W. Huang, J. D. Christensen, M. E. Monaco, T. A. Battista, C. J. Klein, R. L. Howard IV, and G. L. Ray.
2000. Modelling oyster population response to variation in freshwater input. Estuar. Coast. Shelf Sci. 50:655–672.
Loosanoff, V. L.
1966. Time and intensity of setting of the oyster *Crassostrea virginica*, in Long Island Sound. Biol. Bull. (Woods Hole) 130:211–227.
MacKenzie Jr., C. L.
1996. History of oystering in the United States and Canada, featuring the eight greatest oyster estuaries. Mar. Fish. Rev. 58(4):1–78.
Mackin, J. G.
1953. Incidence of infection of oysters by *Dermocystidium* in the Barataria Bay area of Louisiana. Natl. Shellfish. Assoc. Conv. Add. for 1951, p. 22–35.
Mangel, M., B. Marinovic, C. Pomeroy, and D. Croll.
2002. Requiem for Ricker: unpacking *msy*. Bull. Mar. Sci. 70:763–781.
Mangel, M., and C. Tier.
1994. Four facts every conservation biologist should know about persistence. Ecology 75:607–614.

Mann, R., and D. A. Evans.
1998. Estimation of oyster, *Crassostrea virginica*, standing stock, larval production and advective loss in relation to observed recruitment in the James River, Virginia. J. Shellfish Res. 17:239–253.
2004. Site selection for oyster habitat rehabilitation in the Virginia portion of the Chesapeake Bay: a commentary. J. Shellfish Res. 23:41–49.

Mann, R., J. S. Rainer, and R. Morales-Alamo.
1994. Reproductive activity of oysters, *Crassostrea virginica* (Gmelin, 1791) in the James River, Virginia, during 1987–1988. J. Shellfish Res. 13:157–164.

Maunder, M. N.
2003. Is it time to discard the Schaefer model from the stock assessment scientist's toolbox. Fish. Res. 61:145–149.

Maurer, D., and L. Watling.
1973. The biology of the oyster community and its associated fauna in Delaware Bay. *In* Delaware Bay Report series vol. 6 (D. F. Polis, ed.), 97 p. College of Marine Studies, Univ. Delaware, Lewes, DE.

Maurer, D., L. Watling, and R. Keck.
1971. The Delaware oyster industry: a reality? Trans. Am. Fish. Soc. 100:100–111.

May, R. M., J. R. Beddington, J. W. Horwood, and J. G. Shepherd.
1978. Exploiting natural populations in an uncertain world. Math. Biosci. 42:219–252.

McCann, K. S., L. W. Botsford, and A. Hasting.
2003. Differential response of marine populations to climate forcing. Can. J. Fish. Aquat. Sci. 60:971–985.

McGarvey, R., F. M. Serchuk, and I. A. McLaren.
1993. Spatial and parent-age analysis of stock-recruitment in the Georges Bank sea scallop (*Placopecten magellanicus*) population. Can. J. Fish. Aquat. Sci. 50:564–574.

Milke, L. M., and V. S. Kennedy.
2001. Mud crabs (Xanthidae) in Chesapeake Bay: claw characteristics and predation on epifaunal bivalves. Invertebr. Biol. 120:67–77.

Moore, H. F.
1911. Condition and extent of the natural oyster beds of Delaware. U.S. Bur. Fish. 745:1–29.

Myers, R. A., and N. J. Barrowman.
1996. Is fish recruitment related to spawner abundance? Fish. Bull. 94:707–724.

Nixon, S. W., S. Granger, B. A. Buckley, M. Lamont, and B. Rowell.
2004. A one hundred and seventeen year coastal water temperature record from Woods Hole, Massachusetts. Estuaries 27:397–404.

Osman, R. W., R. B. Whitlatch, and R. N. Zajac.
1989. Effects of resident species on recruitment into a community: larval settlement versus post-settlement mortality in the oyster *Crassostrea virginica*. Mar. Ecol. Prog. Ser. 54:61–73.

Oviatt, C. A.
2004. The changing ecology of temperate coastal waters during a warming trend. Estuaries 27:895–904.

Paloheimo, J. E.
1980. Estimation of mortality rates in fish populations. Trans. Am. Fish. Soc. 109:378–386.

Paynter, K. T.
1996. The effects of *Perkinsus marinus* infection on physiological processes in the eastern oyster, *Crassostrea virginica*. J. Shellfish Res. 15:119–125.

Peterman, R. M.
1977. A simple mechanism that causes collapsing stability regions in exploited salmonid populations. J. Fish. Res. Board Can. 34:1130–1142.

Peterson, C. H.
1984. Does a rigorous criterion for environmental identity preclude the existence of multiple stable points? Am. Nat. 124:127–133.

Peterson, C. H., and R. Black.
1987. Resource depletion by active suspension feeders on tidal flats: influence of local density and tidal elevation. Limnol. Oceanogr. 32:145–166.

Peterson, C. H., F. J. Fodrie, H. C. Summerson, and S. P. Powers.
2001. Site-specific and density-dependent extinction of prey by schooling rays: generation of a population sink in top-quality habitat for bay scallops. Oecologia (Berl.) 129:349–356.

Peterson, C. H., and H. C. Summerson.
1992. Basin-scale coherence of population dynamics of an exploited marine invertebrate, the bay scallop: implications of recruitment limitation. Mar. Ecol. Prog. Ser. 90:257–272.

Pierce, G. J., and J. G. Ollason.
1987. Eight reasons why optimal foraging theory is a complete waste of time. Oikos 49:111–117.

Powell, E. N., K. A. Ashton-Alcox, S. E. Banta, and A. J. Bonner.
2001. Impact of repeated dredging on a Delaware Bay oyster reef. J. Shellfish Res. 20:961–975.

Powell, E. N., K. A. Ashton-Alcox, J. A. Dobarro, M. Cummings, and S. E. Banta.
2002a. The inherent efficiency of oyster dredges in survey mode. J. Shellfish Res. 21:691–695.

Powell, E. N., K. A. Ashton-Alcox, and J. N. Kraeuter.
2007. Reevaluation of eastern oyster dredge efficiency in survey mode: application in stock assessment. N. Am. J. Fish. Manag. 27:492–511.

Powell, E. N., K. A. Ashton-Alcox, J. N. Kraeuter, S. E. Ford, and D. Bushek.
2008. Long-term trends in oyster population dynamics in Delaware Bay: regime shifts and response to disease. J. Shellfish Res. 27:729–755.

Powell, E. N., E. A. Bochenek, J. M. Klinck, and E. E. Hofmann.
2002b. Influence of food quality and quantity on the growth and development of *Crassostrea gigas* larvae: a modeling approach. Aquaculture 210:89–117.
2004. Influence of short-term variations in food on survival of *Crassostrea gigas* larvae: a modeling study. J. Mar. Res. 62:117–152.

Powell, E. N., J. J. Gendek, and K. A. Ashton-Alcox.
2005. Fisherman choice and incidental catch: size frequency of oyster landings in the New Jersey oyster fishery. J. Shellfish Res. 24:469–476.

Powell, Eric N., John M. Klinck, K. A. Ashton-Alcox, and John N. Kraeuter.
2009. Multiple stable reference points in oyster populations: implications for reference point-based management. Fish. Bull. 107:133–147.

Powell, E. N., J. M. Klinck, S. E. Ford, E. E. Hofmann, and S. J. Jordan.
1999. Modeling the MSX parasite in Eastern oyster (*Crassostrea virginica*) populations. III. Regional application and the problem of transmission. J. Shellfish Res. 18:517–537.

Powell, E. N., J. M. Klinck, and E. E. Hofmann.
1996. Modeling diseased oyster populations. II. Trigger-

ing mechanisms for *Perkinsus marinus* epizootics. J. Shellfish Res. 15:141–165.

Powell, E. N., J. M. Klinck, E. E. Hofmann, and M. A. McManus.
2003. Influence of water allocation and freshwater inflow on oyster production: a hydrodynamic-oyster (*sic*) population model for Galveston Bay, Texas, USA. Environ. Manag. 31:100–121.

Powell, E. N., J. M. Klinck, E. E. Hofmann, and S. M. Ray.
1994. Modeling oyster populations. IV: rates of mortality, population crashes and management. Fish. Bull. 92:347–373.

Powell, E. N., J. M. Klinck, E. E. Hofmann, E. A. Wilson-Ormond, and M. S. Ellis.
1995. Modeling oyster populations. V. Declining phytoplankton stocks and the population dynamics of American oyster (*Crassostrea virginica*) populations. Fish. Res. 24:199–222.

Powell, E. N., R. J. Stanton Jr., D. Davies, and A. Logan.
1986. Effect of a large larval settlement and catastrophic mortality on the ecologic record of the community in the death assemblage. Estuar. Coast. Shelf Sci. 23:513–525.

Pyke, G. H.
1984. Optimal foraging theory: a critical review. Annu. Rev. Ecol. Syst. 15:523–575.

Ragone Calvo, L. M., R. L. Wetzel, and E. M. Burreson.
2001. Development and verification of a model for the population dynamics of the protistan parasite, *Perkinsus marinus*, within its host, the Eastern oyster, *Crassostrea virginica*, in Chesapeake Bay. J. Shellfish Res. 20:231–241.

Redner, S.
2001. A guide to first-passage processes, 312 p. Cambridge Univ. Press, Cambridge, U.K.

Restrepo, V. R., G. G. Thompson, P. M. Mace, W. K. Gabriel, L. L. Low, A. D. MacCall, R. D.Methot, J. E. Powers, B. L. Taylor, P. R. Wade, and J. F. Witzig.
1998. Technical guidance on the use of precautionary approaches to implementing National Standard 1 of the Magnuson/Stevens Fishery Conservation and Management Act. NOAA Tech. Memo. NMFS-F/SPO-31, 54 p.

Rheault, R. B., and M. A. Rice.
1996. Food-limited growth and condition index in the Eastern oyster, *Crassostrea virginica*. (Gmelin 1791), and the bay scallop, *Argopecten irradians irradians* (Lamarck 1819). J. Shellfish Res. 15:271–283.

Rice, J.
2001. Implications of variability on many time scales for scientific advice on sustainable management of living marine resources. Prog. Oceanogr. 49:189–209.

Rothschild, B. J.
2000. "Fish stocks and recruitment": the past thirty years. ICES J. Mar. Sci. 57:191–201.

Rothschild, B. J., C. Chen, and R. G. Lough.
2005. Managing fish stocks under climate uncertainty. ICES J. Mar. Sci. 62:1531–1541.

Rothschild, B. J., and A. J. Mullen.
1985. The information content of stock-and-recruitment data and non-parametric classification. J. Cons. Cons. Int. Explor. Mer 42:116–124.

Rothschild, B. J., and L. J. Shannon.
2004. Regime shifts and fishery management. Prog. Oceanogr. 60:397–402.

Sakuramoto, K.
2005. Does the Ricker or Beverton and Holt type of stock-recruitment relationship truly exist? Fish. Sci. 71:577–592.

Scavia, D., J. C. Field, D. F. Boesch, R. W. Buddemeier, V. Burkett, D. R. Cayan, M. Fogarty, M. A. Harwell, R. W. Howarth, C. Mason, D. J. Reed, T. C. Royer, A. H. Sallenger, and J. G. Titus.
2002. Climate change impacts on U.S. coastal and marine ecosystems. Estuaries 25:149–164.

Sissenwine, M. P.
1984. Why do fish populations vary? *In* Exploitation of marine communities (R. M. May, ed.), p. 59–94. Springer-Verlag, Berlin.

Sissenwine, M. P., and J. G. Shepherd.
1987. An alternative perspective on recruitment overfishing and biological reference points. Can. J. Fish. Aquat. Sci. 44:913–918.

Soniat, T. M., E. N. Powell, E. E. Hofmann, and J. M. Klinck.
1998. Understanding the success and failure of oyster populations: the importance of sampled variables and sample timing. J. Shellfish Res. 17:1149–1165.

Soniat, T. M., E. N. Powell, J. M. Klinck, and E. E. Hofmann.
In press. Understanding the success and failure of oyster populations: climatic cycles and *Perkinsus marinus*. Int. J. Earth Sci.

Southworth, M., and R. Mann.
1998. Oyster reef broodstock enhancement in the Great Wicomico River, Virginia. J. Shellfish Res. 17:1101–1114.
2004. Decadel scale changes in seasonal patterns of oyster recruitment in the Virginia sub estuaries of the Chesapeake Bay. J. Shellfish Res. 23:391–402.

Steele, J. H., and E. W. Henderson.
1984. Modeling long-term fluctuations in fish stocks. Science. 224:985–987.

Tamburri, M. N., R. K. Zimmer, and C. A. Zimmer.
2007. Mechanisms reconciling gregarious larval settlement with adult cannibalism. Ecol. Monogr. 77:255–268.

Vetter, E. F.
1987. Estimation of natural mortality in fish stocks: a review. Fish. Bull. 86:25–43.

Wallace, R. K., W. Hosking, and S. T. Szedlmayer.
1994. Fisheries management for fishermen: a manual for helping fishermen understand the federal management process. NOAA MASG P-94-012, 56 p.

Ware, D. M.
2000. Aquatic ecosystems: properties and models. *In* Fisheries oceanography: an integrative approach to fisheries ecology and management (P. J. Harrison, and T. R. Parsons, eds.), p. 163–194. Blackwell Science, Oxford, England.

Whitlatch, R. B., and R. W. Osman.
1994. A qualitative approach to manage shellfish populations: assessing the relative importance of trophic relationships between species. J. Shellfish Res. 13:229–242.

Wilson-Ormond, E. A., E. N. Powell, and S. M. Ray.
1997. Short-term and small-scale variation in food availability to natural oyster populations: food, flow and flux. Mar. Ecol. 18:1–34.

Multiple stable reference points in oyster populations: implications for reference point-based management

Eric N. Powell (contact author)[1]
John M. Klinck[2]
Kathryn A. Ashton-Alcox[1]
John N. Kraeuter[1]

Email address for contact author: eric@hsrl.rutgers.edu

[1] Haskin Shellfish Research Laboratory
Rutgers University
6959 Miller Ave.
Port Norris, New Jersey 08349

[2] Center for Coastal Physical Oceanography
Crittenton Hall
Old Dominion University
Norfolk, Virginia 23529

Abstract—In the second of two companion articles, a 54-year time series for the oyster population in the New Jersey waters of Delaware Bay is analyzed to examine how the presence of multiple stable states affects reference-point–based management. Multiple stable states are described by four types of reference points. Type I is the carrying capacity for the stable state: each has associated with it a type-II reference point wherein surplus production reaches a local maximum. Type-II reference points are separated by an intermediate surplus production low (type III). Two stable states establish a type-IV reference point, a point-of-no-return that impedes recovery to the higher stable state. The type-II to type-III differential in surplus production is a measure of the difficulty of rebuilding the population and the sensitivity of the population to collapse at high abundance. Surplus production projections show that the abundances defining the four types of reference points are relatively stable over a wide range of uncertainties in recruitment and mortality rates. The surplus production values associated with type-II and type-III reference points are much more uncertain. Thus, biomass goals are more easily established than fishing mortality rates for oyster populations.

Manuscript submitted 29 November 2007.
Manuscript accepted 9 September 2008.
Fish. Bull. 107:133–147 (2009).

The views and opinions expressed or implied in this article are those of the author and do not necessarily reflect the position of the National Marine Fisheries Service, NOAA.

All federal fisheries, and some state fisheries, are managed under biological reference-point guidelines under which a specific yearly allocation or quota is advised to constrain fishing mortality (e.g., Wallace et al.[1]). The biological reference-point approach for federal fisheries mandated by the Magnuson-Stevens Fishery Conservation and Management Act (Anonymous, 1996) requires management of fish populations at a biomass that provides maximum sustainable yield. In this system, sophisticated survey, analytical, and modeling procedures are used to identify selected biological reference points, such as the target biomass, B_{msy}, and the carrying capacity, K. Fishing mortality is then set in relation to reference point goals. Normally, B_{msy} is defined in relation to carrying capacity, the biomass present without fishing, where natural mortality balances recruitment (e.g., May et al., 1978; Johnson, 1994; Mangel and Tier, 1994; Rice, 2001). This stable point is characterized by a population for which most animals are adults, where natural mortality rates are low, and where recruitment is limited by compensatory processes such as resource limitation constraining fecundity. B_{msy} is most commonly defined as $\frac{K}{2}$, based on the well-known Schaefer model that stipulates the guiding premise that surplus production is highest at $\frac{K}{2}$ (Hilborn and Walters [1992]; see Restrepo et al. [1998] for more details on the federal management system).

The *raison d'être* for reference-point–based management is the development of equilibria between recruitment (and growth) and mortality at target host densities (the archetype being B_{msy}). Unfortunately, for managing oyster populations, obstacles exist in meeting this objective because oyster populations do not appear to be inherently equilibrious, particularly those subjected to MSX, a disease caused by the protozoan *Haplosporidium nelsoni*, or Dermo, a disease caused by the protozoan *Perkinsus marinus*. Time series of oyster abundance typically show wide interannual variations, mediated in no small measure by year-to-year differences in natural mortality rate, although overfishing has also been an important contributing agent (e.g., Mann et al., 1991; Rothschild et al., 1994; Burreson and Ragone Calvo, 1996; Ragone Calvo et al., 2001; Jordan et

[1] Wallace, R. K., W. Hosking, and S. T. Szedlmayer. 1994. Fisheries management for fishermen: A manual for helping fishermen understand the federal management process. NOAA MASG P-94-012, 56 p.

al., 2002; Powell et al., 2008). In the first of two companion contributions, we described the case for oyster populations in Delaware Bay. A 54-year time series documents two regime shifts, circa-1970 and circa-1985, with intervening and succeeding intervals having the attributes of alternate stable states (*sensu* Gray, 1977; Peterson, 1984; Knowlton, 2004). Within these periods are substantial population excursions produced by varying rates of recruitment and natural mortality, but the alternate stable states are demarcated by even larger excursions in abundance. Moreover, these periods of relative stability delineated by regime shifts are persistent and transcend a range of climatic conditions (Soniat et al., in press).

Population dynamics of the Delaware Bay oyster population is not solely a function of disease, but stable-point abundances are at least partially a byproduct of disease, and disease has played a role in regime shifts (Powell et al., 2008). The classic view of carrying capacity fails when disease accounts for a substantial fraction of natural mortality and this compromises an estimate of B_{msy}. Some have attempted to redefine carrying capacity in diseased populations in relation to the abundance (population density in classic disease models, e.g., Kermack and McKendrick [1991], Hethcote and van den Driessche [1995]) at which each diseased animal will produce, in its lifetime, a single infection event (e.g., Heesterbeek and Roberts, 1995; Swinton and Anderson, 1995). This abundance is always below, usually well below, the original K. When abundance rises above this level, the influence of disease increases, as does the chance of epizootic mortality. This increase restrains population abundance below the predisease K (e.g., Kermack and McKendrick, 1991; Hasiboder et al., 1992; Godfray and Briggs, 1995; Frank, 1996). This approach is not well tailored to diseases such as MSX and Dermo for which environment is a potent modulator of effect and in which rapid transmission rates are not requiring of host-to-host contact. Furthermore, the existence of multiple apparently stable states and regime shifts imply that the standard Schaefer model, from which such basic biological references points as B_{msy} are derived, also does not provide the appropriate framework for managing oyster populations because this model has only a single stable state.

These ratiocinations lead to three salient questions pertinent to developing management goals for oyster stocks: 1) Can reference points be defined that consistently permit fishing without jeopardizing the sustainability of the stock? 2) Must management goals be set within the context of each of several multiple stable states? 3) How does regime change affect the usefulness of reference points and can management goals be set to increase the probability of regime shift to a preferred stable state? In this contribution, we use the case of the Delaware Bay oyster stock in New Jersey waters to examine these questions. In a companion contribution, we describe the long-term survey time series and the relationships of broodstock abundance with recruitment and mortality (Powell et al., 2009). In this contribution, we develop a surplus production model to relate these relationships with stock performance over a range of abundances. Following discussion of the results of simulations with this model, we consider the basis for an *MSY*-based management system for oyster populations and the implications of multiple stable states in the decision-making process.

Table 1

The bed groups (by location: upbay and downbay) and subgroups (by mortality rate) for the eastern oyster (*Crassostrea virginica*) collected on twenty beds in Delaware Bay, as shown in Figure 1. Mortality rate divides each of the primary groups, themselves being divided by location, a surrogate for upbay-downbay variations in dredge efficiency and fishery-area management regulations.

Bed group/subgroup	Bed name
Upbay group	
Low mortality	Round Island, Upper Arnolds, Arnolds
Medium mortality	Upper Middle, Middle, Sea Breeze, Cohansey, Ship John
Downbay group	
Medium mortality	Shell Rock
High mortality	Bennies Sand, Bennies, New Beds, Hog Shoal, Hawk's Nest, Strawberry, Vexton, Ledge, Egg Island, Nantuxent Point, Beadons

Model formulations and statistics

Powell et al. (2008, 2009) have provided an overview of the oyster populations in Delaware Bay during the 1953–2006 time period. Analyses of the Delaware Bay oyster resource of New Jersey routinely reveal a division between the upbay group of eight beds (Round Island, Upper Arnolds, Arnolds, Upper Middle, Middle, Sea Breeze, Cohansey, and Ship John [Fig. 1]) and the downbay group of twelve beds (Shell Rock, Bennies Sand, Bennies, New Beds, Nantuxent Point, Hog Shoal, Hawk's Nest, Strawberry, Vexton, Beadons, Egg Island, and Ledge). Salinity, natural mortality rate, and growth rate are higher downbay. Dredge efficiencies are significantly higher downbay (Powell et al., 2002, 2007). Both regions can be subdivided on the basis of natural mortality rate and productivity. In the upbay group, natural mortality rates and growth rates are significantly lower for the upper three beds, Round Island, Upper Arnolds and Arnolds, than for the remaining beds. Henceforth these two groups will be termed the low-mortality and medium-mortality beds (Table 1). In the downbay group, growth rates and mortality rates are lower for Shell Rock, leading to its designation as a medium-mortality bed; the reminder are high-mortality beds (Table 1).

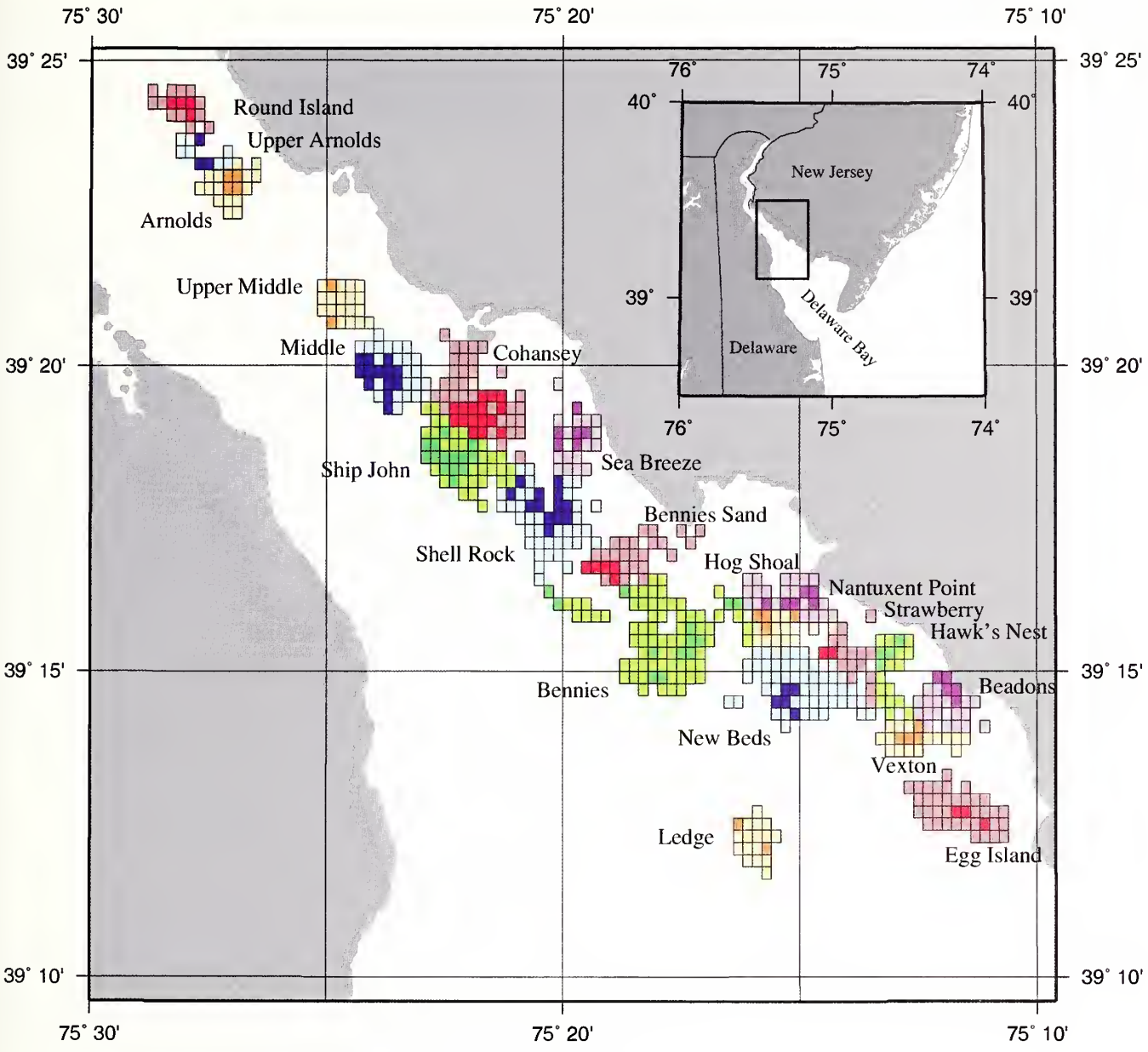

Figure 1

The twenty natural oyster beds of the eastern oyster (*Crassostrea virginica*) in the New Jersey waters of Delaware Bay may be characterized in terms of high-quality (dark shade) and medium-quality (light shade) grids. The term "quality" refers to a relative differential in long-term average oyster abundance (Powell et al, 2008). The footprints for the Middle bed (upper portion of figure) and the beds downbay from it, exceptNew Beds, Egg Island, and Ledge, were updated with data from surveys in 2005 and 2006. The footprints for the remaining beds were based on historical definitions.

Throughout this contribution, we will refer to these bay regions where necessary, but in general, we will model the entire stock. In the following section, we summarize the biological relationships identified by Powell et al. (2009) without further discussion.

Natural mortality fractions were obtained from box counts (*bc*) under the assumption that

$$N_{oysters_{t-1}} = N_{boxes_t} + N_{live\,oysters_t}, \quad (1)$$

where N = the number of individuals.

Hence,

$$\Phi_{bc} = \frac{N_{boxes_t}}{N_{boxes_t} + N_{live\,oysters_t}}, \quad (2)$$

where Φ_{bc} = the fraction of the individuals alive at the end of year t that died during the next year.

The fraction dead determined from box counts is related to the natural mortality rate m_{bc} as

$$m_{bc} = -\frac{\log_e(1-\Phi_{bc})}{t}, \quad 3)$$

where t = time.

Boxes do not adequately measure the mortality of juvenile animals. The fraction dying not recorded by box counts, Φ_0, is obtained by difference:

$$\Phi_0 = \frac{(N_t - N_{t-1}) - (R_{t-1} - \Phi_{bc}N_{t-1} - \Phi_f N_{t-1})}{N_{t-1} + R_{t-1}}, \quad (4)$$

where Φ_f = the fraction taken by the fishery;
R = the number of recruits into the population; and the first parenthetical term on the right-hand side represents the difference in abundance between two consecutive surveys.

The two natural mortality rates, m_{bc} (Eq. 3) and m_0 (Eq. 5), are additive (*sensu* Hassell et al., 1982; Holmes, 1982), as the method for estimation includes the box counts as an input (Eq. 2) in contrast to fishing mortality that can be compensatory under certain fishing season scenarios (Klinck et al., 2001). Φ_0 varied randomly over the time series with a 54-year mean of 0.274 and a 54-year median of 0.311 (Powell et al., 2008). The mortality rate can be obtained from Φ_0 as

$$m_0 = -\frac{\log_e(1-\Phi_0)}{t}. \quad (5)$$

Fishing mortality was calculated as the fraction of the population present at the beginning of the year removed during that year by the fishery (*catch*):

$$\Phi_f = \frac{catch_t}{N_{t-1}}. \quad (6)$$

Additional mortality associated with the dredging process may occur; however, Powell et al. (2001, 2004) determined that this source of mortality was inconsequential in comparison to the catch. Since the late 1950s, the fishery has rarely removed more than 7% of the stock annually, and normally much less, so that the yearly changes in stock abundance in Delaware Bay have been dominantly a product of natural processes over much of the time series (Powell et al., 2008).

A crude estimate of age-frequency pattern was obtained by assuming equilibrium conditions. Yearlings, Y, were estimated from recruits (spat), R, based on observed one-year survivals of recruits between 1953 and 1988 when yearlings were recorded as part of the survey. The yearling-to-spat ratio followed a weakly nonrandom pattern (Fig. 2) that provides a relationship between recruits and yearlings described by

$$Y_{t+1} = 0.434e^{-3.659\times10^{-11}N_t}R_t. \quad (7)$$

Older age groups were modeled by assuming equivalent mortality across all ages. Thus, the number at age a is estimated as

$$N_a = Y e^{-a(m_o+m_{bc})}, \quad (8)$$

where m_0 and m_{bc} are from Equations 5 and 3, respectively.

To model the relationship between broodstock abundance and recruitment, we fit a relationship that produces declining recruitment at high abundance (overcompensation *sensu* Hancock, 1973; McCann et al., 2003), because shellfish can achieve densities sufficient to limit growth and reproduction (e.g., Fréchette and Bourget, 1985; Fréchette and Lefaivre, 1990; Powell et al., 1995). Thus, from Hilborn and Walters (1992)

$$\tilde{R} = \tilde{N}_{t-1}e^{-a\left(1+\frac{\tilde{N}_{t-1}}{\beta}\right)}, \quad (9)$$

where $\tilde{R}$ = the number of spat in millions; and
$\tilde{N}_{t-1}$ = oyster abundance in millions.

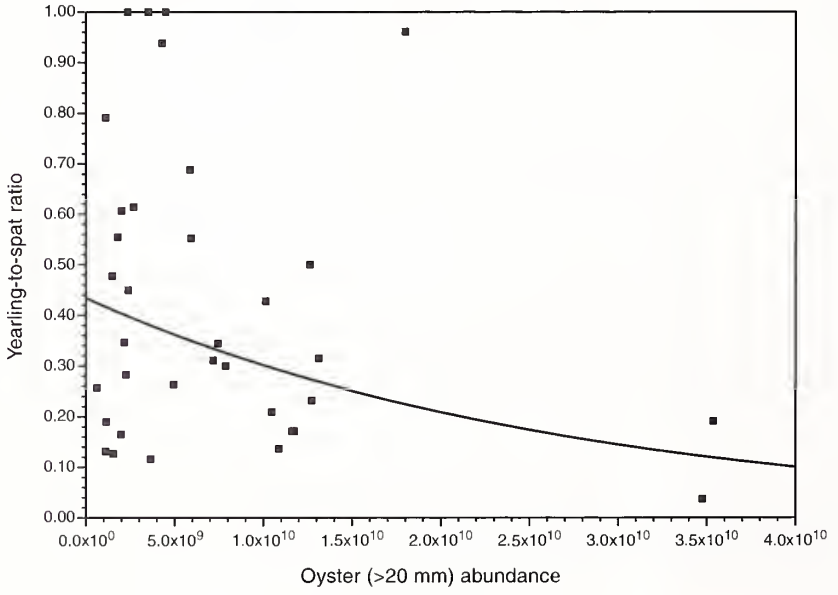

Figure 2

The relationship of yearling abundance to spat in the previous year as a function of population abundance for 1953–88. Line was fitted by following Equation 7.

The recruitment rate $\Gamma_t(\tilde{N}_{t-1})$ is calculated as

$$\Gamma_t(\tilde{N}_{t-1}) = \frac{\log_e\left(1+e^{-a\left(1+\frac{\tilde{N}_{t-1}}{\beta}\right)}\right)}{t}. \quad (10)$$

We compared the results of Equation 10 to that obtained for a best-fit linear regression with zero intercept. The linear relationship is

$$R_t = 0.493N_{t-1}. \quad (11)$$

Note that the linear fit travels through the recruitment values at low abundance slightly below that traversed by the Ricker curve (Fig. 8 in Powell et al., 2009). Powell et al. (2009) provide caveats concerning the use of a single broodstock–recruitment curve for the population over the entire 54-yr time series. The dispersion of the stock over the four bay regions exerts limitations on the ambit of stock performance at any specific time.

Powell et al. (2009) develop an admittedly *ad hoc* empirical relationship to describe the relationship between box-count mortality and abundance:

$$\Phi_{bc_t} = \omega + \kappa \log_e\left(\tilde{N}_{t-1}+\rho\right) - \varphi\tilde{N}_{t-1} + \chi\tilde{N}_{t-1}e^{\left(-\frac{\left(\tilde{N}_{t-1}-\psi\right)^2}{2\upsilon^2}\right)}, \quad (12)$$

where ω=0.055, κ=0.03, ρ=1.0, φ=0.0025, χ=0.1, ψ=2.2, and υ=0.8, with $\tilde{N}$ expressed as billions of animals.

The specific mortality rate, $m_{bc}(N)$, is calculated with Equation 3. Equation 12 has the unique property of eliciting both depensatory and compensatory trends at low abundance. Powell et al. (2009) provide caveats concerning the use of the broodstock–mortality curve. The dispersion of the stock over the four bay regions exerts limitations on the ambit of stock performance at any specific time. At abundances greater than 4×10^9, mortality was low. The fraction dying each year averaged 9.6 % for these nonepizootic years, a nonepizootic year being defined for convenience as a year in which the fraction dying is less than 20%. However, of the 32 years with abundances less than 3×10^9, of which 14 were epizootic years, only one had a fractional mortality between 0.15 and 0.20. Accordingly, two divergent outcomes exist over a range of low abundances. In some years, the fraction dying approximates the long-term mean for high-abundance years, about 9.6%. In other years, epizootic mortalities occur. The likelihood of these two divergent outcomes is substantively affected by the dispersion of the stock (Powell et al., 2009).

Surplus production S is calculated as the difference between additions to the population through recruitment and debits through mortality. The two processes are structurally uncoupled in time, however. First, mortality occurs differentially in time in relation to recruitment. Second, the method of data collection results in a time-integrated value of mortality, but a year ending value for recruitment, inasmuch as the death of recruits between settlement and the time of observation is not recognized as a component of the mortality term (see Keough and Downes, 1982; Powell et al., 1984; Caffey, 1985). Consequently, in the absence of fishing,

$$S_t = N_{t-1}\left(e^{\Gamma t}t-1\right) - N_{t-1}\left(1-e^{-\left(m_{bc_t}+m_{0_t}\right)t}\right), \quad (13)$$

which reduces to the familiar equation

$$S_t = N_{t-1}e^{-\left(m_{bc_t}+m_{0_t}\right)t} + R_t, \quad (14)$$

where t = the time increment between observations of recruitment.

Note that the subscript t–1 is used for the stock abundance value N because the stock survey occurs at the end of the year preceding the year for which surplus production is forecast and for which recruitment is measured.

Modeling of population dynamics—results of simulations and discussion

In the absence of fishing, the population increases when surplus production S_t is positive (Eq. 14). The population decreases when S_t is negative. Abundances where S_t is zero offer potential biological reference points, as do cases where S_t is maximal. Carrying capacity is an example of the former. In this case, mortality and recruitment balance and S_t=0. Surplus production declines as abundance nears carrying capacity and, therefore, the rate of change should be negative, but relatively constant; thus, $\frac{dS}{dN}<0$ and $\frac{d^2S}{dN^2}\sim0$. We will refer to reference points characterized by S_t=0, $\frac{dS}{dN}<0$ and $\frac{d^2S}{dN^2}\sim0$ as type-I reference points (Fig. 3). B_{msy} is defined to be a maximum in surplus production. Surplus production declines as abundance declines below or rises above this point. Hence, $S_t>0$, $\frac{dS}{dN}=0$ and $\frac{d^2S}{dN^2}<0$. We will refer to maxima in surplus production as type-II reference points (Fig. 3). Because the time series under analysis is configured in terms of abundance rather than biomass, the designation N_{msy}, rather than B_{msy}, will be used hereafter.

We present hereafter a series of simulations of the Delaware Bay oyster stock designed to examine the change in surplus production with abundance. We first consider a population for which recruitment rate follows Equation 9, a compensatory curve, with a 54-yr average unrecorded mortality rate (Eq. 5), and with the box-count mortality rate described by Equation 12.

These relationships are depicted in Figures 7 and 10 of Powell et al. (2009). The trajectory for surplus production under these constraints is compared in Figure 3 and detailed in Figure 4. Recruitment rate rises as abundance declines (Fig. 4). This is anticipated from the compensation inherent in the relationship between broodstock and recruitment. The box-count mortality rate shows a maximum somewhat above an abundance of 2×10^9 (Fig. 4). These relationships define a trend between surplus production and abundance that is divergent from the normal Schaefer curve (Ricker, 1975; Hilborn and Walters, 1992; Haddon, 2001; Zabel, 2003), as expected. The single type-I reference point is at $N=9.3\times10^9$. This is an estimate of carrying capacity, K. Typically a single type-II reference point would exist, N_{msy}, at about $\frac{K}{2}$, but in this case two maxima in surplus production exist, one higher, N^H_{msy}, than the other, N^L_{msy}. N^H_{msy} is at $N=4.86\times10^9$. This is the abundance classically interpreted as N_{msy}, and, indeed, surplus production is maximal at this point and the value is approximately $\frac{K}{2}$. The second type-II reference point occurs at $N=1.43\times10^9$. Unlike the simple Schaefer curve depicted in Hilborn and Walters (1992), Haddon (2001), and Zabel (2003), a local minimum in surplus production exists between these two type-II surplus production maxima, at $N=2.57\times10^9$. In this case, surplus production remains above zero, $S_t>0$. An increase in abundance above this level and a decrease in abundance below this level both increase surplus production. This reference point, herein designated type III, always occurs between two maxima in surplus production and is characterized by $\frac{dS}{dN}=0$ and $\frac{d^2S}{dN^2}>0$ (Table 2). The unusual nature of the surplus production curve in Figure 4, that yields the local minimum in surplus production and a secondary surplus production peak at a lower abundance, is produced by the depensatory and compensatory segments of the box-count mortality relationship established by the relationship between the occurrence of epizootics and abundance in the Delaware Bay oyster stock.

Figures 5–7 show three alternative trajectories for the change in surplus production with abundance in the Delaware Bay oyster stock obtained by small modifications of the parameters governing recruitment and mortality. The first is obtained by using the 54-yr median unrecorded mortality rate, rather than the 54-yr mean rate. The median is distinctly higher. Again, the surplus production trajectory includes one type-I, two type-II, and one type-III reference points (Figs. 3 and 5). The abundance associated with the four reference points remains unchanged, although the surplus production values associated with the type-II maxima and type-III minimum are lower than in the preceding case (Table 2).

The second alternative is obtained after a perusal of Figure 10 in Powell et al. (2009) that shows that the mortality rate for stock abundances frequented by epizootics often falls below the curve provided by Equation 12. This is a function of stock dispersion that modulates the likelihood of epizootic mortality rates (Powell et al., 2009). In fact, on the average, box-count mortality rate reaches epizootic levels only half the time. Thus, Figures 3 and 6 show the trend in surplus production when epizootics are assumed to occur only half the time, and box-count mortality rate is expressed as the average of a year with an epizootic and a year without one. The type-III reference point is nearer the N^L_{msy} value in this surplus production trajectory, so that the valley between N^L_{msy} and N^H_{msy} is something more than a shoulder on the surplus production curve. Thus, the value of the surplus production maxima, averaged over a number of years, is strongly influenced by the frequency and intensity of epizootics (Table 2).

The final alternative addresses the uncertainty that exists in the shape of the broodstock–recruitment curve at low abundance. Linearizing the curve at low abundance (Eq. 11) yields a surplus production trajectory depicted in Figure 8 of Powell et al. (2009). The relationship is unique in generating a second type-I reference

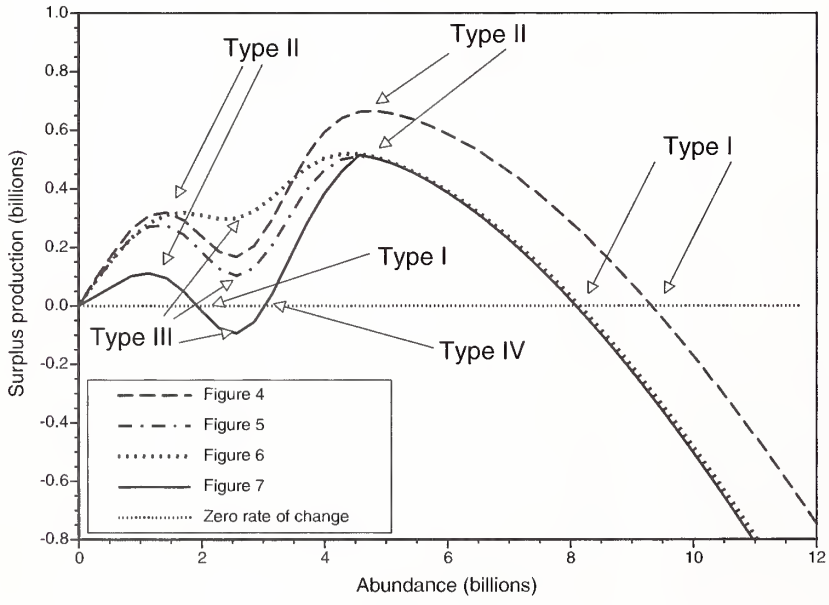

Figure 3

The trajectories of surplus production for cases detailed in Figures 4–7, with the locations of the four types of reference point indicated. Note that a type-IV reference point and two type-I reference points exist in only one case, Figure 7.

point, at $N=1.93\times10^9$. This is a multiple-stable-point system with two carrying capacities, one at K^H and one at K^L. Note that the lower surplus production maximum is closer to K^L than expected by the Schaefer relationship: $N^L_{msy}>\frac{K}{2}$ (Fig. 7). This representation of oyster population dynamics also generates a type-IV reference point at $N=3.03\times10^9$. Type IV, like type I, is characterized by $S_t=0$ and $\frac{d^2S}{dN^2}\sim 0$, but in this case $\frac{dS}{dN}>0$ (Table 2). Figure 8 presents a stylized version of the surplus production trajectory of Figure 7. Note that the type-I reference points are points of convergence. Abundance rising above this value will produce negative surplus production and a return to the abundance level and vice versa for a decline in abundance. On the other hand, type-IV reference points are divergences or points of population instability. They mark thresholds for population collapse. The divergence that is the type-IV reference point is maintained by the competing rates of box-count mortality and recruitment that switch in dominance at this point (Fig. 8). A population reaching a type-IV reference point as abundance declines will see a rapid further decline. Once below this point, the likelihood becomes very low that the population can cross the gulf and re-acquire its high-abundance trajectory.

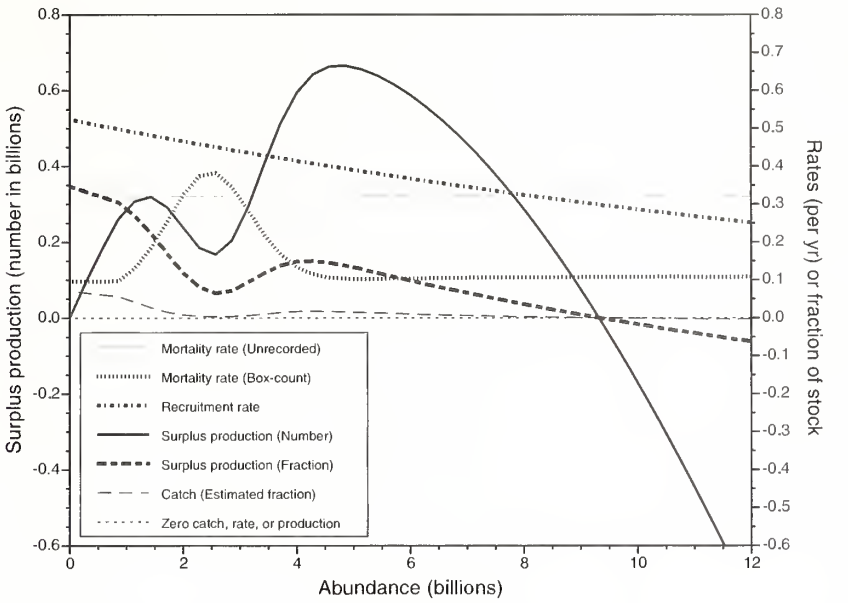

Figure 4

The relationship of surplus production (Eq. 14), the rates of recruitment, unrecorded mortality, box-count mortality, and a conditional estimate of catch expressed as the fraction of the stock, for parameters defined by, for recruitment, Γ_t from Equation 10, m_0 from Equation 5 using the 54-year average Φ_0, and m_{bc} from Equation 12. This simulation assumes compensation in the broodstock–recruitment curve, average unrecorded (mostly juvenile) mortality, and a box-count mortality rate that emphasizes epizootic mortality at low abundance. Catch estimates are conditional on the assumption of long-term persistence of a chosen abundance level and distribution of the entire stock in habitats permitting growth to market size.

Reference-point–based management

Carrying capacity Perusal of the time series suggests that population abundances above about 12×10^9 are unstable. The analyses provided using Equation 14 return this same expectation, that carrying capacity is about 9.3×10^9. This explains the stability of population abundance during the 1970s as the population was at or near carrying capacity (Fig. 9). Abundance rose above this point a number of times between 1970 and 1985, but higher abundances were not sustainable. Interestingly, this carrying capacity is a carrying capacity for a population enzootic for MSX disease. The natural mortality rate during the 1970s is not much different from the few measures that exist for the time frame pre-1957 and the pre-MSX years are not outliers on the broodstock-recruitment diagram. So, MSX was not a significant agent of mortality during this period. Hence, predisease carrying capacity for which no empirical quantitative record exists is likely to have been similar to abundances during the 1970s, with the observed dif-

Table 2

The surplus production values associated with the types I, II, III, and where applicable, IV reference points depicted in the referenced figures and the defining characteristics of each reference point type. Surplus production is expressed in billions of oysters. NA=not applicable.

Figure number	Type I Carrying capacity (K)	Type II N^H_{msy}	Type III S_{min}	Type II N^L_{msy}	Type IV Point of no return
Surplus production					
4	0.0	0.665	0.167	0.319	NA
5	0.0	0.511	0.103	0.275	NA
6	0.0	0.519	0.297	0.318	NA
7	0.0	0.511	−0.094	0.112	0.0
			S	$\frac{dS}{dN}$	$\frac{d^2S}{dN^2}$
Defining characteristics					
Type I			=0	<0	~0
Type II			>0	=0	<0
Type III			>0 or <0	=0	>0
Type IV			=0	>0	~0

ferential in abundance in the 1950s primarily a result of the higher fishing mortality rates during that time.

Carrying capacity is defined by a set of criteria that are normally thought to be unique (Table 2). Interestingly, in Delaware Bay oyster populations, a second type-I reference point may exist, depending on the presence of a reference point of type IV, as considered subsequently. This type-I reference point, if present, is at 1.93×10^9, nearly a factor of 5 lower in abundance than the classic carrying capacity. However, this value is also similar to the abundance observed during the low-abundance phase of the population (Fig. 9), an outcome anticipated of a population with multiple stable points (Gray, 1977; Peterson, 1984) in which community compositions are theorized to resolve themselves into preferred states that can be exchanged only through triggering mechanisms capable of overcoming the inertia of the individual states. Soniat et al. (1998) argued that inertia is an important attribute of oyster population dynamics and that this inertia minimizes the influence of short-term environmental shifts. The 54-year time series of Delaware Bay supports the importance of inertia and suggests some reasons for how population dynamics are internally stabilized.

Both recruitment and mortality have abundance-dependent rates. The high-abundance regime is inherently stable. Mean first passage times (*sensu* Rothschild and Mullen, 1985; Redner, 2001; Rothschild et al., 2005) for transitions to the alternate stable state typically exceed 6 yr (Powell et al., 2009). Given a population at high abundance: that population will tend to maintain itself because high abundance, on the average, generates higher recruitment, and also, on the average, is associated with lower rates of natural mortality. Thus, high abundances have a strong internal self-sustaining mechanism. However, the 1970–85 period occurred prior to the onset of Dermo disease in Delaware Bay. Whether a high abundance state is sustainable under any environmental conditions with Dermo as the principal agent of mortality is unknown.

The low-abundance regime is stable only if the surplus production minimum separating the two maxima is negative. The differential between the two carrying capacities, K^H and K^L, is a factor of 4.82. Powell et al. (2009) discuss the tendency for the Delaware Bay oyster population to contract to a habitat of refuge on the medium-mortality beds (Table 1) as abundance falls. This occurs due to the gradient in natural mortality that increasingly penalizes the population downestuary. The differential in bed area between the entire bay and the medium-mortality beds is a factor of 2.46 excluding the two lowermost and least productive beds, Egg Island and Ledge, or 2.70 including them. Thus, habitat area, though likely a contributor to the differential in the two carrying capacities, does not explain adequately the differential between K^L and K^H, and this agrees with the observation (Figure 5 in Powell et al., 2009) that contracted and dispersed population distributions both prevailed for extended periods during the low-abundance regime.

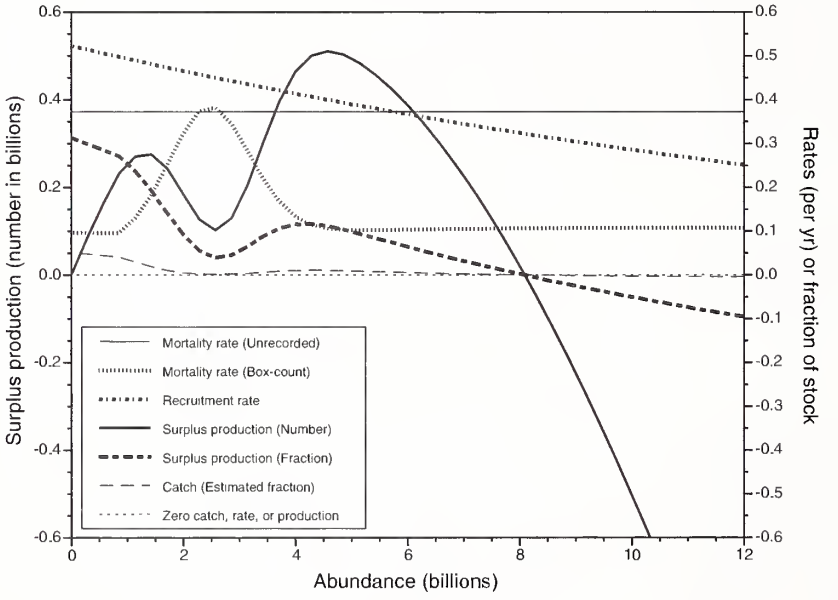

Figure 5

The relationship of surplus production (Eq. 14), the rates of recruitment, unrecorded mortality, and box-count mortality, and a conditional estimate of catch expressed as the fraction of the stock, for parameters defined by, for recruitment, Γ_t from Equation 10, m_0 from Equation 5 using the 54-year median Φ_0, and m_{bc} from Equation 12. This simulation assumes compensation in the broodstock–recruitment curve, median unrecorded (mostly juvenile) mortality, and a box-count mortality rate that emphasizes epizootic mortality at low abundance. This simulation differs from the simulation in Figure 4 in a higher level of unrecorded mortality. Catch estimates are conditional on the assumption of long-term persistence of a chosen abundance level and distribution of the entire stock in habitats permitting growth to market size.

Surplus production targets Beverton et al. (1984) distinguish between short-term catch forecasts used to generate a yearly TAL and long-term strategic assessments used to set abundance goals. The constant-abundance reference point implemented with the model of Klinck et al. (2001) is particularly useful in maintaining a population close to an abundance target and has been used for short-term catch forecasts but does not lend itself to long-term strategic assessments. The purpose of this study was to develop reference points that might be used to set abundance goals.

Four types of reference points are elucidated. Each of them marks critical spots in the ambit of oyster population dynamics that must be included in a successful management plan. If the oyster population in Delaware Bay has two distinct regimes, minimally, two sets of reference points exist. It is a critical corollary of the multiple-stable-state theorem that such should be the case. Modern fisheries management scientists, although cognizant of the importance of regime shifts, have not yet inculcated the concept of multiple stable states into management philosophy and, consequently, continue to focus solely on the highest abundance state.

Maximum sustainable yield generally is considered to occur at half carrying capacity. For the high-abundance regime, N^H_{msy} occurs at almost precisely $\frac{K^H}{2}$ (Figs. 3–7), as expected from standard fisheries theory (Haddon, 2001; Zabel et al., 2003). For the low-abundance regime, N^L_{msy} occurs at a value distinctly above $\frac{K^L}{2}$; thus the lower surplus production dome is distinctly skewed. Some portion of this skewness may be inadequate extrapolation of the population dynamics to abundances below 0.8×10^9 that have not yet been observed. Either N^H_{msy} or N^L_{msy} might be chosen as abundance goals. N^H_{msy} yields the highest surplus production and, consequently, the highest fishery yield, and, all else being equal, would be the desirable goal for rebuilding oyster abundance above present-day levels. Over the 54-year time series for Delaware Bay, the abundance level has been near carrying capacity for about one-third of the years and well below N^H_{msy} for most of the remaining years (Fig. 9). Thus, historical observations provide credence for the viability of this abundance goal.

However, an alternative exists, N^L_{msy}. This second type-II reference point exists at lower abundance and maximizes fishery yield in the low-abundance regime (Fig. 9). The population has been near this level for about two-thirds of the years since 1953 and, for most of this time, this population dynamic has been little influenced by fishing mortality. Thus, a substantive choice exists in managing the Delaware Bay oyster stock. Is it a viable choice to seek through management to transition the population to the high-abundance state and thereby rebuild the population to the higher N^H_{msy} target?

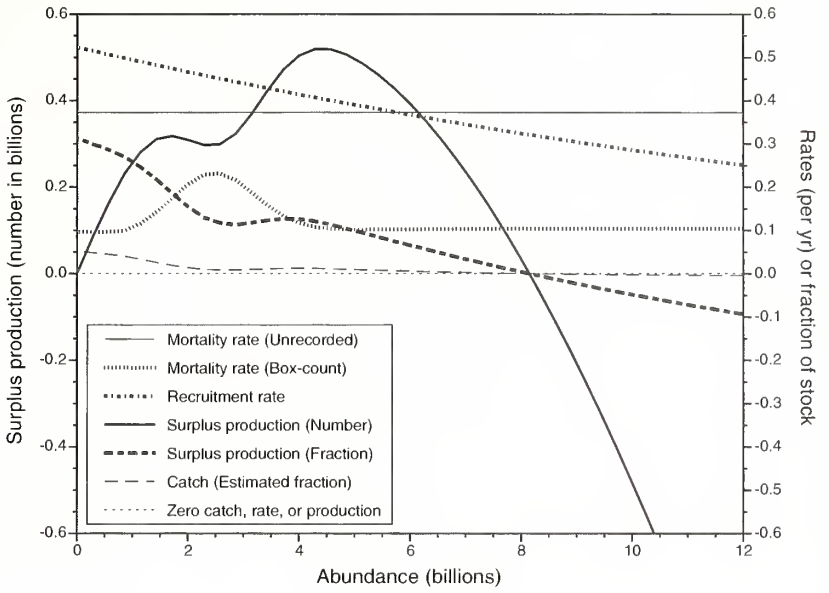

Figure 6

The relationship of surplus production (Eq. 14), the rates of recruitment, unrecorded mortality, and box-count mortality, and a conditional estimate of catch expressed as the fraction of the stock, for parameters defined by, for recruitment, Γ_t from Equation 10, m_0 from Equation 5 using the 54-year median Φ_0, and m_{bc} from Equation 12. This simulation assumes compensation in the broodstock–recruitment curve, median unrecorded (mostly juvenile) mortality, but a box-count mortality rate that de-emphasizes epizootic mortality at low abundance. Epizootics are assumed to occur in half of the years when abundance is in the correct range, in comparison to the simulations shown in Figures 4 and 5. Surplus production as plotted is the average of an epizootic and a nonepizootic year. Catch estimates are conditional on the assumption of long-term persistence of a chosen abundance level and distribution of the entire stock in habitats permitting growth to market size.

The impact of type-III and type-IV reference points

The two other reference points become important at this juncture. The type-III reference point describes the valley between the two surplus production maxima. If negative, two stable states exist, associated with the lower and higher maxima in surplus production (e.g., Fig. 7). If positive, one stable state exists. The other lower maximum in surplus production is a quasi-stable state (e.g., Figs. 4–6). Surrounding the surplus production minimum is a region in which unwise harvest goals could create a region of negative surplus production and establish through overharvesting the second and lower stable state. Thus, this reference point is a measure of the relative degree of impedance present in the population dynamics to transiting to the higher stable state. This impedence exists naturally and is a rebuilding obstacle for management. This impedance can be deepened by inappropriate harvest goals.

If the minimum in surplus production is below zero, the type-IV reference point above it marks the thresh-

old for population collapse or the point-of-no-return abundance (e.g., Collie et al., 2004) below which the population is unlikely to regain the higher abundance state (Fig. 8). It is the critical point generating the regime shift from high abundance to low abundance. That is, once abundance drops to this point, abundance will resolutely fall to the lower carrying capacity and the population subsequently will resist the reverse course even in the absence of fishing (Fig. 8). Once crossed, no anthropogenic manipulation short of Herculean measures to enhance abundance will allow the population to recover. In the years succeeding the 1985 MSX epizootic, population abundance increased to levels representative of the type-III and type-IV reference points a number of times, falling back below these barriers in one to two years (Fig. 9). Two occurrences are noteworthy, one during 1987–89 before the onset of Dermo and one during 1996–98 after Dermo replaced MSX as the dominant disease agent causing mortality. In both cases, the population failed to successfully cross the type-IV barrier. In neither case was fishing responsible for this failure.

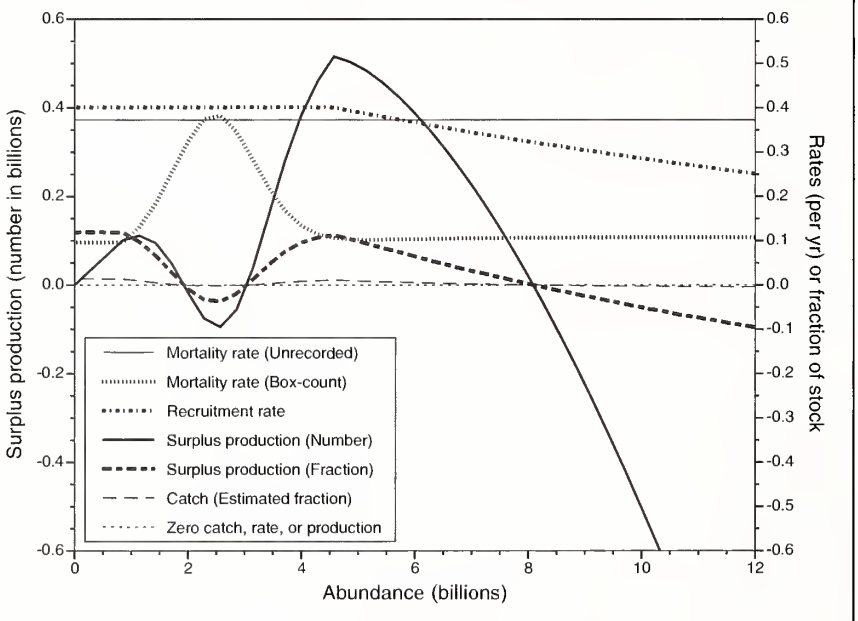

Figure 7

The relationship of surplus production (Eq. 14), the rates of recruitment, unrecorded mortality, and box-count mortality, and a conditional estimate of catch expressed as the fraction of the stock, for parameters defined by, for recruitment, Γ_t from Equation 10 above $N=4.5\times10^9$ and Γ_t from Equation 11 at lower abundance, m_0 from Equation 5 using the 54-year median Φ_0, and m_{bc} from Equation 12. This simulation assumes a linear relationship between broodstock abundance and recruitment at low abundance, median unrecorded (mostly juvenile) mortality, and a box-count mortality rate that emphasizes epizootic mortality at low abundance. In comparison to simulations depicted in Figures 4–6, this simulation has a combination of relatively high natural mortality and relatively low recruitment. Catch estimates are conditional on the assumption of long-term persistence of a chosen abundance level and distribution of the entire stock in habitats permitting growth to market size.

Uncertainty in the natural mortality rate presents a critical impediment to successful stock assessment (e.g., Beverton et al., 1984; Clark, 1999; Bradbury and Tagart, 2000). The population trajectories shown in Figures 3–7 differ principally in the degree and type of uncertainty in mortality and that controls the amplitude of the surplus production excursion between the lower type-II and upper type-II points, as well as the existence of a type-IV reference point. The rarity of regime shifts in the observed time series, the observed stability of the stable states, and the long mean first passage times for some population shifts (Powell et al., 2009) all suggest that the valley between regimes is difficult to cross. Thus, very likely the surplus production minimum in the Delaware Bay oyster stock is below zero or nearly so (Fig. 9). The population "resists" the flip between stable states and the degree of this "resistance" is a function of the depth and breadth of the valley between surplus production maxima.

The existence of the type-IV reference point influences management in two ways. If the population is above it, adequate precaution must be included to limit the probability of a population decline of this magnitude as close to zero as possible. The precautionary approach is a standard component in management (e.g., FAO, 1995; Restrepo et al., 1998), but the assessment of risk is rarely undertaken (e.g., Francis and Shotton, 1997). Note in Figure 7 that the type-IV point is closer to N^H_{msy} than N^H_{msy} is to K^H. Thus, management at *MSY* carries with it an increased risk of stock collapse. On the other hand, if the population is below the type-IV reference point, rebuilding goals must be restrained to the objectives associated with the lower-abundance stable state, N^L_{msy} being the obvious target. The key to this assessment is the value of the type-III reference point and particularly whether that value falls below zero.

Options for rebuilding

Most oyster revitalization programs have rebuilding goals and most are premised on recruitment enhancement (e.g., Haven and Whitcomb, 1983; Abbe, 1988; Leffler, 2002). This is typically accomplished through judicious shell planting, that also improves habitat integrity (Powell et al., 2006; Powell and Klinck, 2007). Both restora-

tion goals and methods have received considerable attention (e.g., Breitburg et al., 2000; Mann, 2000).

Restoration goals are dramatically impacted by the location of type-II reference points in relation to stock abundance. Type II is the goal under *MSY* management objectives, and by the presence of type IV and the differential between types II and III. The difference between type II and type III affects 1) the ease of transition from one stable point to another and 2) the impact on fishery yield during the transition. As the differential increases, from the example in the surplus production trajectory of Figure 6 to that in Figure 7 for instance, the limitation on fishery yield during the transition must increase. The obvious incongruity will be an observed increase in abundance of marketable stock during times of decreased allocation necessitated by the transitory limitation on surplus production coincident with the type-III reference point. This apparent inequity will likely exacerbate the natural adversarial relationship that exists between regulator and industry. The frequently complex relationship between economics and biology in fisheries management is well known (Lipton and Strand, 1992; Mackinson et al., 1997; Imeson et al., 2002). Thus several questions come to the fore. Can rebuilding to N^{H}_{msy} be accomplished? This depends on the existence of type IV. Does one try to rebuild to N^{H}_{msy}? This depends on the willingness of the fishery and management to forgo catch yields during times of increasingly high abundance, possibly for an extended period, so that the population shifts to the higher regime.

Regime shifts of long-term stability almost certainly come with a type-IV reference point. In this case, even the closure of the fishery will not generate enough surplus production to rebuild past the type-III low. Recognizing the existence of such a barrier is critical. Presumably, a massive recruitment enhancement program could be implemented to artificially affect a regime shift. Patience may be the better alternative, using the N_{msy} value of the present regime as the management goal

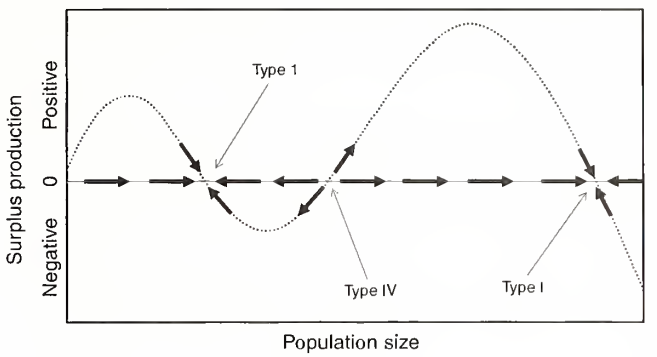

Figure 8

The relationship of the primary trends in population abundance and surplus production associated with the bimodal surplus production trajectory depicted in Figure 7 in which the minimum in surplus production is negative. When surplus production is positive, the population abundance increases. The opposite trend occurs when surplus production is negative. The type-I reference point, the carrying capacity, is a convergence. Trends in surplus production and population abundance converge at this point. The type-IV reference point, the point of no return, is a divergence. Trends in surplus production and population abundance diverge at this point.

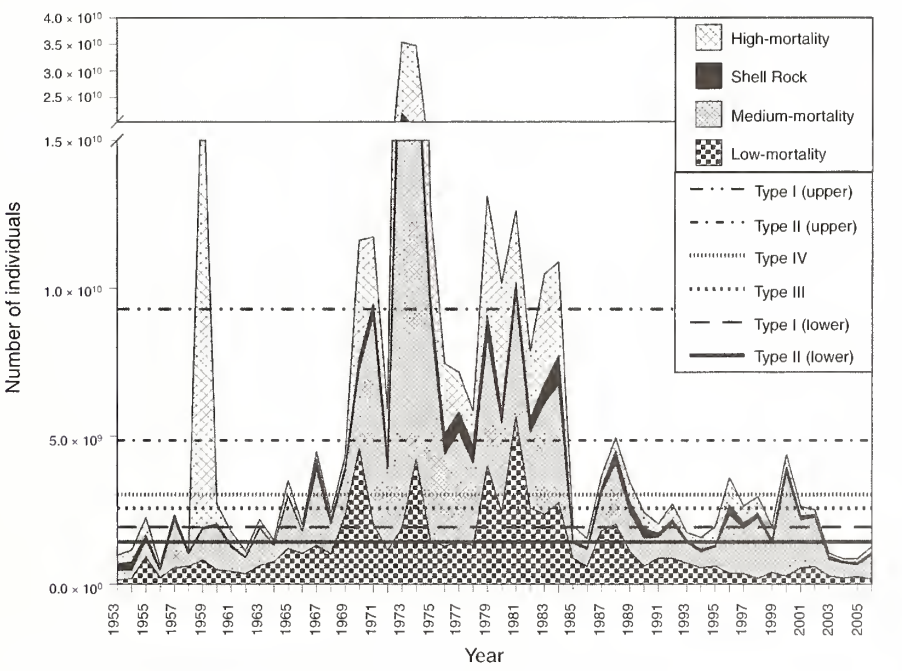

Figure 9

Time series of oyster abundance, by bay region, with the abundance levels associated with types I–IV reference points identified. Regime shifts occurred in 1970 and 1985 (Powell et al., 2009). The 1959 peak is a survey artifact. Total oyster abundance is the cumulative value. Bed groups are defined in Table 1. Bed locations are shown in Figure 1. Reference point legend and symbols are given in order as displayed on the graph, from top to bottom.

while awaiting the rare sequence of events generating a natural transition to the alternate stable state.

Harvest goals

Included in Figures 4–7 is an estimated allowable catch as a fraction of the stock. The values of surplus production given in Figures 4–7 are expressed in numbers, perforce as they are the data source from which the underlying biological relationships are derived. The estimate is provided with some trepidation because the present model does not take into account the differential in growth across the salinity gradient and therefore tends to overestimate the number of animals of market size in the population as a whole. Moreover, the model assumes absolute constancy in the relationship of broodstock to recruitment. Thus, the model may overestimate the fraction of the stock available for harvest in any given year. The formulation of Klinck et al. (2001) is a preferred option to obtain fishery allocations. Finally, the model consistently predicts a higher harvestable fraction at low abundance than at high abundance. An abettor in this trend may be the reliance of setting larvae more and more on the shell resource at low abundance than on the standing crop of living individuals. However, some portion of this outcome is likely due to an inability to accurately extrapolate the primary biological relationships below 0.8×10^9 animals. Such low abundances have not been observed and therefore the extrapolation is likely to be increasingly in error at lower and lower abundances. We do not give complete credence, therefore, to the proportional increase in harvestable fraction at low abundance indicated by the surplus production trajectories depicted in Figures 4–7.

From Figure 3 we observe that the range of abundances assigned to the various reference points varies little among simulations describing a range of assumptions about natural mortality and recruitment rate. By contrast, the range of surplus production is prodigious. Thus, an abundance goal distinguishing an overfished from a sustainable stock, e.g., N_{msy}, is well constrained, whereas an overfishing definition, e.g., f_{msy}, is very poorly delimited. Clearly any successful approach to management must minimize the chance that the added mortality by fishing overcomes the inertia militating against abundance decline. Further, the uncertainty of the level of surplus production at its minimum and maxima (Fig. 5) necessitates precaution as the increased mortality from fishing may be sufficient to stabilize a quasi-stable state at low abundance. Both require, for oysters, that fishing mortality be maintained at a small percentage of the natural mortality rate, thereby permitting the inertia of the system to guard against an abundance decline and reducing the chance that a rare population expansion might be prematurely terminated. Even at N_{msy}, fishing mortality rate is likely not to exceed 5–10% of the stock (Figs. 4–7). The history of the Delaware Bay fishery provides strong corroboration that removals exceeding 15% are not sustainable (Powell et al., 2008) and offers strong evidence that removals below 5% of the stock limit the long-term impact of disease epizootics on abundance. Direct application of the Klinck et al. (2001) model in Delaware Bay has routinely returned values in the range of 1–3%. In addition, Powell and Klinck (2007) discuss the impact of fishing on the shell resource and the degradation of the shell beds upon which the population depends for its existence. That analysis independently argues for fishing mortality rates distinctly below the predisease mortality rate, at approximatly 10%.

It is noteworthy that allowable fishing mortality rates <10% of the stock are more similar to the mortality rates of the longest-lived bivalves, such as geoducks and ocean quahogs (e.g., Bradbury and Tagart, 2000; NEFSC[2]), than other species with life spans of the same order as the oyster, emphasizing the fact that oysters in the Mid-Atlantic region are much more akin in their population dynamics to long-lived k-selected species than to short lived r-selected ones.[3] Low recruitment significantly restricts the ambit of the oyster's population dynamics and significantly constrains allowable fishing mortality rates over a wide range of abundance values. A perusal of the broodstock-recruitment curve (Fig. 7 in Powell et al., 2009) shows that recruitment rate typically falls within the range of 0.25 to 1 spat per adult animal per year. Both this recruitment level and the <10%-per-year natural mortality rate is consistent with theoretical predisease generation times that likely exceeded 10 years (Mann and Powell, 2007) and the fact that reproduction continues to be consistent with an animal characterized by longer generation times.

Conclusions

The oyster population in Delaware Bay exhibits a population dynamics that is not normally described in commercial species. One reason is the presence of distinct and dynamically stable multiple stable points delimited by temporally rapid regime shifts. The result of this complexity is a series of reference points identified by the trajectory of surplus production, which departs dramatically from the simple Schaefer curve (e.g., Zabel et al., 2003). We define four reference point types in terms of surplus production, its derivative, and the rate of change of this derivative (Table 2). In Delaware Bay, the surplus production trajectory likely manifests two stable points and the carrying capacities associated with them and these agree relatively well with the observed stable

[2] NEFSC (Northeast Fisheries Science Center). 2001. 33rd northeast regional stock assessment workshop (33rd SAW): Stock assessment review committee (SARC) consensus summary of assessments. NMFS NEFSC Ref. Doc. 01-18, 281 p.

[3] Gulf of Mexico conditions with rapid growth (Ingle and Dawson, 1952; Butler, 1953; Hayes and Menzel, 1981) and multiple spawns per year (Hopkins, 1954; Hayes and Menzel, 1981; Choi et al., 1993, 1994) are examples of *C. virginica* under more r-selected conditions.

states in the population time series (Fig. 9). For each of these type-I reference points, a maximum in surplus production also exists. The presence of two stable states assures a type-III reference point that is a measure of the ease of transition between the two stable states and provides information on the likelihood that management can artificially impose a transition. In Delaware Bay, the type-III surplus production value may be negative. In this case, a type-IV reference point exists, a point-of-no-return. If the type-III reference point is positive, a quasi-stable state exists at low abundance that can be stabilized by overfishing. The existence of a positive type-III reference point imposes a particular conundrum to management in that rebuilding requires a reduction in fishery yield as abundance increases over a substantive abundance range.

The simulations show the uncertainty imposed by the limitations on accurate knowledge of the biological relationships. One noteworthy observation is that the location of the reference points undefined by a specific surplus production value (e.g., S_t=0), namely types II and III, are relatively stable in position with respect to population abundance over a wide range of uncertainties in recruitment and mortality rates (Table 2). The surplus production values associated with these reference points are much more uncertain (Table 2). Thus, location is much better known than scale. As recommended by Beverton et al. (1984), different models are likely to be needed for short-term catch forecasts and estimation of abundance goals.

We describe reference points in the context of multiple stable states. The simplicity of the B_{msy}–K couple so emphasized in fisheries management fails when multiple stable states exist. That they may often exist is now well considered, although not yet inculcated into the oracle of fisheries management. Multiple stable points assure 1) that a type-III reference point exists, 2) that this point will impede the attainment of imprudently formulated rebuilding goals, 3) that a type-IV point-of-no-return may exist that establishes a barrier to rebuilding, as well as imposing the conditions at high abundance necessary for stock collapse, and 4) that a carrying capacity may exist at abundances well below historically high abundances and well below the simplistic promulgation of B_{msy} as half the carrying capacity established by the higher stable state. Use of the latter may impose impossible requirements for rebuilding a stock because the promulgated goal exceeds the carrying capacity for the controlling regime.

Acknowledgments

We recognize the many people who contributed over the years to the collection of the 54 years of survey data analyzed in this report, with particular recognition of the contributions by H. Haskin, D. Kunkle, and B. Richards. We appreciate the many suggestions on content provided by S. Ford and D. Bushek. The study was funded by an appropriation from the State of New Jersey to the Haskin Shellfish Research Laboratory, Rutgers University, and authorized by the Oyster Industry Science Steering Committee, a standing committee of the Delaware Bay Section of the Shell Fisheries Council of New Jersey.

Literature cited

Abbe, G. R.
1988. Population structure of the American oyster, *Crassostrea virginica*, on an oyster bar in central Chesapeake Bay: Changes associated with shell planting and increased recruitment. J. Shellfish Res. 7:33–40.

Anonymous.
1996. Magnuson-Stevens Fishery Conservation and Management Act. NOAA Tech. Memo. NMFS-F/SPO-23, 121 p.

Beverton, R. J. H., J. G. Cooke, J. B. Csirke, R. W. Doyle, G. Hempel, S. J. Holt, A. D. MacCall, D. J. Policansky, J. Roughgarden, J. G. Shepherd, M. P. Sissenwine, and P. H. Wiebe.
1984. Dynamics of single species group report. *In* Exploitation of marine communities (R. M. May, ed.), p. 13–58. Dahlem Konferenzen, Springer-Verlag, Berlin.

Bradbury, A., and J. V. Tagart.
2000. Modeling geoduck, *Panopea abrupta* (Conrad, 1849) population dynamics II. Natural mortality and equilibrium yield. J. Shellfish Res. 19:63–70.

Breitburg, D. L., L. D. Coen, M. W. Luckenbach, R. Mann, M. Posey, and J. A. Wesson.
2000. Oyster reef restoration: Convergence of harvest and conservation strategies. J. Shellfish Res. 19:371–377.

Burreson, E. M., and L. M. Ragone Calvo
1996. Epizootiology of *Perkinsus marinus* disease of oysters in Chesapeake Bay, with emphasis on data since 1985. J. Shellfish Res. 15:17–34.

Butler, P. A.
1953. Oyster growth as affected by latitudinal temperature gradients. Commer. Fish Rev. 15:7–12.

Caffey, H. M.
1985. Spatial and temporal variation in settlement and recruitment of intertidal barnacles. Ecol. Monogr. 55:313–332.

Choi, K-S., D. H. Lewis, E. N. Powell, and S. M. Ray.
1993. Quantitative measurement of reproductive output in the American oyster, *Crassostrea virginica* (Gmelin), using an enzyme-linked immunosorbent assay (ELISA). Aquacult. Fish. Manag. 24:299–322.

Choi, K-S., E. N. Powell, D. H. Lewis, and S. M. Ray.
1994. Instantaneous reproductive effort in female American oysters, *Crassostrea virginica*, measured by a new immunoprecipitation assay. Biol. Bull. (Woods Hole) 186:41–61.

Clark, W. G.
1999. Effects of an erroneous natural mortality rate on a simple age-structured stock assessment. Can. J. Fish. Aquat. Sci. 56:1721–1731.

Collie, J. S., K. Richardson, and J. H. Steele.
2004. Regime shifts: Can ecological theory illuminate the mechanisms? Prog. Oceanogr. 60:281–302.

FAO (Food and Agriculture Organization of the United Nations).
1995. Technical consultation on the precautionary approach to capture fisheries. Precautionary approach

to fisheries. Part 1: Guidelines on the precautionary approach to capture fisheries and species introductions. FAO Fisheries Tech. Pap. no. 350, part A, 52 p. FAO, Rome.

Francis, R. I. C. C., and R. Shotton.
1997. "Risk" in fisheries management: A review. Can. J. Fish. Aquat. Sci. 54:1699–1715.

Frank, S. A.
1996. Models of parasite virulence. Q. Rev. Biol. 71:37–78.

Fréchette, M., and E. Bourget.
1985. Food-limited growth of *Mytilus edulis* L. in relation to the benthic boundary layer. Can. J. Fish. Aquat. Sci. 42:1166–1170.

Fréchette, M., and D. Lefaivre.
1990. Discriminating between food and space limitation in benthic suspension feeders using self-thinning relationships. Mar. Ecol. Prog. Ser. 65:15–23.

Godfray, H. C. J., and C. J. Briggs.
1995. The population dynamics of pathogens that control insect outbreaks. J. Theor. Biol. 176:125–136.

Gray, J. S.
1977. The stability of benthic ecosystems. Helgol. Wiss. Meeresunters. 30:427–444.

Haddon, M.
2001. Modelling and quantitative methods in fisheries, 406 p. Chapman and Hall, Boca Raton, FL.

Hancock, D. A.
1973. The relationship between stock and recruitment in exploited invertebrates. Rapp. P-v. Réun Cons. Int. Explor. Mer 164:113–131.

Hasiboder, G., C. Dye, and J. Carpenter.
1992. Mathematical modelling and theory for estimating the base reproduction number of canine leishmaniasis. Parasitology 105:43–53.

Hassell, M. P., R. C. Anderson, J. E. Cohen, B. Cujetanović, A. P. Dobson, D. E. Gill, J. C. Holmes, R. M. May, T. McKeown, and M. S. Pereira.
1982. Impact of infectious diseases on host populations. *In* Population biology of infectious diseases (R. M. Anderson, and R. M. May, eds.), p. 15–35. Dahlem Konferenzen, Springer-Verlag, New York, NY.

Haven, D. S., and J. P. Whitcomb.
1983. The origin and extent of oyster reefs in the James River, Virginia. J. Shellfish Res. 3:141–151.

Hayes, P. F., and R. W. Menzel.
1981. The reproductive cycle of early setting *Crassostrea virginica* (Gmelin) in the northern Gulf of Mexico, and its implications for population recruitment. Biol. Bull. (Woods Hole) 160:80–88.

Heesterbeek, J. A. P., and H. G. Roberts.
1995. Mathematical models for microparasites of wildlife. *In* Ecology of infectious diseases in natural populations (B. T. Grenfell, and A. P. Dobson, eds.), p. 90–122. Cambridge Univ. Press, Cambridge, UK.

Hethcote, H. W., and P. van den Driessche.
1995. An SIS epidemic model with variable population size and a delay. J. Math. Biol. 34:177–194.

Hilborn, R., and C. J. Walters.
1992. Quantitative fisheries stock assessment. Choice, dynamics and uncertainty, 570 p. Chapman and Hall, New York, NY.

Holmes, J. C.
1982. Impact of infectious disease agents on the population growth and geographical distributions of animals. *In* Population biology of infectious diseases (R. M. Anderson, and R. M. May, eds.), p. 37–51. Dahlem Konferenzen, Springer-Verlag, New York, NY.

Hopkins, S. H.
1954. Oyster setting on the Gulf coast. Proc. Natl. Shellfish. Assoc. 45:52–55.

Imeson, R. J., J. C. J. M. van den Bergh, and J. Hoekstra.
2002. Integrated models of fisheries management and policy. Environ. Model. Assess. 7:259–271.

Ingle, R. M., and C. E. Dawson Jr.
1950. Variation in salinity and its relation to the Florida oyster. Part One: Salinity variations in Apalachicola Bay. Proc. Natl. Shellfish. Assoc. p. 6–19.

Johnson, L.
1994. Pattern and process in ecological systems: A step in the development of a general ecological theory. Can. J. Fish. Aquat. Sci. 51:226–246.

Jordan, S. J., K. N. Greenhawk, C. B. McCollough, J. Vanisko, and M. L. Homer
2002. Oyster biomass, abundance, and harvest in northern Chesapeake Bay: Trends and forecasts. J. Shellfish Res. 21:733–741.

Keough, M. J., and B. J. Downes.
1982. Recruitment of marine invertebrates: The role of active larval choices and early mortality. Oecologia (Berl.) 54:348–352.

Kermack, W. O., and A. G. McKendrick.
1991. Contributions to the mathematical theory of epidemics—I. Bull. Math. Biol. 53:33–55.

Klinck, J. M., E. N. Powell, J. N. Kraeuter, S. E. Ford, and K. A. Ashton-Alcox.
2001. A fisheries model for managing the oyster fishery during times of disease. J. Shellfish Res. 20:977–989.

Knowlton, N.
2004. Multiple "stable" states and the conservation of marine ecosystems. Prog. Oceanogr. 60:387–396.

Leffler, M.
2002. Crisis and controversy. Does the bay need a new oyster? Chesapeake Quart. 1:2–9.

Lipton, D. W., and I. E. Strand.
1992. Effect of stock size and regulations on fishing industry cost and structure: The surf clam industry. Am. J. Agr. Econ. 74:197–208.

Mackinson, S., U. R. Sumaila, and T. J. Pitcher.
1997. Bioeconomics and catchability: Fish and fishers behaviour during stock collapse. Fish. Res. 31:11–17.

Mangel, M., and C. Tier.
1994. Four facts every conservation biologist should know about persistence. Ecology 75:607–614.

Mann, R.
2000. Restoring the oyster reef communities in the Chesapeake Bay: A commentary. J. Shellfish Res. 19:335–339.

Mann, R., E. M. Burreson, and P. K. Baker.
1991. The decline of the Virginia oyster fishery in Chesapeake Bay: Considerations for the introduction of a non-endemic species, *Crassostrea gigas* (Thunberg, 1793). J. Shellfish Res. 10:379–388.

Mann, R., and E. N. Powell.
2007. Why oyster restoration goals in the Chesapeake Bay are not and probably cannot be achieved. J. Shellfish Res. 26:905–917.

May, R. M., J. R. Beddington, J. W. Horwood, and J. G. Shepherd.
1978. Exploiting natural populations in an uncertain world. Math. Biosci. 42:219–252.

McCann, K. S., L. W. Botsford, and A. Hasting.
2003. Differential response of marine populations to climate forcing. Can. J. Fish. Aquat. Sci. 60:971–985.

Peterson, C. H.
1984. Does a rigorous criterion for environmental identity preclude the existence of multiple stable points? Am. Nat. 124:127–133.

Powell, E. N., and K. A. Ashton-Alcox.
2004. A comparison between a suction dredge and a traditional oyster dredge in the transplantation of oysters in Delaware Bay. J. Shellfish Res. 23:803–823.

Powell, E. N., K. A. Ashton-Alcox, S. E. Banta, and A. J. Bonner.
2001. Impact of repeated dredging on a Delaware Bay oyster reef. J. Shellfish Res. 20:961–975.

Powell, E. N., K. A. Ashton-Alcox, J. A. Dobarro, M. Cummings, and S. E. Banta.
2002. The inherent efficiency of oyster dredges in survey mode. J. Shellfish Res. 21:691–695.

Powell, E. N., K. A. Ashton-Alcox, and J. N. Kraeuter.
2007. Reevaluation of eastern oyster dredge efficiency in survey mode: Application in stock assessment. N. Am. J. Fish. Manag. 27:492–511.

Powell, E. N., K. A. Ashton-Alcox, J. N. Kraeuter, S. E. Ford, and D. Bushek.
2008. Long-term trends in oyster population dynamics in Delaware Bay: Regime shifts and response to disease. J. Shellfish Res. 27:729–755.

Powell, E. N., H. Cummins, R. J. Stanton Jr., and G. Staff.
1984. Estimation of the size of molluscan larval settlement using the death assemblage. Estuarine Coastal Shelf Sci. 18:367–384.

Powell, E. N., and J. M. Klinck.
2007. Is oyster shell a sustainable estuarine resource? J. Shellfish Res. 26:181–194.

Powell, E. N., J. M. Klinck, K. A. Ashton-Alcox, J. N. Kraeuter.
2009. Multiple stable reference points in oyster populations: biological relationships for the eastern oyster (*Crassostrea virginica*) in Delaware Bay. Fish. Bull. 107:109–132.

Powell, E. N., J. M. Klinck, E. E. Hofmann, E. A. Wilson-Ormond, and M. S. Ellis.
1995. Modeling oyster populations. V. Declining phytoplankton stocks and the population dynamics of American oyster (*Crassostrea virginica*) populations. Fish. Res. 24:199–222.

Powell, E. N., J. N. Kraeuter, and K. A. Ashton-Alcox.
2006. How long does oyster shell last on an oyster reef? Estuarine Coastal Shelf Sci. 69:531–542.

Ragone Calvo, L. M., R. L. Wetzel, and E. M. Burreson
2001. Development and verification of a model for the population dynamics of the protistan parasite, *Perkinsus marinus*, within its host, the eastern oyster, *Crassostrea virginica*, in Chesapeake Bay. J. Shellfish Res. 20:231–241.

Redner, S.
2001. A guide to first-passage processes, 312 p. Cambridge Univ. Press, Cambridge, U.K.

Restrepo, V. R., G. G. Thompson, P. M. Mace, W. K. Gabriel, L. L. Low, A. D. MacCall, R. D. Methot, J. E. Powers, B. L. Taylor, P. R. Wade, and J. F. Witzig.
1998. Technical guidance on the use of precautionary approaches to implementing National Standard 1 of the Magnuson/Stevens Fishery Conservation and Management Act. NOAA Tech. Memo. NMFS-F/SPO-31, 54 p.

Rice, J.
2001. Implications of variability on many time scales for scientific advice on sustainable management of living marine resources. Prog. Oceanogr. 49:189–209.

Ricker, W. E.
1975. Computation and interpretation of biological statistics of fish populations. Bull. Fish. Res. Board Can. 191:1–382.

Rothschild, B. J., J. S. Ault, P. Goulletquer, and M. Héral
1994. Decline of the Chesapeake Bay oyster populations: A century of habitat destruction and overfishing. Mar. Ecol. Prog. Ser. 111:29–39.

Rothschild, B. J., C. Chen, and R. G. Lough.
2005. Managing fish stocks under climate uncertainty. ICES J. Mar. Sci. 62:1531–1541.

Rothschild, B. J., and A. J. Mullen.
1985. The information content of stock-and-recruitment data and non-parametric classification. J. Cons. Int. Explor. Mer. 42:116–124.

Soniat, T. M., E. N. Powell, E. E. Hofmann, and J. M. Klinck.
1998. Understanding the success and failure of oyster populations: The importance of sampled variables and sample timing. J. Shellfish Res. 17:1149–1165.

Soniat, T. M., E. N. Powell, J. M. Klinck, and E. E. Hofmann.
In press. Understanding the success and failure of oyster populations: Climatic cycles and *Perkinsus marinus*. Int. J. Earth Sci.

Swinton, J., and R. M. Anderson.
1995. Model frameworks for plant-pathogen interactions. *In* Ecology of infectious diseases in natural populations (B. T. Grenfell, and A. P. Dobson, eds.), p. 280–294. Cambridge Univ. Press, Cambridge, U.K.

Zabel, R. W., C. J. Harvey, S. L. Katz, T. P. Good, and P. S. Levin.
2003. Ecologically sustainable yield. Am. Sci. 91:150–157.

Advances in methods for determining fecundity: application of the new methods to some marine fishes

Peter R. Witthames (contact author)[1]
Anders Thorsen[2]
Hilario Murua[3]
Francisco Saborido-Rey[4]
Lorraine N. Greenwood[2]
Rosario Dominguez[4]
Maria Korta[3]
Olav S. Kjesbu[2]

Email address for contact author: fecund-fish@tiscali.co.uk.

[1] Centre for Environment, Fisheries & Aquaculture Science (Cefas)
Lowestoft, Suffolk NR33 OHT, United Kingdom
Present address:
Fecund Fish Consultancy
40 Plumtrees
Lowestoft, Suffolk NR32 3JH, United Kingdom

[2] Institute of Marine Research (IMR)
P.O. Box 1870
Nordnes, N-5817 Bergen, Norway

[3] AZTI Tecnalia Herrera Kaia
Portualde z/g 20110 Pasaia, Spain

[4] Institute of Marine Research (CSIC)
Eduardo Cabello 6, 36208, Vigo, Spain

Abstract—Estimation of individual egg production (realized fecundity) is a key step either to understand the stock and recruit relationship or to carry out fisheries-independent assessment of spawning stock biomass using egg production methods. Many fish are highly fecund and their ovaries may weigh over a kilogram; therefore the work time can be consuming and require large quantities of toxic fixative. Recently it has been shown for Atlantic cod (*Gadus morhua*) that image analysis can automate fecundity determination using a power equation that links follicles per gram ovary to the mean vitellogenic follicular diameter (the autodiametric method).

In this article we demonstrate the precision of the autodiametric method applied to a range of species with different spawning strategies during maturation and spawning. A new method using a solid displacement pipette to remove quantitative fecundity samples (25, 50, 100, and 200 milligram [mg]) is evaluated, as are the underlying assumptions to effectively fix and subsample the ovary. Finally, we demonstrate the interpretation of dispersed formaldehyde-fixed ovarian samples (whole mounts) to assess the presence of atretic and postovulatory follicles to replace labor intensive histology. These results can be used to estimate down regulation (production of atretic follicles) of fecundity during maturation.

Manuscript submitted 2 May 2008.
Manuscript accepted 3 October 2008.
Fish. Bull. 107:148–164 (2009).

Research on population fecundity (total egg production) has two important applications in the management of renewable marine or freshwater fish resources. Perhaps the most important is to understand the relationship between spawning stock biomass and recruitment because it is increasingly clear that the assumption of direct proportionality (Beverton and Holt, 1957) is not correct (Marshall et al., 1998; Witthames and Marshall, 2008). The link between spawning stock biomass and recruitment varies according to total egg production that in turn is dependent, not only on the length frequency of spawning adults, but also on body weight at length (Marshall et al., 1998, 1999). In summary the stock and recruitment relationship became stronger when stock was expressed as a product of population length frequency and fecundity at length (Marshall et al., 1998).

A second application for fecundity information is to estimate spawning stock biomass independently of data collected from commercial fisheries (Parker, 1980; Lockwood et al., 1981; Lo et al., 1992). In addition to the fecundity count, information is required on a range of parameters associated with the development of fecundity, such as follicular diameter and frequency distribution, spawning rates, and individual realized fecundity, either in one or multiple batches shed during one or more spawning events.

In this article we prefer the following definitions for fecundity (Hunter et al., 1992). Thus the developing fecundity (standing stock of fecundity referred to as "fecundity" [F]) includes follicles containing cortical alveoli (Khoo, 1979) and, in later development, yolk granules (Hunter et al., 1992) but excludes precursor cells such as previtellogenic follicles (PVFs) or oogonia. Relative fecundity (F_{bw}) is the fecundity divided by the total fish weight. We use the term "follicle" to refer to the oocyte and its nurturing follicular layers (Tyler and Sumpter, 1996) during all phases of development from precursor cells to residual postovulatory follicles (POFs) that indicate previous spawning or egg release events.

The species in this study are of interest because they represent three extremes in spawning strategy (Mu-

rua and Saborido-Rey, 2003): 1) group synchronous determinate total spawners (Atlantic herring [*Clupea harengus*], deep water redfish [*Sebastes mentella*] also known as "beaked redfish [FAO, Fisheries and Aquaculture Dept., www.fao.org/fishery/statistics/programme/3.1.1. Accessed Jan., 2009], and golden redfish [*Sebastes marinus*]); 2) group synchronous determinate batch spawners (Atlantic cod [*Gadus morhua*] and European plaice [*Pleuronectes platessa*]); and 3) asynchronous types (European hake [*Merluccius merluccis*] and Atlantic mackerel [*Scomber scombrus*]) that may not be determinate (Greer-Walker et al., 1994). Fecundity in the first two groups included all follicles in the advanced mode to the right of a gap in the follicular size frequency (Hunter et al., 1992) whereas in the latter case the follicular distribution is continuous. Although fecundity may be enhanced during maturation in asynchronous spawning types (indeterminate spawning strategy), it is of practical and theoretical value to study fecundity proliferation whatever classification is applied to the spawning process.

Recent work has shown that not all the fecundity develops into eggs (realized fecundity) and follicular atresia may account for a substantial part of the fecundity in a process referred to as down regulation (see reviews Murua et al., 2003; Thorsen et al., 2006; Kjesbu and Witthames, 2007). In addition, it is also important to differentiate whether an individual female has entered the spawning cycle, thus reducing her fecundity, and how long a POF persists to indicate a previous spawning event (Hunter and Macewicz, 1985a). The latter information is used to assess whether a female still contains her full complement of oocytes for application of the annual egg production method to assess spawning stock biomass applied to fish with a determinate spawning strategy (Armstrong et al., 2001).

To date no single approach has been successful in quantifying follicular stages associated with fecundity development and regression and each has one or more disadvantages. Fish that are very fecund, perhaps containing ovaries weighing more than a kilogram and with millions of follicles, will have to be subsampled for fecundity estimation. In this case, quantitative histological methods (Emerson et al., 1990) requiring sections of the whole ovary are not feasible—meaning only relative proportions of each follicular class can be measured (Andersen, 2003). This approach, however, needs additional information on the fecundity count preferably coupled with measurement of follicular size frequency to exclude smaller PVFs that are not committed to maturation in the current reproductive year. Although it is feasible to release follicles by digesting the ovary in strong acid solutions (either Gilson's fluid (Simpson, 1951) or a less toxic nitric acid formulation (Friedland et al., 2005)), such media have several adverse consequences. These consequences include 1) considerable follicular shrinkage (Witthames and Greer-Walker, 1987), 2) likely loss of atretic follicles and POFs (Klibansky and Juanes, 2007), and 3) incompatibility with histological methods (Hunter and Macewicz, 2003). In view of the need to identify fecundity based on follicular size, there is a need to measure large numbers of follicles greater than a specified lower size limit even if the ovary is subsampled using the gravimetric method (Bagenal and Braum, 1968). Manual measurement of follicular size frequency, even using video technology, is just too demanding on manual labor unless there is some way of automating the collection of data. Although an automatic particle analyzer can provide such data (Witthames and Greer-Walker, 1987), the method requires large quantities of Gilson's fluid and is subject to all the problems listed above. More recently image analysis methods have been adopted to automate collection of size frequency data in Atlantic cod (*Gadus morhua*) (Thorsen and Kjesbu, 2001; Klibansky and Juanes, 2008). In each case the mean fecundity (the independent variable) can be used to estimate the number of follicles per gram (g) of ovary by fitting a power relationship based on a calibration from a data set containing the two variables (the autodiametric method). Fecundity is then determined by raising the number of follicles per g of ovary by the ovarian weight. Although an alternative image analysis method applied to American shad (*Alosa sapidissima*) (Friedland et al., 2005) has advantages as a cost effective method to estimate fecundity, it also has two significant drawbacks: 1) relatively low resolution, and, 2) it uses acid hydrolysis to separate follicles. Thus, the autodiametric method has more general utility because it uses neutral buffered formaldehyde solution (NBF) to fix tissue that is fully compatible with histology. Also Hunter et al. (1992) studying Dover sole (*Microstomus pacificus*) and Öskarsson et al. (2002) studying Atlantic herring (*Clupea harengus*) have shown it possible to identify atretic follicles in NBF-fixed dispersed ovarian samples (whole mounts) suggesting it might be possible to also estimate numbers of different follicular classes.

Accordingly, our first objective is to report on the utility and precision of the autodiametric method to determine fecundity in several species including Atlantic cod, European hake, Atlantic herring, Atlantic mackerel, redfish species (deep water redfish and golden redfish), and European plaice. To emphasize the utility of the method several laboratories 1) AZTI [A] (Pasaia, Spain), 2) Cefas [B](Lowestoft, UK), 3) CSIC [C] (Vigo, Spain), and 4) IMR [D] (Bergen, Norway) used different configurations of image analysis equipment. In order to complete this work, four other objectives were identified linked to the application of fecundity determination using Atlantic cod as the main example and to a lesser extent European hake: 1) ovarian sampling, and follicular homogeneity, 2) evaluate three stains (eosin, rose bengal, and periodic acid-schiff [PAS]) to improve the accuracy of follicular size measurement and counting in relation to the autodiametric method, 3) compare interpretation of NBF-fixed whole mounts with respect to histology to assess maturity, spawning status and quantify the standing stock of atretic follicles, and 4) consideration was also given to the effect of ovarian maturation on down regulation of fecundity in Atlantic

Table 1

Details of the collection date, source, and maturity stage of wild fish (Atlantic cod [*Gadus morhua*], haddock [*Melanogrammus aeglefinus*], European hake [*Merluccius merluccius*], Atlantic herring [*Clupea harengus*], Atlantic mackerel [*Scomber scombrus*], European plaice [*Pleuronectes platessa*], common sole [*Solea solea*], redfish (deep water redfish [*Sebastes mentella*] or golden redfish [*Sebastes marinus*]) used in the study. The samples where taken from commercial or research vessel catches. Collections made in 1995 were used for the study of fecundity down regulation and the later collections from 1998 onward for the study of fecundity methods.

	Atlantic Cod	Haddock	European hake	Atlantic herring	Atlantic mackerel	European plaice	Common sole	Redfish
Date	Jan–Mar 1995, 2003–04, 2007	Feb 2007	Mar 2003	Jan 1998	Mar 2004	Jan–Mar 1995, 2000, 2007	Jan–Feb 1995	Sep-Nov 2000–2001
Source	Lofoten Andenes Norway North and Irish Sea	Irish Sea	Galicia Biscay Celtic Sea	Norwegian-spring spawning stock	Western Atlantic stock	Irish Sea	Irish Sea	Iceland Irminger Sea
Maturity stage	Prespawning and spawning	Pre-spawning	Pre-spawning and spawning	Pre-spawning	Pre-spawning	Pre-spawning	Pre-spawning to near spent	Pre-spawning

cod, European plaice, and common sole (*Solea solea*) and the implications for estimating total fecundity prior to the start of spawning.

Materials and methods

Ovarian sampling, follicle measurement equipment, and homogeneity

Ovarian samples were collected by the four institutes working on two or more of the following species Atlantic cod, Atlantic herring, European hake, Atlantic mackerel, European plaice, and redfish (including deep water redfish and golden redfish) for studies unrelated to this paper (Table 1). Biological information was taken from each fish, but only the information related to this method development (ovarian mass and maturity stage) is used here. Only active ovaries (Hunter et al., 1992) were selected and weighed to better than 2% of their mass, either with a motion-compensated balance (POLS Electronics, Isafjordur, Iceland) when sampled at sea or with a standard balance when on shore. Fish that contained many ovulated eggs (caught in the act of spawning) were not used in the autodiametric calibration because they show a heterogeneous distribution (Witthames, 2003). In each case ovaries or ovarian subsamples were fixed in a minimum of two volumes of NBF for a minimum of 14 days. Quantitative subsamples were taken by one of two methods: 1) from the fresh unfixed ovary (Atlantic cod, Atlantic mackerel) immediately after capture at sea using a Wiretrol II pipette (Drummond Scientific, Broomall, PA), or 2) from the fixed ovary in the laboratory with a scalpel (Atlantic cod, European hake, European plaice, and redfish). The Wiretrol II pipette consists of a Teflon-tipped stainless steel piston within a graduated glass tube with a 1 or 2 millimetre (mm) bore that can remove 26 and 54, or 106 and 212 milligrams (mg), respectively, of tissue when inserted through the ovarian tunica.

Image analysis hardware and software, including the camera resolution and light intensities used by each institute to measure follicular diameter and circularity, varied (Table 2). The follicle data were analyzed with Microsoft Excel to calculate follicular mean, standard deviation, and leading cohort (*Lc*) (defined as the mean of largest 10% of follicles measured). PVFs were excluded from the fecundity count and frequency distribution based on a minimum follicular diameter of 150 and 250 μm in European hake, and Atlantic cod, respectively (Kjesbu, 1991; Murua and Motos, 2006). In the case of Atlantic mackerel there were no published data available, so a diameter of 185 μm was used based on our observation of the smallest follicles containing cortical alveoli and a publication focusing on Atlantic mackerel fecundity determinacy (Greer-Walker et al., 1994). In all other species, where the follicular frequency was not continuous, only dark yolk-bearing follicles in the leading mode were included in the fecundity count. Follicles were disaggregated from the ovarian sample by sucking them in and out of a Pasteur pipette (Thorsen and Kjesbu, 2001) prior to spreading them out in a counting chamber as a single layer completely covered by water. If small clumps of follicles remained they were measured manually as discrete follicles, whereas larger clumps were separated and exposed to more pressure washing by the pipette or a garden spray (Institutes A and C). All the follicles were counted in the subsamples but the method for collecting the follicular measurements differed according to each institute's image

Table 2

Details of the image analysis software ([1]Pilkington Image Analysis Systems,[2] Shareware available at rsb.info.nih.gov/ij/download.html), operating systems, camera, light source, microscope, resolution, grey scale, and staining methods used by each institute: AZTI, Cefas, CSIC, and IMR to analyze whole mounts prepared from each species: Atlantic cod (*Gadus morhua*), European hake (*Merluccius merluccius*, Atlantic herring (*Clupea harengus*), Atlantic mackerel (*Scomber scombrus*), European plaice (*Pleuronectes platessa*), redfish (deep water redfish (*Sebastes mentella*) or golden redfish (*Sebastes marinus*).

Detail	AZTI [A]	Cefas [B]	CSIC [C]	IMR [D]
Software	Visilog 6.11	Myrmica[1] automatic or semi automatic operation	QWin (Leica Imaging System)	Image SXM v. 1.77[2]
Operating system	PC Windows	PC Windows	PC Windows	Mac OS X
Camera	Camedia-4040 Zoom	Pulnix TMC-1000-CL	Leica 1C A	JVC TK-1070E
Light source	3100 High light Olympus	3100 Olympus High light	Leica MZ6	SZX-1LLB200
Microscope	Olympus SZX12	Olympus SZX12	Leica MZ6	Olympus SZX12
Resolution (μm/pixel)	5 (hake)	19.3 (plaice), 10.0 (cod), 4.6 (mackerel)	21.9–27.6 (redfish) 7.02–22.43 (hake)	14.7 (cod) 14.7 (herring)
Gray scale (255 saturated)	230	175	90	205
Staining method	Rose bengal (hake)	PAS (mackerel and cod) Eosin (plaice)	Rose bengal (hake) Unstained redfish	Unstained

analysis system and the size of the follicles comprising the fecundity. Institutes A and C split the sample and took a separate image of each aliquot to ensure that the follicles were evenly spread without overlap in a container that was completely covered within the field of view. Institute B spread the sample in a counting chamber 70 mm long and either 4, 7, or 10 mm wide for Atlantic mackerel, Atlantic cod, and European plaice, respectively. The three widths of counting chamber were used so that three magnifications (Table 2) could be used while still displaying the full width of the chamber. Above the sample the counting chamber tapered outwards in v-shaped profile leading to an upper liquid surface of 25 mm creating a flat meniscus over the channel holding the follicles. Myrmica software (Pilkington image analysis systems, Lindfield, West Sussex, UK) was used to create and archive a series of images and overlays along the horizontal axis of the sample container showing all measurements overlaying the follicles measured. Individual follicles stained PAS were measured in this counting chamber both manually and by image analysis to establish the accuracy of size measurement by image analysis. Institute D working with Atlantic cod and Atlantic herring used a method described previously (Thorsen and Kjesbu, 2001).

In order to investigate whether fixing the ovary in sample aliquots or whole in the tunica affected mean follicular diameter (D_f, μm), circularity, and fecundity per gram of ovary (F_{ow}), replicate samples were taken by pipette and scalpel, respectively, from the central part of the same ovary from Atlantic cod, Atlantic haddock, and European plaice (Table 1). These samples were collected from fish caught in the Irish Sea during February 2007 (Table 1) and fixed for between 63 and 91 days in 1.7 to 9 times their volume of NBF before image analysis (Table 2). Circularity, a function of follicular shape, was measured according to the following equation:

$$Circularity = 4\pi\,(area/perimeter)^2\,. \quad (1)$$

Homogeneity of D_f and F_{ow} were studied in Atlantic cod and European hake ovaries to investigate whether a sample from the center of the ovarian mass was significantly different from samples taken at the extreme ends of each ovary or between the pair of ovaries.

Stain evaluation

Ovarian tissue (whole mounts) stained by the three routines (Table 2) was compared with nonstained tissue in order to improve the identification and measurement of developing (cortical alveoli and vitellogenic) and regressing (postovulatory and atretic) follicles. Nonstained tissue was prepared for analysis as described by Thorsen and Kjesbu (2001), and two of the staining methods applied water soluble 1% eosin or 0.02% rose bengal weight to volume (w/v) dissolved in NBF to color the follicles. A third staining method used the PAS reaction, previously applied to stain cortical alveoli follicles (Greer-Walker et al., 1994). In this procedure the concentration of PAS reagent was 0.1% and 15% w/v, respectively, compared to the histological procedure in order to minimize shrinkage of follicles. Nonbound stain was removed from the tissue subsamples after

staining by washing through mesh sieves that retained all follicles larger than 125 μm using either 1:3 glycerine:water (McBride and Thurman, 2003), 0.9% w/v sodium chloride (Ramsay and Witthames, 1996), or clean water. Replacement of the fixative used for storage by saline or water did not affect the size of follicles during subsequent storage for 5 days at 0–5°C.

Comparison of whole-mount method with histological method

In order to study the morphology of POFs immediately after ovulation, and during advanced regression, ovarian samples were taken from trawl caught Atlantic cod taken from the Irish Sea (Table 1) during the spawning season. In some cases the fish (n=10) were producing copious quantities of ovulated eggs and were expected to contain newly produced POFs created simultaneously with ovulation. After fixation in NBF the whole mounts were examined both unstained and after PAS staining to color both the oocyte chorion and the basement membrane between the granulosa and thecal layers of the follicle. The size frequency of the residual vitellogenic follicles and POFs were also measured at this time. Normal vitellogenic and POFs were tentatively identified in the above preparations based mainly on their shape but also on their internal structure revealed as irregular blotches or shading (Hunter and Macewicz, 1985a, 1985b; Hunter et al., 1992). One fish was chosen from this group because it contained not only large POFs but also illustrated previous spawning activity based on large numbers of small POFs assumed to come from previous ovulation events. Examples of tentatively identified follicular classes were removed from the whole mount and processed into PAS Mallory trichrome stained 2-hydroxyethyl methacrylate (Technovit® 7100 Kulzer GmbH, Wehrheim, Germany) sections (Witthames and Greer- Walker, 1995) in order to compare the accuracy of the identification.

Alpha atretic follicles (Hunter and Macewicz, 1985b) were identified in biopsy samples taken with a Pipelle de Cornier® (Prodimed, Neuilly En Thelle, Picardie, France), a flexible, plastic tube 2.1 mm internal diameter, by endometrial suction after gonad catheterization (Bromley et al., 2000). These samples were taken from sedated captive Atlantic cod available from a separate study carried out at IMR during March 2004 to determine the rate of transition from normal to advanced stage atretic follicles. Each biopsy sample was fixed as above and examined as an unstained and stained whole mount to compare the intensity of follicular atresia found in both preparations. Intensity of atresia (Ia) was defined as

$$Ia = Ni/(Ni + Nj), \quad (2)$$

where Ni and Nj refer to alpha atretic and normal vitellogenic follicles, respectively.

The alpha atresia and more advanced beta follicular stages have been defined previously based on the fragmentation or absence of the chorion (Witthames and Greer-Walker, 1995;Witthames, 2003) following previous studies (Hunter and Macewicz, 1985b). After scoring the intensity of atresia the whole mounts were infiltrated in resin and then polymerized slowly at –10°C over a period of 2 hours that all the follicles lay at the base of the mold. At least 25 to 30 sections of 5 μm were cut and discarded in order to take a section within 125 to 150 μm from the base of the mold to transect all the follicles present in the sample. This section was stained by the PAS Mallory trichrome method to identify and count the transected follicles.

Fecundity maturation and down regulation

In order to study the change in fecundity during maturation D_f and atresia data were taken from Atlantic cod sampled in the Irish and North Seas between January and March during 2003 and 2004 (Table 1), and examined in two ways. In the first case the standing stock of atretic follicles (Ia) was measured as prevalence (proportion of fish containing alpha atretic follicles) and relative intensity (Ia/whole body weight g) as described previously (Witthames and Greer-Walker, 1995). The atresia was determined in histological sections stained by PAS Mallory trichrome. Secondly the overall impact of atresia on relative fecundity F_{bw} = F/total body weight in g) during maturation was determined by assessing the reduction of F_{bw} in relation to D_f as recently described (Thorsen et al., 2006).

$$F_{bw} = a \times \mathrm{Ln}\,(D_f) + b. \quad (3)$$

An additional data set (Table 1) was also available from an annual egg production survey of Atlantic cod, European plaice, and common sole biomass (Armstrong et al., 2001) to assess whether down regulation also occurs in other species with a similar fecundity development process. This data set contained details of fecundity, fish length (cm) total, and ovarian weight (g) for each species and was used to calculate F_{bw} in each case. D_f was predicted from F_{ow} using the ovarian weight and fecundity data in Equation 4 (below) adjusted to make F_{ow} the independent variable.

Autodiametric calibration

A regression line (based on ln-transformed data) was established for each species and institute (Thorsen and Kjesbu, 2001) between D_f and F_{ow} using the following formula where a and b are equation constants.

$$\mathrm{Ln}\,F_{ow} = a \times \ln D_f + b. \quad (4)$$

In one data set the parameters showed some degree of noncovariance and a second polynomial function ($\ln D_f{}^2$) was fitted to the data where a, b and c are constants:

$$\mathrm{Ln}\,F_{ow} = a \times \ln D_f + b \times \ln D_f^2 + c. \quad (5)$$

Table 3

Comparison of mean (standard error [SE]) follicle diameter (D_f, μm), number of follicles per gram ovary (F_{ow}), circularity, and fecundity (F_{ow} × ovary mass [g]), found in samples taken with either a pipette (P, from fresh tissue) or gravimetric method (G, from fixed tissue) from fish caught in the Irish Sea by commercial vessel during 2007. In each case five replicates were taken from a central location of the same ovary in ripe mature Atlantic cod (*Gadus morhua*, cod m), hydrated Atlantic cod (cod h), ripe mature Atlantic haddock (*Melanogrammus aeglefinus*, had), and European plaice (*Pleuronectes platessa*, ple). The mass (g) of the ovary fresh (ovary F) and after storage in fixative for longer than 14 days (ovary S) is also shown.

Parameter	Sample method	Cod m (n=5)	Cod h (n=5)	Had (n=5)	Ple (n=5)	Paired t-test n=15 P
D_f	P	797 (3)	944 (5)	571 (4)	1081 (10)	0.0026
	G	777 (3)	904 (8)	560 (1)	1085 (7)	
F_{ow}	P	3613 (90)	1460 (338)	9355 (338)	1196 (38)	6.652^{-10}
	G	3975 (149)	1706 (33)	10394 (149)	1280 (17)	
Circularity	P	0.986 (0.001)	0.995 (0.001)	0.985 (0.001)	0.990 (0.001)	0.0015
	G	0.966 (0.004)	0.983 (0.001)	0.961 (0.002)	0.977 (0.002)	
Fecundity	P	419,132	388,460	205,804	44,260	
	G	443,191	421,424	218,664	45.980	
Ovary	F	116.0	266.0	22.0	37.0	
Ovary	S	111.5	247.0	21.0	35.9	

Fecundity (F) was calculated from the product of ovarian weight (O) and F_{ow}.

Statistics

Regression analysis was carried out using the "R"(vers. 2.5.0, Free Software Foundation, Boston, MA) and residuals were plotted to check there was no systematic pattern suggesting that the models should be further refined. The coefficient of variation (CV) was determined for predictions with new data to examine the precision of the fecundity estimate for a range of follicular sizes typical for each species.

Results

Ovarian sampling, follicle measurement equipment, and homogeneity

In the course of more extensive use at sea, the pipettes performed well taking samples from maturing ovaries providing that they contained vitellogenic follicles visible to the unaided eye (>400 μm). However, ovaries that were close to being spent or immature did not yield quantitative samples because the connective tissue attached to the follicles pulled the sample out of the pipette as it was withdrawn from the ovary. When this occurred it was clear that the glass tube was only partially filled and the sampling process could be repeated to fill the pipette to avoid under sampling although this was not always successful. In summary we found that replicate subsamples of 25 and 100 μL tissue taken with the pipette from a Atlantic cod ovary equated to a gravimetric sample of 26.0 mg (CV=1.8%, n=10) and 106.0 mg (CV=3.7%, n=10), respectively.

Compared to fixing the ovary whole for the gravimetric method, the pipette procedure for collecting ovarian subsamples was found to significantly increase (P=0.003, P<0.0001, and P=0.002) D_f, circularity of follicles (Table 3), and decrease F_{ow}, respectively. Ovarian weight after fixation over 63–65 days showed a small decease (95% SE=0.9) that was not apparently related (P=0.55, n=4) to the amount of NBF used to fix the ovary. After accounting for a reduction in ovarian mass the overall reduction in fecundity, determined from the pipette samples, was 5.7% (SE=0.3) less compared to gravimetric samples taken from the same ovary fixed whole.

There was a very significant difference in F_{ow}, D_f, and Lc means (P<0.001) between fish but there was no consistent trend either between the pair of ovaries or within the ovary at three sites (anterior, middle, and posterior) where samples were taken (Fig. 1). In two out of the seven fish there was a site effect (left, posterior, and right middle) on D_f and Lc, but their rank order was reversed at other locations. It was also noticed that in more mature Atlantic cod ovaries, where the Lc was larger, the CV of D_f, and Lc amongst replicates also increased. Similarly, sampling site (anterior, middle, or posterior part of one ovary) in 103 European hake indicated that F_{ow}, either classified by cortical alveoli, early, or late vitellegenic follicle development stages, or all classes combined, was not related to ovarian position (P=0.133, 0.149, 0.789, 0.101, respectively).

Stain evaluation

Compared to unstained follicles the use of each stain to color European hake, Atlantic cod, Atlantic mackerel, and European plaice follicles increased the efficiency of image analysis measurement, particularly of semitrans-

parent objects such as PVF, cortical alveoli, hydrated, and POFs. After PAS staining, manual measurements of follicle diameter (F_{dm}) compared closely to automatic measured follicle diameter (F_{di}) calculated from the image analysis:

$$F_{di} = 1.0016 \times F_{dm} + 0.0405 \quad (6).$$
$$(n=42,\ r=0.997,\ 220 \leq \text{manual reading} \leq 1900\ \mu\text{m})$$

Although the eosin solution stained both vitellogenic and hydrated follicles in European plaice, it was much less effective when applied to either Atlantic cod or Atlantic mackerel follicles. A further disadvantage was that the stain was not bound by a chemical reaction and tended to leach out more rapidly compared to PAS stained tissue. This could be countered by extensive washing but this progressively affected the follicle size determined by image analysis. The rose bengal stain was also based on affinity rather than chemically bound and excess stain had to be washed from the sample. It was an effective aid to automatic measurement of PVF and POFs from Atlantic cod, European hake, and Atlantic mackerel, though the coloration was not as intense compared to PAS. Also the PAS stain was particularly useful when applied to whole mounts from Atlantic cod making it easier to identify the outline of small POFs compared to PVF that were less intensely stained.

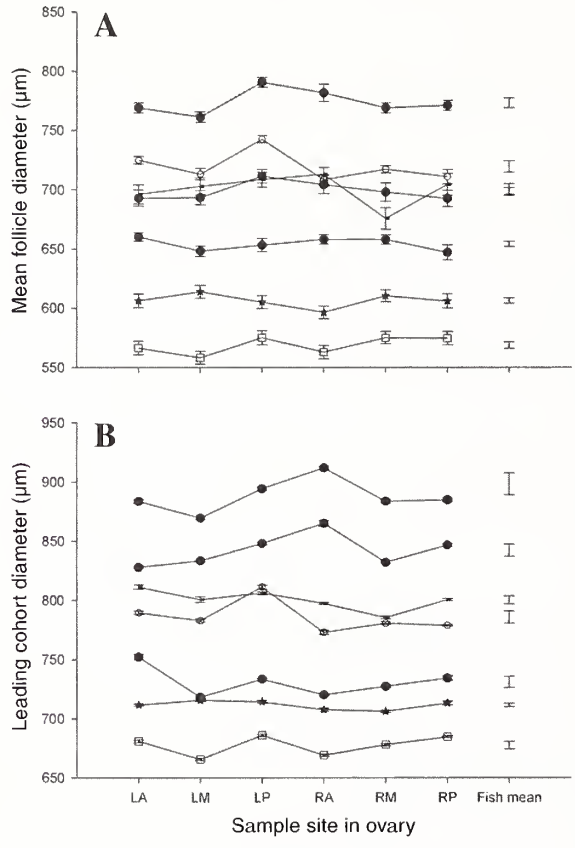

Figure 1

Comparison of mean follicle diameter (**A**) and leading cohort diameter (**B**) ±2 standard error taken from three sites, anterior (LA and RA), middle (LM and RM), and posterior (LP and RP), in each pair (left L or right R, respectively) of seven ovaries of Atlantic cod (*Gadus morhua*) caught by commercial vessel using gill nets landing at Andenes, Norway in 2007 (Table 1). Lines join the sites for each fish. Approximately 200 unstained follicles were measured using image analysis by the Institute of Marine Research Norway at each site. Fish mean refers to the overall mean follicle diameter of all sites for each fish.

Comparison of whole-mount method with histological method

A whole mount prepared from a female Atlantic cod caught during ovulation (Fig. 2A) revealed small POFs from earlier ovulations (Fig. 2B left) and also much larger POFs (Fig. 2B right). The latter appeared as large round membrane structures, about the size of hydrated follicles formed by the thecal and granulosa layers that remain in the ovary to form the POF. A burst zone in the circular membrane was also visible, probably made during the expulsion of the ripe egg. POF shape and morphology was equivalent in whole mounts and section and characterised by deep red staining in section and denser grey scale in stained and unstained whole mount respectively (Fig. 2B left and middle). PVFs in unstained whole mounts appeared quite translucent with a central nucleus that was consistent with their shape and form in section and easily distinguished from POFs.

Atretic follicles were rather easily identified in unstained whole mounts and their morphology could be equated to that seen in histological section (Fig. 3). Comparing these preparations the chorion appeared to be progressively broken down and provided a useful criterion to identify late alpha atretic follicles in whole mounts. A comparison of alpha atretic intensity between the two methods (Fig. 4) indicated that the whole mount preparation could provide an indication of both prevalence and intensity of atresia.

Fecundity maturation and down regulation

Atlantic cod fecundity data from the North and Irish Sea collected in 2003 and 2004 (Table 1) was analysed to investigate whether the relative fecundity declined during maturation. As the ovary matured and D_f increased from 350 to 800 µm the prevalence of atresia increased (Fig. 5). Relative intensity of atresia was absent in ovaries with a D_f of 350 µm and tended to remain at a fairly low level but with one much higher value when the mean follicular diameter was 650 µm. Also during this maturation period there was a drop in predicted mean relative fecundity for all fish in the sample amounting to 49.6% whilst fecundity diameter measured manually or automatically (F_d) increased from 355 to 794 µm. Analysis of the data from the 1995 survey indicated that fecundity was overestimated between 11% (Atlantic cod) and 13% for European plaice

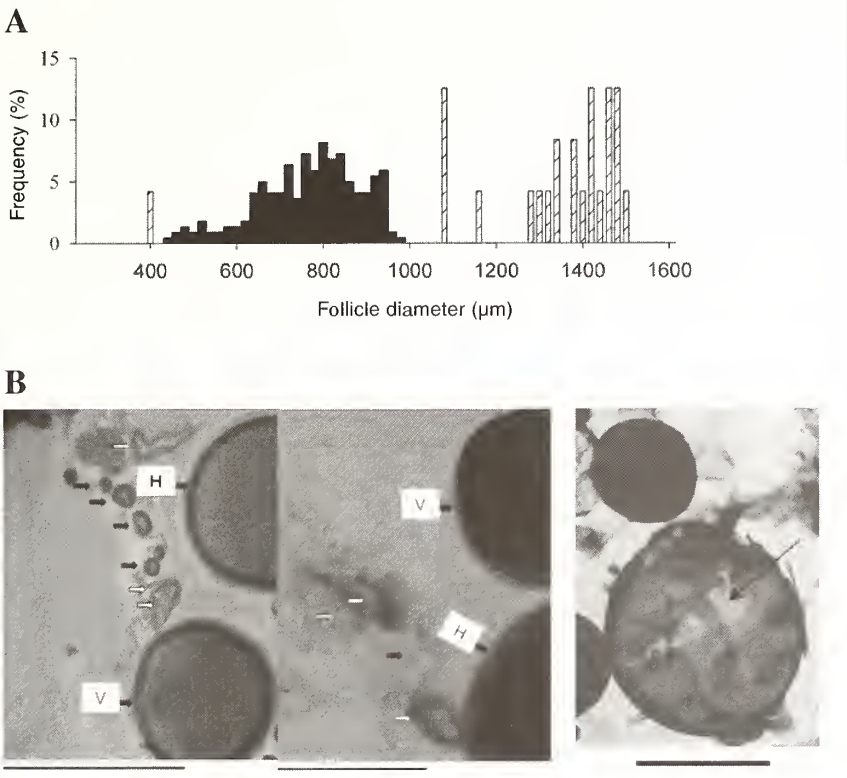

Figure 2

Morphology of ovary samples of Atlantic cod (*Gadus morhua*) taken from a research vessel trawl catch in the Irish Sea during 2003 shown as whole mounts and histological preparations. (**A**) The size frequency distribution measured in a whole mount of residual fecundity (black bars) and postovulatory follicles (POFs striped bars). The POFs from the most recent and previous ovulations appear to the right and left respectively of the residual fecundity. (**B**) (right image) shows the appearance of periodic acid-Schiff stained POF in whole mount from the most recent ovulation with an arrow pointing to the burst zone in the follicle membrane. B (left image) POFs from previous ovulations shown in histological section stained with PAS Mallory (left) and as a whole mount (right). The white and black arrows point to POFs and previtellogenic follicles respectively and box arrows show vitellogenic (V) and early hydration stage (H) follicles. The two scale bars on the left indicate 500 whilst the bar on the right shows 1000 μm.

and common sole (Fig. 6, Table 4). From the perspective of fecundity methodology, the measurement of F_d as well as the standing stock of fecundity make it possible to adjust the fecundity to the same point in maturation, defined by mean follicle size, close to the start of spawning.

Autodiametric calibration

The seven species examined, even when in an advanced stage of maturity, contained very different forms of fecundity size frequency distribution (Fig. 7) ranging from normal (Atlantic herring, European plaice, and redfish) to a more skewed shape (European hake and Atlantic mackerel). In two species (Atlantic cod and European plaice) samples with a hydrated, bimodal distribution were also included in the data set.

The equations (Table 5) from the regression analysis, based on the autodiametric calibration applied individually to Atlantic cod, Atlantic mackerel, Atlantic herring, European plaice, and redfish (Fig. 8) for each institute, made it possible to predict F_{ow} (Eqs. 4 and 5) with high precision in most cases (Table 6). European hake and Atlantic mackerel are examples where the vitellogenic follicle distribution is continuous extending down to overlap with the PVF population (Fig. 7) and produced a higher CV to predict F_{ow} from D_f using Equation 2. In the case of European plaice, Atlantic cod, and European hake, some ovaries contained both maturing and hydrated follicles

exhibiting a bimodal frequency distribution, but in each case the autodiametric calibration made it possible to make estimates of F_{ow} with an acceptable level of precision. Equation 5 gave a small but significant ($P<0.0001$) improved fit, but only for Atlantic cod with hydrated follicles, and reduced the CV of F_{ow} estimates predicted from 450 to 1050 μm D_f. The overall precision after inserting an ascending series of D_f in Equations 4 and 5, spanning the range found in each species was always better than a CV of 3% based on a prediction for new data.

A combination of the data in a general calibration curve (Fig.9A) is provided to show that the auto-diametric method has general application and may be used with other species. However when compared against the individual species model there was difference in the predictions by up to 20% both within species and between institutes (Table 6). The variance was greater in the fish with a continuous follicular distribution, especially in the case of European hake (Fig. 9, B and C).

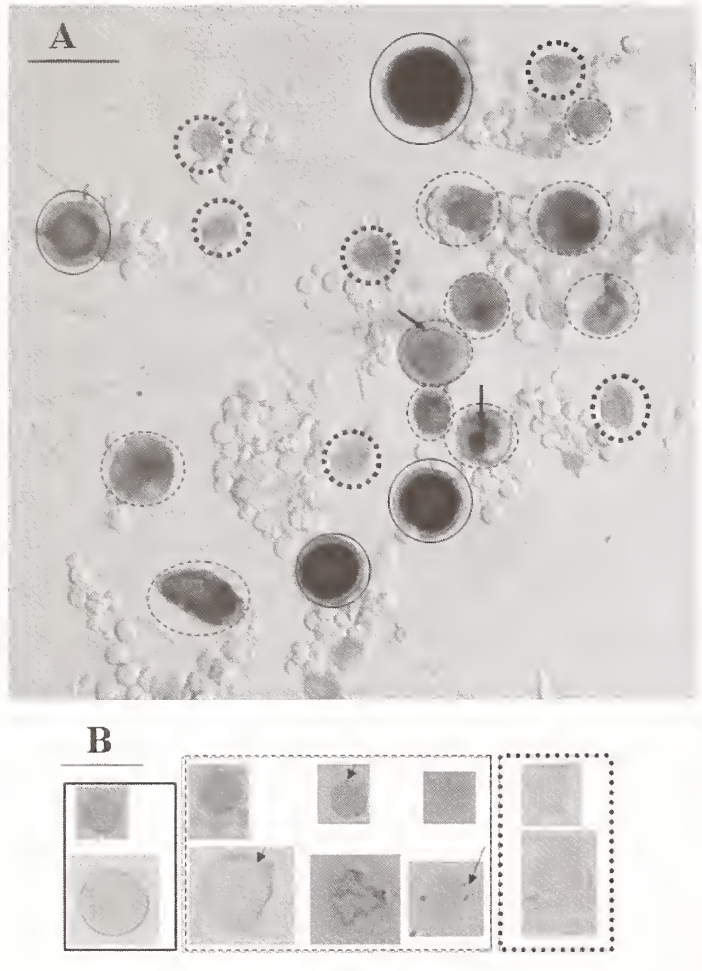

Figure 3

Appearances of atretic oocytes taken from 2 year old aquaculture reared Atlantic cod (*Gadus morhua*) at Institute IMR in 2004. (**A**) Image taken from an unstained whole mount prepared from an ovary biopsy containing high levels of alpha atretic follicles (dashed circles), beta atretic follicles (dotted circles), and normal vitellogenic follicles (black circles). (**B**) Histological section of the biopsy in A showing the same classes of follicle (outlined using the same line key as A) after processing into histological section. In each case arrows point to the disintegrating chorion used for classification of alpha atretic follicles. The scale bars (top left of A and B) = 500 μm.

Discussion

Our results show that the pipette method for sampling fresh ovaries at sea can be used to replace the need to return the whole ovary for the gravimetric fecundity method (Bagenal and Braum, 1968), provided ovarian weight can be recorded precisely onboard. Although the pipette fecundity was slightly lower (94.7%) compared to the gravimetric fecundity, we feel that the scale of difference can be easily nullified by a small correction factor and is small compared to the reported variability in fecundity over time (Rijnsdorp, 1991) and space (Witthames et al., 1995). Our confidence in making this statement is increased because of a direct comparison between both methods for the same ovary and because the autodiametric calibrations are very similar without large residuals attached to either method. A previous report described a cut down plastic syringe to suck up standard sized ovarian samples of 1.54 g (CV=3.7 n=155), but the commercially available alternative described in this paper has two advantages: 1) it is already calibrated for a range of sample sizes (25, 50, 100, and 200 μL), and 2) it is suited to taking small samples appropriate for fecundity determination in species such as Atlantic mackerel and European hake. In our results ovarian weight showed on average a small decline (–5%) from fresh to fixed weight for each species which was considerably different from a previous report (Klibansky and Juanes, 2007) at +5% or less. The reasons for the difference are not apparent but do not involve the ratio of fixative to weight of ovarian tissue because the range used in this work (1.7 to 9.1 times NBF to ovarian weight) spans the ratio of four times where a positive weight change was recorded.

Collection of fecundity samples in this way has clear advantages: 1) require small amounts (1.2 compared to more than 5000 ml for species like Atlantic cod) of NBF (classed as a carcinogen), 2) reduced exposure because of the smaller free surface for evaporation, 3) lower environmental impact for disposal of fixed tissue and waste fixative, 4) it is more feasible to collect fecundity samples on com-

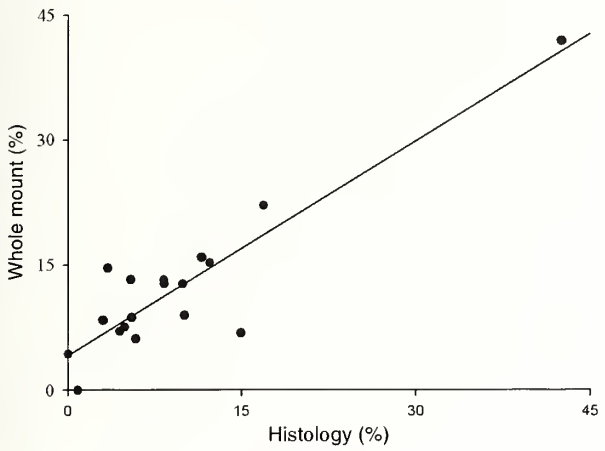

Figure 4

Comparison of atretic follicles as a percentage of atretic follicles divided by the sum of vitellogenic and atretic follicles in whole mount and histology, respectively found in 2 year old aquaculture reared Atlantic cod (*Gadus morhua*) at Institute IMR in 2004. The equation for the fitted line is W=H×0.85+4.20 (n=18, r^2=0.79, P <0.001).

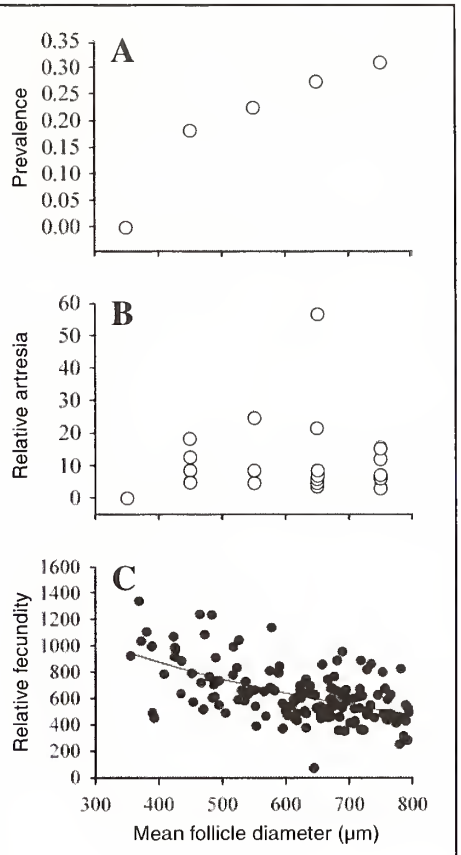

Figure 5

Down regulation of fecundity during maturation in North and Irish Sea Atlantic cod (*Gadus morhua*) collected in 2003 and 2004. (**A**) Prevalence of atretic follicles (proportion of fish with atresia) plotted against the mean follicle diameter of the fecundity (D_f, μm). (**B**) Relative intensity of atretic follicles (atretic follicles per g female whole weight) plotted against D_f (μm). (**C**) The decline in relative fecundity (F_{bw}=fecundity/body weight [g]) in relation to D_f (μm). The fitted line is from the equation F_{bw}=a×ln D_f + b where a=−581.9 and b=4360 (r^2=0.30, P for a and b <0.0001). Open circles are used in A and B because they refer to regressing follicles and filled circles are used in C to denote normal vitellogenic follicles.

mercial vessels, 4) easily portable samples that can be distributed at lower cost to facilitate exchange of samples between laboratories carrying out international egg production based stock assessments (Armstrong et al., 2001) and, not least, 5) better preservation of histological detail to identify and determine proportions of atretic and postovulatory follicles. Our finding that POF in recently ovulated ovaries are spherical and not collapsed, compared to previous studies, may be attributed to less compression in a biopsy compared to ovaries fixed whole.

A small difficulty in not returning the whole ovary back to the laboratory for subsampling means the ovary must be weighed at sea, sometimes in rough conditions, but this can be achieved using motion-compensated balances. Although this equipment is perhaps beyond some research budgets it has been successful even on commercial vessel in rough conditions providing the mass for weighing is less than 75% of the upper weighing range. Also balances are available with a resolution of 0.01 g making it feasible to weigh ovaries from probably all commercial species with an acceptable accuracy. If it is not feasible to use motion-compensated balances, it has been reported that ovaries can be returned for weighing after the end on of the cruise providing the ovary is packed to prevent water loss (Klibansky and Juanes, 2008). A further recommendation, in connection with using the pipette, is to complete at least duplicate samples and the follicles should not be larger than the pipette internal bore of 2 mm although exception can be made for hydrated follicles just larger than 2 mm.

In this study it was shown that the ovary is homogenous in regard to F_{ow} and D_f both for Atlantic cod and European hake. Homogenous packing has also been reported for hydrated oocytes prior to ovulation in European hake (Murua et al., 2006). The posterior region of the ovary is the most variable and in some fish this part can be packed with significantly different sized follicles and should be avoided. However, it should not be assumed that F_d is universally independent of location because small differences (2%) in F_d heterogeneity have been reported in flatfish species such as yellowfin

sole *Limanda asper* (Nichol and Acuna, 2001) and European plaice (Kennedy et al., 2007). Samples used for the auto-diametric calibration and in subsequent determination of F_{ow} should have the same fixation history because fixing conditions affect D_f, F_{ow}, and circularity and also affects the ovarian weight (Klibansky and Juanes, 2007) used to raise F_{ow} to fecundity.

We would not recommend the general use of PAS stain for image analysis in mature fish because it obscures the chorion detail which is used to classify atretic from normal vitellogenic follicles (Kjesbu et al., 1991). The main advantages of PAS, compared to the other stains evaluated, was that it was the most color fast, worked with all the species where it was tried, and provided specific staining to color more transparent objects such as cortical alveoli, hydrated, and postovulatory follicles. It is however more laborious to apply, but has been successful in all applications where it has been tried previously (Kennedy et al., 2007) and performed well in the comparison of manual versus automatic measurements. Similar results have also been found for nonstained follicles, although not reported in the results section.

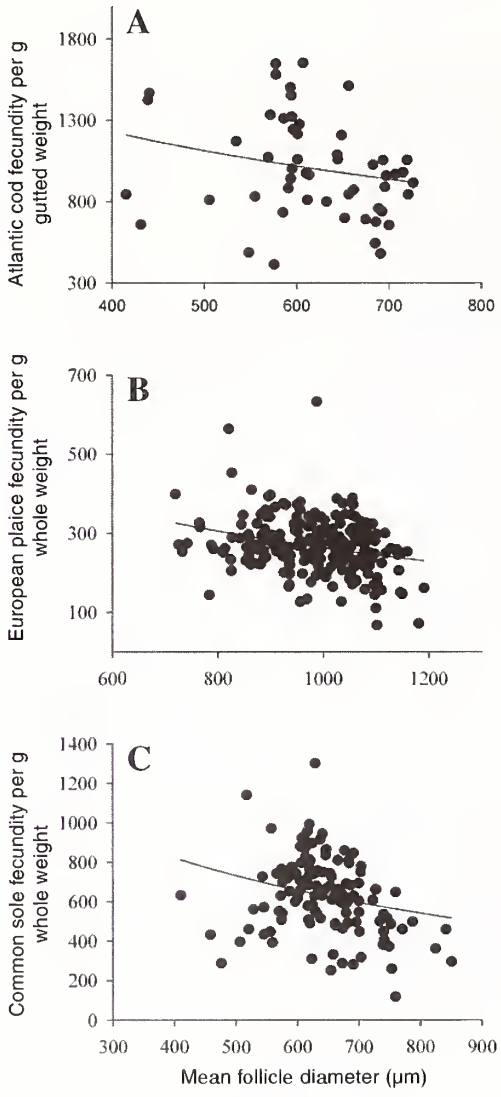

Figure 6

Reduction in relative fecundity (F_{bw}) during maturation, measured as mean follicle diameter (D_f, μm) in Atlantic cod (*Gadus morhua*), European plaice (*Pleuronectes platessa*), and common sole (*Solea solea*) (A–C, respectively) collected from the Irish Sea during 1995. The equation for the fitted line and regression coefficients are shown in Table 4.

Based on our results and earlier reports (Witthames and Greer-Walker, 1995; Kurita et al., 2003; Thorsen et al., 2006; Kennedy et al., 2007) fecundity is down regulated by the production of atretic follicles during maturation. If samples are taken close to spawning season, down regulation is not significant (Öskarsson and Taggart, 2006), but the timing of sampling should be considered especially when studying multiyear collections for example: Atlantic cod (McIntyre and Hutchings, 2003), European plaice (Horwood et al., 1986; Rijnsdorp, 1991) and common sole (Witthames et al., 1995). Using the autodiametric method, it was possible to predict D_f, providing data on ovarian weight and fecundity is reported using a rearranged Equation 4. This method was used in this study for 1995 survey data to standardize fecundity for maturity and indicated that the spawning stock biomass of Atlantic cod, European plaice, and common sole may have been overestimated by about 12% based on follicle diameters of 650, 1100, and 600 μm, respectively. Although we consider that follicular atresia was an important cause of negative fecundity residuals in this study, we do not exclude an alternative explanation that more fecund individuals within a fecundity sample produce smaller eggs, and vice versa (i.e., a trade off between fecundity and egg size). Such a trade off is likely in a comparison between stocks such as Atlantic herring (Winters et al., 1993) but has not, to our knowledge, been proven to occur within one stock. One report referring to Atlantic cod from the Norwegian coast (Kjesbu et al., 1996a) indicates that much of the variability in egg size occurs during the final maturation rather than variability in follicular size when final maturation occurs. Overall our view is that the relationship used for fecundity standardisation should be documented, including the follicle size reference point along with the unadjusted results.

Different image analysis configurations used by four institutes to collect the autodiametric calibration data produced a low CV of fecundity estimates for new predictions. The data can be accumulated without intervention (Thorsen and Kjesbu, 2001) in automatic mode and has utility for a number of species. Since it is an automatic process it is important that all follicular classes of interest are measured with equal selectivity, including cortical alveoli, atretic, or hydrated follicles. We suspect that the cause of the higher fecundity CV

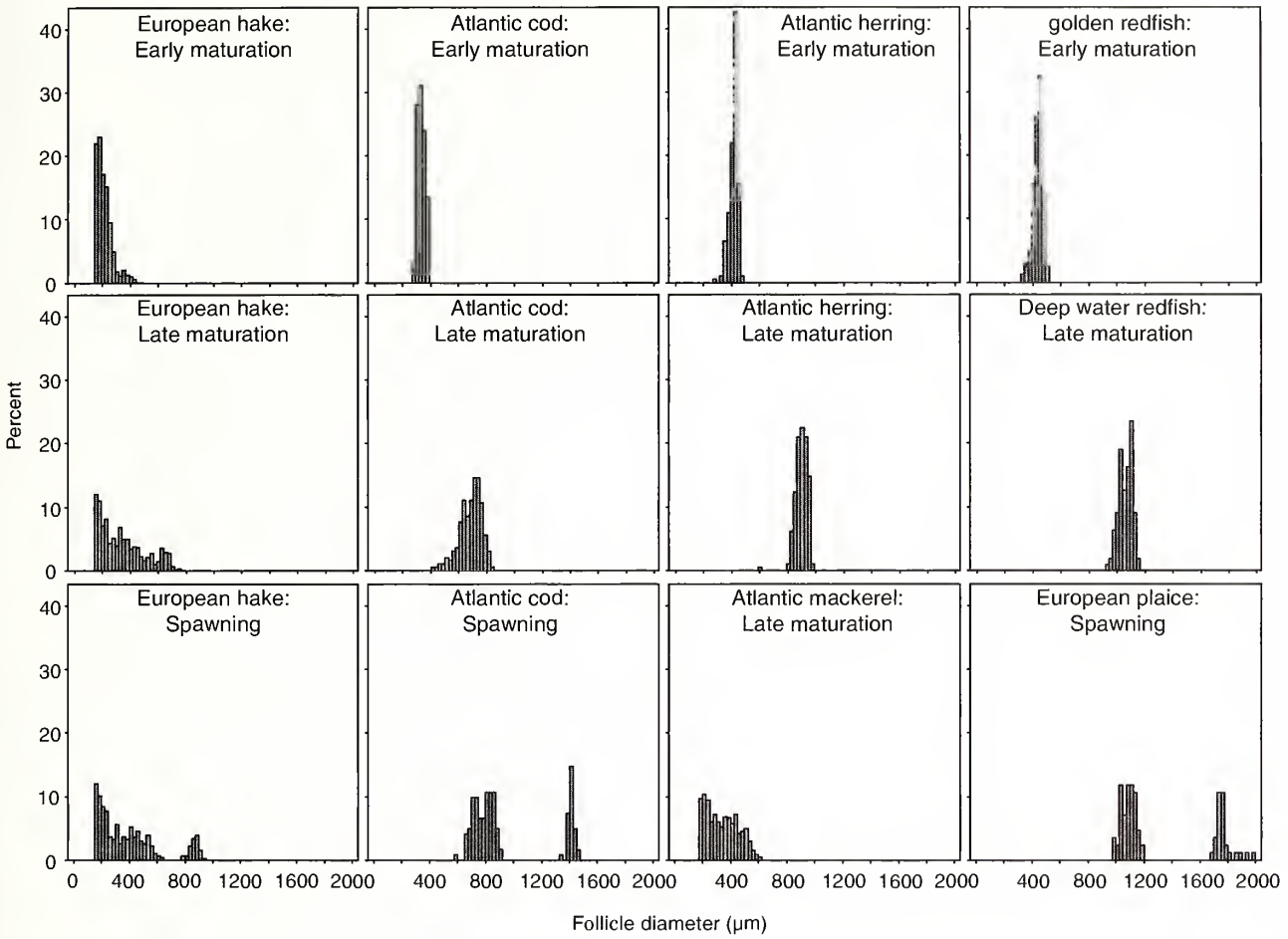

Figure 7

Follicle number per g of ovary (percentage of total count) per 25-μm class interval follicle diameter found in Atlantic cod (*Gadus morhua*), European hake (*Merluccius merluccius*), Atlantic herring (*Clupea harengus*), Atlantic mackerel (*Scomber scombrus*), European plaice (*Pleuronectes platessa*), redfish (deep water redfish [*Sebastes mentella*] or golden redfish [*Sebastes marinus*]) used to produce the autodiametric calibrations (Table 5) by Institutes AZTI (A, stained rose bengal), Cefas (B, stained with periodic acid Schiff's, except European plaice with eosin), CSIC (C, hake rose bengal, redfish unstained), and IMR (D, unstained).

Table 4

Regression coefficients used to fit relative potential fecundity (F_{bw}) with mean follicle diameter (D_f, μm) in the following equation $F_{bw} = a \times \mathrm{Ln}(D_f) + b$ using data collected from Atlantic cod (*Gadus morhua*), European plaice (*Pleuronectes platessa*), and common sole (*Solea solea*) caught in the Irish Sea during 1995.

Species	Coefficient		SE	t	P
Atlantic cod, n=54	b	4356	2039	4.6	<0.0001
	a	−521	317	−1.6	0.1068
European plaice, n=220	b	1578	318	55.0	<0.0001
	a	−190	46	−4.1	<0.0001
Common sole, n=129	b	3257	929	6.8	<0.0001
	a	−406	143	−2.8	0.0055

Table 5

Details of the autodiametric calibration relating follicle number (F_{ow}) to follicle diameter (D_f μm) using a linear equation $\ln F_{ow} = a \times \ln D_f + b$ and polynomial equation (5) $\ln F_{ow} = a \times \ln D_f + b \times \ln D_f^2 + c$ fitted to data collected by each institute: AZTI, Cefas, CSIC, and IMR for each species: Atlantic cod (*Gadus morhua*), European hake (*Merluccius merluccius*), Atlantic herring (*Clupea harengus*), Atlantic mackerel (*Scomber scombrus*), European plaice (*Pleuronectes platessa*), and redfish (deep water redfish [*Sebastes mentella*] or golden redfish [*Sebastes marinus*].

Species	Institute	*a*	*b*	*c*	*N*	r^2
Atlantic cod	Cefas	−3.106	28.777		28	0.972
Atlantic cod	Cefas polynomial	17.234	−1.5497	−37.864	28	0.986
Atlantic cod	IMR	−2.700	26.088		47	0.988
European hake	AZTI	−2.157	22.293		157	0.774
European hake	CSIC	−2.196	22.758		245	0.780
Atlantic herring	IMR	−2.718	26.287		23	0.971
Atlantic mackerel	Cefas	−2.528	25.030		78	0.761
European plaice	Cefas	−2.910	27.442		150	0.980
Redfish	CSIC	−2.551	25.040		147	0.948
General (excluding European hake)	All institutes except AZTI	−2.750	26.371		475	0.979

reported for species like European hake or Atlantic mackerel maybe attributed to the ovary being packed with a larger, and perhaps more variable partial volume of PVF associated with a continuous follicular distribution. Further analysis to determine the source of variation in the autodiametric calibration for fish with a continuous follicular frequency distribution is therefore considered worthwhile. Calibration data that included spawning Atlantic cod was best described by a polynomial model, although the additional term was not significant for the European plaice, even though the data included fish with hydrated follicles and POF. The difference may arise because European plaice produce fewer egg batches, about five (Urban, 1991), compared to between 14 and 21 in Atlantic cod (Kjesbu et al., 1996b). Thus, residual POFs in Atlantic cod ovaries should take up increasingly more space in the ovary towards the end of the spawning season changing the relative partial volume taken up by residual vitellogenic follicles.

An alternative to full automation is to use a semi-automatic analysis so that follicles that are not measured by the automatic analysis can still be measured manually. In practice, the dominant fecundity follicles were measured in automatic mode and then other follicular types, such as POFs or atretic follicles, are manually assigned and measured accumulating the measurements in user defined classes. This information can be used for more qualitative aspects, such as an overview of atresia intensity or confirming fish are at an advanced state of maturity, and also to provide a means to exclude fish that have started spawning. Our experience shows that POFs will arise from a synchronous ovulation that will produce a cohort of POFs of similar size and shape thus making their identification more certain. In practice we keep a tally of identified POFs in a separate class and reject the fish from the fecundity data set to apply the annual egg production method if five or more POFs with similar structures are found. The hydrated cohort were split from the vitellogenic mode to determine the batch fecundity by inspection of the frequency distribution produced from the follicular measurements. This provides a further advantage for the study of batch fecundity because it is easier to see and separate the next batch compared to the traditional gravimetric method described previously (Hunter and Macewicz, 1985a).

In conclusion the present study has shown that image analysis and the autodiametric method have wider application than originally reported (Thorsen and Kjesbu, 2001; Klibansky and Juanes, 2008). Although one report (Friedland et al., 2005) indicated caution in this respect, the range of spawning strategies and institutes participating in this study indicate that for species with a discontinuous follicular frequency distribution, the method is also reliable. However, the authors have demonstrated that a calibration should be done to validate the method in all new applications whether it involves new species, equipment, or situation. The use of the pipette makes it possible to take quantitative fecundity samples in situations were accurate balances, measuring to an accuracy of 0.1 mg, will not function. In addition this provided a means to calibrate the autodiametric method for routine quality control and substantially reducing the use of toxic fixative. Substantial histology costs can be avoided by improving the interpretation of whole mounts and the approach has great utility to study the fate of fecundity during the spawning season.

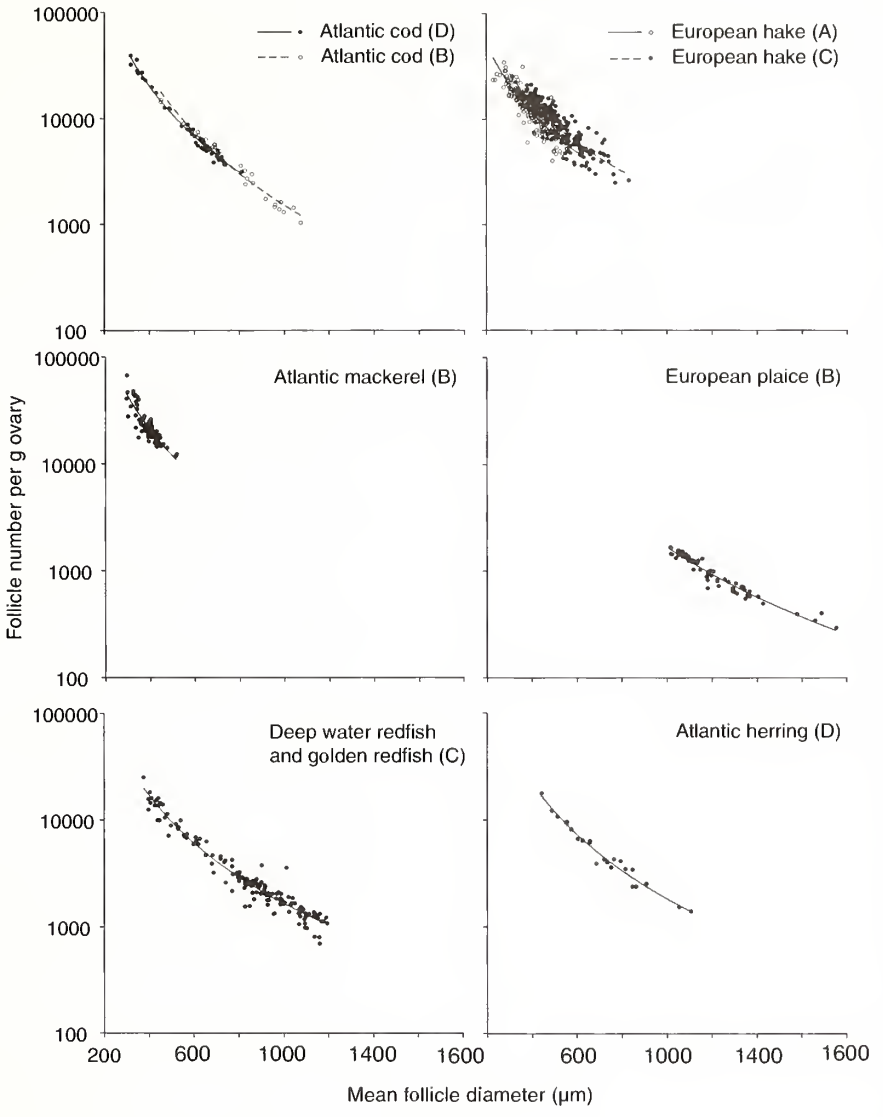

Figure 8

Autodiametric calibrations shown as scatter plots and fitted lines for Atlantic cod (*Gadus morhua*), European hake (*Merluccius merluccius*), Atlantic herring (*Clupea harengus*), Atlantic mackerel (*Scomber scombrus*), European plaice (*Pleuronectes platessa*), redfish (deep water redfish [*Sebastes mentella*] or golden redfish [*Sebastes marinus*]) used to produce the autodiametric calibrations (Table 5) by Institutes AZTI (A stained Rose Bengal), Cefas (B stained with periodic acid Schiff's, except European plaice with eosin), CSIC (C hake Rose Bengal, redfish unstained), and IMR (D unstained).

Acknowledgments

This study was jointly funded under European Union Frame Work V Q5RS-2002-01825 and the Institutes in England (Department of the Environment, Food, and Rural Affairs), Norway (Institute of Marine Research), and Spain (Consejo Superior de Investigaciones Científicas, and AZTI Tecnalia (publication number 424)). The first author would like to acknowledge the contribution of J. Pilkington who wrote the software code for Myrmica. This software will be distributed at no charge under a Free Software Foundation License at www.myrmica.co.uk.

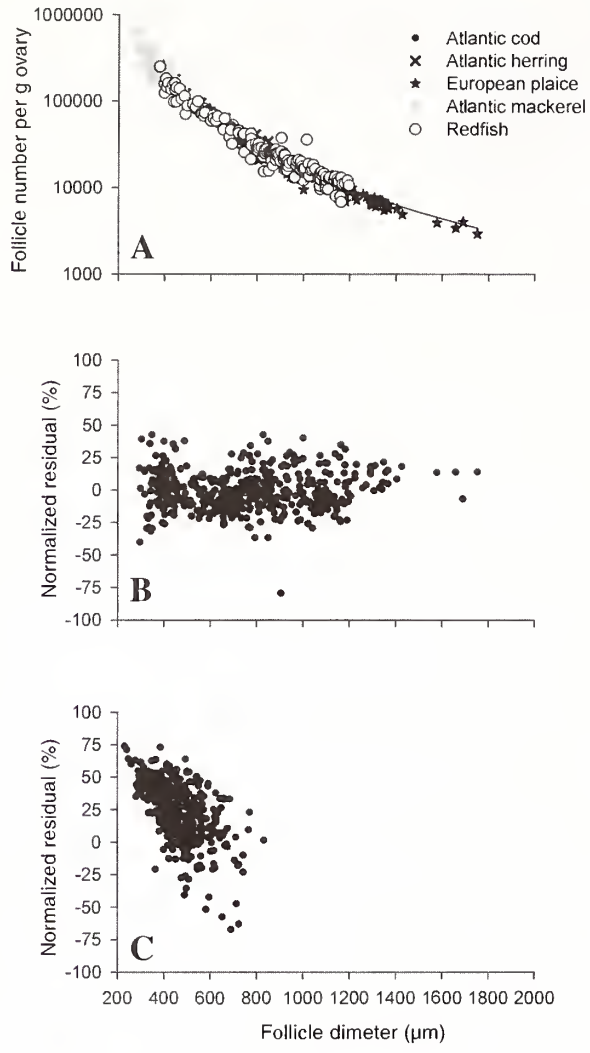

Figure 9

(**A**) General autodiametric calibration for Atlantic cod (*Gadus morhua*), Atlantic herring (*Clupea harengus*), Atlantic mackerel (*Scomber scombrus*), European plaice (*Pleuronectes platessa*), redfish (deep water redfish [*Sebastes mentella*]) or golden redfish (*Sebastes marinus*) used to produce the autodiametric calibrations (Table 5) by Institutes Cefas (B, stained with periodic acid Schiff's, except European plaice with eosin), CSIC (C, hake rose bengal, redfish unstained), and IMR (D, unstained) based on the combined data D_f and follicle number (F_{ow}). The parameters (Table 5) for the fitted line were based on Equation 4 ($\ln F_{ow} = a \times \ln D_f + b$). P for a and b was <0.001. (**B**) Plot of normalised residual $(F-O_s)/F \times 100$ where O_s=observed value for Atlantic cod, Atlantic herring, Atlantic mackerel, European plaice, and redfish (deep water redfish (*Sebastes mentella*) or ocean perch (*Sebastes marinus*) and F=fitted value based on F_{ow} against D_f (Eq. 4). (**C**) Plot of normalized residual $(F-O_h)/F \times 100$ where O_h=observed fecundity for European hake (*Merluccius merluccius*), and F=fitted fecundity value based on the observed F_d for hake substituted in the general model (Eq. 4).

Table 6

Predicted values (coefficient of variation) of follicle number per gram of ovary (F_{ow}) from mean follicle diameter (D_f, µm) using a linear equation $\ln F_{ow} = a \times \ln D_f + b$ and polynomial equation [1] $\ln F_{ow} = a \times \ln D_f + b \times \ln D_f^2 + c$ fitted and regression parameters in Table 5 specific for each species (Atlantic cod [*Gadus morhua*], European hake [*Merluccius merluccius*], Atlantic herring [*Clupea harengus*], Atlantic mackerel [*Scomber scombrus*], European plaice [*Pleuronectes platessa*], redfish (deep water redfish [*Sebastes mentella*] or golden redfish [*Sebastes marinus*]) and institute (AZTI, Cefas, CSIC, IMR).

	D_f values substituted in the linear and polynomial [1] equations									
Species: Institutes	300	450	600	750	900	1050	1200	1350	1500	1650
Atlantic cod: IMR		14665 (0.87)	6744 (0.94)	3692 (1.01)						
Atlantic cod: Cefas		18033 (1.57)	7380 (1.63)	3690 (1.75)	2094 (1.89)	1297 (2.07)				
Atlantic cod[1]: Cefas		14488 (1.18)	7358 (1.11)	3819 (1.21)	1993 (1.31)	1061 (1.55)				
European hake: AZTI	21742 (2.20)	9065 (2.41)	4873 (2.62)	3011 (2.84)						
European hake: CSIC	27700 (2.20)	11368 (2.38)	6043 (2.56)	3684 (2.73)						
Atlantic herring: IMR		15990 (1.35)	7315 (1.38)	3988 (1.47)	2430 (1.60)	1598 (1.75)				
Atlantic mackerel: Cefas	43056 (1.68)	15448 (1.82)								
European plaice: Cefas		15703 (1.73)	6798 (1.48)	3551 (1.59)	2089 (1.70)	1334 (1.81)	904 (1.91)	642 (2.02)	472 (2.13)	358 (2.2)
Redfish: CSIC		12703 (1.97)	6097 (2.11)	3450 (2.25)	2166 (2.19)	1462 (2.52)	1040 (2.65)			

Literature cited

Andersen, T. E.
2003. Unbiased stereological estimation of cell numbers and volume fraction: the disector and the principles of point counting. *In* Fisken Havet 2003(12): Report of the working group on modern approaches to assess fecundity and maturity of warm- and cold-water fish and squids (O. S. Kjesbu, J. R. Hunter, and P. R. Witthames, eds.), p. 11–18. The Institute of Marine Research, Bergen, Norway.

Armstrong, M. J. P., P. Conolly, R. D. M. Nash, M. G. Pawson, E. Alesworth, P. J. Coulahan, M. Dickey-Collas, S. P. Milligan, M. F. O'Neill, P. R. Witthames, and L. Woolner.
2001. An application of the annual egg production method to estimate the spawning biomass of cod (*Gadus morhua* L), plaice (*Pleuronectes platessa* L) and sole (*Solea solea* L.) in the Irish Sea. ICES J. Mar. Sci. 58:183–203.

Bagenal, T. B., and E. Braum.
1968. Eggs and early life history. *In* Methods of assessment of fish production in fresh waters (W. E. Ricker, ed.), p. 165–201. Blackwell Sci. Publ., Oxford, U.K.

Beverton, R. J. H., and S. J. Holt.
1957. On the dynamics of exploited fish populations. Fish. Invest Ser. II Mar. Fish. G.B. Minist. Agric. Fish Food 19:1–553.

Bromley, P. J., C. Ravier, and P. R. Witthames.
2000. The influence of feeding regime on sexual maturation, fecundity and atresia in first time spawning turbot. J. Fish Biol. 56:264–278.

Emerson, L. S., M. Greer-Walker, and P. R. Witthames.
1990. A stereological method for estimating fish fecundity. J. Fish Biol. 36:721–730.

Friedland, K. D., D. Ama-abasi, M. Manning, L. Clarke, G. Kligys, and R. C. Chambers.
2005. Automated egg counting and sizing from scanned images: rapid sample processing and large data volumes for fecundity estimates. J. Sea Res. 54:307–316.

Greer-Walker, M., P. R. Witthames, and I. Bautista de los Santos.
1994. Is the fecundity of the Atlantic mackerel (*Scomber scombrus:* Scombridae) determinate? Sarsia 79:13–26.

Horwood, J. W., R. C. A. Bannister, and G. J. Howlett.
1986. Comparative fecundity of North Sea plaice (*Pleuronectes platessa* L.). Proc. R. Soc. Lond. Ser. B. 228:401–431.

Hunter, J. R., and B. J. Macewicz.
1985a. Measurement of spawning frequency in multiple spawning fishes. *In* An egg production method for estimating spawning biomass of pelagic fish: application to the northern anchovy, *Engraulis mordax* (Lasker, ed.), p. 79–94. NOAA Tech. Rep. NMFS 36, Springfield, VA.
1985b. Rates of atresia in the ovary of captive and wild northern anchovy, *Engraulis mordax*. Fish. Bull. 83:119–136.
2003. Improving the accuracy and precision of reproductive information used in fisheries. *In* Fisken Havet 2003(12): Report of the working group on modern approaches to assess fecundity and maturity of warm- and cold-water fish and squids (O. S. Kjesbu, J. R. Hunter, and P. R. Witthames, eds.), p. 57–68. The Institute of Marine Research, Bergen, Norway.

Hunter, J. R., B. J. Macewicz. N. C. H. Lo, and C. A. Kimbrell.
1992. Fecundity, spawning, and maturity of female Dover sole *Microstomus pacificus*, with an evaluation of assumptions and precision. Fish. Bull. 90:101–128.

Kennedy, J., P. R. Witthames, and R. D. M. Nash.
2007. The concept of fecundity regulation in plaice (*Pleuronectes platessa* L.) tested on three Irish Sea spawning populations. Can. J. Fish. Aquat. Sci. 64:587–601.

Khoo, H. K.
1979. The histochemistry and endocrine control of vitellogenesis in goldfish ovaries. Can. J. Zool. 57:617–626.

Kjesbu, O. S.
1991. A simple method for determining the maturity stages of Northeast Arctic cod (*Gadus morhua* L.) by in vitro examination of oocytes. Sarsia 75:335–338.

Kjesbu, O. S., J. Klungsoyr, H. Kryvi, P. R. Witthames, P. R., and M. Greer-Walker.
1991. Fecundity, atresia, and egg size of captive Atlantic cod (*Gadus morhua*) in relation to proximate body composition. Can. J. Fish. Aquat. Sci. 48:2333–2343.

Kjesbu, O.S., H. Kryvi, and B. Norberg.
1996a. Oocyte size and structure in relation to blood plasma steroid hormones in individually monitored, spawning Atlantic cod. J. Fish Biol. 49:1197–1215.

Kjesbu, O. S., P. Solemdal, P. Bratland, and M. Fonn.
1996b. Variation in annual egg production in individual captive Atlantic cod (*Gadus morhua*). Can. J. Fish. Aquat. Sci. 53:610–620.

Kjesbu, O. S., and P. R. Witthames.
2007. Evolutionary pressure on reproductive strategies in flatfish and groundfish: Relevant concepts and methodological advancements. J. Sea Res. 58:23–34.

Klibansky, N., and F. Juanes.
2007. Species-specific effects of four preservative treatments on oocytes and ovarian material of Atlantic cod (*Gadus morhua*), haddock (*Melanogrammus aeglefinus*), and American plaice (*Hippoglossoides platessoides*). Fish. Bull. 105:538–547.
2008. Procedures for efficiently producing high-quality fecundity data on a small budget. Fish. Res. 89:84–89.

Kurita, Y., O. S. Kjesbu, and S. Meier.
2003. Oocyte growth and fecundity regulation by atresia of Atlantic herring (*Clupea harengus*) in relation to body condition throughout the maturation cycle. J. Sea Res. 49:203–219.

Lo, N. C. H., J. R. Hunter, H. G.. Moser, P. E. Smith, and R. D. Methot.
1992. The daily fecundity reduction method: A new procedure for estimating adult fish biomass. ICES J. Mar. Sci. 49:209–215.

Lockwood, S. J., J. H. Nichols, and W. A. Dawson.
1981. The estimation of a mackerel (*Scomber scomber* L.) spawning stock size by plankton survey. J. Plankton Res. 3:217–233.

Marshall, T. C., O. S. Kjesbu, N. A. Yaragina, P. Solemdal, and Ø. Ulltang.
1998. Is spawning stock biomass a sensitive measure of the reproductive potential of Northeast Arctic cod? Can. J. Fish. Aquat. Sci. 55:1766–1783.

Marshall, T. C., N. A. Yaragina, Y. Lambert, and O. S. Kjesbu.
1999. Total lipid energy as a proxy for total egg production by fish stocks. Nature 402:288–290.

McBride, R. S., and P. E. Thurman.
2003. Reproductive biology of *Hemiramphus brasiliensis*

and *H. balao* (Hemiramphidae): Maturation, spawning frequency, and fecundity. Biol. Bull. 204:57–67.

McIntyre, T. M., and J. A. Hutchings.
2003. Small-scale temporal and spatial variation in Atlantic cod (*Gadus morhua*) life history. Can. J. Fish. Aquat. Sci. 60:1111–1121.

Murua, H., G. Kraus, F. Saborido-Rey, P. R. Witthames, A. Thorsen, and S. Junquera.
2003. Procedure to estimate fecundity of marine fish species in relation to their reproductive strategy. J. Northwest Atl. Fish. Sci. 33:33–54.

Murua H., P. Lucio, M. Santurtun, and L. Motos.
2006. Seasonal variation in egg production and batch fecundity of European hake *Merluccius merluccius* (L.) in the Bay of Biscay. J. Fish Biol. 69:1304–1316.

Murua, H., and L. Motos.
2006. Reproductive strategy and spawning activity of the European hake, *Merluccius merluccius* L., in the Bay of Biscay. J. Fish Biol. 69:1288–1303.

Murua, H., and F. Saborido-Rey.
2003. Female reproductive strategies of marine fish species of the North Atlantic. J. Northwest Atl. Fish. Sci. 33:23–31.

Nichol, D. G., and E. I. Acuna.
2001. Annual and batch fecundities of yellowfin sole, *Limanda aspera*, in the eastern Bering Sea. Fish. Bull. 99:108–122.

Óskarsson, G. J., O. S. Kjesbu, and A. Slotte.
2002. Predictions of realized fecundity and spawning time in Norwegian spring-spawning herring (*Clupea harengus*). J. Sea Res. 48:59–79.

Óskarsson, G. J., and C. T. Taggart.
2006. Fecundity variation in Icelandic summer-spawning herring and implications for reproductive potential. ICES J. Mar. Sci. 63:493–503.

Parker, K.
1980. A direct method for estimating northern anchovy, *Engraulis mordex*, spawning biomass. Fish. Bull. 78:541–544.

Ramsay, K., and P. R.Witthames.
1996. Using oocyte size to assess seasonal ovarian development in *Solea solea* (L.). J. Sea Res. 36:275–283.

Rijnsdorp, A. D.
1991. Changes in fecundity of female North Sea plaice (*Pleuronectes platessa* L.) between three periods since 1900. ICES J. Mar. Sci. 48:253–280.

Simpson, A. C.
1951. The fecundity of the plaice. Fish. Invest. Ser. II Mar Fish. G.B. Minist. Agric. Fish Food 17:1–27.

Thorsen, A., and O. S. Kjesbu.
2001. A rapid method for the estimation of oocyte size and potential fecundity in Atlantic cod using computer-aided particle analysis system. J. Sea Res. 46:295–308.

Thorsen, A., C. T. Marshall, and O. S. Kjesbu.
2006. Comparison of various potential fecundity models for north-east Arctic cod *Gadus morhua*, L. using oocyte diameter as a standardizing factor. J. Fish Biol. 69:1709–1730.

Tyler, C. R., and J. P. Sumpter.
1996. Oocyte growth and development in teleosts [Review]. Rev. Fish Biol. Fish. 6:287–318.

Urban, J.
1991. Reproductive strategies of North Sea plaice, *Pleuronectes platessa,* and North Sea sole, *Solea solea*: batch spawning cycle and batch fecundity. Meeresforschung 33:330–339.

Winters, G. H., J. P. Wheeler, and D. Stansbury.
1993. Variability in the reproductive output of spring-spawning herring in the north-west Atlantic. ICES J. Mar. Sci. 50:15–25.

Witthames, P. R.
2003. Methods to assess maturity and realized fecundity illustrated by studies on Dover sole *Solea solea*. *In* Fisken Havet 2003(12): Report of the working group on modern approaches to assess fecundity and maturity of warm- and cold-water fish and squids (O. S. Kjesbu, J. R. Hunter, and P. R. Witthames, eds.), p. 125–137. The Institute of Marine Research, Bergen, Norway.

Witthames, P. R., and M. Greer-Walker.
1987. An automated method for counting and sizing fish eggs. J. Fish Biol. 30:225–235.
1995. Determination of fecundity and oocyte atresia in sole (*Solea solea*) (Pisces) from the Channel, the North Sea and the Irish Sea. Aquat. Living Resour. 8:91–109.

Witthames, P. R., M. Greer-Walker, M. T. Dinis, and C. L. Whiting.
1995. The geographical variation in the potential fecundity of Dover sole *Solea solea* (L) from European Shelf edge waters during 1991. J. Sea Res. 34:45–58.

Witthames, P. R., and C. T. Marshall.
2008. The importance of reproductive dynamics in fish stock assessments. *In* Advances in fisheries science: 50 years on from Beverton and Holt (A. Payne, J. Cotter, and T. Potter, eds.), p. 306–324. Blackwell Publ., Oxford, U.K.

Anadromous fish as marine nutrient vectors

Stephen E. MacAvoy (contact author)[1]
Greg C. Garman[2]
Stephen A. Macko[3, 4]

Email address for contact author: macavoy@american.edu

[1] Department of Environmental Science
American University
4400 Massachusetts Ave. NW
Washington, DC 20016

[2] Center for Environmental Studies
Virginia Commonwealth University
1000 W. Cary St., Suite 111
Richmond, Virginia 23284

[3] Environmental Science Department
University of Virginia
291 McCormick Rd.
Charlottesville, Virginia 22903

[4] Program in Geobiology and Low Temperature Geochemistry
U.S. National Science Foundation
4201 Wilson Boulevard
Arlington, Virginia 22230

Abstract—The tidal freshwater of Virginia supports anadromous herring (*Alosa* spp.) spawning runs in the spring; however, their importance as nutrient delivery vectors to the freshwater fish food web remains unknown. The stable isotope signatures of fishes from 21 species and four different guilds (predators, carnivores, generalists, and planktivores) were examined in this study to test the hypothesis that marine derived nutrients (MDNs) brought by anadromous fish would be traced into the guilds that incorporated them. Spawning anadromous fish were ^{13}C and ^{34}S-enriched ($\delta^{13}C$ and $\delta^{34}S$ of approximately 18‰ and 17.7‰, respectively) relative to resident freshwater fish. Of the guilds examined, only predators showed ^{13}C and ^{34}S-enrichment similar to the anadromous fish; however, some generalist catfish also showed enriched signatures. Specific fatty acid $\delta^{13}C$ signatures for gizzard shad (*Dorosoma cepedianum*), blue catfish (*Ictalurus furcatus*), and alewife (*Alosa pseudoharengus*), show a 10‰ range among fishes, clearly reflecting isotopically distinct dietary sources. The $\delta^{13}C$ and $\delta^{34}S$ distribution and range among the freshwater fishes suggest that both autochthonous and allochthonous (terrestrial C3 photosynthetic production and MDN) nutrient sources are important to the tidal freshwater fish community.

Manuscript submitted 25 June 2008.
Manuscript accepted 20 October 2008.
Fish. Bull. 107:165–174 (2009).

Streams in which anadromous fish spawn are often nutrient poor and the spawning anadromous fish may be an important source of nutrients to them (Kline et al., 1993; Wipfli et al., 2003). Sometimes spawning anadromous fish even fertilize near-stream terrestrial environments (Ben-David et al., 1998; Koyama et al., 2005). The spawning fish are frequently semelparous and deliver marine derived nutrients (MDN) to the freshwater as moribund biomass, excreted ammonium ion (NH_4^+), or through gamete release (Cederholm et al., 1989; Browder and Garman, 1994; Wipfli et al., 2003). Several studies in Alaska and the Pacific Northwest of North America have demonstrated the importance of marine nutrients brought to freshwater streams by anadromous salmonids (Bilby et al., 2003; Kline et al., 1993; Francis et al., 2006). In the Gulf of Mexico, migrating Gulf menhaden (*Brevoortia patronus*) transported estuarine nutrients into inshore environments (Deegan, 1993), and returning salmon contributed to the productivity of Lake Ontario tributaries (Rand et al., 2002). However, less work has been done on the East Coast of the United States where coastal development has been much more intense and the dominant anadromous species (*Alosa* spp.; herring (*A. aestivalis*), American shad (*A. sapidissima*), and alewife (*A. pseudoharengus*)) are often not highly abundant (Deegan, 1993; Garman and Macko, 1998). Although the *Alosa* spp. on the east coast tend towards an iteroparous life cycle rather than a semelparous one, they do experience heavy postspawning mortality (alewife postspawning mortality has been measured as 41% (Havey, 1961) and between 39% and 57% (Durbin et al., 1979)). Because tidal freshwater streams receive nutrients from marine and freshwater primary productivity at different times, the incorporation of these nutrients by consumers may be different depending on feeding guilds. Fish found in the same area in a stream may derive nutrition from local or translocated productivity. In nutrient poor systems, such as East Coast United States tidal freshwater areas, it is important to understand nutrient sources to different feeding guilds (e.g., predators, carnivores, generalists, and planktivores).

For more than 20 years now, carbon and nitrogen stable isotopes (re-

ported as a ratio of heavy to light isotopes and given δ notation with units of ‰, see *Materials and methods* section for more detail) have been used to determine the importance of MDN in freshwater systems, and to characterize the trophic structure within those systems (Kline, et al., 1993; Vander-Zanden et al., 1999). For example, carbon and nitrogen isotopes have shown that anadromous Pacific salmon (*Oncorhynchus* spp.) were a significant source of allochthonous nitrogen to coastal streams where spawning occurs (Kline et al., 1993).

Hesslein et al. (1991) used sulfur isotopes to differentiate freshwater migratory and non-migratory fishes in the Mackenzie River Basin, Canada. On the East Coast of the United States, anadromous river herring (*Alosa* spp.) retain their marine isotope signal after spending part of the spring spawning in freshwater, and that some freshwater piscivores are ^{34}S and ^{13}C-enriched after preferentially consuming migrating *Alosa* spp. during the spawning run (Garman and Macko, 1998; MacAvoy et al., 2000).

An additional tool for determining origins and transformations of organic material from different sources is the stable isotope ratio of specific compounds. Isolating a specific compound, or class of compounds, then measuring the isotope ratio on those compounds, may offer a more robust technique to trace biologically significant compounds (such as fatty or amino acids) than would be possible from bulk isotope analysis alone. For example, examining the carbon isotopic composition of fatty acids from an animal, particularly essential fatty acids, allows the direct determination of dietary sources that contribute to the fatty acid pool of that animal (Stott et al., 1997). Although bulk isotope analysis can be an effective nutrient tracer in systems with isotopically distinct nutrient sources (Peterson et al., 1985), the isotopes of specific fatty acids may provide more confidence in identifying sources (Canuel et al., 1997).

Carnivorous heterotrophs are unable to synthesize fatty acids longer than 18-carbons, nor can they desaturate carbon-carbon bonds between the ninth and terminal methyl carbon, therefore, these essential fatty acids must be obtained from diet (Olsen 1999). Because essential fatty acids are not influenced by subsequent metabolism within a eukaryotic heterotroph, they retain their original isotope composition (Stott et al., 1997). Fatty acids synthesized by marine plankton and incorporated into marine fish would be highly enriched in ^{13}C relative to those produced by freshwater primary producers or C3 photosynthesis. Additionally, short chain fatty acids, used as precursors in the biosynthesis of unsaturated or longer chain saturated fatty acids, should be ^{13}C enriched in relation to biosynthesized fatty acid products (Murphy and Abrajano, 1994). In this study, the fatty acid nomenclature used is carbon number:number of double bonds. For example, 18:2 is an 18-carbon fatty acid with two points of unsaturation. The desaturation of 16:0 to 16:1 and 18:0 to 18:1–18:2 occurs by a systematic fractionation of roughly 2‰ per desaturation (DeNiro and Epstein, 1977; Monson and Hayes, 1982). Also, studies have shown that the elongation of fatty acids by *de novo* synthesis results in a 2‰ per 2-carbon acetyl group addition. These fractionations allowed the identification of fatty acids that were directly incorporated from symbiotic bacterial sources in mussels as opposed to those obtained through *de novo* synthesis (Murphy and Abrajano, 1994).

In this study we compared the $\delta^{15}N$, $\delta^{13}C$, $\delta^{34}S$ of bulk tissues, plus the $\delta^{13}C$ of specific fatty acids among four guilds of fish plus anadromous *Alosa* spp. in a tidal freshwater stream on the East Coast of the United States. Our objective was to determine if anadromous fish, captured more than 40 km from the salt-wedge, were isotopically distinct from freshwater residents, and to determine if freshwater guilds showed the incorporation of marine allochthonous organic material.

Materials and methods

Field collections by boat electrofisher were made in the tributaries and main-stem of the Rappahannock River, VA (within a 40-mile area between Fredericksburg and Tappahannock, VA) during March and May 1997 and 1998 (Fig. 1). The Rappahannock River is tidal in this region (tidal range: 0.1 to 1 meter) and shares many physicochemical characteristics with other tidal freshwater rivers in the region (Garman and Nielsen, 1992). Fishes were collected and placed on ice in the field, transported back to the laboratory, and muscle tissue samples were taken, which were then dried for later analysis. Analysis of the sulfur and compound specific fatty acid samples took several years and were completed by 2002.

The fishes were placed into four different guilds based on feeding strategies taken from Jenkins and Burkhead's (1993) seminal work on Virginia freshwater fishes, plus an anadromous life cycle group (Table 1).

Bulk isotope tissue analysis, elemental analyzer, and isotope ratio mass spectrometry

Samples of dorsal muscle tissue were dried at 60°C for three days and homogenized in preparation for analysis. The tissues were then lipid extracted by refluxing them in dichloromethane for 35 minutes (Knoff et al., 2002), except for those samples selected for compound specific analysis, which were soxlet extracted (see below; gas chromatography-mass spectrometry (GC-MS) and compound specific stable isotope analysis (CSIA)). One milligram (mg) of dried, lipid-extracted muscle was used for $\delta^{13}C$ and $\delta^{15}N$ analysis. Six mg was used for $\delta^{34}S$ analysis. A Carlo Erba elemental analyzer (EA) (Fisons/VG/Micromass, Manchester, UK) coupled to a Micromass Optima isotope ratio mass spectrometer (IRMS) (Fisons/VG/Micromass, Manchester, UK) was used to obtain $\delta^{13}C$, $\delta^{15}N$ and $\delta^{34}S$ values. The $\delta^{13}C$ and $\delta^{15}N$ were obtained concurrently, and $\delta^{34}S$ was determined during separate analytical runs.

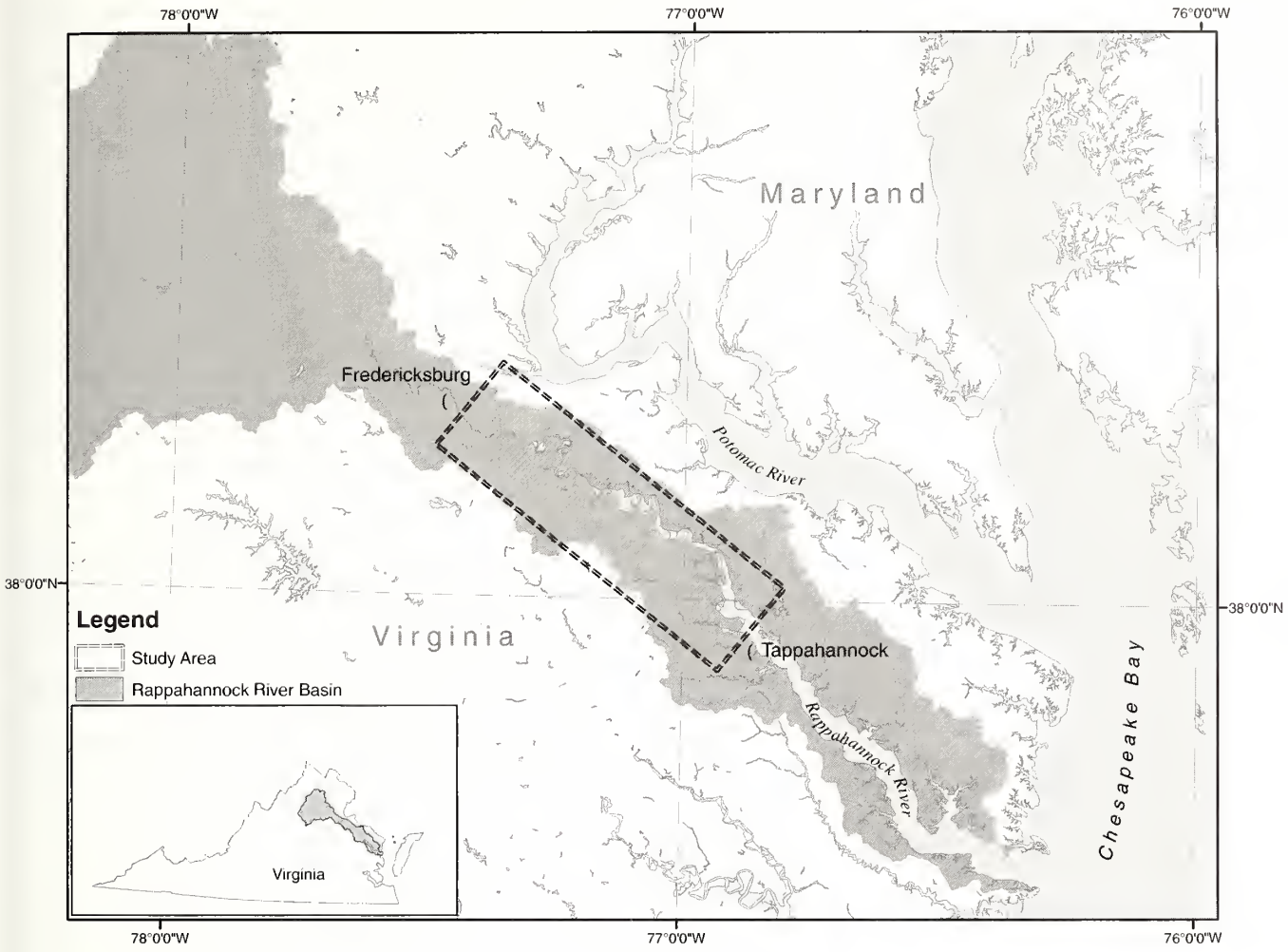

Figure 1

The boxed area indicates the section of the Rappahannock River, Virginia, between the towns of Fredericksburg and Tappahannock, where all fish were captured to determine the role of anadromous fish as marine nutrient vectors to the freshwater environment. Boat electrofishing was conducted between February and May 1997 and 1999. Sampling was conducted so that fish were captured before, during and after the spring spawning run of the anadromous *Alosa* spp.

The isotope compositions are reported in relation to standard material and follow the same procedure for all stable isotopic measurements, as follows:

$$\delta^x E = [({}^xE/{}^yE)\text{sample}/({}^xE/{}^yE)\text{standard}] - 1) \times 1000, \quad (1)$$

where E = the element analyzed (C, N, or S);
x = the molecular weight of the heavier isotope; and
y = lighter isotope (x=13, 15, 34, and y=12, 14, 32 for C, N, and S, respectively).

The standard materials to which the samples are compared are Pee Dee Belemnite for carbon, air N_2 for nitrogen, and Canyon Diablo Triolite for sulfur. Reproducibility of all measurements was typically 0.2‰ or better. Between every 12 samples, a laboratory standard was analyzed. In a typical run of 60 samples (+5 standards, 65 measurements total) the standard deviations for $\delta^{15}N$ and $\delta^{13}C$ were <0.2‰. For $\delta^{34}S$, standard deviations were <0.3‰.

Gas chromatograph-mass spectrometer (GC-MS)

Once dried, muscle samples selected for compound specific isotope analysis (CSIA) were lipid extracted (Soxhlet method from Ballentine et al., 1996) and the fatty acids had a methyl group added to the carboxyl end (derivitized) so they could be characterized by gas chromatography (GC). This was done by heating with BF_3CH_3OH for eight minutes (Ballentine et al., 1996). The fatty acid methyl esters (FAME) were analyzed by GC-MS using a Hewlett Packard 5890 Series II gas chromatograph (Palo Alto, CA) interfaced to a Hewlett Packard 5971A mass sensitive detector (Palo Alto, CA), with helium gas as the carrier. A 60-meter J&W DB-5

column (J&W Scientific, Folsom, CA) was used for FAME separation. The GC oven temperature program used was as follows: 100°C for 2 minutes, ramp at 3°C/min. to 210°C, hold for 20 min, ramp 1°C/min. to 220°C, hold for 10 min.

Compound specific stable isotope analysis (CSIA)

The FAMEs were analyzed for their stable carbon isotope compositions using a Hewlett Packard 5890 Series II gas chromatograph interfaced through a combustion furnace with a VG Isoprime IRMS (Fisons/VG/Micromass, Manchester, UK). The GC was equipped with the same column that was used for the GC-MS analysis and helium was the carrier gas. The GC oven temperature program was identical to that used for the GC-MS FAME identification. Time elution was used to identify peaks. The CO_2 combustion products of the fatty acids eluting from the column were introduced into the mass spectrometer after passing through a water trap.

All FAME $\delta^{13}C$ values were corrected for the addition of the methyl group to the original fatty acid. The derivatization of the fatty acids to their methyl esters results in a predictable and reproducible isotope effect (Ballentine et al., 1996; Uhle et al., 1997). Adding a methyl group to the fatty acid alters its isotope signature. However, if the isotopic ratio of the methanol (in this case $\delta^{13}C$=–46‰, measured by injecting the methanol into the mass spectrometer through the GC) and the fatty acid methyl ester are known, then the isotopic signature of the original fatty acid can be determined using a mass balance Equation 2.

$$\delta^{13}C_{\text{FAME}} = f_{\text{FA}}\delta^{13}C_{\text{FA}} + f_{\text{Methanol}}\,\delta^{13}C_{\text{Methanol}} \quad (2)$$

where $\delta^{13}C_{FAME}$, $\delta^{13}C_{FA}$, and $\delta^{13}C_{Methanol}$ = the carbon isotope signatures of the FAME, the underivatized fatty acid, and the methanol, respectively; and

f_{FA} and $f_{Methanol}$ = the fractions of carbon in the FAME due to the underivatized fatty acid and methanol, respectively (Ballentine et al., 1996; Uhle et al., 1997).

Each sample was injected four to eight times (depending on the reproducibility of the analysis). Only $\delta^{13}C$ values that were within 1.5‰ of each other were considered to reflect the $\delta^{13}C$ of the FAME (MacAvoy et al., 2002). Therefore, the $\delta^{13}C$ reported for each FAME identified is represented by an average value and a standard deviation. Every sixth sample injected was an internal, laboratory standard (naphthalene-d, $\delta^{13}C$–25.7‰) to insure consistent performance of the GC, oxidation furnace, and mass spectrometer.

Table 1

Fish species examined by guild (including an anadromous group) from the Rappahannock River to assess the role of marine fish as nutrient vectors. Guild assignments are based on diet as reported in Jenkins and Burkhead (1993).

Guild	Species name	Common name
Predator	*Ictalurus furcatus*	blue catfish
	Lepisosteus osseus	longnose gar
Carnivore	*Micropterus salmoides*	largemouth bass
	Lepomis gibbosus	pumpkinseed
	Hybognathus regius	eastern silvery minnow
	Notemigonus crysoleucas	golden shiner
	Lepomis macrochirus	bluegill
	Perca flavescens	yellow perch
Generalist	*Anguilla rostrata*	American eel
	Ameiurus catus	white catfish
	Ameiurus nebulosus	brown bullhead
	Ictalurus punctatus	channel catfish
Planktivore	*Menidia beryllina*	inland silverside
	Dorosoma cepedianum	gizzard shad
	Erimyzon oblongus	creek chubsucker
Anadromous	*Alosa aestivalis*	blueback herring
	Alosa pseudoharengus	alewife
	Alosa sapidissima	American shad
	Morone saxatilis	striped bass
	Morone americana	white perch

Statistical analysis

Kruskal-Wallis nonparametric procedures were used to test for differences in isotopic values among anadromous fish and the different guilds (predators, carnivores, generalists, and planktivores, (α=0.05)). The Dunn procedure was used to examine differences between groups (Rosner, 1990). Statview SE + Graphics (Abacus Concepts, Inc., Cary, NC), JMP In (SAS, Cary, NC) and Microsoft Excel version 5.0 (Microsoft, Inc., Redmond, WA) were used for statistical tests. The Dunn procedure reduces the risk of type-1 error inherent in multiple comparison techniques. It does so by increasing the Z-score needed to reject the null hypothesis as the number of individual groups being compared increases. In the present study, a Z-score of ±3.02 (0.9975 confidence) was needed for a difference to be significant.

Results

The first objective of this study was to establish that the spawning anadromous fish retained the marine isotope signal more than 40 km upstream from saline waters. This was the case for all three isotopes examined.

Table 2

Isotope values for all fish used in this study seperated by Family. "A" indicates anadromous, * indicates euryhaline range. Guild assingments are based on diet as reported in Jenkins and Burkhead (1993). "C" indicates a group with some isotope data derived from MacAvoy et al. (2000). White perch (*Morone americana*) shows elevated ^{13}C content is probably not marine protein given the low $\delta^{34}S$ ratio; *M. americana* is a secondary carnivore and the high $\delta^{13}C$ reflect this. Standard deviation is given after the ± and N is in parentheses.

Family and Species	Common name	Guild: food types	$\delta^{13}C$	$\delta^{15}N$	$\delta^{34}S$
Anguillidae					
Anguilla rostrata	American eel	generalist: insects, snails, fish, clams	–24.7±0.7 (3)	11.2±0.8 (3)	0.9±2.4 (3)
Atherinidae					
Menidia beryllina	inland sliverside	planktivore	–23.8±0.9 (3)	15.5±0.2 (3)	10.0±0.9 (3)
Catostomidae					
Erimyzon oblongus[C]	creek chubsucker	planktivore: planktonic crustaceans	–28.1 (1)	10.9 (1)	5.1 (1)
Centrarchidae					
Micropterus salmoides	smallmouth bass	carnivore	–23.0±1.9 (5)	14.5±1.3 (5)	7.6±3.2 (5)
Lepomis gibbosus	pumpkinseed	carnivore: insects, worms	–25.4±1.1 (8)	13.1±1.3 (8)	6.5±2.3 (9)
Lepomis macrochirus	bluegill	carnivore: insects, worms	–23.7±2.2 (5)	14.7±1.8 (5)	4.7±2.0 (5)
Clupeidea					
Alosa pseudoharengus[A, C]	alewife spawning	anadromous: copepods, diatoms, ostracods, shrimp, fish	–17.4±1.1 (7)	12.8±0.8 (7)	17.9±0.8 (6)
Alosa aestivalis[A, C]	blueback herring spawning	anadromous: copepods, cladocerans	–19.0±0.6 (7)	13.2±0.3 (7)	17.5±0.4 (7)
Alosa sapidissima[A, C]	juvenile American shadspawning	anadromous: copepods, small invertebrates	–20.2±0.6 (4)	12.6±0.4 (4)	8.0±2.2 (4)
Dorosoma cepedianum	gizzard shad	planktivore: filter feeder	–20.2±2.1 (7)	14.0±0.9 (7)	7.8±2.5 (7)
Cyprinidae					
Hybognathus regius	eastern silvery	minnowcarnivore: diatoms, algae, ooze detritus	–23.0±2.1 (6)	12.4±3.4 (6)	6.5±2.5 (6)
Notemigonus crysoleucas	golden shiner	carnivore: microcrustaceans insects	–24.8±1.1 (5)	13.1±1.6 (5)	2.5±1.7 (5)
Ictaluridae					
Ictalurus furcatus[C]	blue catfish	carnivore/piscivore	–21.6±1.9 (43)	15.4±2.0 (43)	9.2±3.0 (43)
Ictalurus punctatus	channel catfish	opportunistic generalist	–20.5±2.0 (3)	13.4±1.2 (3)	8.5±3.2 (3)
Ameirus nebulosus	brown bullhead	generalist/omnivorous	–24.0±0.8 (3)	13.2±0.5 (5)	5.3±1.6 (5)
Ameirus catus	white catfish	generalist/omnivorous	–21.2±2.7 (10)	15.8±2.3 (10)	8.7±4.7 (10)
Lepisosteidae					
Lepisosteus osseus	longnose gar	predator, piscivore	–23.1	16.8	8.34
Moronidae					
Morone saxatilis[A]	striped bass	generalist, piscivorous	–25.0±2.3 (2)	13.3±2.4 (2)	3.4±4.3 (2)
Morone americana[A*]	white perch	carnivorous: worms, shrimp, fish	–20.7±1.2 (5)	16.7 ±1.4 (5)	7.5±3.9 (5)
Percidae					
Perca flavescens[C]	yellow perch	carnivore: insects small fish	–25.1±2.1 (6)	14.3±2.2 (6)	6.9±1.6 (6)

The second objective was to test whether the different guilds of fish showed the incorporation of the marine isotope signal brought to the tidal freshwater by the anadromous fishes. This was observed, but largely limited to the predator guild.

Of the groups examined, the anadromous fish were the most ^{13}C-enriched, with mean values of approximately –19‰, followed by predators and planktivores (means –21.8‰ and –22.0‰, respectively), which were not significantly different from each other. This suggests that, of the remaining two guilds, carnivores were significantly ^{13}C-depleted relative to generalists (mean –24.1‰ and –23.5‰, respectively; Table 2). There was approximately a 10‰ range in $\delta^{13}C$ among the exclusively freshwater guilds (Table 2, Fig. 2).

Anadromous fish have elevated $\delta^{15}N$ values relative to freshwater fish with similar feeding strategies. However, the trophic enrichment and diet-tissue discrimination associated with $\delta^{15}N$ signatures make using nitrogen a less effective tracer for source than carbon or sulfur. In this study there was less variability within the guilds $\delta^{15}N$ signatures, relative to $\delta^{13}C$, although the range (‰)

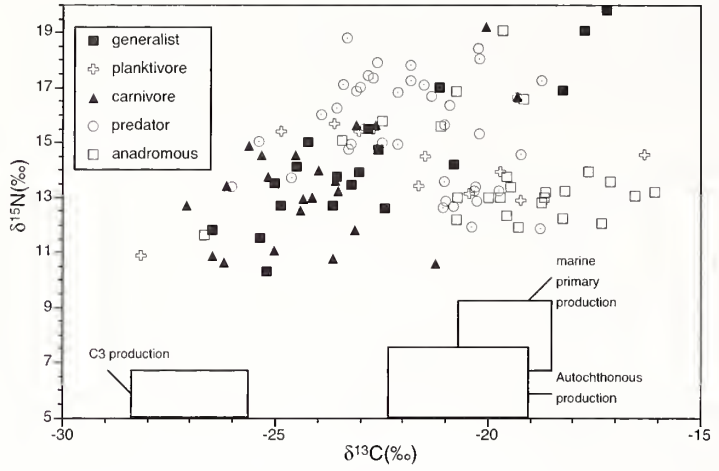

Figure 2

$\delta^{15}N$ vs. $\delta^{13}C$ values for the four guilds and anadromous *Alosa* species, showing that most resident freshwater fishes are approximately two trophic levels above primary producers (C3 or autochthonous production), in contrast to the *Alosa* spp., whose $\delta^{15}N$ reveals that they are one trophic level above marine primary production. Boxes indicate the isotope signature of C3 terrestrial plant primary production, freshwater autochthonous production, and marine primary production. *Alosa* spp. are ^{13}C-enriched relative to most freshwater residents, reflecting marine primary production.

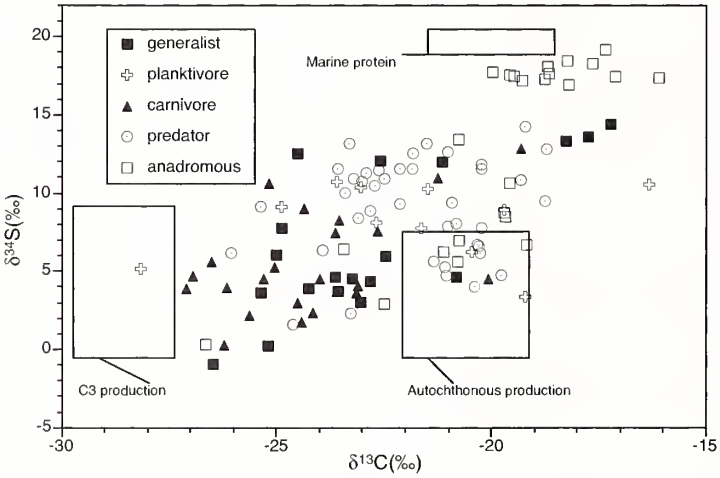

Figure 3

$\delta^{34}S$ vs. $\delta^{13}C$ values for the four guilds and anadromous *Alosa* species, with boxes to indicate the isotope signature of C3 terrestrial plant primary production, freshwater autochthonous production, and marine primary production. *Alosa* spp. are highly ^{34}S-enriched relative to most freshwater residents, reflecting marine sulfate (which becomes incorporated into primary producers and *Alosa* spp. while they grow in the Atlantic Ocean). Predators are the only guild showing elevated $\delta^{34}S$, indicating the incorporation of marine protein derived from *Alosa* spp.

of $\delta^{15}N$ values among all fishes was similar to that observed for $\delta^{13}C$ (10‰). The anadromous fish had the lowest $\delta^{15}N$ values and generally grouped between 12‰ and 13‰; however, their values were not lower than generalists or carnivores. The predators were the most ^{15}N-enriched of any group (Table 2). There were no significant differences among the $\delta^{15}N$ values for carnivores, generalists, and planktivores (Table 2).

Sulfur isotopes were hypothesized to be the most useful for tracing marine protein into freshwater, owing to extreme differences between the $\delta^{34}S$ of marine plankton and various sulfur sources in freshwater. Predator fishes and anadromous *Alosa* spp. showed elevated ^{34}S signals relative to other resident freshwater fishes, indicating that the predators incorporated *Alosa* spp. sulfur (protein). The range of $\delta^{34}S$ values among all the fish captured was from approximately 0‰ to 20‰, a considerably larger range than observed for the other two isotopes (Table 2, Fig. 3). Significant differences were observed in $\delta^{34}S$ among several of the separate groups. Anadromous species were highly ^{34}S-enriched relative to all resident freshwater fish (Table 2, Fig. 2), although the striped bass (40 cm total length (TL)) had values between 0.3‰ and 6.4‰, the lowest of the anadromous $\delta^{34}S$ values. Predators were the most ^{34}S-enriched of the resident fish, followed by planktivores (a trend also observed for $\delta^{13}C$). Carnivores and generalists were the most ^{34}S-depleted of the guilds and were not significantly different from each other (Table 2). Sulfur was the only stable isotope that completely separated the anadromous *Alosa* spp. from the full time freshwater residents. All of the *Alosa* spp. individual values were ^{34}S-enriched and outside the ranges observed in the other groups (Table 2).

Fatty acid analysis

Fatty acid (FA) isotope values show that some predators derive fats from anadromous fish and that there is a large variation among FA isotope values. FA $\delta^{13}C$ values were determined for one alewife (anadromous), one gizzard shad (*Dorosoma cepedianum*, a native freshwater planktivore), and two blue catfish (*Ictalurus furcatus*, an introduced piscivorous predator). For the blue catfish bulk $\delta^{13}C$ and $\delta^{34}S$ values from muscle tissue showed that one individual (A in Table 3) was significantly ^{13}C and ^{34}S-depleted relative to the other. This was also the case for the respective $\delta^{13}C$ values of their individual FAs. The anadromous alewife and the more ^{13}C-enriched blue

Table 3

Fatty acid (FA) $\delta^{13}C$ values for Rappahannock River fish. Means ± 1 Standard Deviation. (n=3). Values are corrected for CH4OH derevitization. FAs show that carbon from anadromous fish has been incorporated by *Ictalarus furcatus* but not by other resident fishes. Bulk isotope values show trends similar to the FAs and are as follows: alewife *A. pseudoharengus*, $\delta^{13}C$ –19.3‰, $\delta^{15}N$ 11.9‰, $\delta^{34}S$ 17.1‰; blue catfish *Ictalarus furcatus* (A) $\delta^{13}C$ –26.0‰, $\delta^{15}N$ 13.3‰, $\delta^{34}S$ 6.1‰; *I. furcatus* (B) $\delta^{13}C$ –19.3‰, $\delta^{15}N$ 16.6‰, $\delta^{34}S$ 10.8‰; gizzard shad *Dorosoma cepedianum* $\delta^{13}C$ –21.5‰, $\delta^{15}N$ 14.5‰, $\delta^{34}S$ 10.2‰.

Fatty acid	*Alosa pseudoharengus* alewife (‰)	*Ictalurus furcatus* blue catfish (‰)	*A Ictalurus furcatus* blue catfish (‰)	*B Dorosoma cepedianum* gizzard shad (‰)
12:0	–22.4 (0.4)	–28.5 (0.5)	–22.5 (0.9)	–27.4 (1.0)
14:0	–27.4 (1.8)	–33.6 (0.9)	–26.9 (0.6)	–25.5 (1.4)
16:1	–26.8 (0.8)	–35.4 (0.6)	–25.6 (0.7)	–27.4 (0.6)
16:0	–22.1 (0.1)	–30.3 (0.2)	–23.3 (0.3)	–25.7 (0.6)
18:1	–23.3 (0.6)	–30.5 (0.6)	–24.5 (0.7)	–28.7 (0.4)
18:0	–19.9 (1.8)	–28.8 (0.7)	–20.4 (1.1)	–23.5

catfish (B) had $\delta^{13}C$ FA values that, for the most part, overlapped with each other. Their 16 and 18 carbon length FAs were generally ^{13}C-enriched relative to the gizzard shad and the second blue catfish (A) (Table 3). For all fish, except gizzard shad, the saturated 12:0, 16:0, and 18:0 FAs were more enriched (2‰ to 6‰) than the 14:0, 16:1 and 18:1 FAs. 14:0 FAs are not elongated to 16 or 18 carbons in animals, which is why they are ^{13}C-depleted relative to saturated 16:0 and 18:0 (see Discussion). For the gizzard shad, the 12:0 FAs were 2‰ depleted relative to the 14:0 FAs. The blue catfish (B) with low $\delta^{13}C$ and $\delta^{34}S$ bulk values, generally had more ^{13}C-depleted FAs than other fishes. There was up to a 10‰ range among the FAs within an individual fish, with unsaturated FAs ^{13}C-depleted relative to saturated, and longer saturated chains being generally ^{13}C-depleted relative to shorter chain FAs (Table 3).

Discussion

The fact that the anadromous *Alosa* spp. were the most ^{13}C-enriched of the groups examined was expected because they retain the ^{13}C-enriched (relative to freshwater) signal of marine carbon fixation (Garman and Macko, 1998, MacAvoy et al., 2000, Hoffman et al., 2007). High $\delta^{13}C$ in freshwater systems with anadromous fish does not necessarily indicate trophic status (Garman and Macko, 1998; MacAvoy et al., 2000; Gregory-Eaves et al., 2007). The ^{13}C-enriched predators (mostly piscivorous catfish) show a wide range in $\delta^{13}C$, from –16 to –27‰ (white perch also show elevated $\delta^{13}C$ relative to most resident freshwater fish, but they also are ^{34}S-depleted, indicating that their carbon signature reflects their status as a secondary carnivore, not marine carbon). The most ^{13}C-enriched of the predators reflect the consumption of marine material, probably spawning adult *Alosa* spp., which had the most ^{13}C-enriched values of any prey item found. A number of predators, however, clearly derive very little carbon from marine migrants; they are strictly freshwater feeders, as shown by their ^{13}C-depleted carbon isotope values. Among the remaining three guilds, the planktivores (within which the anadromous *Alosa* spp., mainly filter feeders, were not included) were the most ^{13}C-enriched, driven largely by the migratory and filter-feeing gizzard shad (Jenkins and Burkhead, 1993). Gizzard shad ^{13}C enrichment probably reflects consumption of autochthonous production and not marine derived nutrients, because the gizzard shad $\delta^{34}S$ are too low to reflect substantial marine material (Table 2 and see below). The $\delta^{13}C$ range among the resident freshwater fishes suggest, not surprisingly, that both autochthonous and allochthonous production contribute to carbon fixation in this tidal freshwater stream. Indeed, in the York River estuary, a few kilometers south of the Rappahannock River, Raymond and Bauer (2001) estimate that between 38% and 56% of dissolved organic carbon was derived from internal (autochthonous) sources.

Only a small percent of the residents show an exclusive allochthonous signal in the region of the Rappahannock River examined, and most of the resident freshwater fish show an autochthonous $\delta^{13}C$ signature, which is characteristic of small tributaries close to the main stem of a large piedmont river. The $\delta^{13}C$ range of allochthonous productivity in Virginia tidal freshwater streams is between –25‰ and –28‰ (Garman and Macko, 1998; Hoffman et al., 2007). Because CO_2 solubility is limited in water, systems dominated by autochthonous production tend to be ^{13}C-enriched relative to C3 plants that appear in small streams dominated by C3 allochthonous production (Michener and Schell, 1994). Garman and Neilson (1992) note that the presence of gizzard shad and detritivores in Virginia tidal freshwater suggest that autochthonous production is important in these systems relative to non-tidal areas upstream, where fishes primarily consume terrestrial arthropods (Garman, 1991). Most of the guilds examined in this study reflected the predominance of autochthonous production and have $\delta^{13}C$ values that are lower

than would be expected for a C3 dominated system. The anadromous *Alosa* spp. were also ^{13}C-enriched relative to other guilds. All of their $\delta^{13}C$ values cluster between –22‰ and –16‰, whereas all other guilds range to approximately –28‰ range (the most ^{13}C-depleted values reflecting allochthonous production). This ^{13}C enrichment in *Alosa* spp. is not due to incorporating autochthonous freshwater production. The ^{13}C-enrichment is a signal from the marine environment from which the *Alosa* spp. biomass was derived. This interpretation is supported by the markedly ^{34}S-enriched values of the *Alosa* spp., which are in most cases 7‰ greater than any other fish in this study ($\delta^{34}S$ value of sulfur fixed from marine SO_4 in the ocean at present is highly enriched relative to freshwater [Kaplan et al., 1963]). Therefore, the ^{13}C enrichment of the *Alosa* spp. biomass (and other anadromous fishes) is due to a marine influence, not an autochthonous influence.

Of the guilds examined, predators show the highest $\delta^{34}S$ value after the *Alosa* spp., but are not significantly enriched in ^{13}C relative to other guilds. The elevated ^{34}S in predators (many of whom are piscivores) shows that more marine sulfur is incorporated by this guild relative to others. The predator's elevated $\delta^{15}N$ values place them at the top of the fish food web, although some smaller individuals (blue catfish), feed at lower trophic levels while young (Jenkins and Burkhead, 1993).

The link between anadromous *Alosa* spp. and the predators is also supported by the fatty acid carbon isotope signatures. *Alosa* spp. 16 and 18 carbon FAs were generally the most ^{13}C-enriched of the fish examined (Table 3). The two large (53cm TL) blue catfish show two very different FA isotope profiles. One blue catfish (B in Table 3) had a series of highly ^{13}C-enriched FAs (bulk muscle tissue $\delta^{13}C$ and $\delta^{34}S$ are also enriched in this individual) and the other had FAs with isotope signatures similar to allochthonus primary production (also consistent with bulk muscle tissue $\delta^{13}C$ and $\delta^{34}S$). Shorter chain (12 carbon) and more saturated FAs reveal the original $\delta^{13}C$ of the fats in the diet. Longer chain and unsaturated FAs can be subject to *de novo* transformations, which result in well established fractionations as chain length is systematically increased or as a double bond between carbons is created (making a point of unsaturation in a saturated FA). Generally, there is a 2‰ depletion in $\delta^{13}C$ arising from each unsaturation and another 2‰ depletion for each two carbon acetyl group addition (Deniro and Epstein, 1977). The most conservative tracer of dietary FAs, are the enriched precursors to long chain and unsaturated FAs. Among the FAs analyzed, the 12:0, 16:0, and 18:0 yield the best $\delta^{13}C$ estimate for dietary FAs, which clearly show distinct isotope signals depending on the carbon sources listed below: 1) ^{13}C-enriched marine isotope signals (represented by alewife and blue catfish B), 2) allochthonus production (represented by blue catfish A), or 3) a mix of autochthonous and allochthonus production, with the possibility of marine influences (represented by gizzard shad, although their $\delta^{34}S$ values do not reflect the typical marine signal).

The $\delta^{13}C$ and $\delta^{34}S$ distribution and range among the freshwater fishes suggest, not surprisingly, that both autochthonous and allochthonous nutrient sources, with the allochthonous sources being terrestrial C3 vegetation and marine primary production inwelling to this tidal freshwater stream, more than 40 km from the Chesapeake Bay. Unlike streams on the West Coast of the United States, where marine derived nitrogen and carbon can be an important nutrient source to inland ecosystems (Kline et al., 1993; Bilby et al., 2003; Chaloner et al., 2002), for all fish guilds in the study reported here, except the predators, there was not significant marine nutrient uptake. Several West Coast studies have shown that marine derived nitrogen, and some marine derived carbon, contributed to invertebrates (Francis et al., 2006; Hicks et al., 2005), primary producers, and juvenile fish within or near the sites receiving the spawning anadromous fish (Bilby et al., 2003; Koyama et al., 2005). For example, Bilby et al. (1996) found that 17% and 30% of the nitrogen in collector-gathers and juvenile coho salmon *(Oncorhynchus kisutch)* in Washington, were derived from spawning salmon. Ben-David et al. (1998) found that salmon carcasses may have contributed to the nitrogen incorporated by some terrestrial plants, as well as deer mice, squirrels, and voles; and Wipfli et al. (2003) found that salmon carcasses fueled increased growth rates among young salmonids. However, those studies show that only some material from decaying salmon makes its way into invertebrates and riparian vegetation (Bilby et al., 1996, 1998; Francis et al., 2006). There is strong evidence however, that the nutrients deposited as a result of the postspawning death of anadromous adults did significantly sustain fry the following year (Bilby et al., 1996, 1998).

In the East Coast stream examined here, carnivores and generalists, which consume benthic invertebrates as part of their diet, did not show a marine signal. Compared with anadromous salmonids on the West Coast, East Coast herring have a lower postspawning mortality and their runs have less biomass. Both of these facts indicate that a limited amount of marine protein and nitrogen maybe be delivered to spawning streams unless it is consumed directly by predatory fish. This is consistent with findings suggesting benthic insects in *Alosa* spp. spawning streams do not accumulate large amounts of marine derived material, even if they are living closely with post-spawning anadromous fish carcasses (Francis et al., 2006; Garman, 1992). It should be noted that in West Coast streams associated with spawning salmon, invertebrate uptake can be substantial (Hicks et al., 2005; Chaloner et al., 2002). Unlike most West Coast streams however, some tidal streams in Virginia have large piscivorous fish (introduced from Texas, Louisiana, or Mississippi in the 1970s) and these fish clearly incorporate marine material. So, while salmon (and presumably herring) on the West Coast import nutrients to the base of the food web (terrestrial autotrophs, young-of-the-year fish, and some invertebrates), in the steams examined here the marine material enters the top of the aquatic food web

where spawning adult anadromous fish are consumed by piscivorous fish. In order to fully understand the importance of a migratory or transitory nutrient source to consumers, the time required for that nutrient to be incorporated must be understood, thereby allowing a temporal evaluation of ecosystem structure. While the results of this study suggest that marine material does not form a substantial nutrient source to most of the fish community, more work needs to be done to investigate marine inputs derived from spawning anadromous fish, to other, lower order components of East Coast United States tidal freshwater systems.

Acknowledgments

We thank Mark King, Steve McIninch, and William Shuart at Virginia Commonwealth University, Department of Environmental Studies. This work was partially supported by the NOAA-Chesapeake Bay Office, a Moore Award from The University of Virginia, and a Mellon Award from American University.

Literature cited

Ballentine, D. C., S. A. Macko, V. C. Turekian, W. P. Gilhooly, and B. Martincigh.
1996. Compound specific isotope analysis of fatty acids and polycyclic aromatic hydrocarbons in aerosols: implications for biomass burning. Org. Geochem. 25(1/2):97–104.

Ben-David, M., T. A. Hanley, and D. M. Schell.
1998. Fertilization of terrestrial vegetation by spawning Pacific salmon: the role of flooding and predator activity. Oikos 83:47–55.

Bilby, R. E., E. W. Beach, B. R. Fransen, and J. K. Walter.
2003. Transfer of nutrient from spawning salmon to riparian vegetation in western Washington. Trans. Am. Fish. Soc. 132:733–745.

Bilby, R. E., B. R. Fransen, and P. A. Bisson.
1996. Incorporation of nitrogen and carbon from spawning coho salmon into the trophic system of small streams: evidence from stable isotopes. Can. J. Fish. Aquat. Sci. 53:164–173.

Bilby, R. E., B. R. Fransen, P. A. Bisson, and J. K. Walter.
1998. Response of juvenile coho salmon (*Oncorhynchus kisutch*) and steelhead (*Oncorhynchus mykiss*) to the addition of salmon carcasses to two streams in southwestern Washington, USA. Can. J. Fish. Aquat. Sci. 55:1909–1918.

Browder, R. G. and G. C. Garman.
1994. Increased ammonium concentrations in a tidal freshwater stream during residence of migratory clupeid fishes. Trans. Am. Fish. Soc. 123:993–996.

Canuel, E. A., K. H. Freeman, and S. G. Wakeham.
1997. Isotopic compositions of lipid biomarker compounds in estuarine plants and surface sediments. Limnol. Oceanogr. 42(7):1570–1583.

Cederholm, C. J., D. B. Houston, D. L. Cole, and W. J. Scarlett.
1989. Fate of coho salmon (*Oncorhynchus kisutch*) carcasses in spawning streams. Can. J. Fish. Aquat. Sci.46:1347–1355.

Chaloner, D. T., K. M. Martin, M. S. Wipfli, P. H. Ostrom, and G. A. Lamberti.
2002. Marine carbon and nitrogen in southwestern Alaska stream food webs: evidence from artificial and natural streams. Can. J. Fish. Aquat. Sci. 59:1257–1265.

Deegan, L. A.
1993. Nutrient and energy transport between estuaries and coastal marine ecosystems by fish migration. Can. J. Fish. Aquat. Sci. 50:74–79.

DeNiro, M. J., and S. Epstein.
1977. Mechanism of carbon isotope fractionation associated with lipid synthesis. Science 197:261–263.

Durbin, A. G., S. W. Nixon, and C. A. Oviatt.
1979. Effects of the spawning migrations of the alewife, *Alosa pseudoharengus*, on freshwater ecosystems. Ecology 60(1):8–17.

Francis, T. B., D. E. Schindler, and J. W. Moore.
2006. Aquatic insects play a minor role in dispersing salmon-derived nutrients into riparian forests in southwestern Alaska. Can. J. Fish. Aquat. Sci. 63(11):2543–2552.

Garman, G. C.
1991. Use of terrestrial arthropod prey by a stream-dwelling cyprinid fish. Environ. Biol. Fishes 30:325–331.
1992. Fate and potential significance of postspawning anadromous fish carcasses in an Atlantic costal river. Trans. Am. Fish. Soc. 121:390–394.

Garman, G. C. and S. A. Macko.
1998. Contribution of marine-derived organic matter to an Atlantic coast, freshwater, tidal stream by anadromous clupeid fishes. J. North Am. Benthol. Soc. 17(3):277–285.

Garman, G. C., and L. A. Nielsen.
1992. Medium-sized rivers of the Atlantic coastal plain. *In* Biodiversity of the Southeastern United States (C. Hackney, S. Adams, W. Martin, eds.), p. 315–349. John Wiley and Sons, New York.

Gregory-Eaves, I., M. J. Demers, L. Kimpe, E. M. Krummel, R. W. MacDonald, B. P. Finney, and J. M. Blais.
2007. Tracing salmon-derived nutrients and contaminants in freshwater food webs across a pronounced spawner density gradient. Environ. Toxicol. Chem. 26(6):1100–1108.

Havey, K. A.
1961. Restoration of anadromous alewives at Long Pond, Maine. Trans. Am. Fish. Soc. 90:281–286.

Hesslein, R. H., M. J. Capel, D. E. Fox, and K. A. Hallard.
1991. Stable isotopes of sulfur, carbon, and nitrogen as indicators of trophic level and fish migration in the lower Mackenzie River, Canada. Can. J. Fish. Aquat. Sci 48:2258–2265.

Hicks, B. J., M. S. Wipfli, D. W. Lang, and M. E. Lang.
2005. Marine-derived nitrogen and carbon in freshwater-riparian food webs of the Copper River Delta, south-central Alaska. Oecologia 144:558–569.

Hoffman, J. C, D. A. Bronk, and J. E. Olney.
2007. Contribution of allochthonous carbon to American Shad production in the Mattaponi River, Virginia, using stable isotopes. Estuaries and Coasts 30(6):1034–1048.

Jenkins, R. E. and N. M. Burkhead.
1993. Freshwater fishes of Virginia. Am. Fish. Soc., Bethesda, MD.

Kaplan, I. R., K. O. Emery, and S. C. Rittenberg.
1963. The distribution and isotopic abundance of sulfur in recent marine sediments off southern California. Geochim. Cosmochim. Acta 27:297–331.

Kline, T. C., J. J. Goering, O. A. Mathisen, P. H. Poe, and P. L. Parker.
1993. Recycling of elements transported upstream by runs of Pacific Salmon: II. $\delta^{15}N$ and $\delta^{13}C$ evidence in the Kvichak River watershed, Bristol Bay southwestern Alaska. Can. J. Fish. Aquat. Sci. 50:2350–2365.

Knoff, A. J., S. A. Macko, R. M. Erwin, and K. M. Brown.
2002. Stable isotope analysis of temporal variation in the diets of pre-fledged Laughing Gulls. Waterbirds 25(2):142–148.

Koyama, A., K. Kavanagh, and A. Robinson.
2005. Marine nitrogen in central Idaho riparian forests: evidence from stable isotopes. Can. J. Fish. Aquat. Sci. 62:518–526.

MacAvoy, S. E., S. A. Macko, and G. C. Garman.
1998. Tracing marine biomass into tidal freshwater ecosystems using stable sulfur isotopes. Naturwissenschaften 85(11):544–546.

MacAvoy, S. E., S. A. Macko, and S. B. Joye.
2002. Fatty acid carbon isotope signatures in chemosynthetic mussels and tube worms from gulf of Mexico hydrocarbon seep communities. Chem. Geol. 185: 1–8.

MacAvoy, S. E., S. A. Macko, S. P. McIninch, and G. C. Garman.
2000. Marine nutrient contributions to freshwater apex predators. Oecologia 122:568–573.

Michener, R. H., and D. M. Schell.
1994. Stable isotope ratios as tracers in marine aquatic food webs. *In* Stable isotopes in ecology and environmental science (K. Lajtha, and R. H. Michener, eds.) p. 138–157. Blackwell, Oxford, U.K.

Monson, D. K., and J. M. Hayes.
1982. Carbon isotopic fractionation in the biosynthesis of bacterial fatty acids. Ozonolysis of unsaturated fatty acids as a means of determining the intramolecular distribution of carbon isotopes. Geochim. Cosmochim. Acta. 46:139–149.

Murphy, D. E., and T. A. Abrajano, Jr.
1994. Carbon isotope compositions of fatty acids in mussels from Newfoundland estuaries. Estuar. Coast. Shelf Sci. 39:261–272.

Olsen, V.
1999. Lipids and essential fatty acids in aquatic food webs: what can freshwater ecologists learn from mariculture? *In* Lipids in freshwater ecosystems (M. T. Arts, B. C. Wainman, eds), p. 161–202. Springer-Verlag, New York.

Peterson, B. J., R. W. Howarth, and R. H. Garritt.
1985. Multiple stable isotopes used to trace the flow of organic matter in estuarine food webs. Science 227:1361–1363.

Rand, P. S., C. A. S. Hall, W. H. McDowell, N. H. Ringler, and J. G. Kennen.
2002. Factors limiting primary productivity in lake Ontario tributaries receiving salmon migrations. Can. J. Fish. Aquat. Sci. 49:2377–2385.

Raymond P. A., and J. E. Bauer.
2001. DOC cycling in a temperate estuary: A mass balance approach using natural 14C and 13C isotopes. Limnol. Oceanogr. 46(3):655–667.

Rosner, B.
1990. Fundamentals of biostatistics, 3rd ed. PWS-Kent Publ. Co., Boston, MA.

Stott, A. W., E. Davies, R. P. Evershed, and N. Tuross.
1997. Monitoring the routing of dietary and biosynthesised lipids through compound-specific stable isotope ($\delta^{13}C$) measurements at natural abundance. Naturwissenschaften 84:82–86.

Uhle, M. E., S. A. Macko, H. J. Spero, M. H. Engel, and D. W. Lea.
1997. Sources of carbon and nitrogen in modern planktonic foraminifera: the role of algal symbionts as determined by bulk and compound specific stable isotopic analyses. Org. Geochem. 27(3/4):103–113.

Vander Zanden, M. J., J. M.Casselman, and J. B. Rasmussen.
1999. Stable isotope evidence for the food web consequences of species invasions in lakes. Nature 401:464–467.

Wipfli, M. S., J. P. Hudson, J. P. Caouette, and D. T. Chaloner.
2003. Marine subsidies in freshwater ecosystems: salmon carcasses increase the growth rates of stream-resident salmonids. Trans. Am. Fish. Soc. 132:371–81.

Description of early life history stages of the northern sculpin (*Icelinus borealis* Gilbert) (Teleostei: Cottidae)

Rachael L. Cartwright

Email address: rachcart@hotmail.com

National Marine Fisheries Service, NOAA
Alaska Fisheries Science Center
7600 Sand Point Way NE, Building 4
Seattle, Washington 98115

Abstract—Larvae of the genus *Icelinus* are collected more frequently than any other sculpin larvae in ichthyoplankton surveys in the Gulf of Alaska and Bering Sea, and larvae of the northern sculpin (*Icelinus borealis*) are commonly found in the ichthyofauna in both regions. Northern sculpin are geographically isolated north of the Aleutian Islands, Alaska, which allows for a definitive description of its early life history development in the Bering Sea. A combination of morphological characters, pigmentation, preopercular spine pattern, meristic counts, and squamation in later developmental stages is essential to identify *Icelinus* to the species level. Larvae of northern sculpin have 35–36 myomeres, pelvic fins with one spine and two rays, a bony preopercular shelf, four preopercular spines, 3–14 irregular postanal ventral melanophores, few, if any, melanophores ventrally on the gut, and in larger specimens, two rows of ctenoid scales directly beneath the dorsal fins extending onto the caudal peduncle. The taxonomic characters of the larvae of northern sculpin in this study may help differentiate northern sculpin larvae from its congeners, and other sympatric sculpin larvae, and further aid in solving complex systematic relationships within the family Cottidae.

Manuscript submitted 18 September 2007.
Manuscript accepted 29 October 2008.
Fish. Bull. 107:175–185 (2009).

The views and opinions expressed or implied in this article are those of the author and do not necessarily reflect the position of the National Marine Fisheries Service, NOAA.

The sculpin family, Cottidae, is a speciose, morphologically diverse group of fishes with a worldwide distribution comprising as many as 275 species in about 70 genera (Nelson, 2006). Greatest diversity occurs in the Northeast Pacific Ocean and Bering Sea with 96 species in 34 genera where they are found in almost every benthic habitat from the intertidal to the upper continental slope (Mecklenburg et al., 2002; Nelson, 2006; Pietsch and Orr, 2006). Cottids are primarily predators of smaller fish and crustaceans, and many species are preyed upon by larger fishes and marine mammals, particularly pinnipeds (Browne et al., 2002; Pietsch and Orr, 2006). Cottids are one of several prey species exploited by the harbor seal (*Phoca vitulina*). Cottid species, including the northern sculpin (*Icelinus borealis*), are abundant in waters surrounding rookeries of Steller sea lions (*Eumetopias jubatus*) where they contribute to the diversity of available prey species (Mueter and Norcross, 2000; Browne et al., 2002; Fritz and Hinckley, 2005). New cottid species continue to be described; however, the systematics and life histories of most species are poorly known. A more complete understanding of the diversity of the family is necessary to fully understand their role in the dynamics of North Pacific ecosystems (Hoff, 2006; Pietsch and Orr, 2006).

Icelinus borealis is the most common species of *Icelinus* in the Gulf of Alaska and the only species of *Icelinus* known from the Bering Sea. It is reported to be an important component of the ichthyofauna in both regions (Mueter and Norcross, 2000; Mecklenburg et al., 2002). Adults are distributed from Attu Island in the Aleutian Islands and Bristol Bay in the eastern Bering Sea to southern Puget Sound, Washington, at depths of 4–247 m, on nearly all types of substrate (Mecklenburg et al., 2002). Larvae of *Icelinus* are the most frequently collected larval cottids in the Northeast Pacific Ocean and Bering Sea, occurring in 9.3% (ranked 12th of all taxa collected) of ichthyoplankton samples collected by the Alaska Fisheries Science Center (AFSC).

Larvae of *Icelinus* have primarily been collected in continental shelf and slope waters of the Bering Sea, through Unimak Pass to the Gulf of Alaska and Shelikof Sea Valley, around Kodiak Island, and southward to the west coast of the United States. In the Shelikof Sea Valley, they are most often collected along the northern side, closest to the Alaska Peninsula (Matarese et al., 2003). *Icelinus* comprises 11 species that are diagnosed by pelvic fins having one spine and two rays, four preopercular spines (the dorsalmost is longest and bifid or trifid), two rows of ctenoid scales directly beneath the dorsal fins, and gill membranes that are united and free from the isthmus (Bolin, 1936; Yabe et al., 1983; Yabe et al., 2001; Nelson et al., 2004; Rosenblatt and Smith, 2004). Adult *I. borealis* reach 10 cm standard length and lack distinct postocular spines, possess a long cirrus at the base of the nasal spine, the first or second

dorsal-fin spines are not longer than the third or fourth, and the two rows of ctenoid scales below the dorsal fins extend onto the caudal peduncle (Bolin, 1936; Mecklenburg et al., 2002).

This study is the first to identify and describe the larval and juvenile stages of *I. borealis*. Previous descriptions were based on misidentified specimens or were made at a more conservative generic level because of difficulty distinguishing among species of *Icelinus* and between *Icelinus* and other sympatric cottid larvae. Larvae of *Icelinus quadriseriatus* from the coast of California are currently the only *Icelinus* larvae described (Feeney, 1987). Larvae tentatively identified as *I. borealis* in early literature were misidentified as *Ruscarius meanyi* based on a pelvic-fin ray count of 1, 2—a count diagnostic of *Icelinus* but also occurring rarely in *R. meanyi* (Blackburn, 1973; Richardson, 1977; Richardson and Pearcy, 1977; Richardson and Washington, 1980; Washington, 1981; Begle, 1989). Current literature has continued to identify larvae of *Icelinus* at the generic level; however, Matarese et al. (1989, 2003) have cautiously identified illustrations as *I. borealis*. *Icelinus borealis* has cautiously been identified at the species level because three other species of *Icelinus* with unidentified larvae (*I. burchami*, *I. filamentosus*, and *I. tenuis*), and other unidentified cottid larvae (e.g., *Icelus*) are also found in the Gulf of Alaska.

Uniformity between larval *Icelinus* and other cottid larvae is noted in the assignment of phenetic groups based on shared larval characters (e.g., preopercular spine pattern, body shape, and pigmentation) (Richardson, 1981). *Icelinus* is included in phenetic group 2, which includes *Paricelinus*, *Triglops*, *Icelus* (tentatively), and *Chitonotus*, and is characterized by a slender body shape, pointed snout, and four prominent preopercular spines (Richardson, 1981). Further study of phenetic groups has increased the size of group 2, the "*Myoxocephalus* group," to include a total of 13 genera (Matarese et al., 1989; Moser et al., 1996). The *Myoxocephalus* group includes the genera previously included in group 2 as well as the genera *Myoxocephalus*, *Ruscarius*, *Ascelichthys*, *Orthonopias*, *Enophrys*, *Radulinus*, *Gymnocanthus*, and *Synchirus* (Matarese et al., 1989; Moser et al., 1996). Members of the *Myoxocephalus* group have four preopercular spines and are defined by a unique larval character, namely a bony preopercular shelf (Moser et al., 1996).

Larvae of *Icelinus* are reported to be the most frequently collected larval cottids in the Northeast Pacific Ocean and Bering Sea. Although collected in large numbers, the size range of specimens is limited, which has hindered compiling the developmental series necessary for description. Increased ichthyoplankton sampling conducted in the Bering Sea in the 1990s has provided the specimens necessary to describe larvae of *I. borealis* using meristic counts and morphological characters, including pigmentation and preopercular spination. This study presents an illustrated developmental series and general aspects of osteological development for *I. borealis*.

Methods

A total of 53 specimens (7.4–51.7 mm standard length [SL]) collected during AFSC research cruises in the Bering Sea and Gulf of Alaska between 1979 and 2002 were examined (Fig. 1). Specimens were collected at depths to 400 m, primarily using 60-cm bongo nets and Methot trawls. Specimens were initially preserved in 5% formalin buffered with sodium borate, then later transferred to 70% ethanol. Nineteen specimens were cleared and stained using the method of Potthoff (1984). Twenty-two adult *Icelinus borealis* specimens were radiographed to verify the vertebral count of 35–36 recorded in literature.

Specimens were grouped using the series method, by positively identifying juveniles using known adult characteristics then linking those specimens to progressively smaller specimens using shared characteristics (Neira et al., 1998). Larvae were identified using reported generic characters for *Icelinus* including 35–36 vertebrae (myomeres) and four distinct preopercular spines, if developed. Illustrated *Icelinus* (tentatively identified as *I. borealis*) from Matarese et al. (1989) were also used to compare general morphological and pigment characters.

Meristic counts are reported for ossified elements using cleared and stained or radiographed material. Morphometric measurements were taken following Richardson and Washington (1980) using a digital image analysis system with Image Pro Plus, vers. 4.5 software (Media Cybernetics, Inc., Silver Spring, MD). Both body length and proportional measurements are in SL unless otherwise noted. Developmental terminology follows Kendall et al. (1984). Nomenclature describing caudal-fin development follows Matarese and Marliave (1982).

Only melanistic pigmentation is described. Nomenclature describing pigment pattern follows Busby and Ambrose (1993). The term "band" refers to an aggregation of melanophores oriented vertically; "bar" refers to an aggregation that is oriented horizontally. Illustrations were rendered using a camera lucida attached to a dissecting stereomicroscope.

Material examined

Larvae: 53 specimens examined, 7.4–51.7 mm. UW 105110, 1 (16.7 mm), Bering Sea, 52°35.9′N, 173°25.6′W, 137 m depth, 2 August 1997, FV *Vesteraalen*; UW 105111, 1 (13.4 mm), Bering Sea, 56°31.9′N, 166°25.4′W, 88 m depth, 16 July 1994, RV *Miller Freeman*; UW 105113, 2 (14.4–15.1 mm), Bering Sea, 56°30.6′N, 168°60.0′W, 95 m depth, 23 July 2001, TS *Oshoro maru*; UW 105114, 1 (12.1 mm), Bering Sea, 54°59.7′N, 166°58.9′W, 100 m depth, 19 July 1995, TS *Oshoro maru*; UW 105116, 1 (14.5 mm), Bering Sea, 56°59.6′N, 170°00.4′W, 62 m depth, 25 July 1996, TS *Oshoro maru*; UW 105117, 2 (13.4–14.3 mm), Bering Sea, 57°01.1′N, 171°00.2′W, 94 m depth, 25 July 1996, TS *Oshoro maru*; UW 105119, 2 (14.3–16.3 mm), Bering Sea, 55°00.9′N, 166°01.4′W,

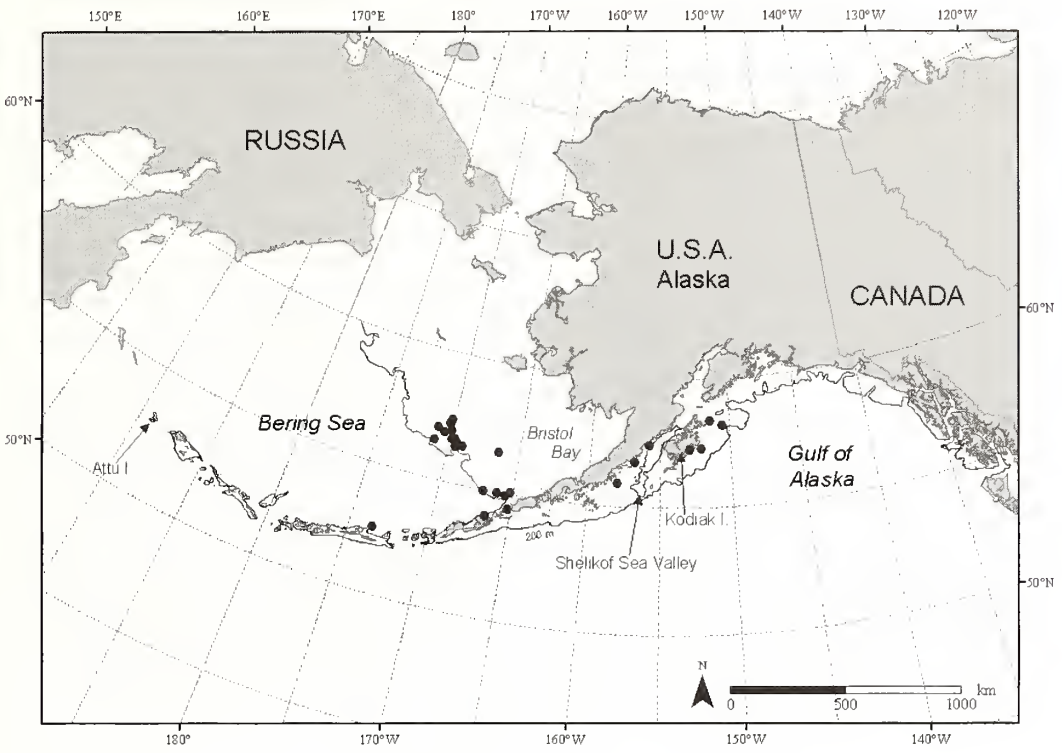

Figure 1

Station locations (•) in the Bering Sea and Gulf of Alaska where larval and juvenile northern sculpin (*Icelinus borealis*) were collected by the Alaska Fisheries Science Center, National Marine Fisheries Service (1979–2002).

100 m depth, 21 July 1997, TS *Oshoro maru*; UW 105121, 1 (32.1 mm), Gulf of Alaska, 58°12.1′N, 150°27.0′W, 115 m depth, 16 May 1985, RV *Poseidon*; UW 105122, 1 (7.9 mm), Bering Sea, 54°01.3′N, 166°33.9′W, 100 m depth, 25 April 1993, RV *Miller Freeman*; UW 105124, 1 (51.7 mm), Gulf of Alaska, 55°55.5′N, 157°56.0′W, 94 m depth, 23 June 1998, RV *Wecoma*; UW 105125, 2 (10.7–15.2 mm), Gulf of Alaska, 58°22.1′N, 151°22.2′W, 100 m depth, 1 June 2002, RV *Miller Freeman*; UW 105127, 1 (8.3 mm), Bering Sea, 54°55.5′N, 165°29.1′W, 119 m depth, 23 May 2003, RV *Miller Freeman*; UW 105129, 2 (9.2–9.3 mm), Bering Sea, 56°27.3′N, 169°28.3′W, 94 m depth, 12 July 1997, RV *Wecoma*; UW 105131, 1 (8.8 mm), Bering Sea, 56°27.3′N, 169°28.3′W, 30 m depth, 12 July 1997, RV *Wecoma*; UW 105133, 2 (8.5–12.5 mm), Bering Sea, 56°30.2′N, 169°28.5′W, 78 m depth, 10 July 1997, RV *Wecoma*; UW 105134, 1 (14.9 mm), Bering Sea, 56°41.4′N, 169°48.5′W, 74 m depth, 8 July 1997, RV *Wecoma*; UW 105136, 2 (8.0–9.2 mm), Bering Sea, 56°42.6′N, 169°35.9′W, 64 m depth, 10 July 1997, RV *Wecoma*; UW 105138, 1 (13.2 mm), Bering Sea, 56°42.6′N, 169°35.9′W, 25 m depth, 10 July 1997, RV *Wecoma*; UW 105140, 2 (10.0–14.1 mm), Bering Sea, 56°42.6′N, 169°36.1′W, 70 m depth, 9 July 1997, RV *Wecoma*; UW 105142, 1 (14.9 mm), Bering Sea, 56°42.7′N, 169°36.5′W, 72 m depth, 9 July 1997, RV *Wecoma*; UW 105144, 1 (10.2 mm), Bering Sea, 56°53.2′N, 170°26.7′W, 87 m depth, 6 July 1997, RV *Wecoma*; UW 105146, 2 (15.4–16.5 mm), Bering Sea, 57°17.3′N, 170°10.1′W, 30 m depth, 6 July 1997, RV *Wecoma*; UW 105148, 1 (14.5 mm), Bering Sea, 57°21.2′N, 170°08.3′W, 50 m depth, 13 July 1997, RV *Wecoma*; UW 105149, 1 (7.4 mm), Bering Sea, 54°24.9′N, 165°09.0′W, 140 m depth, 25 April 1997, RV *Miller Freeman*; UW 105151, 3 (43.2–45.9 mm), Gulf of Alaska, 57°18.5′N, 152°02.8′W, 74 m depth, 13 September 1993, RV *Miller Freeman*; UW 105152, 1 (41.7 mm), Gulf of Alaska, 57°15.7′N, 152°53.7′W, 87 m depth, 16 September 1993, RV *Miller Freeman*; UW 105154, 1 (14.1 mm), Bering Sea, 56°32.0′N, 166°25.4′W, 88 m depth, 16 July 1994, RV *Miller Freeman*; UW 105156, 1 (19.6 mm), Bering Sea, 57°24.9′N, 170°05.6′W, 52 m depth, 13 September 1999, RV *Miller Freeman*; UW 105157, 1 (11.6 mm), Gulf of Alaska, 56°46.2′N, 156°46.7′W, 101 m depth, 27 May 1995, RV *Miller Freeman*; UW 105159, 1 (9.4 mm), Gulf of Alaska, 57°24.5′N, 155°48.6′W, 100 m depth, 28 May 1995, RV *Miller Freeman*; UW 105160, 1 (17.9 mm), Bering Sea, 55°04.4′N, 165°08.0′W, 108 m depth, 26 July 1996, RV *Miller Freeman*; UW 105162, 2 (13.4–15.8 mm), Bering Sea, 56°28.3′N, 169°26.9′W, 87 m depth, 1 August 1996, RV *Miller Freeman*; UW 105164, 2 (11.1–12.9 mm), Bering Sea, 56°30.3′N, 171°02.5′W, 119 m depth, 4 August 1996, RV *Miller Freeman*; UW 105165, 3 (14.8–16.0 mm), Bering Sea, 56°32.7′N, 169°27.4′W, 63 m depth, 2 August 1996, RV *Miller Freeman*; UW 105167, 1 (13.8 mm), Bering Sea, 56°34.6′N, 169°24.3′W, 44 m depth, 2 August 1996, RV

Table 1

Body proportions of larvae and juveniles of northern sculpin (*Icelinus borealis*). Values for each body proportion are expressed as percentage of standard length (SL) or head length (HL): mean, standard deviation, and range.

Body proportion	Flexion	Postflexion	Juvenile
Sample size	9	27	8
Standard length	9.1 ±0.74 (8.0–10.2)	14.9 ±2.40 (11.1–22.7)	38.6 ±10.3 (24.1–51.7)
Head length/SL	25.2 ±0.02 (22.2–28.4)	34.3 ±0.04 (26.2–41.5)	37.9 ±0.02 (35.2–39.8)
Snout length/HL	27.9 ±0.04 (24.8–37.9)	26.8 ±0.03 (20.0–32.4)	27.9 ±0.05 (21.8–39.0)
Eye diameter/HL	31.0 ±0.03 (25.3–33.7)	24.3 ±0.02 (20.2–30.3)	27.8 ±0.01 (26.1–30.6)
Snout-to-anus length/SL	44.6 ±0.03 (38.7–48.6)	47.2 ±0.03 (42.3–54.0)	50.6 ±0.04 (46.4–57.7)
Body depth/SL	20.3 ±0.02 (17.6–23.2)	21.9 ±0.02 (17.6–27.1)	20.5 ±0.02 (17.4–22.7)
Pectoral-fin length/SL	10.1 ±0.02 (6.6–13.4)	24.2 ±4.30 (13.8–32.4)	24.5 ±2.80 (19.6–28.8)

Miller Freeman; UW 105169, 1 (24.9 mm), Bering Sea, 56°31.2′N, 169°28.8′W, 68 m depth, 11 September 1997, RV *Miller Freeman*; UW 105172, 1 (24.1 mm), Bering Sea, 57°17.3′N, 170°09.3′W, 39 m depth, 16 September 1997, RV *Miller Freeman*; UW 105174, 1 (22.7 mm), Bering Sea, 57°16.3′N, 170°11.0′W, 16 September 1997, RV *Miller Freeman*.

Adults: 22 specimens examined, 32.0–77.0 mm. UW 027383, 4 (41.0–50.0 mm), eastern North Pacific, 60°12.0′N, 147°45.0′W, 30 m depth, 1 August 1989, RV *Discovery*, J. W. Orr; UW 029499, 5 (32.0–55.0 mm), eastern North Pacific, 60°21.0′N, 147°49.0′W, 40 m depth, 6 August 1989, RV *Discovery*, J. W. Orr; UW 040432, 3 (45.0–64.0 mm), eastern North Pacific, 60°18.0′N, 147°50.0′W, 142 m depth, 31 July 1989, RV *Discovery*, C. Eaton; UW 111416, 2 (55.0–62.0 mm), eastern North Pacific, 52°39.8′N, 169°21.6′W, 114 m depth, 24 May 2003, FV *Northwest Explorer*, J. W. Orr; UW 040955, 4 (44.0–45.0 mm), eastern North Pacific, 60°33.2′N, 147°35.0′W, 40 m depth, 1 October 1989, A. M. Shedlock; UW 027174, 4 (60.0–77.0 mm), eastern North Pacific, Gulf of Alaska, Yakutat Bay, FV *Resolution*.

Results

Morphology

The smallest larva examined in this study was 7.4 mm notochord length (NL) and in preflexion (Fig. 2A). Notochord flexion began at approximately 8.0 mm and was complete around 11.0 mm (Fig. 2B). Postflexion larvae were 11.0–16.0 mm (Fig. 2C). Transformation to the juvenile stage occurred between 16.0 mm and 24.0 mm (Fig. 2D). Specimens larger than 24.0 mm were considered juveniles and identified using adult characters (Fig. 2E).

During preflexion, the head was small and round, measuring 18% SL, increasing to 38% SL by the juvenile stage (Table 1). The snout was initially rounded, but became notably pointed by flexion; snout length was 24% head length (HL) during preflexion, increasing to approximately 28% HL during flexion through the juvenile stage. Snout-to-anus length steadily increased from 39% SL during preflexion to 51% SL in juveniles. Body depth was initially 17% SL during preflexion, but increased to approximately 20% SL in later stages.

Pigmentation

Two preflexion specimens were available for study: one 7.4 mm NL and one 7.9 mm NL. Both specimens were lightly pigmented (Fig. 2A). A single melanophore was present on the lower jaw angle. Pigment on the gut consisted of one to three individual melanophores anteriorly, and moderate pigmentation on the anus. A single row of nine postanal ventral melanophores (PVMs) was present on both specimens. Pigmentation on the caudal finfold was present on the 7.4 mm NL specimen. Pigment on the head, gut, and anus steadily increased during flexion (Fig. 2B).

Twenty-six postflexion and transforming specimens were examined. Melanophores were present dorsally over the mid- and hind-brain (Fig. 2C). Minute melanophores were present on the orbital rim. Loosely grouped melanophores were present in postorbital and suborbital regions, upper and lower jaws, on the cheek, operculum, chin, and isthmus. Pigment was present on the nape. The gut was pigmented along the anterodorsal surface and extended dorsolaterally toward the anus. Three to 14 PVMs were present on specimens between preflexion and postflexion stages; nine was the modal value (Table 2). The size, shape, and location of PVMs were variable among specimens. Lateral body pigment developed as vertical (dorsal to ventral) bands that were composed of densely aggregated small melanophores. The anterior (first) lateral band was located directly under the first dorsal fin and extended ventrally to the gut. The second band developed as a small aggregation of melanophores located mediolaterally on the body. When fully developed, the second band extended from the anterior portion of the second dorsal fin to the mediolateral part of the body. Pigment developed on the first dorsal fin, particularly on the membrane between

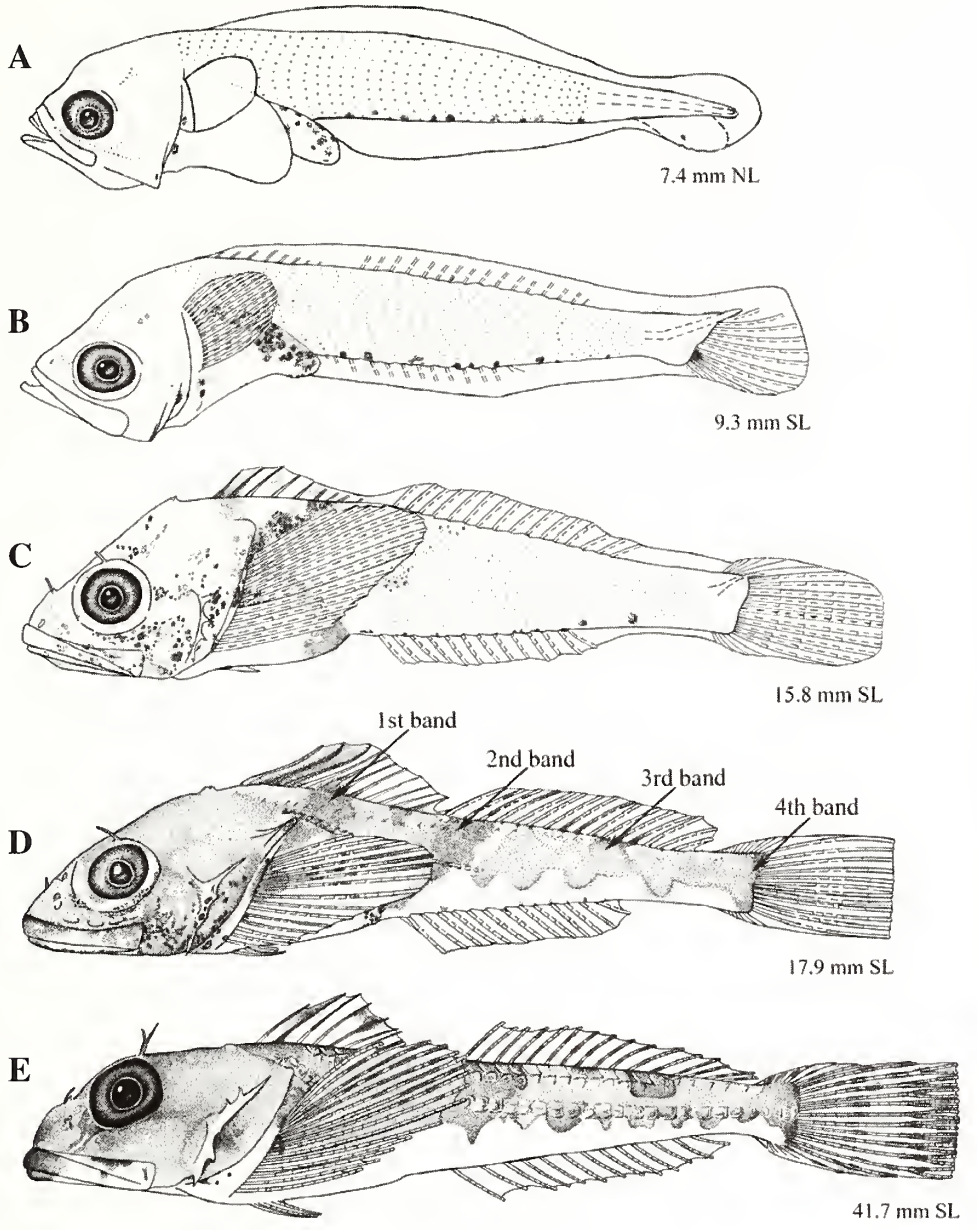

Figure 2

Developmental series of northern sculpin (*Icelinus borealis*): (**A**) preflexion larva, 7.4 mm NL, UW 105149, Bering Sea, 54°24.9′N, 165°09.0′W, 140 m depth, 25 April 1997; (**B**) flexion larva, 9.3 mm SL, UW 105129, Bering Sea, 56°27.3′N, 169°28.3′W, 94 m depth, 12 July 1997; (**C**) postflexion larva, 15.8 mm SL, UW 105162, Bering Sea, 56°28.3′N, 169°26.9′W, 87 m depth, 1 August 1996; (**D**) transformation larva, 17.9 mm SL, UW 105160, Bering Sea, 55°04.4′N, 165°08.0′W, 108 m depth, 26 July 1996; (**E**) juvenile, 41.7 mm SL, UW 105152, Gulf of Alaska, 57°15.7′N, 152°53.7′W, 87 m depth, 16 September 1993. Abbreviations: NL=notochord length; SL=standard length. Illustrations by R. L. Cartwright.

the first two or three spines. Rays of the second dorsal fin were also pigmented in some specimens. Large, dark melanophores were present on the pectoral-fin base, and some pigmentation developed on the rays near the base. One or two melanophores were present on or near the pelvic-fin base.

Throughout transformation of larvae of *I. borealis* into the juvenile stage, pigmentation continued to in-

crease on the head until the entire area was nearly covered with small melanophores (Fig. 2D). Gut pigment was less visible. The first and second lateral pigment bands were fully developed. The third lateral pigment band developed directly beneath the posterior portion of the second dorsal fin approximately between fin rays 11 and 13. Pigment in the fourth band was located on the caudal peduncle and extended posteriorly onto the caudal fin. Pigment was also scattered mediolaterally, giving the appearance of a horizontal bar posterior to the second band. Pigment developed on the caudal-fin rays.

At the beginning of the juvenile stage, lateral bands were well defined by dark pigment (Fig. 2E). Larval pigmentation (e.g., PVMs) was still present until at least 24.9 mm, but by 33.0 mm no residual larval pigment remained. Scattered melanophores on the mediolateral part of the body between the second and fourth bands were retained and looked like small pigment blotches.

Table 2

Total postanal ventral melanophores (PVMs) of larvae and juveniles of northern sculpin (*Icelinus borealis*). Specimens between dotted lines (-----) are undergoing notochord flexion; specimens between lines (- — -) are in transformation stage. Abbreviation: SL = standard length.

Body length (mm SL)	Postanal ventral melanophores
7.4	—
7.9	9
8.8	9
10.2	4
11.6	9
13.4	14
14.3	9
14.8	9
14.9	7
15.1	11
15.8	9
16.0	8
16.3	10
17.9	7
19.6	5
22.7	3
24.1	3
24.9	7
32.1	0
41.7	0
43.2	0
45.1	0
45.9	0
51.7	0

Cirri

Cirri developed during the postflexion stage. Supraocular cirri were first to develop. Supraocular cirri are typically bifid or trifid, but occasionally have more than three terminal filaments. The development of nasal and postorbital cirri followed supraocular cirri. During transformation into the juvenile stage, cirri developed posterodorsally on the maxilla. By 25.0 mm, one small cirrus was present both anteriorly and posteriorly of the parietal and nuchal spines, and more than one opercular cirrus may develop per side (two cirri were present dorsally on each opercle of a 46.0-mm specimen). A full complement of supraocular, nasal, postorbital, maxillary, occipital, and opercular cirri was present in juveniles.

Meristic features

Except for the dorsal-fin spines and rays and the superior procurrent caudal-fin rays, fins ossified by 14.3 mm (Table 3). Dorsal-fin spines and rays were completely ossified at 15.8 mm, as were the superior procurrent caudal-fin rays. Vertebral centra (9–11 abdominal + 24–27 caudal) ossified at 14.3–15.8 mm. By 15.0 mm, lateral line scales began to develop; by 15.8 mm, two dorsal scale rows began to develop immediately beneath the dorsal fins. Lateral line scales and the two dorsal scale rows were ossified by 24.0 mm. Pterygiophores of the dorsal and anal fins ossified by 24.1 mm. Adult radiographs resulted in vertebral counts of 35–36.

Spination

Head spines developed during flexion. At 8.8 mm, parietal spines were minute but ossified. Four preopercular spines were present; the dorsalmost spine was most pronounced. At 11.6 mm, small nuchal spines, approximately half the size of the parietals, were present. By 14.3 mm, nasal spines were ossified. Parietal and nuchal spines fused together at their tips to form parietal sensory canals. By 16.0 mm, the dorsalmost preopercular spine was bent upward and the ventralmost spine downward and forward. The fused parietal and nuchal spines were less prominent. Nasal spines were well developed and slightly curved posteriorly by 22.7 mm. At approximately 24.0 mm, the dorsalmost preopercular spine was very large and bifurcate; the dorsalmost spine may become trifurcate by the juvenile stage.

Caudal skeleton

The caudal skeleton consisted of one ural centrum, preural centra, neural and haemal spines, three epurals, two uroneurals, one superior hypural (HY_{4-5}), one inferior hypural (HY_{1-3}), and 25–31 caudal-fin rays (7–11, 6 + 6, 4–8) (Fig. 3). At 8.8 mm, HY_{1-3} and HY_{4-5} were fused and all 12 principal caudal-fin rays (6 + 6) were present (Fig. 3A). Three epurals formed by 12.0 mm. Each preural centrum had one neural and one haemal spine; however, in some specimens the first preural centrum had

Table 3

Meristic counts of larvae and juveniles of northern sculpin (*Icelinus borealis*). Specimens between dotted lines (-----) are undergoing notochord flexion; specimens between dashed lines (- — -) are undergoing transformation. Abbreviation: SL = standard length.

Body length (mm SL)	Dorsal-fin		Anal-fin rays	Pectoral-fin rays		Pelvic-fin spine & rays		Caudal-fin rays							Branchiostegal rays
								Superior		Inferior		Vertebrae			
	Spines	Rays		Left	Right	Left	Right	Procurrent	Principal	Principal	Procurrent	Abdominal	Caudal	Total	
7.4	—	—	—	—	—	—	—	—	—	—	—	—	—	—	—
7.9	—	—	—	—	—	—	—	—	—	—	—	—	—	—	—
*8.8	—	—	—	—	—	—	—	—	—	—	—	—	—	—	—
*10.2	—	—	—	—	—	—	—	—	—	—	—	—	—	—	—
*11.6	—	—	—	—	—	—	—	—	—	—	—	—	—	—	—
*13.4	—	—	—	—	—	—	—	—	—	—	—	—	—	—	—
*14.3	—	—	13	16	16	I, 2	I, 2	—	6	6	7	9	26	35	6
*14.8	—	—	—	—	—	—	—	—	6	6	—	—	—	—	—
*14.9	—	—	—	16	16	—	—	—	—	—	—	—	—	—	6
*15.1	—	—	—	16	16	—	—	—	—	—	—	—	—	—	6
*15.8	X	17	14	16	17	I, 2	I, 2	9	6	6	7	10	25	35	6
*16.0	—	—	—	16	16	I, 2	I, 2	—	6	6	—	—	—	—	6
*16.3	X	16	13	16	16	I, 2	I, 2	10	6	6	8	11	25	36	6
+17.9	X	16	#	15	15	I, 2	I, 2	11	6	6	8	11	25	36	6
*19.6	XI	16	12	16	16	I, 2	I, 2	10	6	6	7	10	25	35	6
*22.7	XI	16	13	16	15	I, 2	I, 2	10	6	6	4	10	25	35	6
*24.1	X	16	13	16	16	I, 2	I, 2	10	6	6	8	#	#	36	6
+24.9	IX	16	13	16	16	I, 2	I, 2	9	6	6	8	10	26	36	6
+32.1	X	16	13	16	16	I, 2	I, 2	10	6	6	7	10	26	36	6
+41.7	IX	16	13	16	16	I, 2	I, 2	10	6	6	7	11	25	36	6
+43.2	X	16	13	16	16	I, 2	I, 2	8	6	6	6	11	25	36	6
+45.1	X	15	12	16	16	I, 2	I, 2	9	6	6	8	#	#	36	6
+45.9	#	15	12	15	15	I, 2	I, 2	9	6	6	8	11	25	36	6
+51.7	IX	14	12	16	16	I, 2	I, 2	9	6	6	8	11	25	36	6

* Cleared and stained specimens.
\+ Radiographed specimens.
\# Could not obtain accurate count.

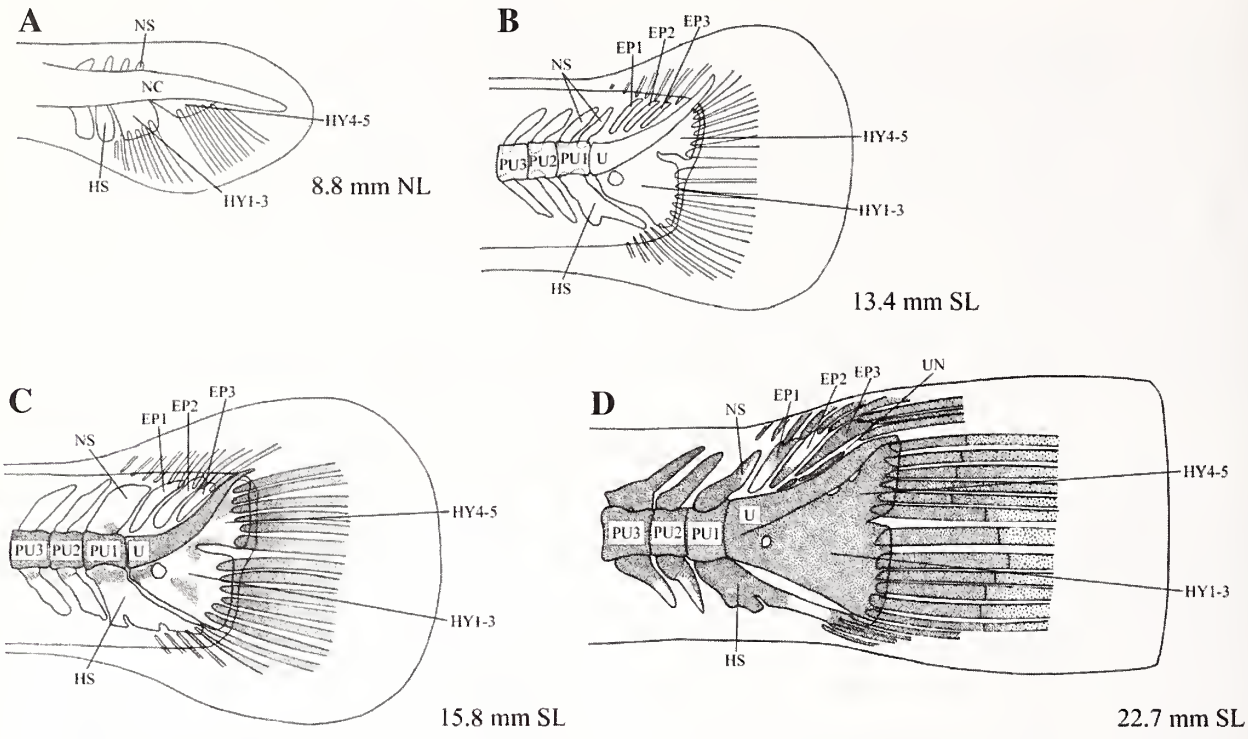

Figure 3

Development of caudal skeleton of northern sculpin (*Icelinus borealis*). (**A**) Flexion larva, 8.8 mm NL, UW 105131, Bering Sea, 56°27.3′N, 169°28.3′W, 30 m depth, 12 July 1997; (**B**) postflexion larva, 13.4 mm SL, UW 105111, Bering Sea, 56°31.9′N, 166°25.4′W, 88 m depth, 16 July 1994; (**C**) postflexion larva, 15.8 mm SL, UW 105162, Bering Sea, 56°28.3′N, 169°26.9′W, 87 m depth, 1 August 1996; (**D**) juvenile, 22.7 mm SL, UW 105174, Bering Sea, 57°16.3′N, 170°11.0′W, 16 September 1997. Abbreviations: NL=notochord length; SL=standard length; HY_{1-3}=hypurals 1–3; HY_{4-5}=hypurals 4–5; EP (1, 2, 3)=epural(s) (1, 2, 3); NS=neural spine; HS=haemal spine; NC=notochord; U=ural centrum; PU (1, 2, 3)=preural centra (1, 2, 3); UN=uroneural. Illustrations by R. L. Cartwright.

two neural spines (Fig. 3B). All five hypurals (HY_{1-5}) fused by 13.4 mm. By 15.8 mm, the ural centrum, preural centra, and principal caudal-fin rays ossified (Fig. 3C). Hypurals ossified by 16.0 mm. Two uroneurals were present and ossified by 20.0 mm; neural and haemal spines on the first preural centrum and procurrent caudal-fin rays were ossified. Epurals ossified by 22.7 mm (Fig. 3D). By the juvenile stage at approximately 24.0 mm, development of the caudal skeleton was complete.

Discussion

Information about the early life history of *Icelinus* is conspicuously sparse in literature. This study presents the first description of larval and juvenile *Icelinus borealis*. *Icelinus borealis* larvae exhibit a unique geographic distribution in the Bering Sea and are geographically isolated north of the Aleutian Islands—which provides for a definitive description of its development. A combination of morphological characters, pigmentation, preopercular spine pattern, meristic counts, and squamation in later developmental stages is essential to identify *Icelinus* at the species level. Larvae of *I. borealis* have 35–36 myomeres. The body is lightly pigmented, and the most useful character is the presence of 3–14 (mode=9) irregular PVMs that persist through transformation into the juvenile stage. Four prominent preopercular spines and three rows of spiny ctenoid scales develop during transformation into the juvenile stage; one row is along the lateral line and two are directly beneath the dorsal fins. Identification of *I. borealis* larvae in other geographic areas, such as the Gulf of Alaska, is complicated by the co-occurrence of other species of *Icelinus*.

Icelinus filamentosus is found with *I. borealis* throughout the Gulf of Alaska but, if collected, has not been identified in ichthyoplankton samples (Matarese et al., 1989; Mecklenburg et al., 2002). Larvae of *I. borealis* differ from *I. filamentosus* primarily by having an anal-fin ray count of 11–14 (vs. 13–16) and a vertebral count of 35–36 (vs. 34–37) (Table 4). *Icelinus burchami* and *I. tenuis* also are found with *I. borealis*; however, the northernmost extent of their geographic ranges is

Southeast Alaska and do not extend farther north into the Gulf of Alaska or into the Bering Sea (Matarese et al., 1989; Mecklenburg et al., 2002). Larvae of *I. burchami* and *I. tenuis* have not been identified, but there are subtle differences in meristic counts of juveniles and adults between these species and *I. borealis* (Table 4). Juvenile *Icelinus* may be distinguished by using adult characters in any geographic location (e.g., by the presence of elongated, threadlike first two dorsal spines in *I. filamentosus*).

Icelinus quadriseriatus is the only species of *Icelinus* with currently identifiable and described early life history stages. *Icelinus quadriseriatus* is distributed from Sonoma County, California, south to Cabo San Lucas, Baja California, Mexico (Feeney, 1987). Although *I. borealis* and *I. quadriseriatus* are geographically separated and their distributions do not overlap, it is important to compare the larvae of these species. Larvae of *I. borealis* and *I. quadriseriatus* are similarly pigmented; however they differ primarily in number of PVMs and ventral gut pigment. *Icelinus borealis* PVMs number from three to 14 (vs. 25–63). *Icelinus borealis* may have a few, individual melanophores present on the ventral gut during preflexion, whereas *I. quadriseriatus* has ventral gut pigment consisting of one to six rows of melanophores aligned anteroposteriorly in early development. *Icelinus quadriseriatus* retains ventral gut pigment throughout its larval development (Feeney, 1987). *Icelinus borealis* differs from *I. quadriseriatus* by having an analfin ray count of 11–14 (vs. 10–15), and a vertebral count of 35–36 (vs. 33–35) (Table 4). *Icelinus borealis* and *I. quadriseriatus* also undergo flexion at different times (8.0–11.0 mm vs. 5.2–7.6 mm, respectively) (Feeney, 1987).

After examining all available putative larval specimens of *Icelinus* from the Bering Sea, it was found that the majority of larvae at AFSC were not *I. borealis* but probably members of the closely

Table 4

Comparison of meristic counts of *Icelinus* and *Icelus* (Yabe et al., 1980; Matarese et al., 1989; Moser et al., 1996; Yabe et al., 2001; Mecklenburg et al., 2002; Rosenblatt and Smith, 2004; Tsuruoka et al., 2006). Counts in parentheses (*I. borealis*) indicate the mode. Abbreviations: C=central; S=southern; SE=southeast; SS=south of southern.

			Fins				
Species	Common name	Distribution	Dorsal	Anal	Pectoral	Pelvic	Vertebrae
Icelinus borealis	northern sculpin	Washington–Bering Sea	IX–XI + 14–17 (X + 16)	11–14 (13)	14–17 (16)	I,2	35–36*
I. burchami	dusky sculpin	S California–SE Alaska	VIII–XI + 15–18	10–14	16–19	I,2	33–37
I. cavifrons	pit–head sculpin	SS California–C California	IX–XII + 12–15	11–13	14–16	I,2	35–37
I. filamentosus	threadfin sculpin	S California–Gulf of Alaska	IX–XII + 15–18	13–16	16–18	I,2	34–37
I. fimbriatus	fringed sculpin	S California–British Columbia	X–XI + 12–14	12–14	16–18	I,2	35–37
I. japonicus	Futasuji–kajika	Japan	IX–X + 12–13	10–11	15–17	I,2	33
I. limbaughi	canyon sculpin	S California	IX–X + 13–15	8–12	15–17	I,2	31–36
I. oculatus	frogmouth sculpin	S California–British Columbia	X–XI + 15–17	13–14	17	I,2	37
I. pietschi	Hime–futasuji–kajika	Onagawa, Japan–Iturup I., Kuril Is.	X + 13–14	11–12	16	I,2	32–34
I. quadriseriatus	yellowchin sculpin	SS California–C California	VII–X + 12–16	10–15	15–17	I,2	33–35
I. tenuis	spotfin sculpin	SS California–SE Alaska	IX–XI + 16–19	13–17	15–17	I,2	37–39
Icelus canaliculatus	blacknose sculpin	Gulf of Alaska–Bering Sea	VII–VIII + 22–25	18–20	15–19	I,3	37–39
I. euryops	wide–eye sculpin	Gulf of Alaska–Bering Sea	VIII–X + 20–23	15–19	16–18	I,3	41–42**
I. spatula	spatulate sculpin	Gulf of Alaska–Arctic	VII–XI + 18–22	13–18	16–20	I,3	39–41
I. spiniger	thorny sculpin	British Columbia–Bering Sea	VIII–X + 19–23	15–19	17–20	I,3	40–42
I. uncinalis	uncinate sculpin	Bering Sea	IX + 19–20	14–16	17–18	I,3	37–40

* Counts obtained from literature and radiographs of adult specimens.
** Counts obtained from radiographs of adult specimens.

related genus, *Icelus*. The majority of larvae had higher myomere counts (37–42) than *Icelus* (35–36) and a different pelvic-fin count (1, 3) than *I. borealis* (1, 2) (Table 4). Larvae of *I. borealis* and *Icelus* had the same general body shape, presence of irregular PVMs (size, shape, location), similar pigmentation on the head, gut, and anus, four prominent preopercular spines, and a distinctive bony shelf on the anterior portion of the preopercle. *Icelinus* and *Icelus* were also placed in the same phenetic group by Richardson (1981) based on shared larval characters. There are five species of *Icelus* in the Bering Sea; however, *Icelus spatula* and *I. spiniger* are most abundant in the geographic area where *Icelinus borealis* is found (Matarese et al., 1989).

This study provides a sound method for identifying larval *I. borealis* in the Bering Sea and is applicable to juvenile specimens as far south as southern Puget Sound, Washington. Although only two preflexion specimens were available for study, morphological characters and patterns of pigmentation at this stage of development are an important contribution. Taxonomic characters presented here could elucidate distinctiveness or similarity of *Icelinus* among other cottid genera (e.g., *Ruscarius*, *Icelus*) and co-occurring species (e.g., *Icelinus filamentosus*)—an important beginning to solving the complicated systematic relationships within the family Cottidae (Richardson, 1981). Although *I. borealis* larvae were identified in this study from the Bering Sea, definitive identification of larval *I. borealis* in other geographic areas will depend on the comparison of *I. borealis* with its congeners and other sympatric cottid larvae.

Acknowledgments

The author thanks J. Orr (AFSC), M. Busby, A. Matarese, and J. Napp for reviewing the manuscript. Data for adult groundfish and specimens of *Icelinus* and *Icelus* juveniles and adults were supplied by J. Orr and D. Stevenson (AFSC), who also granted use of the Resource Assessment and Conservation Engineering Groundfish Systematics Laboratory and digital radiograph machine. J. Benson (AFSC) and M. Busby provided ArcView–GIS training and support. K. Maslenikov, University of Washington, provided radiographs and specimens of *Icelus*. This research is contribution EcoFOCI-0636 to the National Oceanic and Atmospheric Administration's Fisheries-Oceanography Coordinated Investigations.

Literature cited

Begle, D. P.
1989. Phylogenetic analysis of the cottid genus *Artedius* (Teleostei: Scorpaeniformes). Copeia 1989:642–652.

Blackburn, J. E.
1973. A survey of the abundance, distribution and factors affecting distribution of ichthyoplankton in Skagit Bay. M.S. thesis, 136 p. Univ. Washington, Seattle, WA.

Bolin, R. L.
1936. A revision of the genus *Icelinus* Jordan. Copeia 1936:151–159.

Browne, P., J. L. Laake, and R. L. DeLong.
2002. Improving pinniped diet analyses through identification of multiple skeletal structures in fecal samples. Fish. Bull. 100:423–433.

Busby, M. S., and D. A. Ambrose.
1993. Development of larval and early juvenile pygmy poacher, *Odontopyxis trispinosa*, and blacktip poacher, *Xeneretmus latifrons* (Scorpaeniformes: Agonidae). Fish. Bull. 91:397–413.

Feeney, R. F.
1987. Development of the eggs and larvae of the yellowchin sculpin, *Icelinus quadriseriatus* (Pisces: Cottidae). Fish. Bull. 85:201–212.

Fritz, L. W., and S. Hinckley.
2005. A critical review of the regime shift – "junk food" – nutritional stress hypothesis for the decline of the western stock of Steller sea lion. Mar. Mammal Sci. 21(3):476–518.

Hoff, G. R.
2006. Biodiversity as an index of regime shift in the eastern Bering Sea. Fish. Bull. 104:226–237.

Kendall, A. W., Jr., E. H. Ahlstrom, and H. G. Moser.
1984. Early life history of fishes and their characters. *In* Ontogeny and systematics of fishes, spec. publ. 1 (H. G. Moser, W. J. Richards, D. M. Cohen, M. P. Fahay, A. W. Kendall Jr., and S. L. Richardson, eds.), p. 11–22. Am. Soc. Ichthyol. Herpetol., Allen Press, Lawrence, KS.

Matarese, A. C., D. M. Blood, S. J. Picquelle, and J. L. Benson.
2003. Atlas of abundance and distribution patterns of ichthyoplankton from the Northeast Pacific Ocean and Bering Sea ecosystems based on research conducted by the Alaska Fisheries Science Center (1972–1996). U.S. Dep. Commer., NOAA Prof. Paper NMFS 1, 281 p.

Matarese, A. C., A. W. Kendall Jr., D. M. Blood, and B. M. Vinter.
1989. Laboratory guide to early life history stages of Northeast Pacific fishes. U.S. Dep. Commer., NOAA Tech. Rep. NMFS 80, 652 p.

Matarese, A. C., and J. B. Marliave.
1982. Larval development of laboratory-reared rosylip sculpin, *Ascelichthys rhodorus* (Cottidae). Fish. Bull. 80:345–355.

Mecklenburg, C. W., T. A. Mecklenburg, and L. K. Thorsteinson.
2002. Fishes of Alaska, 1037 p. Am. Fish. Soc., Bethesda, MD.

Moser, H. G., R. L. Charter, P. E. Smith, D. A. Ambrose, S. R. Charter, C. A. Myer, E. M. Sandknop, and W. Watson.
1996. Distributional atlas of fish larvae and eggs in the California Current region. Calif. Coop. Oceanic Fish. Invest. Atlas 33. 1505 p. Scripps Inst. Ocean., La Jolla, CA.

Mueter, F. J., and B. L. Norcross.
2000. Species composition and abundance of juvenile groundfishes around Steller sea lion *Eumetopias jubatus* rookeries in the Gulf of Alaska. Alaska Fish. Res. Bull. 7:33–43.

Neira, F. J., A. G. Miskiewicz, and T. Trnski.
1998. Larvae of temperate Australian fishes—laboratory guide for larval fish identification, 474 p. Univ. Western Australia Press, Nedlands, Western Australia.

Nelson, J. S.
2006. Fishes of the World, 4th ed., 601 p. John Wiley and Sons, Inc., Hoboken, NJ.

Nelson, J. S., E. J. Crossman, H. Espinosa-Pérez, L. T. Findley, C. R. Gilbert, R. N. Lea, and J. D. Williams.
2004. Common and scientific names of fishes from the United States, Canada, and Mexico, 6th ed., 386 p. Am. Fish. Soc. Spec. Publ. 29, Bethesda, MD.

Pietsch, T. W., and J. W. Orr.
2006. *Triglops dorothy*, a new species of sculpin (Teleostei: Scorpaeniformes: Cottidae) from the southern Sea of Okhotsk. Fish. Bull. 104:238–246.

Potthoff, T.
1984. Clearing and staining techniques. *In* Ontogeny and systematics of fishes, spec. publ. 1 (H. G. Moser, W. J. Richards, D. M. Cohen, M. P. Fahay, A. W. Kendall Jr., and S. L. Richardson, eds.), p. 35–37. Am. Soc. Ichthyol. Herpetol., Allen Press, Lawrence, KS.

Richardson, S. L.
1977. Larval fishes in ocean waters off Yaquina Bay, Oregon: Abundance, distribution, and seasonality, January 1971–August 1972, 72 p. OSU Sea Grant Publ. ORESU-T-77-003.
1981. Current knowledge of larvae of sculpins (Pisces: Cottidae and allies) in Northeast Pacific genera with notes on intergeneric relationships. Fish. Bull. 79:103–121.

Richardson, S. L., and W. G. Pearcy.
1977. Coastal and oceanic fish larvae in an area of upwelling off Yaquina Bay, Oregon. Fish. Bull. 75: 125–145.

Richardson, S. L., and B. B. Washington.
1980. Guide to identification of some sculpin (Cottidae) larvae from marine and brackish waters off Oregon and adjacent areas in the Northeast Pacific. NOAA Tech. Rep. NMFS 430, 56 p. [With errata sheet dated May 1981.]

Rosenblatt, R. H., and W. L. Smith.
2004. *Icelinus limbaughi*: A new species of sculpin (Teleostei: Cottidae) from southern California. Copeia 2004:556–561.

Tsuruoka, O., T. Abe, H. Munehara, and M. Yabe.
2006. Record of a cottid fish, *Icelinus pietschi*, collected from Hokkaido and Miyagi Prefecture, Japan. Jap. J. Ichthyol. 53(1):89–93.

Washington, B. B.
1981. Identification and systematics of larvae of *Artedius*, *Clinocottus*, and *Oligocottus* (Scorpaeniformes: Cottidae). M.S. thesis, 202 p. Oregon State Univ., Corvallis, OR.

Yabe, M., S. Maruyama, and K. Amaoka.
1983. First records of five cottid fishes and a psychrolutid fish from Japan. Jap. J. Ichthyol. 29(4):456–464.

Yabe, M., A. Soma, and K. Amaoka.
2001. *Icelinus pietschi* sp. nov. and a rare species, *Sigmistes smithi*, from the southern Kuril Archipelago (Scorpaeniformes: Cottidae). Ichthyol. Res. 48(1):65–70.

Yabe, M., K. Tsumura, and M. Katayama.
1980. Description of a new cottid fish, *Icelinus japonicus*, from Japanese waters. Jap. J. Ichthyol. 27(2):106–110.

Management of fishing capacity in a spiny lobster (*Panulirus argus*) fishery: analysis of trap performance under the Florida spiny lobster Trap Certificate Program

Nelson M. Ehrhardt (contact author)
Vallierre K. W. Deleveaux

Email address for contact author: nehrhardt@rsmas.miami.edu

Division of Marine Biology and Fisheries
Rosenstiel School of Marine and Atmospheric Science
University of Miami
4600 Rickenbacker Causeway
Miami, Florida 33149

Abstract—The spiny lobster (*Panulirus argus*) fishery in Florida was operationally inefficient and overcapitalized throughout the 1980s. The Trap Certificate Program initiated during the 1992–93 season was intended to increase gear efficiency by reducing the number of traps being used while maintaining the same catch level in the fishery. A depletion model was used to estimate trap fishing efficiency. The costs of fishing operations and the value of the catch were used to determine the revenues generated by the fishery under different trap levels. A negative functional relationship was found between the catchability coefficient and the number of traps, which indicated that the fewer traps operating under the trap reduction scheme were more efficient. Also, the financial analyses indicated that the higher catch efficiency resulting from fewer traps generated significantly higher revenues, despite lower stock abundances. This study indicates that the trap reduction program had improved a situation that would have been much worse.

Manuscript submitted 9 May 2008.
Manuscript accepted 4 November 2008.
Fish. Bull. 107:186–194 (2009).

The Florida spiny lobster (*Panulirus argus*) fishery has been exploited since the early 20th century (Labisky et al., 1980); however, demand for lobster products in the U.S. markets did not materialize until the early 1960s. Rapid growth of the fishery took place in the late 1960s and early 1970s and since then total landings have varied between 1800 and 2700 metric tons (t) whole weight, with no discernible pattern. Fishing effort expanded from 250,000 traps in the early 1970s to approximately 940,000 traps by the 1991–92 fishing season (August–March). This fishery development took place mainly in the Florida Keys, where today over 90% of Florida's harvest is landed with a dockside value exceeding $40 million. Therefore, the spiny lobster fishery is one of the most important fisheries in the State. High fishing intensity, overcapitalization, negative environmental impacts, and gear conflicts characterized the fishery until the Florida Legislature enacted a trap reduction program in 1991.

The Trap Certificate Program (TCP) was implemented in the Florida spiny lobster fishery taking the 1992–93 fishing season as a base. One of the goals of the TCP was to increase the efficiency of the traps used in the fishery. Seasonal catch per trap in the Florida Keys fishery decreased from about 24.1 kg per trap using about 97,000 traps in the 1969–70 fishing season to about 3.1 kg per trap from about 851,000 traps in the 1991–92 fishing season. While the catch per trap decreased, the total seasonal landings were sustained at an average of 2.8 million kg whole weight through most of the fully developed fishery (1975 to 2004). The TCP proposed a steady reduction in the number of traps while keeping the total landings unaffected. This desirable objective was thought possible because total landings were sustained over the wide range of traps used in the fishery.

There was an operational assumption that the trap catchability (the fraction of the seasonal stock biomass taken by each trap) would increase because there would be less competition for the fixed seasonal spiny lobster biomass as the trap numbers were reduced. Under the TCP, the total number of traps was to be reduced annually by a fixed percentage of the number of traps used during the previous fishing season, starting with the 1993–94 season. However, this strategy was modified several times in the ensuing years, mainly due to economic hardships resulting from environmental impacts, e.g., Hurricane George in September 1998, and a perceived decrease in stock abundance. This TCP was the first limited access system to be implemented in the southeastern United States.

By the early 2000s the spiny lobster trap fishermen expressed reservations about whether the TCP would be able to resolve the economic hardship that they had faced. Therefore, in order to

address the fishermen's concerns regarding the TCP, the Florida Fish and Wildlife Conservation Commission (FWC) implemented a project to assess the status of the TCP under the existing conditions of the spiny lobster stocks and costs of the fishery. A comprehensive cost and social survey analysis was conducted in 2004 with FWC support. An assessment of the financial impact of different levels of stock abundance on the TCP was performed. As a corollary, one of the first tasks for the project was to test the hypothesis that the seasonal trap catchability should have been positively affected by the TCP. In this article we present the results of the research on the effects of the TCP on trap catch efficiency, at both a fishery-wide and regional scale, and its financial impacts.

Methods and Materials

Evaluation of trap catch efficiency under the TCP

A quantitative model was developed to estimate the seasonal catchability coefficient, q, and to study the resulting trends as the trap reduction schedules were implemented. A seasonal depletion model similar to those used in the scientific literature concerning fishery assessments (Chien and Condrey, 1985; Sanders, 1988; Rosemberg et al., 1990) was adopted using Pope's (1972) approximation to Baranov's catch equation. This approximation assumes that the total catch (C_t) realized in a given month (t) will be taken instantaneously at the middle of the month. Such an approximation generates unbiased estimates of population abundance at the beginning (N_t) and end (N_{t+1}) of the time units given that the natural mortality rate (M) is not greater than 0.3/yr and fishing mortality rates are not greater than 1.2/yr. Hence, the basic population equation is expressed as

$$N_{t+1} = \frac{\frac{N_t}{e^{M/2}} - C_t}{e^{M/2}}, \quad (1)$$

and the average population abundance is expressed as

$$\overline{N_t} = \frac{N_t}{e^{M/2}} - \frac{C_t}{2}. \quad (2)$$

Also, the relative stock abundance expressed as the catch in numbers per unit of effort (CPUE) in the time period t is assumed directly proportional to the average abundance. Hence,

$$CPUE_t = q_i * \overline{N_t}, \quad (3)$$

and therefore,

$$q_i = \frac{CPUE_t}{\overline{N_t}}. \quad (4)$$

Application of Equation 1 to express seasonal depletion in the spiny lobster fishery requires that N_t varies with monthly fishing and natural mortality. However, at the beginning of the fishing season (August) the stock abundance is composed of the remainder of the previous season's stock abundance that escaped natural and fishing mortality (N_t), plus the new recruits (R_{t+1}) that accumulated during the closed season (April–July). In this manner, the abundance at the start of the season (August t+1) is expressed as

$$N_{t+1} = \frac{N_t}{e^{4M}} + R_{t+1}. \quad (5)$$

The seasonal depletion model expressed by Equations 1 and 5 was fitted to the monthly catch in numbers per unit of effort data for the period including the 1991–92 through the 2002–03 fishing seasons, i.e., from the season previous to the base year for implementation of the TCP to the last fishing season when no further trap reductions were implemented. For this purpose the FWC provided landings and effort data for the commercial fishery extracted from the Marine Fisheries Information System. This system consists of all wholesale seafood dealers receipts of salt-water product purchases (trip tickets). Trip tickets show landings, fishing effort, gear, location, and date of landings per trip. The information used in this research is limited to the Florida Keys where most of the spiny lobster landings occur. Counts of the total number of traps deployed during the 1991–92 and 1992–93 fishing seasons were obtained from the National Marine Fisheries Service. Trap numbers for subsequent seasons were obtained from the trap certificates issued by the State of Florida according to the TCP. Numbers of commercial trips per season were obtained from the trip ticket system for those records containing lobster landings. Numbers of recreational spiny lobster landings were obtained from the FWC. The FWC transforms the weight of commercial landings into numbers using sex and size frequency samples collected by the FWC and the National Marine Fisheries Service. The number of undersized lobsters used as attractants in the trap fishery was provided by the FWC from their observer program established in 1993. This program measures the total catch on selected commercial lobster fishing trips.

The catchability coefficient was assumed to vary among the seasons following a random walk model of the type:

$$q_i = q_{i-1} e^{\varepsilon_i}, \quad (6)$$

where the ε_i are annualized, and normally distributed with mean zero and variance σ_e^2. The model was fitted by minimizing the negative log-likelihood objective function using the Solver minimization tool in Excel (Microsoft Corp., Redmond, WA):

$$\frac{n}{2}\sum_t \left(\ln(U_t) - \ln(\hat{U}_t)\right)^2 + \frac{\sum_i \varepsilon_i^2}{\sigma_\varepsilon^2}, \quad (7)$$

where n represents the number of months, U_t represents CPUE in month t, and σ_e^2 was fixed to achieve a coefficient of variation of 20% in log space—a percentage that was adopted to represent the likely response of the change in q to trap reductions.

The monthly CPUE was measured in numbers of spiny lobsters caught per trap day per trip, where a trip is defined as the day when a set of traps was serviced. The difference between trips represents the effective soak time measured in days. Therefore, any seasonal change in catchability would refer directly to a per-trap-day condition defined between fishing trips. One important consideration in the preparation of the data to fit the model using the objective function (Eq. 7) was the realization that soaking times may vary throughout the fishing season, with an increasing trend expected as the fishing season progresses and local population abundance is depleted. The soaking time may also vary among fishing seasons as a consequence of differences in seasonal abundance. Therefore, if these variations in soaking times occur, the catch per trap day per trip would have to be standardized to the changing seasonal soaking time.

Financial performance under the trap reduction program

The financial analysis to assess the results of the TCP was based on monthly and seasonal revenue estimations that required information on the average unit price paid for product landed per trap day per trip, and the cost per trap day per trip incurred in the realization of the landings. The average monthly price paid per kilogram of spiny lobster landed was obtained from the trip ticket database provided by the FWC for each of the fishing seasons covered in this analysis (1991–2002). The average cost data (indirect and direct) was obtained from a census carried out from February 2003 through January 2004 sponsored by the FWC, which included interviews of 221 fishermen operating in the spiny lobster fishery.

The information collected in the 2003–04 cost survey included the general characteristics of the fishermen and their historical involvement in the multispecies fisheries associated with spiny lobster in South Florida. Other data important to this analysis provided by the FWC were the fraction of the total effort dedicated to spiny lobster operations, as well as the variable and direct costs associated with the fishermen's participation in the spiny lobster fishery. The variable cost information per trip included fuel and oil, bait, ice, food and supplies, and other costs. The direct cost data used in the analysis consisted of the value of the vessel and the age of the vessel so that vessel depreciation could be analyzed, annual dockage cost, trap costs (including repairs and labor), principal and interest on loans (IP), and protection and indemnity (PI) payments. The average costs for docking, IP, and PI included the zero costs reported by many fishermen who used dock facilities without cost or did not have debts on loans or insurance, and as such these were considered in the average direct cost estimation.

The cost analyses conducted in this study considered that the direct costs related to vessel depreciation, dockage, and vessel repairs should be proportionally distributed between the spiny lobster fishing operations and other fishing operations carried out by the same vessels. In the survey, the combined data for the entire fishery provided an average of 66% of fishing time allocated to spiny lobster. This proportion, therefore, was applied to the direct cost components pertaining to docking, IP and PI payments, and vessel repairs as directed to spiny lobster fishing on a fishery-wide scale. Similarly, the regional spiny lobster direct costs for the segregated areas were estimated by the average percent participation in spiny lobster fishing in each region declared in the survey.

The average total number of trips carried out seasonally per vessel and the average number of traps serviced per trip necessary to estimate costs on a per-trap-day-per-trip basis were also obtained from the survey data.

The vessel depreciation life was estimated at 18 years with data from the 2003–04 FWC survey. The age structure of the fleet, generated from the 2003–04 survey data, indicated that a large fraction of the vessels are in or above the 16–20 year class range that includes the depreciation life span of the vessels. Therefore, the cost analysis considered only the cost associated with the fishery-wide average payments on principal and interest that fishermen were paying for their vessels since most of the vessels are already paid off. The seasonal direct costs were converted to a per-trip basis by dividing by the average number of spiny lobster fishing trips.

The financial analyses were assessed on a fishery-wide and regional basis. Thus, it was necessary to consider the seasonal changes in stock abundance, and the dynamic changes in the catchability coefficient that occurred as a consequence of the trap reduction schedule. Because the cost data pertain only to the 2003–04 fishing season, the financial analyses were designed as case scenarios, where the CPUE was a function of the average population abundance, and the value of the CPUE was assumed for a fishing season of reference. In order to generate the catch per trap day per trip scenarios, results from the application of the assessment methods (Eqs. 1–7) were used as follows:

1 The average monthly abundance for the season with the highest abundance (1997–98), the lowest abundance (2001–02), and an intermediate abundance were used to estimate seasonal catch per trap day per trip according to Equation 3.
2 The catchability coefficient, q, required for the estimation of the catch per trap day per trip in Equation 3 was selected for the following conditions: a) low q—when the number of traps was high (1991 fishing season); b) high q—when the number of traps was low (2001 fishing season); and c) intermediate q—corresponding to the trap levels achieved by the TCP during the 1997–98 season.

3 The monthly net revenue generated on a per trap day per trip basis under each of the above scenarios was estimated as the difference between the monthly value of the catch per trap day per trip and the average cost of operating per trap day per trip based on the 2003–04 census. Total revenue for the season was simply the product of the average revenue per trap day per trip and the average number of traps serviced per trip and the average number of trips per season.

In the analyses pertaining to a fishery-wide scale the case scenarios were as follows:

1 The catch per trap per trip referred to the following three conditions: if fishing took place during the season with the highest (1997–98), or the lowest (2001–02), stock abundance during the TCP, or with the stock abundance of the season just prior to the implementation of the TCP (1991–92), and
2 The catchability coefficient condition resulted from the number of traps operated in the fishery that corresponded to the three CPUE scenarios expressed above.

Thus, it was possible to use the value per kilogram landed per trap day per trip and the cost per trap day per trip data to simulate the financial consequences for a maximum range of catchability and abundance combinations.

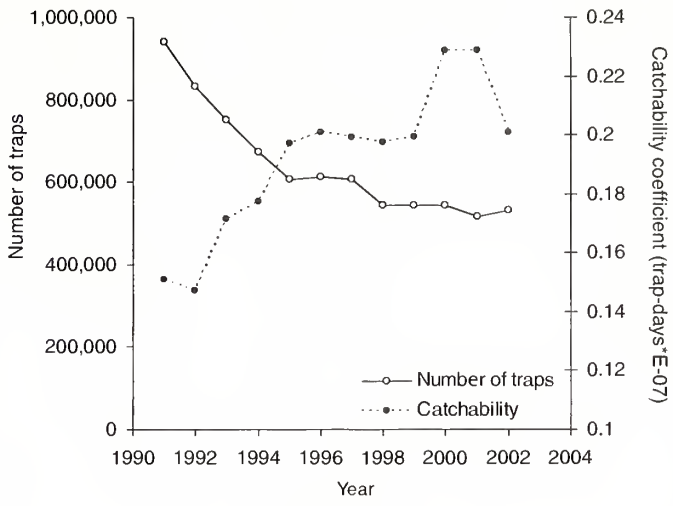

Figure 1

Number of traps under the Trap Certificate Program (○) and catchability coefficient trend (●) for spiny lobster (*Panulirus argus*) in the Florida fishery from 1991 to 2002.

Results

Trap catch efficiency

The assumption that the trap catchability would increase with the reduction of traps used in the Florida lobster fishery was verified during the TCP (Fig. 1) The trap soaking time was found to vary throughout the fishing season, with an increasing trend as the fishing season progressed and local population abundance was depleted. The soaking time also varied among fishing seasons (Fig. 2) as a consequence of differences in seasonal abundance. Therefore, the catch per trap day per trip was standardized to the changing seasonal soaking time. For this purpose an average monthly soaking time was estimated for every month in each season from the records in the trip ticket database. The resulting CPUE was consequently the average catch in numbers per trap day per trip. The seasonal CPUEs are plotted in Figure 3 where a persistent pattern of stock depletion is observed. A consistent fit of the depletion model was obtained for most years (Fig. 3) when the monthly natural mortality rate (M) commonly used in Caribbean spiny lobster assessments (FAO, 2001) was 0.0317 (or 0.38 annually). The overall fit resulted in a residual sum of squares (RSS) of 1.277.

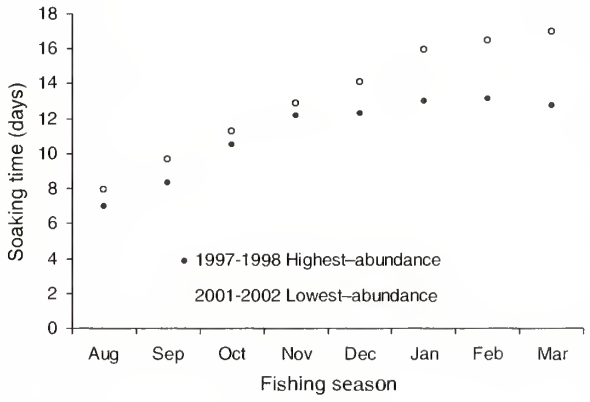

Figure 2

Average trap soaking time in number of days for fishing seasons with highest spiny lobster stock abundance (1997–98) (●) and lowest stock abundance (2001–02) (○) in the Florida fishery.

The 1991–92 fishing season had a higher stock abundance than the 2001–02 fishing season (which actually had the lowest abundance observed during the study period). The catchability coefficients were lowest during the 1991–92 seasons when the number of traps operating in the fishery was at the highest level. Meanwhile the highest catchability coefficient was found in the 2001–02 season when the fewest traps were used in the fishery. Figure 4 clearly shows a negative functional correlation between the historic trends in

seasonal catchability estimates and trap reductions under the TCP. This relationship, when the fishing effort is by passive fishing units (e.g., traps, longlines, gillnets, etc.), has also been reported for the spiny lobster fisheries of Australia (Groeneveld et al., 2003), Brazil (Ehrhardt, 2005), and Nicaragua (Ehrhardt (2005); crawfish (Romaire and Pfister, 1983; Fouilland and Fossati, 1996); and cod (Angelsen and Olsen, 1987). Figure 4 indicates a significant increase in the fraction of the stock that was taken per trap-day as the number of interacting traps was reduced from about 851,000 to about 550,000. It is observed that during the period of the TCP, the 1991–92 to the 2002–03 fishing seasons, the fishing effort expressed in traps-days became at least 50% more efficient due to changes in trap catching efficiency. This increase was independent of the decreasing stock abundance levels.

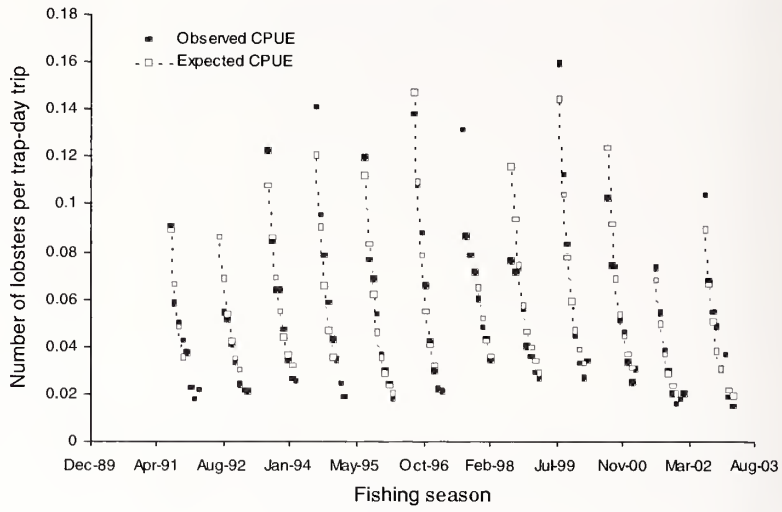

Figure 3

Observed (●) Florida seasonal spiny lobster (*Panulirus argus*) catch in number of lobsters per trap per day per trip (CPUE) corrected by soaking time in days and expected (○) CPUE obtained by fitting the depletion model to the observed data during the 1991 to 2002 fishing seasons. Fishing seasons are from August to April.

Financial performance

Fishery-wide analysis The fishery-wide financial performance was assessed based on monthly revenues using the costs per trap day per trip and the average monthly value paid per kilogram of lobster landed in the 2002–03 season estimated from the trip ticket database. The average seasonal direct costs and indirect costs per trip were transformed to a per-trap-day-per-trip condition based on the average number of 347.8 (standard deviation=213) traps pulled per trip and 78 trips per season reported in the 2003–04 survey. Therefore, it was possible to judge the consequences of the increases in the catching efficiency of the traps due to the TCP and the decreasing trend in stock abundance observed in the period of analysis.

Analysis of the different scenarios considered in this study indicates highly significant differences regarding the seasonal dissipation of revenues as a function of the number of traps used in the fishery. However, such dissipation is dramatically influenced by the lower catchabilities observed when a large number of traps are deployed in the fishery. For example, Figure 5A shows the monthly revenues of the 1991–92 scenario of high abundance and lowest q fishing season, prior to the TCP implementation, and the 2001–02 fishing season with the lowest abundance and highest q. The figure indicates that revenues dissipated quickly and became negligible by March in both cases. The total seasonal revenue per vessel was $17,701 and $13,405 for the 1991–92 and 2001–02 fishing seasons, respectively. Thus, although a much larger stock abundance was present during the 1991–92 fishing season relative to the 2001–02 season, the less efficient traps at that time generated a catch per trap day per trip that did not contribute significantly to the total revenues. If the catchability coefficient of 2001–02 could have been applied to the stock abundance available in the 1991–92 season, the total annual revenue per vessel would have been $38,654, or about 2.18 times larger than that which was actually obtained.

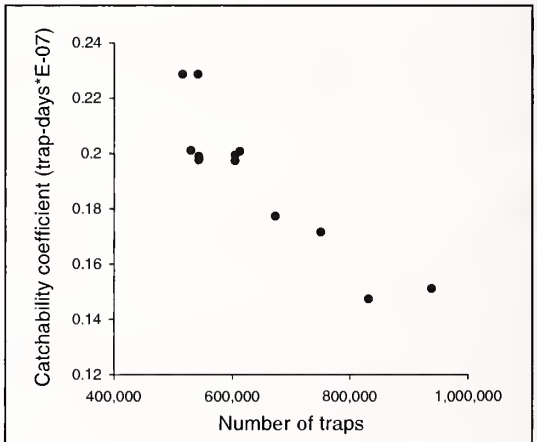

Figure 4

Trend of decreasing catchability (measured in trap days) with increasing number of traps in the spiny lobster (*Panulirus argus*) fishery in Florida from 1991 to 2002 fishing seasons.

In the scenario under which the TCP would not have been established, very small revenues would have been generated by the fishery. This case compares the revenue conditions for the 2001–02 fishing season abun-

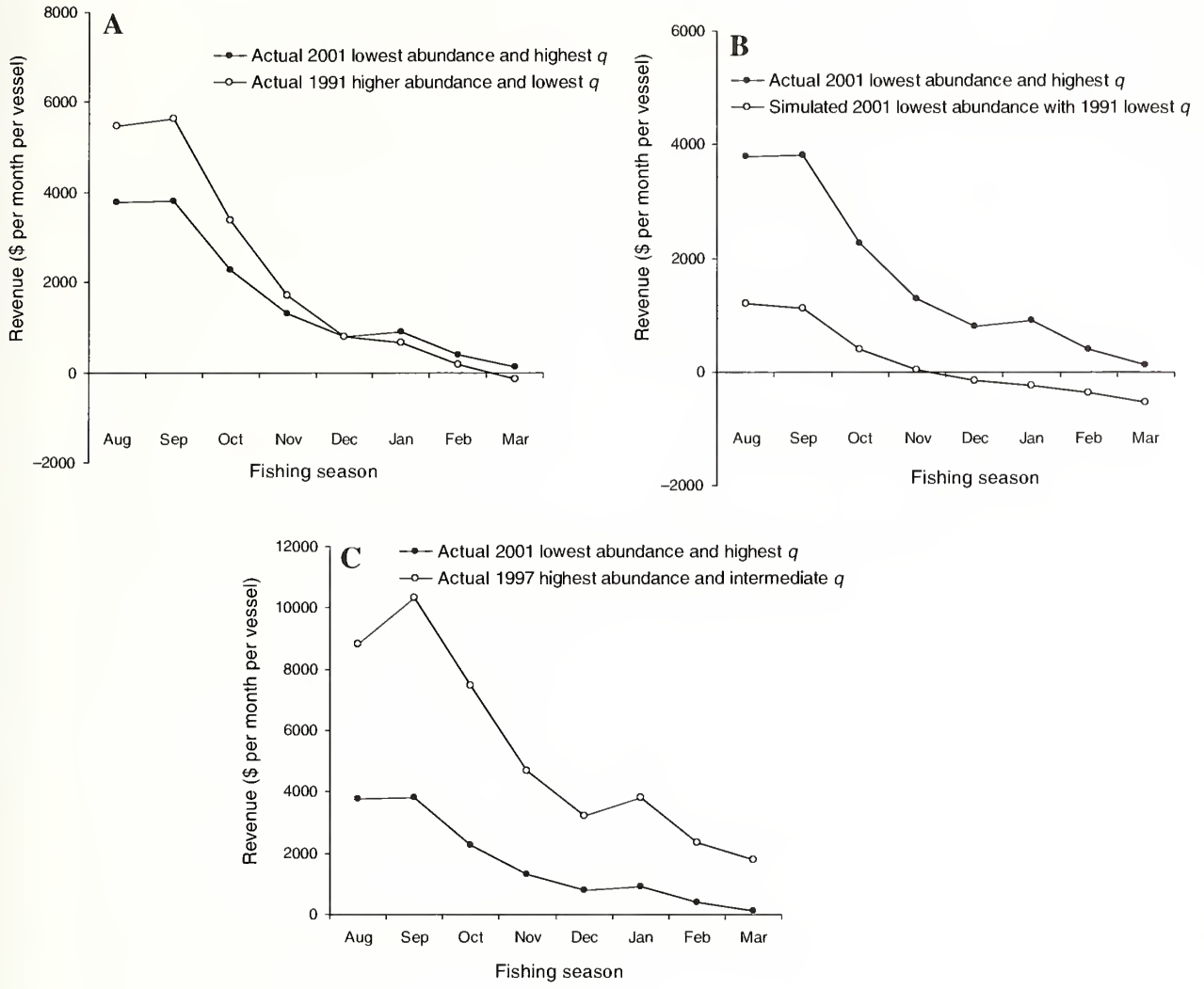

Figure 5

Average Florida regional monthly revenues per trap-fishing vessel under (**A**) the 1991 spiny lobster (*Panulirus argus*) high abundance and lowest q (○) and the 2001 lowest abundance and highest q (●); (**B**) the 2001 lowest abundance and highest q (●) and a simulated condition of the 2001 abundance subjected to the 1991 lowest q (○), and (**C**) the 2001 lowest abundance and highest q and the 1997 abundance and the intermediate q estimated for that season.

dance under the exploitation of the catchability coefficients before the TCP (the 1991–92 fishing season) and the actual 2001–02 catchability (Fig. 5B). In the absence of the TCP, the revenues per vessel would have been close to zero by November, and negative starting in December, resulting in total seasonal revenues of only $1,470 instead of the $13,405 that was actually obtained due to the increased CPUE that resulted as a consequence of the TCP implementation.

In the case scenario corresponding to the highest fishing season stock abundance observed during the study period (1997–98), the reduced number of traps generated an intermediate value of q; hence, the total seasonal revenue for the 1997–98 scenario was $42,468 compared with $13,405 for the 2001–02 scenario (Fig. 5C). If the reduced number of traps of the 2001–02 season had existed in the 1997–98 fishing season, the annual expected revenue under the 1997–98 stock abundance would have been $51,608.

Regional analysis Direct costs were calculated on a per trap day per trip condition for each region. The total costs (direct and indirect) per trip show a significant decreasing trend from Key West (including the Dry Tortugas) through the Upper Keys, and Miami shows an intermediate total cost per trip. The total cost per trap day per trip varied among the regions because of the different number of traps serviced per trip in each of the regions and hence the total cost per trap day per trip did not follow a marked regional trend.

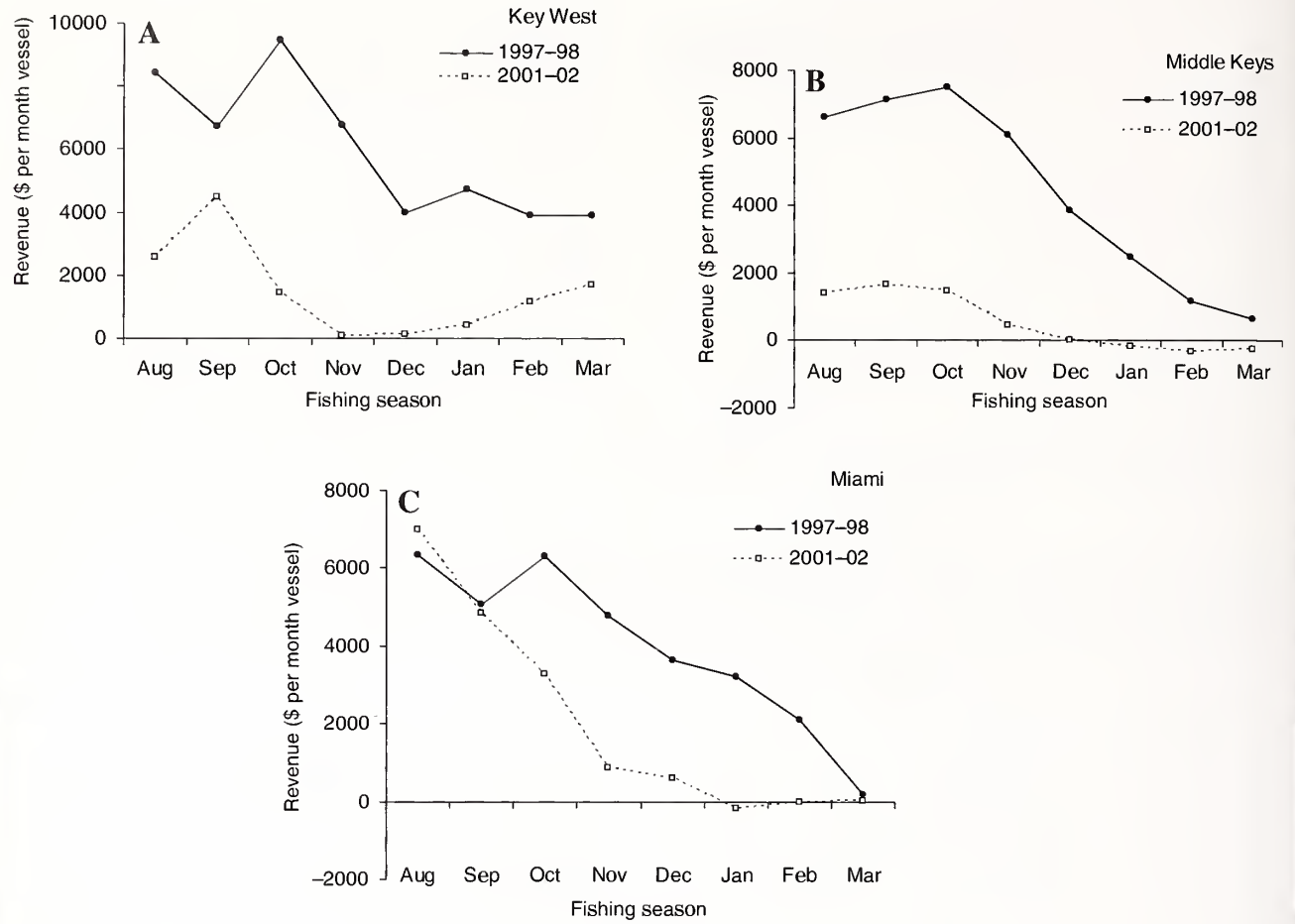

Figure 6

Average monthly revenues resulting for the season with highest (1997–98) (●) and lowest (2001–02) (○) spiny lobster (*Panulirus argus*) stock abundance and their respective *q* estimates for the trap fishery in three regions in South Florida: (**A**) Key West, (**B**) Middle Keys, and (**C**) Miami.

The total costs results were used in the seasonal financial analysis for the outcome of fishing for lobsters in the regions. The case scenarios in the regional analyses considered 1) the estimated CPUEs for the seasons with the highest (1997–98), and lowest (2001–02) stock abundance, and 2) the estimated CPUEs for the seasons with the highest and the lowest abundance standardized to the catchability coefficients corresponding to the 1991–92 fishing season (prior to the TCP) and to the 2001–02 fishing season (ten years later).

Case scenario 1: For Key West, two very different monthly revenue trends resulted for the fishing seasons with the highest and the lowest stock abundance relative to the 2003–04 costs and values per kilogram (Fig. 6A). The difference in stock abundance had a very significant and striking financial impact, the total seasonal revenue was $47,922 for 1997–98 (highest abundance) and $11,985 for 2001–02 (lowest abundance). In the case of the Lower Keys the monthly revenues for 2001–02 were almost negligible. In the Lower Keys the total seasonal revenues were $15,851 for the 1997–98 fishing season, and $3227 for the 2001–02 season. The seasonal revenue trends for the Middle Keys indicate that the revenue differences were very significant between the two seasons. The total seasonal revenues for the Middle Keys were $35,505 and $4,266 for the 1997–98 and 2001–02 fishing seasons, respectively (Fig. 6B). The seasonal revenue trends for the Upper Keys show that the total seasonal revenues were very different: $31,204 for the 1997–98, and $6324 for the 2001–02 fishing seasons. In the case scenario results for Miami the total seasonal revenues were $31,619 for the 1997–98 fishing season, and $16,422 for the 2001–02 fishing season (Fig. 6C).

Generally, the 2001–02 monthly revenues in each of the regions were indicative of a fishery undergoing significant economic troubles given that revenues after November were insufficient to maintain a viable fishery. This generic condition is clearly due to the low abundance of the resource adopted in this particular

Table 1

Simulated total seasonal revenues in dollars per vessel for the highest (1997–98) and lowest (2001–02) spiny lobster (*Panulirus argus*) stock abundance seasons with catch per unit of effort standardized to the lowest (1991–92) and highest (2001–02) trap fishing seasons observed during the study period in the Florida trap fishery.

		Region				
Abundance	Catchability	Key West	Lower Keys	Middle Keys	Upper Keys	Miami
High	Low	36,298	12,006	26,893	23,635	23,949
High	High	54,920	18,165	40,690	35,761	36,236
Low	Low	7,919	2,132	2,819	4,178	10,851
Low	High	11,985	3,227	4,266	6,324	16,422

scenario, which had distinct effects on the different regions.

Case scenario 2: In this case scenario the catch per trap day per trip for the 1997–98 and 2001–02 fishing seasons were each standardized to the 1991–92 and 2001–02 catching efficiencies. The trap catching efficiencies were estimated as the simple ratio of the corresponding catchability coefficients estimated for each season to those obtained for the 1991–92 and the 2001–02 seasons. The results of the case scenarios are presented in Table 1.

The total revenues in Table 1 are indicative of the significant impact of the TCP on the potential revenues for each region under conditions of the minimum and maximum stock abundance observed during the study period. The greater catching efficiency of the traps, as reflected by the higher 2001–02 catchability coefficient relative to the 1991–92 catchability, generated much larger revenues. In the absence of the TCP those generated revenues are much less than those that created the recent economic hardships in the fishery.

Conclusions

The analyses in this study indicate several very fundamental impacts of the TCP. First, it generated a significant increase in the catching efficiency of the traps used in the fishery. Second, if the TCP had not been implemented, given the significant decrease in the stock abundance observed since the mid-1990s, the fishermen most likely would have encountered much greater economic hardships.

There are many positive consequences of the TCP, the traps are now more efficient because they retain a higher fraction of the fishable stock, and the fishery-wide investment on traps is at least 40% less than during the 1991–92 fishing season. It is important to note, however, that fewer fishermen now participate in the fishery and the number of traps per fisherman appears to have increased. Thus, the trap certificates are allotted among fewer fishermen; hence, the revenue of the resource is now distributed among fewer participants.

The revenues by regions are very different, portraying the economic conditions that differ among the regions. The TCP appears to have benefited the overall economics of the participating fishermen but the decreased stock abundance observed in the last few seasons of the study period has had a profound and different impact on the economics of fishing operations within the regions.

Finally, this assessment demonstrates that the TCP had succeeded with regard to its original objectives. The truly significant problem is the reduction in the stock abundance, which may not only be due to the local exploitation.

Acknowledgments

We thank the sponsors of this project, the Florida Fish and Wildlife Conservation Commission. Special thanks are given to J. Hunt and R. Muller of the FWC for their support and guidance regarding the spiny lobster database used in this research. Thanks are also extended to M. Shivlani of the University of Miami who was responsible for the collection of the socio-economic data in the FWC census carried out in 2003–04. We thank three anonymous reviewers for their comments that significantly improved the paper.

Literature cited

Angelsen, K., and S. Olsen.
1987. Impact of fish density and effort level on catching efficiency of fishing gear. Fish. Res. 5:271–278.

Chien, Y., and R. E. Condrey.
1985. A modification of the DeLury method for use when natural mortality is not negligible. Fish. Res. 3:23–28.

Ehrhardt, N.
2005. Population dynamic characteristics and sustainability mechanisms in key Western Central Atlantic spiny lobster, *Panulirus argus*, fisheries. Bull. Mar. Sci. 76:501–526.

FAO (Food and Agriculture Organization of the United Nations).
2001. Report on the FAO/DANIDA/CFRAMP/WECAFC regional workshops on the assessment of the Caribbean

spiny lobster (*Panulirus argus*). FAO Fish. Rep. 619 (ISSN 0429-9337), 381 p. FAO, Rome.

Fouilland, E., and O. Fossati.
1996. Trapping efficiency of plastic bottle "wickertraps" for population assessment of river *Macrobrachium* (Crustacea: Decapoda). Fish. Res. 28:343–351.

Groeneveld, J. C., D. S. Butterworth, J. P. Glazer, G. M. Branch, and A. C. Cockcroft.
2003. An experimental assessment of the impact of gear saturation on an abundance index for an exploited rock lobster resource. Fish. Res. 65:453–465.

Labisky, R. F., D. R. Gregory Jr., and J. A. Conti.
1980. Florida's spiny lobster fishery: an historical perspective. Fisheries 5:28–37.

Pope, J. G.
1972. An investigation of the accuracy of virtual population analysis using cohort analysis. ICNAF Res. Bull. 9:65–74.

Romaire R. P., and V. A. Pfister.
1983. Effects of trap density and diel harvesting frequency on catch of crawfish. Am. J. Fish. Manag. 3:419–24.

Rosemberg, A. A., G. P. Kirkwood, J. A. Crombie, and J. R. Beddington.
1990. The assessment of stocks of annual squid species. Fish. Res. 8:335–350.

Sanders, M. J.
1988. Mean population number and the DeLury and Leslie methods. Fish. Res. 6:153–165.

Assessment of fish populations and habitat on Oculina Bank, a deep-sea coral marine protected area off eastern Florida

Stacey L. Harter (contact author)[1]
Marta M. Ribera[1]
Andrew N. Shepard[2]
John K. Reed[3]

Email address for contact author: stacey.harter@noaa.gov

[1] National Marine Fisheries Service
Southeast Fisheries Science Center
3500 Delwood Beach Rd.
Panama City, Florida 32408

[2] NOAA Undersea Research Center
University of North Carolina at Wilmington
5600 Marvin Moss Lane
Wilmington, North Carolina 28409

[3] Harbor Branch Oceanographic Institute
Florida Atlantic University
5600 U.S. 1 North
Ft. Pierce, Florida 34946

Abstract—A portion of the Oculina Bank located off eastern Florida is a marine protected area (MPA) preserved for its dense populations of the ivory tree coral (*Oculina varicosa*), which provides important habitat for fish. Surveys of fish assemblages and benthic habitat were conducted inside and outside the MPA in 2003 and 2005 by using remotely operated vehicle video transects and digital still imagery. Fish species composition, biodiversity, and grouper densities were used to determine whether *O. varicosa* forms an essential habitat compared to other structure-forming habitats and to examine the effectiveness of the MPA. Multivariate analyses indicated no differences in fish assemblages or biodiversity among hardbottom habitat types and grouper densities were highest among the most complex habitats; however the higher densities were not exclusive to coral habitat. Therefore, we conclude that *O. varicosa* was functionally equivalent to other hardbottom habitats. Even though fish assemblages were not different among management areas, biodiversity and grouper densities were higher inside the MPA compared to outside. The percentage of intact coral was also higher inside the MPA. These results provide initial evidence demonstrating effectiveness of the MPA for restoring reef fish and their habitat. This is the first study to compare reef fish populations on *O. varicosa* with other structure-forming reef habitats and also the first to examine the effectiveness of the MPA for restoring fish populations and live reef cover.

Manuscript submitted 26 March 2008.
Manuscript accepted 14 November 2008.
Fish. Bull 107:195–206 (2009).

The views and opinions expressed or implied in this article are those of the author and do not necessarily reflect the position of the National Marine Fisheries Service, NOAA.

Like shallow tropical coral reefs, deep-sea coral habitats support important ecosystem functions, for example, as hotspots for biodiversity and biomass production (Husebo et al., 2002; Jonsson et al., 2004; George et al., 2007) and as important fish habitat (Gilmore and Jones, 1992; Fosså et al., 2002; Ross and Quattrini, 2007). Like their shallow-water counterparts, deep-sea coral ecosystems are affected by human activities. As harvests have declined in shallow ecosystems, fishing pressure has moved further offshore (Watling and Norse, 1998; Koslow et al., 2000; Roberts, 2002), thus raising interest in deep-sea coral ecosystem protection. With the passage of the Magnuson-Stevens Fishery Management and Conservation Act of 1996, an ecosystem approach to fishery management in the United States has been encouraged by linking the preservation of essential fish habitat with protection of fishery resources. Reauthorization of the Act in 2006 mandated the conservation and studies of deep-sea coral ecosystems. These mandates are expected to lead to the increasing use of marine protected areas (MPAs) as a fishery management tool (Allison et al., 1998; Bohnsack, 1998; Guenette et al., 1998).

One of the world's first deep-sea coral ecosystems to be designated a marine protected area is located approximately 37 km off Florida's east coast in depths of 60–120 m. This area is known as the Oculina Bank, a series of reefs and high-relief bioherms (thickets of live coral, capping mounds of sediment and coral rubble, built upon an underlying lithified base structure) constructed by the scleractinian ivory tree coral (*Oculina varicosa*). This species lives in water depths of 49 to 152 m without zooxanthellae and may form extensive thickets 1 m tall, which over thousands of years have built up mounds and ridges extending as much as 200 m laterally and 35 m above the surrounding seafloor (Reed, 1980). These *O. varicosa* bioherms are known to exist only off the east coast of Florida from Ft. Pierce to St. Augustine, a stretch of almost 150 km along the edge of the Florida-Hatteras slope and beneath the western edge of the Gulf Stream. Surface water currents may exceed 150 cm/sec and bottom currents may exceed 50 cm/sec (Reed, 2002a). Intact, live *O. varicosa* sup-

ports a diverse and dense assemblage of invertebrates and fishes (Avent et al., 1977; Reed, 2002a, 2002b; Koenig et al., 2005), and it may serve as spawning grounds for a number of economically important or threatened reef fish species (Gilmore and Jones, 1992; Koenig et al., 2005).

A portion of the Oculina Bank known as the Oculina Habitat Area of Particular Concern (OHAPC) first received protection in 1984 (Koenig et al., 2005; Reed et al., 2005). Current management regulations established by the South Atlantic Fishery Management Council include a 1029 km^2 (300 nm^2) OHAPC (Fig. 1), within which bottom-fishing gear such as trawls, dredges, longlines, traps, and anchors are not permitted, in order to protect the fragile coral. Within the OHAPC, the 315 km^2 (92 nm^2) Oculina Experimental Closed Area (OECA) (Fig. 1) was designated in 1994 in response to the rapidly diminishing grouper (*Mycteroperca* and *Epinephelus* spp.) populations and excludes all bottom fishing, including fishing with hook-and-line gear, in order to assess the use of a MPA for recovering over-fished reef fish populations, especially those of grouper.

Management requirements to protect many deep-sea coral ecosystems have been delayed owing to the difficulty in quantifying, monitoring, and restoring damaged reefs (Pyle, 2000). Despite efforts to understand and protect the Oculina Bank, extensive damage to the fragile coral had already occurred from fishing gear prior to the implementation of management regulations (Koenig et al., 2000; Reed et al., 2007). When the first management action was taken in 1984, only about 30% of the reef system was afforded protection (Reed et al., 2005). Fishing, including shrimp trawling, was allowed to continue in the northern section of the Oculina Bank until the OHAPC was expanded in 2000. Decades of shrimp trawling and scallop dredging before protection had reduced most of the 150-km stretch of healthy reefs to coral rubble (Reed et al., 2007). Remotely operated vehicle (ROV) transects and multi-beam mapping surveys since 2000, however, have indicated that Jeff's Reef and Chapman's Reef, both located in the southern portion of the OECA, still contain a large amount of intact live *O. varicosa* (Fig. 1) (Reed et al., 2005).

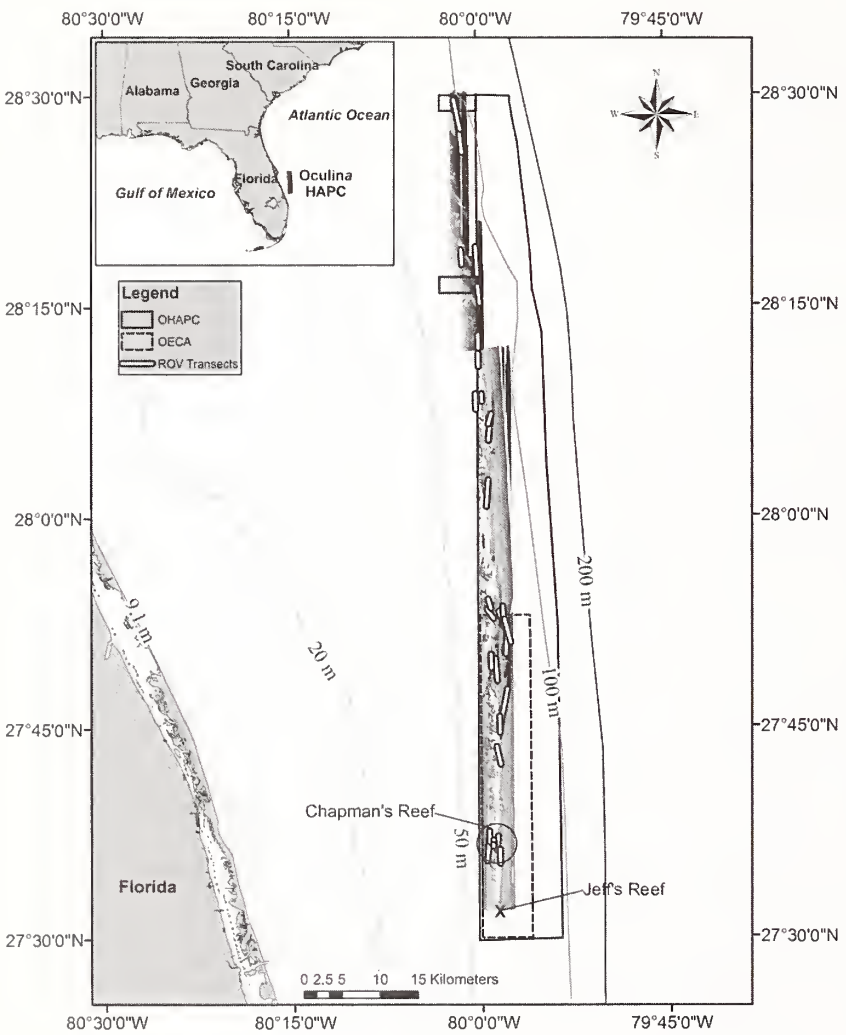

Figure 1

Remotely operated vehicle (ROV) transects overlain on the multibeam map of the Oculina marine protected area (MPA) off eastern Florida. Location of the OHAPC and OECA (OHAPC=areas where all bottom gear except hook and line are restricted, i.e., excluding the OECA, and OECA=inside the MPA where all bottom gear, including hook and line fishing, are restricted) are shown along with Chapman's and Jeff's Reefs. ROV transects were conducted during April–May 2003 and October 2005.

Over-fishing has significantly diminished populations of reef fishes, especially those of groupers (Koenig et al., 2000, 2005). Historical observations made during the 1970s and 1980s indicate that *O. varicosa* reefs were once dominated by large groupers, but later surveys found grouper populations greatly diminished and the reefs dominated by small, non-fishery species like small sea basses (*Serranus* and *Centropristis* spp.), butterflyfishes (*Chaetodon* spp.), and damselfishes (*Chromis* spp.) (Koenig et al., 2005).

A current topic of discussion regarding deep water corals is whether they serve as essential habitat for some fish species or whether any type of 3-dimensional structure (e.g., rock ledges) is important. Auster (2005) proposed that examination of the distribution of fish in relation to all available habitats is one method to assess the "essential"

role of deep water corals. Several studies have concluded that deep water corals were no more important to fishes than other reef structures (Auster, 2005; Tissot et al., 2006) suggesting an opportunistic fish association with deep corals. Ross and Quattrini (2007), however, found that deep reef habitats along the southeast United States slope contain a unique and possibly obligate assemblage of fish. No previous studies have examined whether *O. varicosa* supports a distinct assemblage of fish compared to other structure-forming, hardbottom habitats.

In 2014, the South Atlantic Fishery Management Council will re-evaluate the effectiveness of the OECA. To aid the Council in making future management decisions, our goals for this project were to (1) compare fish assemblage composition, biodiversity, and grouper densities among hardbottom reef habitat types to examine whether *O. varicosa* is an essential habitat structure compared to other structure-forming reef habitats; (2) compare fish assemblage composition, biodiversity, and grouper densities inside and outside managed areas to assess the effectiveness of the MPA; and (3) quantify the percent cover of all hardbottom habitat types.

Materials and methods

Sampling design

In 2002 and 2005, multibeam maps (3-m resolution) were produced for a portion of the Oculina Bank. Coverage included 90% of *O. varicosa* bioherms thought to occur inside the OHAPC, and a portion of bioherms outside the OHAPC between the two satellite areas (Fig. 1). These maps were used to select remotely operated vehicle (ROV) transect stations (April–May 2003, October 2005) so that all habitat types and management areas were examined. Management areas sampled included open (any area outside the OHAPC open to fishing), OHAPC (areas where all bottom gear except hook and line are restricted, i.e., excluding the OECA), and OECA (inside the MPA where all bottom gear, including hook and line fishing, are restricted).

Locations of ROV dive transects were non-random and were based on conducting an equal number of dives in each management area. Due to high current speeds, all dives were conducted in a northerly direction (drifting with prevailing Gulf Stream current with minimal east-west maneuvering). The starting points were chosen *a priori* in order to have each dive cover a range of the major substrate types (described below) as indicated from the multibeam maps. Dives ranged from 0.5 to 3.5 hours.

In addition to management area, fish assemblages were analyzed among five major hardbottom habitat types. Habitat types used were a subset of the Southeast Area Monitoring and Assessment Program (SEAMAP) habitat classification scheme and included pavement, rubble, rock outcrops, standing dead *O. varicosa* coral, and live *O. varicosa* coral. One difference between our habitat classification and that of SEAMAP is that we distinguished between live and dead coral. Pavement habitat was fairly flat rock pavement often with small cracks or crevices present. Rubble habitat consisted of small coral fragments exhibiting little to no relief. Rock outcrop habitat was small rock outcrops approximately 0.3–0.9 m relief, occasionally 1.2–1.8 m relief. *O. varicosa* existed mostly as small individual heads (about 0.3–0.9 m relief), but occasionally as larger mounds and thickets.

Collection methods

The *Phantom Spectrum II* ROV (National Undersea Research Center, University of North Carolina at Wilmington) was used to conduct video and digital still transects to estimate fish densities and characterize habitat. A downweight (~145 kg) was tethered to the umbilical cable of the ROV and the ROV was tethered to a 30-m leash, which allowed it to run just above the seafloor (<1 m) at a controlled over-the-ground speed of approximately 0.39 m/s (range 0.26 to 0.77 m/s). The geographic position of the ROV was constantly recorded throughout each dive using a slant range positioning system linked to the ship's Global Positioning System (GPS). The ROV was equipped with lights, lasers, forward-looking video camera, and down-looking still camera. Lasers projected parallel beams 10 cm apart for measuring fish and habitat features. The forward-looking color video camera provided continuous video while the down-looking high-resolution digital still camera captured images of fish and habitat.

Fish population analyses

Fishes were identified to the lowest discernable taxonomic level and counted and the habitat types were classified from video covering 50-m (±2.5 m) transects. Excluded from the analysis were sections of video recorded when the ROV was in non-hardbottom habitats, video clouded by stirred up sediment, video that zoomed in on a species of interest, or video recorded when the camera was elevated in the water column.

Fish densities (numbers/hectare) were determined by estimating the area viewed during video transects from transect length (L) and width (W). Transect length was calculated from latitude and longitude recorded by the ROV tracking system. Width of each transect was calculated using the following equation:

$$W = 2(\tan(^1/_2A))D, \quad (1)$$

where A = horizontal angle of view (a constant property of the video camera); and
D = distance from the camera at which fishes could be identified with certainty.

D was usually 5 m except for some dives in 2005 where visibility was reduced to 2–3 m. In 2003, a set of three lasers was mounted to the ROV. The lasers were set up

so that when they were projecting out at a distance of 5 m, two of the lasers overlapped. The third laser was spaced 10 cm apart from the two overlapping lasers, which allowed measurements to be made. This was initially used to train the eye to determine the distance at which fishes could be identified. Distance was then estimated on subsequent dives in 2005. Transect area (*TA*) was then calculated as:

$$TA = (LW) - {}^1/_2\,(WD) \quad \text{(Koenig et al., 2005).} \qquad (2)$$

Mean *TA* was 372.9 m^2 ±1.8 m^2. Density of all observed fish species was calculated for each transect in 2003 and 2005. Initial analyses demonstrated that no statistical differences were evident between years, so data from both years were combined for all analyses.

Multivariate ecological analyses were conducted using PRIMER 5.0 (Primer–E Ltd, Plymouth, U.K.) to examine fish assemblage composition among habitat types and management areas. A non-metric multi-dimensional scaling (MDS) ordination of ROV transects was constructed from a Bray-Curtis similarity matrix of square root transformed fish densities. A square root transformation was used to reduce the disparity between uncommon and abundant species by downweighting abundant species relative to uncommon species (Clarke, 1993). Prior to analyses, transects in which no fishes were observed were deleted, as the same reason may not apply to why two samples are devoid of species. Species comprising <0.01% of the total abundance of fish were also removed to minimize rare species confounding the cluster analysis. All pelagic species were removed from PRIMER analyses because we wanted to focus on benthic fish species associated with reef habitat. A two-way crossed analysis of similarity (ANOSIM) and pairwise comparisons were used to detect significant differences in fish assemblages among habitat types and management areas.

PRIMER was also used to examine biodiversity among habitats and management areas by calculating average taxonomic distinctness (Δ^+). This statistic uses the taxonomic distance between every pair of species in a given assemblage as the basis for determining relative diversity (Clarke and Warwick, 1998). Unlike conventional diversity indices such as the Shannon-Weiner Index, Δ^+ is independent of sampling effort. To calculate Δ^+, a total list of species observed from ROV transects was used. The following taxonomic categories were utilized: species, genus, family, order, class, and phylum. Each of these represents a node in determining taxonomic distances between species pairs. This list along with fish density data were used to run a TAXDTEST which produces funnel plots where Δ^+ is plotted in comparison with the mean and 95% confidence limits.

Densities of grouper were singled out for analysis because their declining abundances led the South Atlantic Fishery Management Council to establish the OECA. A generalized linear model (GLM) (Minitab 13.32, State College, PA) was used to test for significant differences in grouper densities among management areas and habitat types. Individual species of grouper were not abundant enough to analyze separately, so all grouper species were combined. One-way analysis of variance (ANOVA) was used to test for significant differences in grouper densities among management areas within each habitat type. A significance level of $P \leq 0.05$ was applied to all analyses, and log transformations were applied to correct for unequal variances. Pairwise comparisons were performed using Tukey's honestly significant differences (HSD).

Habitat quantification analyses

A digital still image of the seafloor (taken pointing straight down from the ROV, perpendicular to the seafloor) was taken every 1–3 min during ROV transects to quantify habitat type among management areas. These images were imported into an image analysis program written at the University of North Carolina-Wilmington, emulating the area/length analysis tool of Coral Point Count software (CPCe, Dania Beach, FL) (Kohler and Gill, 2006). Within each image, a polygon was drawn around each distinctive hardbottom area and a habitat type assigned to it. Habitat types were the same as those used for video analyses with the addition of human artifacts (e.g., fishing line, bottles) and shadow, where all or part of an image was blurred, usually from sand being stirred up by the ROV. The program then calculates the percentage of each habitat type within an image based on the number of pixels in each polygon. The area of each habitat type was calculated using paired lasers (set at a known distance of 10 cm apart) on each image. Mean area of still images was 1.2 m^2 ±0.05 m^2. One-way ANOVAs were then used to test for significant differences in habitat type percentages among management areas.

Results

Fish assessment

Forty-two ROV dives (65 hours of video footage) were completed in 2003 and 2005, resulting in 512 hardbottom 50-m transects: 236 in the OECA, 184 in the OHAPC, and 92 in the open area. Among habitat types, 72 transects were in pavement, 186 in rubble, 210 in rock outcrops, 11 in standing dead *O. varicosa*, and 33 in live *O. varicosa*. A total of 62 fish species were observed (Table 1). The previously unexplored bioherms discovered outside the OHAPC between the two satellite areas turned out to be comprised mostly of coral rubble, therefore, even though some live and standing dead *O. varicosa* were observed in the open areas, there wasn't enough of it to produce any 50-m transects to be used in the analyses. No fish species were exclusive to *O. varicosa* coral (live or standing dead). No grouper species were found on pavement except scamp (*Mycteroperca phenax*), the most abundant grouper. Tattlers (*Serranus phoebe*), one of the most abundant small sea basses were

Table 1

Relative abundance (%) of all fish species observed from remotely operated vehicle (ROV) transects on the Oculina Bank during April/May 2003 and October 2005. Species are listed by management area (open= any area outside the OHAPC open to fishing, OHAPC=areas where all bottom gear except hook and line are restricted, i.e., excluding the OECA, and OECA= inside the MPA where all bottom gear, including hook and line fishing, are restricted) and habitat (PAV=pavement, RUB=rubble, OUT=rock outcrops, SD=standing dead *Oculina*, LO=live *Oculina*). There were no SD or LO transects in the open area. A dash indicates 0.00% relative abundance.

	open			OHAPC					OECA				
	PAV	RUB	OUT	PAV	RUB	OUT	SD	LO	PAV	RUB	OUT	SD	LO
Muraenidae													
Gymnothorax spp.	—	—	—	—	—	—	—	—	—	0.07	—	—	—
Undetermined	—	—	—	—	—	—	—	—	—	0.15	—	—	—
Ophicithidae													
Undetermined	—	—	—	—	—	—	—	—	—	—	0.10	—	0.14
Engraulidae													
Anchoa spp.	—	—	—	—	—	—	—	—	—	7.14	—	—	0.28
Synodontidae													
Synodus intermedius	—	—	—	—	0.13	—	—	—	1.49	—	—	—	0.15
Synodus spp.	—	—	—	—	0.14	0.15	—	—	0.76	—	—	—	—
Ogcocephalidae													
Ogcocephalus corniger	—	—	0.12	—	—	—	—	—	—	0.07	—	—	—
Ogcocephalus spp.	—	0.20	—	—	—	—	—	—	—	—	—	—	—
Holocentridae													
Holocentrus rufus	—	—	0.27	—	—	0.38	—	—	—	—	—	—	—
Holocentrus spp.	—	—	—	—	—	—	—	—	—	0.07	0.50	—	—
Myripristis jacobus	—	—	0.13	—	—	—	—	—	—	—	—	—	—
Syngnathidae													
Hippocampus spp.	—	—	—	—	0.14	0.15	—	—	2.34	—	0.50	—	—
Scorpaenidae													
Helicolenus dactylopterus	—	—	0.39	—	—	0.46	—	—	—	0.56	—	—	—
Undetermined	—	0.81	0.39	—	—	0.23	—	—	—	1.60	—	—	1.13
Triglidae													
Prionotus spp.	—	—	—	—	—	—	—	—	—	0.07	—	—	—
Serranidae													
Anthiinae	—	—	3.30	—	11.24	9.06	30.85	25.22	—	16.80	45.22	—	43.79
Centropristis ocyurus	6.63	4.06	8.95	20.91	2.18	8.21	8.29	1.18	16.92	4.13	1.62	7.98	5.16
Centropristis spp.	—	39.93	11.68	38.02	4.52	14.04	4.97	1.19	9.70	3.53	3.15	14.27	5.76
Centropristis striata	—	—	0.12	5.91	—	—	0.83	—	12.26	1.03	0.80	—	0.43
Epinephelus adscensionis	—	—	—	—	—	—	—	—	—	0.07	—	—	—
Epinephelus drummondhayi	—	—	—	—	—	—	—	—	—	—	0.09	—	0.14
Epinephelus morio	—	—	—	—	0.14	0.31	—	—	—	0.07	0.10	2.23	0.28
Epinephelus niveatus	—	—	0.13	—	—	0.15	—	—	—	—	0.19	—	0.14
Hemanthias vivanus	—	5.13	6.69	—	3.00	5.26	3.31	3.41	—	2.21	4.81	—	—
Liopropoma eukrines	—	—	1.93	—	0.42	0.76	0.81	—	—	0.14	1.35	—	1.16
Pronotogrammus martinicensis	—	8.02	31.47	—	17.49	18.74	15.53	13.33	—	4.92	8.55	—	0.14
Mycteroperca microlepis	—	—	—	—	—	0.08	—	—	—	—	—	—	—
Mycteroperca phenax	—	0.20	0.90	2.97	0.13	1.13	4.89	1.76	0.46	0.58	1.59	2.16	1.70
Mycteroperca spp.	—	0.20	—	—	—	—	—	—	—	—	—	—	—
Rypticus maculatus	—	—	—	—	—	—	—	—	—	0.14	—	—	—
Serranus annularis	—	0.20	0.25	—	0.28	—	—	—	—	0.07	—	—	—
Serranus notospilus	—	5.16	0.64	1.00	1.67	1.37	3.30	0.57	1.24	0.40	—	—	0.86
Serranus phoebe	60.57	13.16	10.17	17.74	13.51	16.92	7.53	1.79	27.14	14.91	8.67	14.33	5.16

continued

Table 1 (continued)

	open			OHAPC					OECA				
	PAV	RUB	OUT	PAV	RUB	OUT	SD	LO	PAV	RUB	OUT	SD	LO
Anthiinae (cont.)													
Serranus spp.	—	0.42	0.12	—	—	0.22	—	—	—	0.36	—	—	—
Serranus subligarius	—	—	—	—	—	—	—	—	—	0.36	—	—	0.71
Undetermined grouper	—	—	—	—	—	0.08	—	0.59	0.93	—	0.20	—	0.15
Undetermined small sea bass	—	0.60	0.13	1.02	0.97	0.29	4.19	1.17	2.54	0.11	—	—	—
Priacanthidae													
Priacanthus arenatus	—	—	0.26	—	—	0.74	—	—	—	—	0.57	—	—
Pristigenys alta	13.20	0.20	1.93	3.93	—	4.27	—	—	6.79	0.60	4.47	1.15	0.28
Undetermined	—	—	—	—	—	0.23	—	—	—	—	—	—	—
Apogonidae													
Apogon pseudomaculatus	—	—	—	0.94	—	0.43	—	—	0.94	0.07	0.10	1.09	1.32
Apogon spp.	—	—	0.39	—	—	1.28	—	—	—	0.36	1.07	1.17	0.86
Rachycentridae													
Rachycentron canadum	—	—	—	—	—	0.15	—	—	—	—	—	—	—
Carangidae													
Seriola dumerili	—	—	0.50	—	—	0.79	1.62	—	0.93	0.42	0.29	—	—
Seriola rivoliana	—	—	—	—	0.27	—	—	—	—	—	—	—	—
Seriola spp.	6.91	—	0.13	—	0.41	0.40	—	—	0.47	0.29	0.40	—	0.14
Seriola zonata	—	—	0.13	—	—	—	—	—	0.49	0.14	—	—	—
Lutjanidae													
Lutjanus campechanus	—	—	—	—	—	0.08	—	—	—	—	—	—	—
Lutjanus spp.	—	—	0.13	—	—	—	—	—	—	—	—	—	—
Ocyurus chrysurus	—	—	—	—	—	—	—	—	—	0.08	—	—	—
Haemulidae													
Haemulon aurolineatum	—	—	—	—	—	—	—	—	—	5.03	—	—	—
Haemulon spp.	—	—	—	—	—	—	—	—	—	1.43	—	—	—
Sparidae													
Pagrus pagrus	—	—	0.37	—	—	—	—	—	—	0.14	0.10	—	—
Undetermined	12.69	—	0.13	—	—	0.12	—	—	1.43	0.36	0.39	—	0.42
Sciaenidae													
Equetus acuminatus	—	—	—	0.98	0.14	—	—	—	—	0.49	—	—	—
Equetus spp.	—	—	0.13	—	—	—	—	—	—	—	—	—	—
Equetus umbrosus	—	—	—	—	—	—	—	—	—	—	0.10	—	3.56
Micropogonias undulatus	—	—	—	—	—	—	—	—	—	0.18	—	—	—
Pareques iwamotoi	—	—	—	1.97	—	0.30	—	—	—	—	—	—	—
Chaetondontidae													
Prognathodes aya	—	1.43	2.95	—	2.49	1.66	4.95	2.96	—	7.53	4.02	3.22	10.06
Chaetodon ocellatus	—	—	0.27	—	—	0.15	—	1.74	—	0.07	0.49	—	—
Chaetodon sedentarius	—	0.39	1.04	—	1.65	0.90	—	1.00	—	1.66	1.27	—	0.56
Chaetodon spp.	—	—	0.25	—	0.27	0.08	—	0.59	—	0.79	—	—	—
Pomacanthidae													
Holacanthus bermudensis	—	—	0.66	—	—	0.22	2.44	2.34	—	0.43	1.00	2.13	0.70
Holacanthus ciliaris	—	—	—	—	—	0.07	—	—	—	—	—	—	—
Holacanthus spp.	—	—	—	—	—	—	—	—	—	0.07	—	—	—
Pomacentridae													
Chromis enchrysurus	—	12.32	7.60	—	36.71	5.66	5.68	29.27	8.01	17.56	5.93	44.43	12.55
Chromis scotti	—	0.85	—	—	—	—	—	—	—	0.14	—	—	—
Chromis spp.	—	0.20	0.14	—	0.14	—	—	0.61	—	0.08	—	—	—
Microspathodon chrysurus	—	—	—	—	—	—	—	—	—	0.37	—	—	—
Labridae													
Bodianus pulchellus	—	—	—	—	—	0.15	—	—	—	0.07	0.19	—	—
Bodianus rufus	—	—	—	—	—	—	—	—	—	0.14	—	—	—
Decodon puellaris	—	—	0.12	—	—	0.15	—	—	—	0.07	0.26	5.83	0.14
Halichoeres bathyphilus	—	0.21	—	—	—	—	—	—	—	0.30	—	—	—
Halichoeres spp.	—	3.22	4.45	—	1.54	3.06	—	2.29	—	0.28	1.29	—	0.70

continued

Table 1 (continued)

	open			OHAPC					OECA				
	PAV	RUB	OUT	PAV	RUB	OUT	SD	LO	PAV	RUB	OUT	SD	LO
Sphyraenidae													
Sphyraena barracuda	—	—	—	—	—	—	—	—	—	0.07	—	—	—
Bothidae													
Cyclopsetta fimbriata	—	—	—	—	—	—	—	—	—	—	—	—	0.14
Undetermined	—	—	0.14	0.98	—	—	0.83	—	2.44	—	0.10	—	0.29
Balistidae													
Balistes capriscus	—	—	—	—	—	—	—	—	—	—	0.10	—	—
Monacanthidae													
Aluterus monoceros	—	—	—	—	—	—	—	—	—	0.07	—	—	—
Stephanolepis hispidus	—	—	—	—	—	0.07	—	—	—	—	0.10	—	—
Monacanthus spp.	—	—	—	—	—	0.19	—	—	—	0.07	—	—	—
Ostraciidae													
Lactophrys quadricornis	—	—	—	—	—	—	—	—	—	0.21	—	—	—
Lactophrys spp.	—	—	—	—	—	—	—	—	—	—	0.17	—	—
Tetraodontidae													
Sphoeroides spengleri	—	2.88	0.51	3.62	0.41	0.42	—	—	2.72	0.83	0.16	—	0.44
Sphoeroides spp.	—	—	—	—	—	0.34	—	—	—	0.07	—	—	0.57
Diodontidae													
Chilomycterus spp.	—	0.20	—	—	—	—	—	—	—	—	—	—	—

found in every habitat and management area. Rock hind (*Epinephelus adscensionis*), speckled hind (*E. drummondhayi*), grey triggerfish (*Balistes capriscus*), and grunts (family Haemulidae) were only observed in the OECA.

Multivariate analyses based on 39 fish species across 473 transects indicated no differences in fish assemblages among hardbottom habitat types or management areas. MDS ordination portrayed a potentially useful representation of relationships among ROV transects in two-dimensional space (stress=0.2; see Clarke and Warwick, 2001) and showed no distinct groupings (Fig. 2). ANOSIM results confirmed these conclusions, fish assemblages were not significantly different among hardbottom habitat types (ANOSIM, Global R=0.128, P=0.001) or management areas (ANOSIM, global R=0.061, P=0.002). For ANOSIM, the P value is highly sensitive to sample number and, therefore, the likelihood of committing a type-I error is high. For that reason, the R value is more important than the P value. R equals 0 when groups are the same and R equals 1 when groups are different (Clarke and Warwick, 2001).

Among habitat types, species richness was highest on rock outcrops and lowest for standing dead *O. varicosa* (Fig. 3). Average taxonomic distinctness (Δ^+) was

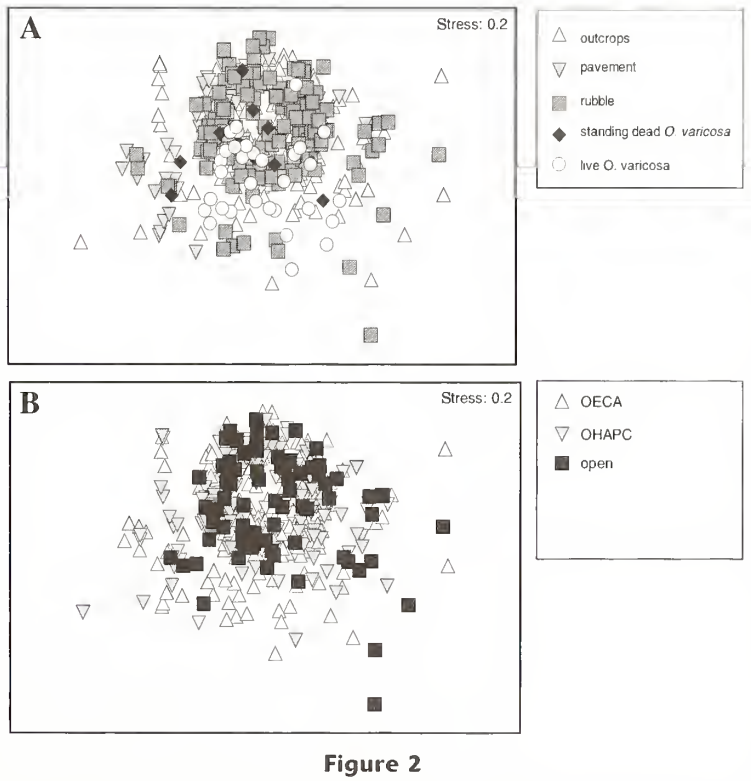

Figure 2

Multidimensional scaling (MDS) ordination of habitats (**A**) and management areas (**B**) based on the Bray-Curtis similarity matrix calculated from square root transformed fish densities (39 species). Data were collected from remotely operated vehicle (ROV) transects conducted on the Oculina Bank during April-May 2003 and October 2005.

highest for rock outcrops followed by pavement, rubble, and live *O. varicosa*, all of which were within the 95% confidence limits. Species richness (Δ^+) for standing dead habitat, however, was less than expected and fell below the 95% confidence limits. Among management areas, species richness was higher in the OECA and OHAPC compared to the open management area (Figure 3). Average taxonomic distinctness (Δ^+) for the OECA and OHAPC were within the 95% confidence limits, however, Δ^+ for the open area was less than expected falling below the 95% confidence limits.

Grouper densities were significantly different among habitat types (GLM, $P<0.001$) and management areas (GLM, $P=0.033$) (Fig. 4). Observed grouper species include speckled hind, red grouper (*E. morio*), snowy grouper (*E. niveatus*), scamp, gag (*M. microlepis*), and rock hind (*E. adscensionis*). Pairwise comparisons revealed that grouper densities were significantly higher ($P<0.05$) on live *O. varicosa*, rock outcrops, and standing dead *O. varicosa* compared to pavement and rubble. Grouper densities were also higher in the OECA compared to both the OHAPC and open management areas. When compared within each single habitat, grouper densities were significantly different on rock outcrops (One-way ANOVA, $P=0.023$) and pairwise comparisons revealed that densities were higher in the OECA compared to both the OHAPC and open areas ($P<0.05$). Grouper densities among management areas were not significantly different ($P>0.05$) for any of the other habitat types.

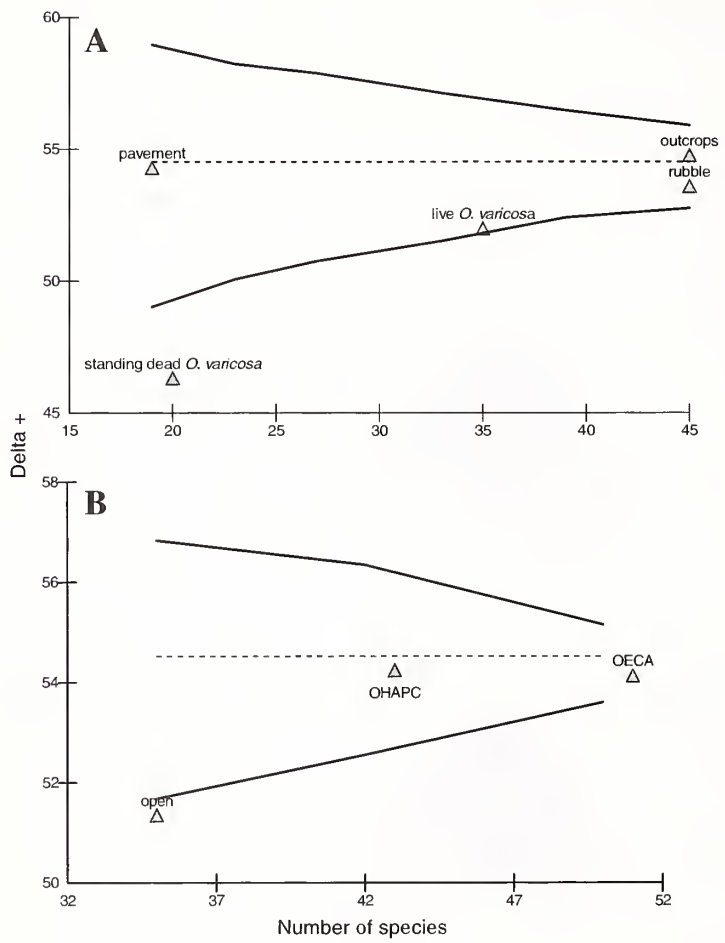

Figure 3

Average taxonomic distinctness (Δ^+) of fish assemblages relative to the mean Δ^+ (dashed line) and the 95% confidence intervals (solid lines) by habitat (**A**) and management area (open = any area outside the OHAPC open to fishing, OHAPC = areas where all bottom gear except hook and line are restricted, i.e., excluding the OECA, and OECA = inside the MPA where all bottom gear, including hook and line fishing, are restricted) (**B**) from remotely operated vehicle (ROV) transects conducted on the Oculina Bank during April–May 2003 and October 2005.

Habitat assessment

Analysis of digital stills revealed the highest percentage of live coral habitat was found in the OECA making up only 1.9% of the total habitat observed (Fig. 5). A total of 1307 digital still images were taken in 2003 and 2005 and used for analysis. There was significantly more live *O. varicosa* located within the OECA compared to the OHAPC and open (One-way ANOVA, $P=0.025$). The percentage of rock outcrops was significantly higher in the OHAPC compared to the open and OECA as well as in the open compared to the OECA (One-way ANOVA, $P<0.001$). Significantly more rubble was found in the OECA and open compared to the OHAPC (One-way ANOVA, $P<0.001$). The percentage of pavement was significantly higher in the OECA and OHAPC compared to the open area (One-way ANOVA, $P=0.003$) and, finally, there was significantly more standing dead *O. varicosa* in the OECA than the open (One-way ANOVA, $P=0.032$). Location of video transects and digital still images containing live *O. varicosa* are shown in Figure 6.

Discussion

This is the first study to address the functionality of coral habitat and to compare fish assemblages among areas with different management levels on the Oculina Bank. Prior to this study, the last survey conducted on the Oculina Bank was in 2001 (Koenig et al., 2005), however, several differences exist between the two and new findings have emerged from the current survey. Koenig et al. (2005) targeted high relief sites within the OECA, used side-scan sonar to locate sites, and compared fish densities among three general habitat types (no coral, sparse live and dead *O. varicosa*, and dense live and dead *O. varicosa*). The current study had updated multibeam maps to target sites,

compared areas not only within the OECA but also included the OHAPC and open areas, and examined an expanded range of habitats.

While it is well known that deep coral habitat supports a high diversity and densities of fish species (Costello et al., 2005; Koenig et al., 2005; Parrish, 2006; Stone, 2006; Ross and Quattrini, 2007), it is unclear whether fish are attracted to live coral or just structure made by corals. Our study addressed this question by comparing fish assemblages, densities, and diversity among several structure-forming habitat types including coral. We found no significant difference in the composition of fish assemblages or diversity among all hardbottom habitat types. Grouper densities were significantly higher on the most structurally complex habitats (live *O. varicosa*, standing dead *O. varicosa*, and rock outcrops) compared to the less complex ones (pavement and rubble). Therefore, higher grouper densities were not exclusive to coral habitats. According to Auster (2005), one of the ways to define functionally equivalent habitats is those that support a similar density of fishes, therefore, we conclude that *O. varicosa* was functionally equivalent to the other hardbottom habitats on the Oculina Bank. Similar results were found in the Gulf of Maine (Auster, 2005). No difference in fish communities was found between habitats dominated by dense corals and those dominated by dense epifauna with or without corals. In addition, Tissot et al. (2006) concluded that fishes in southern California were associated with sponges and corals, but no functional relationship was present. In Hawaii, fish densities were higher in areas with deep-water corals, but when bottom relief and depth were accounted for, these densities were not higher than those for surrounding areas without corals (Parrish, 2006). Ross and Quattrini (2007) concluded that deep slope reefs function much like shallow corals reefs, hosting a unique, probably obligate, ichthyofauna, however other hardbottom habitats were not examined.

Even though our study demonstrated that *O. varicosa* serves a similar role for fishes as other hardbottom habitats, corals are still important and are major contributors to deep-sea habitat complexity and structure (Roberts et al., 2006). Significant numbers of gag and scamp aggregate on and use *O. varicosa* for spawning habitat and juvenile speckled hind use the coral for shelter suggesting a nursery value of the coral (Gilmore and Jones, 1992; Koenig et al., 2000; Koenig et al., 2005). Intact coral is not only valuable for fish, but invertebrates as well. As long as the coral is standing (live or dead), living space within the colony branches supports dense and diverse communities of associated invertebrates (Reed et al., 2002a, 2002b; Reed et al., 2007). However, once reduced to unconsolidated coral rubble, little living space is left except for infauna (George et al., 2007). A hypothetical trophic model of the *O. varicosa* ecosystem indicates significant loss of habitat, in particular intact

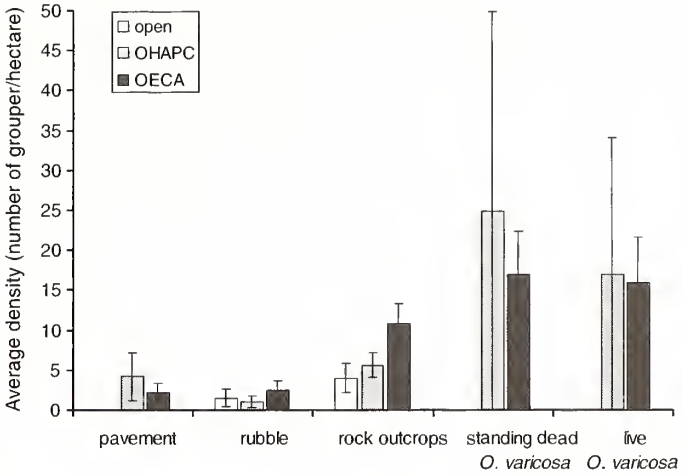

Figure 4

Average grouper densities (no./hectare) (±SE) for each management area by habitat type observed from remotely operated vehicle (ROV) transects conducted on the Oculina Bank during April/May 2003 and October 2005. Average grouper density for pavement in the open area was 0.0 fish/hectare, however, there were no live or standing dead *Oculina varicosa* transects for the open area.

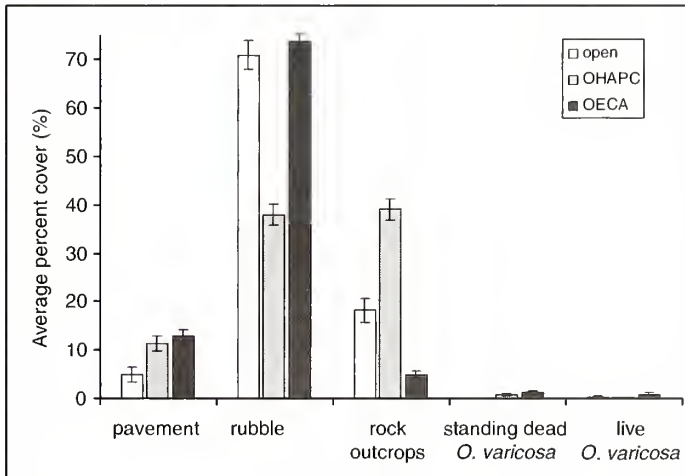

Figure 5

Average percent cover (±S.E.) of habitat types in each of the three management areas (open = any area outside the OHAPC open to fishing, OHAPC = areas where all bottom gear except hook and line are restricted, i.e., excluding the OECA, and OECA = inside the MPA where all bottom gear, including hook and line fishing, are restricted) from analysis of digital stills taken during remotely operated vehicle (ROV) transects on the Oculina Bank during April–May 2003 and October 2005.

live and dead standing coral, could bring dramatic shifts in the ecosystem (George et al., 2007). Conservation efforts, however, should focus on the intrinsic value of corals such as their slow growth, high sensitivity to disturbance, and questionable potential for recovery (Auster, 2005). A restoration project utilizing artificial reef structures is currently ongoing within the OECA. Between 1996 and 2001, a total of 125 large and 900 small restoration modules were deployed in a series of experiments to test their efficacy in the recovery of degraded coral and depleted fish populations (Koenig et al, 2005). The theory is that this will help *O. varicosa* restoration by providing stable settlement habitat, which may, in turn, provide suitable habitat for fish populations to recover. Early evidence (ROV dives from this study) found new coral recruits growing on the structures and groupers associated with them as well (Reed et al., 2005). While the scale of the artificial reefs is likely too small for fisheries replenishment, this experiment will provide insight to whether this tool is effective for coral restoration.

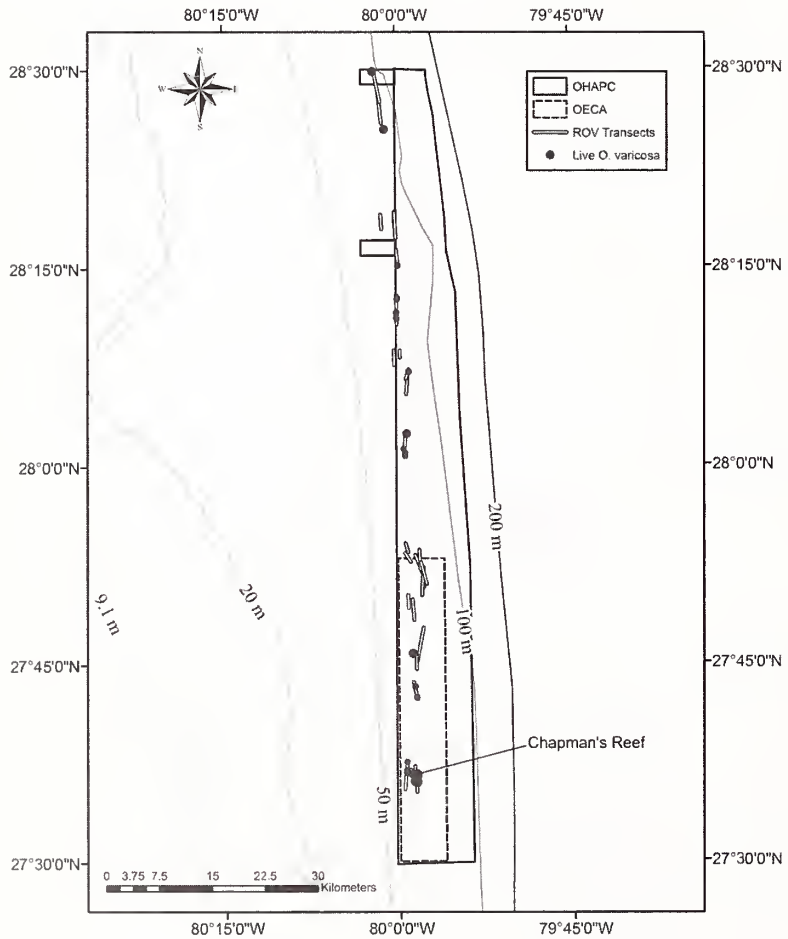

Figure 6

Locations of live *Oculina varicosa* (ivory tree coral) from video and digital stills collected during remotely operated vehicle (ROV) transects during April–May 2003 and October 2005.

Being the first study to compare fish assemblages among areas with different management levels on the Oculina Bank, the results are important to the South Atlantic Fishery Management Council as they evaluate the effectiveness of the OECA; this study and future surveys will help determine the fate of the closed area when it is reconsidered by the Coral and Habitat Advisory Panels in 2014. While MDS and ANOSIM analyses revealed no significant differences in the composition of fish assemblages among management areas, other positive effects of the closure were observed. Fish diversity was higher inside the OHAPC and OECA compared to the open area. Grouper densities were significantly higher in the OECA, particularly on rock outcrops, than in the OHAPC or open areas. Also, more coral was found in the OECA suggesting the restriction of fishing activity may have aided in conserving what little *O. varicosa* had not been destroyed by trawling. Habitat quantification analyses demonstrated there was significantly more live and standing dead *O. varicosa* in the OECA compared to the OHAPC and open.

An important observation from the ROV transects was the presence of black sea bass (*Centropristis striata*) in 2005. Prior to that time, black sea bass had not been observed on the *O. varicosa* reefs since the 1980s when they dominated the area (Koenig et al., 2000). While black sea bass in the 1980s were large, mature individuals, most individuals in 2005 were small juveniles, ranging in length from 10 to 20 cm, suggesting initial stages of recovery for this species. Another significant discovery was the sighting of the first juvenile speckled hinds since the 1980s. All of these findings combined present initial evidence demonstrating effectiveness of the MPA for restoring reef fish and their habitat.

Sustained enforcement remains an ongoing problem for MPAs (Riedmiller and Carter, 2001; Rogers and Beets, 2001). Even relatively moderate levels of poaching can quickly deplete gains achieved by closure (Roberts and Polunin, 1991; Russ and Alcala, 1996). As of 2003, all trawling vessels working in the Oculina Bank area are required to have vessel monitoring systems, but this doesn't solve the problem of poaching by hook and line fishing. Between 2003 and 2007, illegal trawlers and fishers were observed within the MPA during our cruises, and several vessels have been cited and fined by the United States Coast Guard. ROV observations from this study indicate recent trawl nets, bottom long lines, and fishing lines inside the MPA long after these gears were banned from the area. Continued trawling and bottom fishing in the OHAPC likely will thwart management objectives.

In summary, unlike shallow-water ecosystems, understanding of the ecological and functional role of deep-water corals has only recently emerged. The current study is in agreement with most other recent literature, demonstrating that corals are functionally equivalent to other deep-sea structural habitats. Deep-sea corals, however, are clearly an important provider of structural habitat for fishes and are sensitive to fishing gear impacts and vulnerable to destruction due to their fragility and slow growth rates. Therefore, protection remains crucial. While an ecosystem approach to management has become widely accepted and MPAs have become a primary tool to manage deep-sea coral ecosystems, little evidence has been provided demonstrating MPA effectiveness. This study, however, revealed several positive effects of the closure including higher biodiversity, grouper densities, and percentage of intact coral suggesting initial effectiveness of the *Oculina* MPA.

Acknowledgments

We thank the United Space Alliance (USA), National Aeronautics and Space Administration (NASA), and the crews of the MV *Liberty Star* and MV *Freedom Star* for providing vessel support. L. Horn and G. Taylor of University of North Carolina at Wilmington/National Underwater Research Center (UNCW/NURC) provided ROV support. Funding was provided by National Oceanographic and Atmospheric Administration (NOAA) Office of Exploration, National Marine Fisheries Service Southeast Fisheries Science Center (NMFS SEFSC), NOAA Coral Reef Conservation Program (CRCP), and NOAA Undersea Research Center at UNCW. M. Miller of NMFS SEFSC acted as NOAA CRCP representative. A. Maness of UNCW/NURC provided the image analysis program. We also thank C. Koenig and S. Brooke whose comments helped to improve the manuscript.

Literature cited

Allison, G. W., J. Lubchenco, and M. H. Carr.
1998. Marine reserves are necessary but not sufficient for marine conservation. Ecol. Appl. 8:S79–S92.

Auster, P. J.
2005. Are deep-water corals important habitats for fishes? *In* Cold-water corals and ecosystems (A. Freiwald and J. M. Roberts, eds.), p. 747–760. Springer, Berlin, Heidelberg.

Avent, R. M., M. E. King, and R. H. Gore.
1977. Topographic and faunal studies of shelf-edge prominences off the central eastern Florida coast. Hydrobiol. 62(2):185–208.

Bohnsack, J. A.
1998. Application of marine reserves to reef fisheries management. Aust. J. Ecol. 23:298–304.

Clarke, K. R.
1993. Non-parametric multivariate analyses of changes in community structure. Aust. J. Ecol. 18:117–143.

Clarke, K. R. and R. M. Warwick.
1998. A taxonomic distinctness index and its statistical properties. J. Appl. Ecol. 35:523–531.
2001. Change in marine communities: an approach to statistical analysis and interpretation, 2nd ed. PRIMER-E, Plymouth, U.K.

Costello, M. J. M. McCrea, A. Freiwald, T. Lundälv, L. Jonsson, B. J. Bett, T. C. E. van Weering, H. de Haas, J. M. Roberts, and D. Allen.
2005. Role of cold-water *Lophelia pertusa* coral reefs as fish habitat in the NE Atlantic. *In* Cold-water corals and ecosystems (A. Friewald and J. M. Roberts, eds.), p. 771–805. Springer-Verlag, Berlin, Heidelberg.

Fosså, J., P. Mortensen, and D. Furevik.
2002. The deep-water coral *Lophelia pertusa* in Norwegian waters: distribution and fishery impacts. Hydrobiol. 471:1–12.

George, R. Y., T. A. Okey, J. K. Reed, and R. P. Stone.
2007. Ecosystem-based fisheries management of seamount and deep-sea coral reefs in U. S. waters: conceptual models for proactive decisions. *In* Conservation and adaptive management of seamounts and deep-sea coral ecosystems (R. Y. George and S. D. Cairns, eds.), p. 9–30. Rosentiel School of Marine Science and Atmospheric Science, Univ. Miami, Miami, FL.

Gilmore, R. G. and R. S. Jones.
1992. Color variation and associated behavior in the epinepheline groupers, *Mycteroperca microlepis* (Goode and Bean) and *M. phenax* Jordan and Swain. Bull. Mar. Sci. 51(1):83–103.

Guenette, S., T. Lauck, and C. Clark.
1998. Marine reserves; from Beverton and Holt to the present. Rev. Fish Biol. Fish. 8:251–272.

Husebo, Å., L. Nottestad, J. H. Fosså, D. M. Furevik, and S. B. Jorgensen.
2002. Distribution and abundance of fish in deep coral habitats. Hydrobiol. 471:91–99.

Jonsson, L. G., P. G. Nilsson, F. Floruta, and T. Lundaelv.
2004. Distributional patterns of macro- and megafauna associated with a reef of the cold-water coral *Lophelia pertusa* on the Swedish west coast. Mar. Ecol. Prog. Ser. 284:163–171.

Koenig, C. C., F. C. Coleman, C. B. Grimes, G. R. Fitzhugh, K. M. Scanlon, C. T. Gledhill, and M. Grace.
2000. Protection of fish spawning habitat for the conservation of warm-temperate reef-fish fisheries of shelf-edge reef of Florida. Bull. Mar. Sci. 66(3):593–616.

Koenig, C.C., A. N. Shepard, J. K. Reed, S. D. Brooke, J. Brusher, and K. M. Scanlon.
2005. Habitat and fish populations in the deep-sea *Oculina* coral ecosystem of the western Atlantic. Am. Fish. Soc. Sym. 41:795–805.

Kohler, K. E. and S. M. Gill.
2006. Coral point count with Excel extensions (CPCe): a visual Basic program for the determination of coral and substrate coverage using random point count methodology. Computers and Geosciences 32(9):1259–1269.

Koslow, J. A., G. W. Boehlert, J. D. M. Gordon, R. L. Haedrich, P. Lorance, and N. Parin.
2000. Continental slope and deep sea fisheries: implications for a fragile ecosystem. ICES J. Mar. Sci. 57:548–557.

Parrish, F. A.
2006. Precocious corals and subphotic fish assemblages. Atoll Res. Bull. 543:425–438.

Pyle, R. L.
2000. Assessing undiscovered fish biodiversity on deep coral reefs using advanced self-contained diving technology. Mar. Tech. Soc. J. 34:82–91.
Reed, J. K.
1980. Distribution and structure of deep-water *Oculina varicosa* coral reefs off central eastern Florida. Bull. Mar. Sci. 30(3):667–677.
2002a. Deep-water *Oculina* coral reefs of Florida: biology, impacts, and management. Hydrobiol. 471:43–55.
2002b. Comparison of deep-water coral reefs and lithoherms off southeastern USA. Hydrobiol. 471:57–69.
Reed, J. K., C. C. Koenig, and A. N. Shepard.
2007. Impacts of bottom trawling on a deep-water *Oculina* coral ecosystem off Florida. Bull. Mar. Sci. 81:481–496.
Reed, J. K., A. N. Shepard, C. C. Koenig, K. M. Scanlon, and R. G. Gilmore Jr.
2005. Mapping, habitat characterization, and fish surveys of the deep-water *Oculina* coral reef marine protected area: a review of historical and current research. *In* Cold-water corals and ecosystems: proceedings of the second international symposium on deep sea corals (A. Freiwald, J. Roberts, eds.), p. 443–465. Springer-Verlag, Berlin Heidelberg.
Riedmiller, S. and E. Carter.
2001. The political challenge of private sector management of marine protected areas: The Chumbe Island Case, Tanzania. ACP-EU Fish. Res. Rep. no. 10, p. 141–153.
Roberts, C. M.
2002. Deep impact: the rising toll of fishing in the deep sea. Trends Ecol. Evol. 17:242–245.
Roberts, C. M. and N. V. C. Polunin.
1991. Are marine reserves effective in management of reef fisheries? Rev. Fish Biol. Fish. 1:65–91.
Roberts, J. M., A. J. Wheeler, and A. Friewald.
2006. Reefs of the deep: the biology and geology of cold-water coral ecosystems. Science 312:543–547.
Rogers, C. S. and J. Beets
2001. Degradation of marine ecosystems and decline of fishery resources in marine protected areas in the US Virgin Islands. Environ. Conserv. 28(4):312–322.
Ross, S. W. and A. M. Quattrini.
2007. The fish fauna associated with deep coral banks off the southeastern United States. Deep-Sea Research I. 54:975–1007.
Russ, G. R. and A. C. Alcala.
1996. Marine reserves: rate and patterns of recovery and decline of large predatory fish. Ecol. Appl. 6:947–961.
Stone, R. P.
2006. Coral habitat in the Aleutian Islands of Alaska: depth distribution, fine-scale species associations, and fisheries interactions. Coral Reefs 25:229–238.
Tissot, B. N., M. M. Yoklavich, M. S. Love, K. York, and M. Amend.
2006. Benthic invertebrates that form habitat on deep banks off southern California, with special reference to deep sea coral. Fish. Bull. 104:167–181.
Watling, L. and E. A. Norse.
1998. Disturbance of the seabed by mobile fishing gear: a comparison to forest clearcutting. Conserv. Biol. 12(6):1180–1197.

Changes in body composition and fatty acid profile during embryogenesis of quillback rockfish (*Sebastes maliger*)

Fletcher F. Sewall (contact author)

Cara J. Rodgveller

Email address for contact author: Fletcher.Sewall@noaa.gov

National Marine Fisheries Service, NOAA
Alaska Fisheries Science Center
Auke Bay Laboratories
Ted Stevens Marine Research Institute
17109 Pt. Lena Loop Road
Juneau, Alaska 99801

Abstract—We investigated developmental changes in the body compositions and fatty acid (FA) profiles of embryos and preparturition larvae of the quillback rockfish (*Sebastes maliger*). Comparisons of proximate composition data from early-stage embryos with data from hatched preparturition larvae taken from wild-caught gravid females indicated that embryos gain over one-third their weight in moisture while consuming 20% of their dry tissue mass for energy as they develop into larvae. Lipid contributed 60% of the energy consumed and was depleted more rapidly than protein, indicating a protein-sparing effect. Oil globule volume was strongly correlated with lipid levels, affirming its utility as an indicator of energetic status. FA profiles of early embryos differed significantly from those of hatched larvae. Differences in the relative abundances of FAs between early embryos and hatched larvae indicated different FA depletion rates during embryonic development. We conclude that some metabolically important FAs may prove useful in assessing the condition of embryos and preparturition larvae, particularly 20:4n-6, which cannot be synthesized by many marine fish and which is conserved during embryogenesis. Variability in body composition and energy use among rockfish species should be considered when interpreting any measures of condition.

Manuscript submitted April 14, 2008.
Manuscript accepted November 19, 2008.
Fish. Bull. 107:207–220 (2009).

The views and opinions expressed or implied in this article are those of the author and do not necessarily reflect the position of the National Marine Fisheries Service, NOAA.

The nutritional condition of fish during their early life histories may play a major role in determining the strength of year classes because larvae must have energy stores sufficient to ensure survival to first feeding. The survival rates of early planktonic rockfish larvae may be influenced by differences in the amounts and use of endogenous protein and lipid sources during embryonic development (MacFarlane and Norton, 1999). Despite this potential importance, little is known about the biochemistry of developing rockfish embryos and larvae. Because utilization of lipid and protein may vary by species (e.g., MacFarlane and Norton, 1999) and life history stage (e.g., Norton et al., 2001), it is important to examine these variables by species at the appropriate life stage.

Quillback rockfish (*Sebastes maliger*) are a long-lived, slow-growing species of commercial importance, for which biochemical data on early life stages are lacking. Like other rockfish species of the genus *Sebastes*, they bear live young, and embryos (as post fertilization, prehatching individuals with the chorion intact) develop and hatch as larvae (individuals free of the chorion envelope) inside the maternal female before being extruded (Yamada and Kusakari, 1991). Survival during the larval phase can be vital in determining the eventual size of a rockfish cohort (Ralston and Howard, 1995). The utilization of lipids is of particular importance, as triacylglycerols (TAGs) and polar lipids (mainly phospholipids) may be the primary energy sources during rockfish embryogenesis (MacFarlane and Norton, 1999). Endogenous TAG is thought to reside mainly in an oil globule, the volume of which was identified as a main correlate of survival of black rockfish larvae (*S. melanops*) (Berkeley et al., 2004). In that study, total lipid concentration was not related to oil globule volume (OGV) or later larval survival; however, lipid levels have been correlated with survival for many other fish species (reviewed in Kamler, 1992). Research with wild-caught shortbelly rockfish (*S. jordani*) (pre-flexion larvae through juvenile stages) has indicated that the relationship of TAG to total lipids, and the usefulness of TAG as an indicator of nutritional status, depends upon life stage (Norton et al., 2001). Given this variability, it is unclear what trends may occur in total lipid levels and oil globule TAG reserves in developing quillback rockfish embryos. If OGV can be shown to be a reliable indicator of lipid levels, using this measurement would represent a substantial savings in time and cost as compared with analytical chemistry techniques.

Embryos and larvae of quillback rockfish are likely incapable of synthesizing essential fatty acids (EFAs), either entirely or at a rate which will meet their metabolic needs for growth and survival, as is the case for adults of other fish species (e.g., as reviewed

Table 1

Sample sizes for determinations of body composition and fatty acid profiles of quillback rockfish (*Sebastes maliger*) embryos (early and middle stages) and hatched, preparturition larvae (late stages). The sample unit was one maternal female, from which subsamples of embryos or larvae were obtained for use in biochemical analyses. Sample sizes varied due to inadequate subsample masses being available for some analytical procedures.

	Sample size		
Variable	Early stages (1–3)	Middle stages (4–9)	Late stages (10)
Developmental stage	5	6	4
Oil globule volume	3	4	4
Wet tissue mass	3	4	4
Moisture, protein	3	4	4
Ash	2	4	3
Lipid	3	4	4
Fatty acids	4	4	4

in Watanabe, 1982). Fish are capable of selectively catabolizing particular fatty acids (FAs) while retaining others (reviewed in Tocher, 2003). Differences in rates of individual FA use during embryogenesis would be reflected by changes in overall FA profiles as embryos develop into hatched larvae. Assessing net differences in the amounts of individual FAs present may reveal which FAs potentially contribute to variability in larval survival (e.g., due to deficiencies in particular EFAs resulting from inadequate maternal provisioning).

Our study was driven by three objectives. First, we sought to describe the amount and sources of energy consumed during quillback rockfish embryogenesis, by measuring changes in lipid and protein levels from early to late stages of development. Second, to assess the usefulness of OGV as an indicator of the energetic status of embryos and preparturition larvae, we investigated how well changes in OGV were correlated with changes in stage and biochemical composition. Last, we reduced lipids to their FA components and compared the overall FA profiles of embryos to preparturition larvae, to determine whether all FAs were used at the same rate as the total lipid during embryonic development, or whether some were used disproportionately fast while others were conserved.

Methods

Sampling

Quillback rockfish were caught 15–28 April 2006 by hook and line in southeastern Alaska on the northwest side of Chichagof Island (58°10′N, 136°21′W). Fish were caught within approximately 1 km of shore at depths of 30 to 75 m. Fifteen gravid females ranging in size from 360 to 480 mm (fork length) were transported live to Auke Bay Laboratory in Juneau, where they were kept in flow-through seawater tanks at 3.5–4°C. During a 2-week holding period, the females did not feed and did not release larvae naturally. Females were then sacrificed and a sample of embryos or larvae was manually expressed from each fish. Sample sizes available for biochemical analysis varied occasionally because each analytical procedure was destructive and required separate subsamples of embryos or larvae, and sample masses were below the minimum needed to ensure accurate analysis in some cases (Table 1). One sample of stage seven embryos was omitted from analysis due to the apparent degradation and possible resorption of embryos by the parent.

Changes in lipid and protein levels during development

Developmental stages We ranked embryos or larvae from each female in order of development (stages 1–10, from immediately after fertilization through posthatching; Fig. 1) following the descriptions of kurosoi rockfish (*S. schlegelii*) by Yamada and Kusakari (1991), and incorporating our own observations for quillback rockfish (Table 2). In quillback rockfish, we found that the retina went through many stages of pigmentation and that body pigment appeared relatively early in development and became more pronounced through time. Yamada and Kusakari (1991) include only one stage for retinal pigmentation and one for peritoneal pigment (stages 25 and 29, respectively), so we further divided the embryo stages based on these characteristics.

Developmental stages were then used for tracking changes in body composition during embryonic development. Because the durations (in days) of stages vary widely (Eldridge et al., 2002), they are not strictly appropriate for statistical analyses with linear models. In any model using developmental stage categories, the assumption that the stages represent equal intervals can distort the true patterns of change over time. Quantitative statements about rates of change in body composition ideally would be based on time since fer-

Table 2

Developmental staging scheme for quillback rockfish (*Sebastes maliger*) embryogenesis. Stages 1 through 9 represent progressively developing embryos, whereas stage-10 samples contained many hatched larvae. Equivalent stages from Yamada and Kusakari (1991) are included for comparison.

Stage	Description	Yamada and Kusakari (1991) stage
1	Embryonic shield (very small germ disc on one pole of egg)	15
2	Head fold	16
3	Optic vesicles	17
4	Optic cups, increased orbital definition	20
5	Early retinal pigmentation	25
6	Retinal pigment light, spreading throughout eye; body pigment appears as scattered dark dots along ventral side of tail	25–28
7	Very slight eye shimmer appears; body pigment increased slightly, still ventral	25–28
8	Eye shimmer increases, scattered throughout the darkening retina; body pigment increases >2×, still ventral, spots merging to form a line	25–28
9	Retina dark with a lot of shimmer scattered throughout, some black still visible; pigmentation on gut behind yolk sac and dorsally along tail	25–28
10	Dark retina covered with shimmer, body pigment blended into a dark line on ventral side of tail, spots also on dorsal side of tail and on peritoneal wall; hatched/hatching imminent; yolk not depleted	29–31

tilization; however, we did not possess data on the gestation period for quillback rockfish. The period of gestation seems to vary widely among rockfish species (e.g., 29 days for *S. flavidus* [Eldridge et al., 2002], 48 days for *S. schlegelii* [Yamada & Kusakari, 1991]), as well as the time spent at each stage of development, so we did not feel confident in assigning estimated time durations to each stage based on studies of other rockfish. However, we were more concerned with general trends during development, and net differences in body composition as embryos become larvae, than the precise rates of change among stages. In addition, other studies have reported developmental changes in body composition using stages assumed to represent equal intervals (e.g., MacFarlane and Norton, 1999); to facilitate comparisons, we also chose to follow this convention.

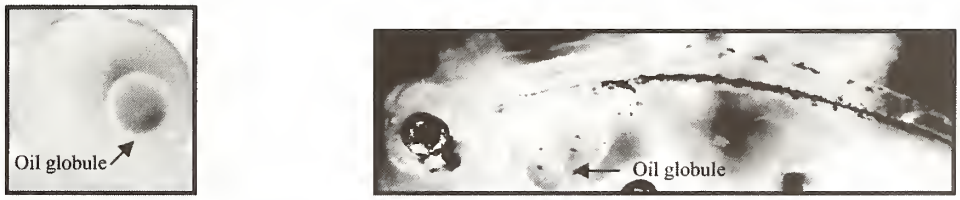

Figure 1

Quillback rockfish (*Sebastes maliger*) stage-1 embryo (left) and stage-10 hatched larva (right).

To assess net changes in body composition that occurred over the course of embryogenesis (i.e., differences between early embryos versus hatched, preparturition larvae), data on body compositions were averaged from three samples at the earliest available stages (stages 2 and 3) and compared with values averaged from four late-stage samples (stage 10). To describe trends and variability in lipid and protein use across all stages of development, protein and lipid masses were plotted against developmental stage and the strengths of the correlations were calculated. Samples at stages 1 and 9 were excluded from biochemical analyses due to technical constraints, such as insufficient sample masses for some processes.

Wet tissue mass The average wet tissue mass of embryos and larvae at each developmental stage was determined for use in calculations of body composition. A subsample of ~100 embryos or larvae removed from a maternal fish was placed on filter paper to drain intraovarian fluid. The subsample was then weighed to the nearest 0.1 mg, and individuals were counted under a dissecting microscope. This was repeated three times per female, and data from the three replicates were used to calculate an average wet mass per embryo or larva. These subsamples were discarded to prevent degraded or oxidized samples from being included in biochemical analyses.

The remaining embryos or larvae from a female were placed in a 20 ml glass vial capped with nitrogen and stored in a freezer at −80°C to prevent oxidation and tissue degradation prior to further processing.

Moisture, protein, and ash content A subsample of approximately 2–4 g (wet mass) of embryos or larvae, representing a composite of thousands of individuals, was used from each sample for analysis of moisture, protein, and ash (inorganic components such as phosphorous, calcium, and other minerals). To determine percent moisture, samples were placed in crucibles in a Leco Thermogravimetric Analyzer 601 (TGA 601) (Leco Corporation, St. Joseph, MI), heated to 135°C to boil off moisture, and wet and dry sample masses were compared. Percent ash was determined gravimetrically by further heating samples to 600°C to combust all organic components and weighing the remaining mass.

The dry mass percent protein was calculated as the observed nitrogen content multiplied by a factor of 6.25, based on the assumption that nitrogen accounts for 16% of the protein mass (Craig et al., 1978). Nitrogen content was determined following the Dumas method (Horwitz, 2002), using a Leco FP 528 nitrogen analyzer (Leco Corporation, St. Joseph, MI), with approximately 0.1 g dry sample mass burned at 850°C and the released nitrogen measured by thermal conductivity.

A National Institute of Standards and Technology Standard Reference Material (SRM) 1546 (pork and chicken homogenate) was used to calibrate the Leco TGA 601, and Leco calibration sample ethylenediaminetetraacetic acid (EDTA, 9.57 ± 0.04% nitrogen) was used to calibrate the Leco FP 528. Two quality assurance samples, Chinook salmon (*Oncorhynchus tshawytscha*) homogenate and walleye pollock (*Theragra chalcogramma*) homogenate, were subjected to proximate analysis along with the larval samples to verify the accuracy of protein, moisture, and ash measurements. Replicate measurements of nitrogen content were taken as a check for precision, with a target error limit of less than 15% coefficient of variation.

Carbohydrate content was not analyzed in this study because fish eggs typically have very low levels of carbohydrates, averaging 2.6% of dry mass (Kamler, 1992). Adult fish also do not typically store carbohydrates in any appreciable quantities (Brett, 1995).

Lipid content A subsample of 0.2 to 0.3 g wet mass containing hundreds of embryos or larvae was used from each of the samples for lipid analysis. Samples were processed by a modified Folch's method as described by Christie (2003). A 2:1 solution of chloroform and methanol, with 0.1 g/L butylated hydroxytoluene (BHT) to minimize oxidation, was used to extract lipids under high temperature (120°C) and pressure (1200 psi) on a Dionex ASE 200 Accelerated Solvent Extractor (Dionex Corporation, Sunnyvale, CA). Extracts were washed with 0.88% KCl followed by a 1:1 (by volume) methanol/deionized water solution, both added at 25% of the extract volume, to remove co-extractables (e.g., glycerol) from the solution containing the extracted lipids. The resulting extract volume was reduced to less than 1 mL by evaporating excess solvent with a Yamato RE 540 rotary evaporator system (Yamato Scientific America, Inc., Santa Clara, CA), then drawn up by electronic pipette with sufficient chloroform to bring the volume to 1000 μL. For gravimetric analysis of total percent lipid, a 500-μL aliquot of the extract was placed in aluminum weighing pans in a fume hood overnight, allowing the solvent to evaporate and leave behind the extracted lipids. The remaining half of the extract was capped with nitrogen and stored at −80°C to minimize oxidation until further processing for FA analysis.

In quality assurance tests, the extraction method consistently yielded wet tissue lipid concentration values not exceeding 15% error compared with the certified value for Standard Reference Material 1946 (lake trout [*Salvelinus namaycush*]). Three quality control samples were also processed concurrently with the larval samples. A method blank containing no sample was used to verify that any contaminants or residues that could bias the observations of lipid mass were less than 0.01% of the average sample mass. As a check for accuracy, extraction of Pacific herring (*Clupea pallasii*) reference tissue yielded lipid concentrations that varied by less than 8% from the average value established in prior analyses. As a check for precision, one larval sample was split into two portions that yielded percent lipid values with less than 1% coefficient of variation.

Energy estimates

Total energy content, energy density, and the relative energetic contributions of protein and lipid were estimated from protein and lipid masses. Protein mass was expressed as its energy equivalent by calculating the product of protein mass and an energy density of 20.1 J/mg, and a similar calculation was made for lipids using an energy density of 36.4 J/mg—figures which are conversions of the average energy density values reported by Brett (1995). For samples having both protein and lipid analyses completed, these were combined to estimate the total energy content per individual embryo or larva, and expressed in relation to sample wet and dry masses to obtain energy density values.

Oil globule volume

Subsamples of 16 to 37 embryos or larvae (mean=24) from each female were placed in Petri dishes and photographed digitally under a dissecting microscope. Using the Clever Ruler 3.0 software (shareware published by zcstar.com), we measured two perpendicular oil globule diameters for each larva from the photos. An average oil globule volume (OGV) for each was then converted to millimeters using a stage micrometer at the same magnification. The change in OGV was determined as the difference in average OGV between early embryonic stage samples and hatched larval samples. To describe trends and variability in OGV across all stages of devel-

opment, OGV was plotted against developmental stage and the strength of the correlation calculated. The relationship between OGV and energetic status of larvae was assessed by treating lipid mass, lipid concentration, and protein mass as response variables and OGV as a predictor variable in simple linear models. Significance tests were performed with a one-way analysis of variance (ANOVA).

Fatty acid analysis

FA composition of total lipid extracts was determined by gas chromatography and mass spectrometry. To prepare lipid extracts for FA analysis, whole lipid extracts underwent acid-catalyzed transesterification to fatty acid methyl esters (FAMEs), following a procedure outlined by Christie (2003). Two mL of Hilditch reagent (0.5 N sulfuric acid [H_2SO_4] in methanol) was added to an aliquot of lipid extract which contained 0.3 mg of lipid. Before transesterification, 2050 nanograms (ng) of 19:0 FA in 50.0 μL hexane was added to each sample as an internal standard for quantification. The solution was incubated at 55°C for approximately 18 hours, and then washed with 5 mL of 5% aqueous sodium chloride (NaCl). To separate and extract the FAMEs from the aqueous solution, 4 mL of hexane was added, the solution was stirred on a vortex mixer, and the hexane layer transferred by pipette to a second container; this process was repeated with another 4 mL of hexane. Four milliliters of 2% potassium bicarbonate ($KHCO_3$) was added to the hexane containing the FAMEs to quench the esterification reaction and neutralize any remaining acid. The hexane-FAME layer was run through a sodium sulfate (Na_2SO_4) drying column to remove any residual co-extractables and water, and the resulting hexane-FAME volume reduced to approximately 1 mL in a Labconco Rapidvap (Labconco Corporation, Kansas City, MO). Prior to GC analysis, 2040 ng of 21:0 FAME in 50.0 μL hexane as an instrumental internal standard was added to each sample for use in sample recovery calculations. The FAMEs were then eluted with a temperature gradient on a Hewlett Packard 6890 gas chromatograph (Hewlett-Packard Company, Palo Alto, CA) with a 5973 mass selective detector by using a 30-m Omegawax 250 fused silica column (Sigma-Aldrich, St. Louis, MO). Five-point calibration curves were created from known concentrations of a Supelco FAME-37 standard mix (Supelco, Bellefonte, PA). Thirty of the 32 FAMEs investigated yielded calibration curves with a coefficient of determination $r^2 \geq 0.990$. As a quality assurance measure, selected calibration standards were re-injected and quantified, and the average across all FAME analytes fell within ±1.5% of the known value.

Along with the samples, quality control samples from the lipid extraction step were subjected to the transesterification procedure. Concentrations of 23 of the 28 FAMEs detected in the Standard Reference Material 1946 were within 25% of the average values obtained from six previous analyses, with none exceeding 35% error. Duplicate larval samples yielded FA concentrations with coefficients of variation less than 10% for 26 of the 29 FAs present. Six FAMEs were detected in the method blank (in order of mass: 18:0, 16:0, 22:1n-9, 17:0, 18:1n-9 *cis* and *trans*, and 14:0) and the masses of these were subtracted from the masses of those FAMEs found in each of the samples as a correction.

Statistical analysis

To determine whether FA profiles of early-stage embryos differed from hatched, preparturition larvae, raw data on FA concentrations (ng of FA per g of wet sample mass) were first converted to proportions of total FAs per sample. The relative proportions of individual FAs present in four samples of early-stage embryos were then compared to those found in four late-stage samples by analysis of similarities (ANOSIM), a nonparametric, multivariate statistical test suitable for compositional studies (Clarke and Warwick, 1994). ANOSIM was performed on a dissimilarity matrix based on the Aitchison distance (Aitchison, 1992) between all possible pairs of samples. The Aitchison distance ($D_{Aitchison}$) between two samples, A and B, is derived from the differences between the log ratios of pairs of FAs present in the two groups:

$$D_{Aitchison}(A,B) = \sqrt{\sum_{i<j}\left(\log\frac{A_i}{A_j} - \log\frac{B_i}{B_j}\right)^2}, \quad (1)$$

where j takes on values up to the number of analytes investigated—in this case, 32.

The Aitchison distance cannot be calculated in cases where the concentrations of a FA are zero in any of the samples being compared. This proved not to be a significant limitation because only one FA, 18:1n-11, was present in measurable quantities in some samples but not in others. This FA was excluded from ANOSIM analysis, but included in estimates of FA mass losses. Three other FAs (15:1n-5, 17:1n-7, and 18:2n-6 *trans*) were also excluded from analysis because they yielded zero values for all samples. We used ANOSIM to compare the ranked Aitchison distances among samples within groups and among samples between groups. This yielded the ANOSIM R statistic, which can range in value from –1 to 1, with a zero value indicating identical groups (i.e., all FAs were used at the same rate, resulting in no difference between FA compositions of embryos and hatched larvae), positive values indicating dissimilarity between groups (i.e., FAs were used at different rates, resulting in changes to the FA compositions of embryos as they developed into larvae), and negative values indicating greater dissimilarity within than between groups (i.e., a study design problem). The significance value was determined through permutations where the observed R value is compared to simulated R values assuming no difference between groups

Table 3

Quillback rockfish (*Sebastes maliger*) body composition data averaged for early-stage embryos and hatched preparturition larvae (mean ±1 SD). Comparisons of early versus late-stage samples revealed net changes that occurred during embryogenesis. "Early" included stages 2–3 embryos, and sample size (n) was 3 maternal females, except for ash (n=2). "Late" included stage-10 larvae, n=4, except ash (n=3). Comparisons only included those samples for which all proximate composition data, except ash, were available. Each sample was a composite of hundreds of embryos or larvae from the same parent. Dry masses did not sum to exactly 100% because lipid was determined by a separate process from protein and ash.

	Early	Late	% Change
Wet mass per individual (μg)	649 ±60	884 ±72	36.2
Moisture (%)	78.5 ±1.7	87.3 ±0.8	11.3
Dry mass per individual (μg)	140 ±13	112 ±15	–19.5
Protein mass per individual (μg)	90.3 ±9.9	73.0 ±12.1	–19.2
Lipid mass per individual (μg)	43.5 ±6.8	28.9 ±4.7	–33.6
Ash mass per individual (μg)	8.61 ±0.57	9.71 ±0.90	12.8
Protein (% wet mass)	13.9 ±1.08	8.22 ±0.74	–41.0
Lipid (% wet mass)	6.70 ±0.85	3.25 ±0.35	–51.4
Lipid (% dry mass)	31.0 ±1.9	25.7 ±2.2	–17.3
Total energy content per individual (J)	3.40 ±0.44	2.52 ±0.40	–25.9
Energy density (J/mg wet mass)	5.24 ±0.52	2.84 ±0.24	–45.9
Energy density (J/mg dry mass)	24.3 ±0.9	22.4 ±0.8	–7.9
Oil globule volume (nL)	27.8 ±1.2	13.7 ± .8	–50.6

(i.e., each time the ANOSIM p is calculated for a given R, its values will vary slightly).

A multidimensional scaling (MDS) plot was constructed using XLStat (Addinsoft, New York, NY) based on the Aitchison distance matrix, to illustrate the degree to which the early-stage embryonic and hatched, preparturition samples were separated based on their FA compositions. Any differences in the rates at which individual FAs were depleted during embryogenesis were expected to change the overall FA profiles over time; any net change in overall FA profile that occurred between early embryonic and later larval stage samples were revealed in the MDS plot.

In order to describe which individual FAs were responsible for the differences in overall FA profiles between early and late stage samples, we calculated the percentages of mass lost (*IML*) for each individual FA:

$$IML = \frac{\overline{m_e} - \overline{m_l}}{\overline{m_l}} \times 100\%, \quad (2)$$

where $\overline{m_e}$ = the average mass of a FA in four samples of early-stage embryos; and
$\overline{m_l}$ = the average mass of a FA in four samples of hatched larvae.

Comparison to the percentage of total lipid mass lost enabled us to describe which FAs had been depleted most rapidly, and which had been largely conserved. Because the importance of any FA in metabolism may be revealed in a combination of the rates of use and the absolute mass used (i.e., its contribution to the overall loss of lipid), we also described changes in mass of each FA between early and late stage samples and the percentage of total FA mass loss (*TML*) they accounted for:

$$TML = \frac{\overline{m_e} - \overline{m_l}}{\overline{TM_e} - \overline{TM_l}} \times 100\%, \quad (3)$$

where $\overline{TM_e}$ = the average total mass of all FAs in four samples of early-stage embryos; and
$\overline{TM_l}$ = the average total mass of all FAs in four samples of hatched larvae.

It is important to note that total lipid masses of samples were independently determined by separate processes from the FA analysis, so total lipid did not simply reflect the summed FA masses.

Results

Body composition and energy use

As they developed, quillback rockfish embryos took on water to gain size while they consumed their stored lipids and, to a lesser extent, protein as energy sources. A typical quillback rockfish embryo gained over one-third its weight in water and lost nearly 20% of its dry mass through the observed course of development, from early embryonic stages to preparturition, hatched larvae (Table 3). Dry mass loss was comprised of 54% protein and 46% lipid.

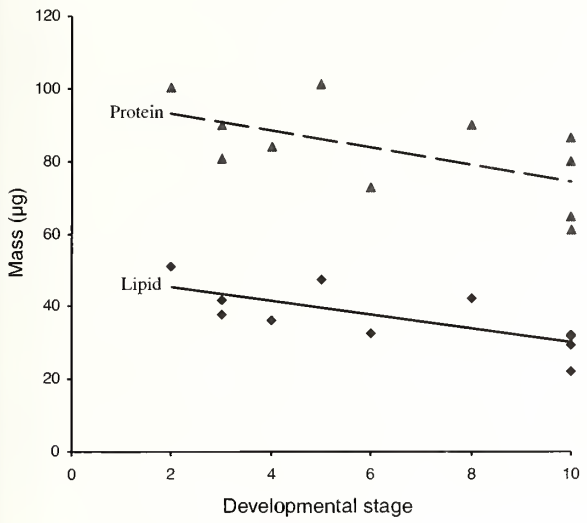

Figure 2

Protein mass (▲) and lipid mass (●) per embryo or larva by developmental stage for quillback rockfish (*Sebastes maliger*). Development progresses from left to right: Stage 2=early embryos (postfertilization); stage 10=hatched larvae (preparturition). Each point represents a single measurement of a composite sample of hundreds of embryos/larvae from one maternal female (n=11 maternal females). Only data from samples for which protein and lipid analyses were both completed are included. For lipid mass, two stage-10 points overlap and are indistinguishable. Lipid: r^2=0.54, y=–1.90x+48.96. Protein: r^2=0.35, y=–2.37x+98.02.

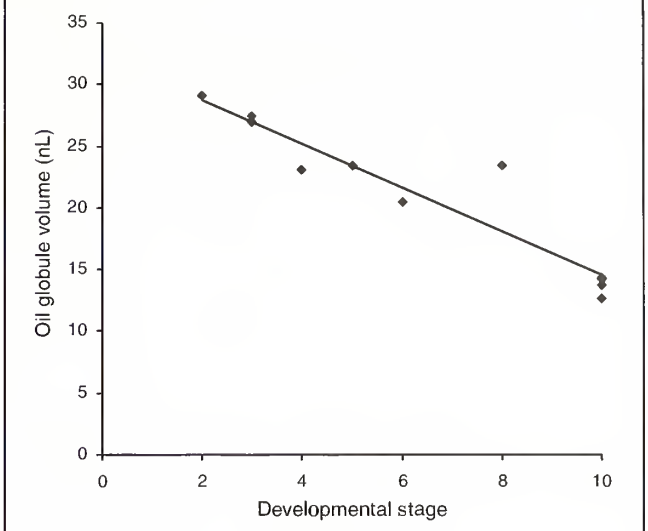

Figure 3

Oil globule volume in nanoliters (nL) by developmental stage for quillback rockfish (*Sebastes maliger*) embryos and larvae. Development progresses from left to right: Stage 2=early embryos (postfertilization); stage 10=hatched larvae (preparturition). Each point represents the mean oil globule volume calculated from diameter measurements of approximately 24 embryos or larvae from each maternal female (n=11 maternal females); two stage-10 points overlap and are indistinguishable. Only data from samples for which protein and lipid analyses were both completed are included. r^2=0.89, y=–1.78x+32.27.

While lipid and protein were both consumed in significant amounts, lipid was lost at a greater rate as a proportion of initial lipid mass (34%) than was protein (19%). Though both declined during development, there was greater variability and a weaker correlation between protein mass and developmental stage than lipid mass and stage (Fig. 2).

Using these mass losses to estimate energy use (Table 3), a developing embryo consumed a minimum of 0.88 J of energy, on average, with approximately 0.53 J (60%) coming from lipid and 0.35 J (40%) from protein. The slight decrease (8%) in the energy density of dry tissue mass was due to greater proportional losses of lipids than proteins. The 26% decline in total energy content per individual was thus more a reflection of the 20% loss in total dry mass than of the changes in proportions of lipid and protein.

Oil globule volume

The volume of the oil globule in rockfish embryos and larvae reflected both their developmental stage and body composition. OGV declined by 51% from early-stage embryos to hatched larvae. The OGV was highly correlated with developmental stage (Fig. 3). As embryos progressed through developmental stages, changes in OGV indicated trends in overall lipid and protein levels. Simple linear regression analysis indicated that total lipid was significantly dependent upon OGV (Table 4); this held true whether lipid was expressed as lipid mass per individual, or concentration (percentage of wet or dry tissue mass). Protein mass also decreased with OGV, though this relationship was weaker.

Fatty acid profiles

The proportions of fatty acids (FAs) present in quillback rockfish appeared to change during their early development, as indicated by the significantly different FA compositions of early embryos versus hatched larvae (ANOSIM R=0.677, α=0.05, n=8). An MDS plot of the samples based on their Aitchison matrix distances showed a distinct separation of the early and late-stage FA profiles (Fig. 4).

The highest percentage mass losses (> 60%) of individual FAs were found to occur among the n-11 monounsaturated fatty acids (MUFAs) 18:1n-11, 20:1n-11 and 22:1n-11; and the polyunsaturated fatty acids (PUFAs) 18:3n-3 (alpha-linolenic acid) and 20:3n-3 (eicosatrienoic acid) (Eq. 2; Fig. 5). The lowest percentage losses (<20%) occurred for the saturated fatty acid (SFA) 18:0 (stearic acid), the MUFA 24:1n-9 (nervonic acid), and

Table 4

Simple linear regression parameters relating body composition (response variables) to oil globule volume for quillback rockfish (*Sebastes maliger*) embryos and preparturition larvae. Each sample was a composite of hundreds of larvae from the same parent (n=11 maternal females). Only data from samples for which protein and lipid analyses were both completed were included.

Response variable	Slope	Intercept	r^2	ANOVA F	P
Lipid mass	1.13	0.0133	0.672	$F_{1,9}$=18.45	0.002
Lipid (% wet mass)	247	−0.101	0.943	$F_{1,9}$=150.14	<0.001
Lipid (% dry mass)	403	20.3	0.701	$F_{1,9}$=99.41	0.001
Protein mass	1.40	0.0537	0.432	$F_{1,9}$=6.85	0.028

the PUFA 20:4n-6 (arachidonic acid). No groups of FAs based on degree of saturation were apparently depleted more rapidly than others, as the percentage mass losses of SFAs, MUFAs, and PUFAs were approximately equivalent to the percentage of total FA mass loss (Fig. 5).

Some FAs showed relatively little contribution to total FA mass loss despite having large initial masses, indicating that they were conserved, particularly the SFA 18:0; and the PUFA 20:4n-6 (Eq. 3, Table 5). Meanwhile, the largest absolute mass losses were found for the SFA 16:0 (palmitic acid); the MUFA 18:1n-9 (oleic acid); and the n-3 PUFAs 22:6n-3 (docosahexaenoic acid, DHA) and 20:5n-3 (eicosapentaenoic acid, EPA), which together accounted for 71% of the total loss in FAs. Thus, there were clear differences in the contributions of different FAs to the overall lipid use.

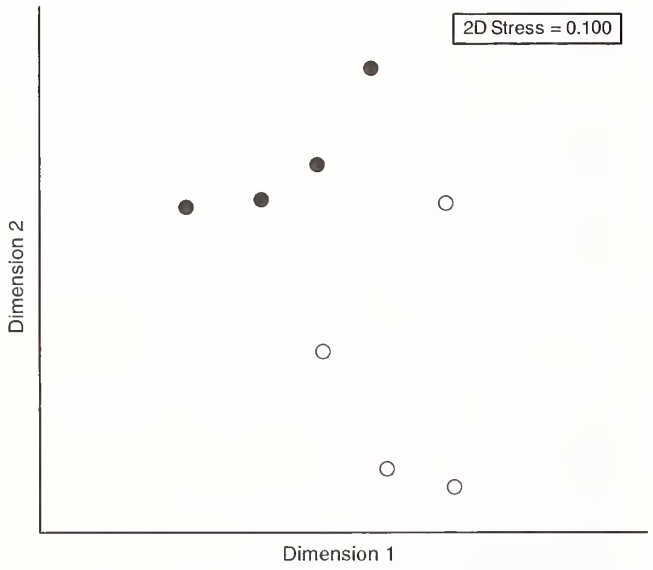

Figure 4

Multidimensional scaling plot of quillback rockfish (*Sebastes maliger*) early-stage embryos (●) and hatched, preparturition larvae (○) according to their fatty acid compositions based on an Aitchison distance matrix. Developmental stage for each sample is given in parentheses. Each sample was a composite of hundreds of larvae from the same parent (n=8 maternal females). Comparisons only included those samples for which lipid data were available.

Discussion

We found that while both lipid and protein mass are consumed by quillback rockfish embryos during development, lipid is used more rapidly and contributes a larger portion of total energy than protein. This is consistent with results from other studies of rockfish, and affirms the importance of measuring lipid levels when assessing larval condition. However, we also found differences in the specific rates of use of protein and lipid compared to other rockfish, which illustrates the diversity of patterns of energy use and changes in body composition among species.

In our study, OGV was highly correlated with lipid content. This relationship could be important for future studies researching the energetic status of rockfish embryos and preparturition larvae. Using OGV as an indicator of energy reserves at any stage of development, and knowing the relationship between OGV and developmental stage, may allow for interpreting the energetic health of embryos at any developmental stage. This is a considerable advantage for field-based studies, given the difficulty of capturing significant numbers of gravid females with embryos or larvae at the same developmental stage, and the risks of introducing experimental effects when parents are held until larvae are released. Our results also illustrate that indicators of condition applied to different species should be interpreted with differences in their biochemistries in mind (e.g., in quillback rockfish OGV is strongly related to total lipid, whereas in black rockfish the two are unrelated) (Berkeley et al., 2004).

Our study represents the first attempt to characterize FA use during embryogenesis for a rockfish species. Although aquaculture studies have investigated FA requirements for rockfish, these have typically involved manipulating the diets of adults and juveniles (e.g., Lee, 2001) and likely

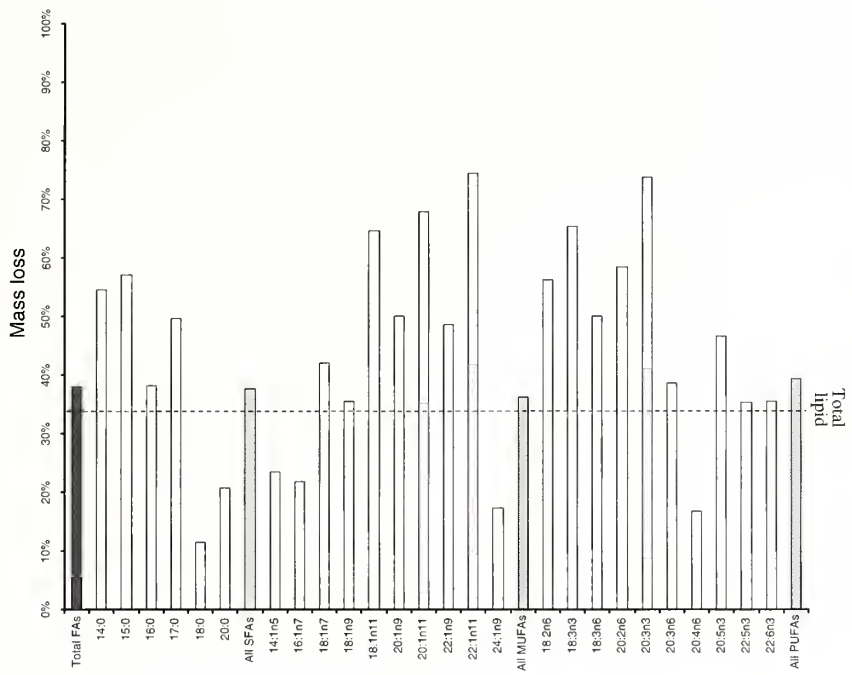

Figure 5

Percentage of individual fatty acid (FA) masses lost during embryogenesis of quillback rockfish (*Sebastes maliger*) larvae. Percentage mass losses represent differences between average FA masses per larva of four early embryonic samples and four hatched larval samples, in relation to masses present in early embryonic samples. Each sample was a composite of hundreds of larvae from the same parent (n=8 maternal females). Dashed line indicates difference in total lipid mass between embryos and larvae in relation to lipid mass in embryos.

cannot be generalized to developing rockfish embryos and larvae. Although we did not attempt to directly assess the influence of specific FAs on larval survival, our results show FAs are depleted at different rates during embryogenesis. When used in conjunction with data on total lipid levels, the relative abundances of specific conserved FAs of known metabolic importance (e.g., 20:4n-6) may be useful in assessing the condition of embryos and preparturition larvae collected from wild-caught female rockfish.

Body composition and energy use

Comparisons with other studies of rockfish revealed substantial diversity in the body compositions and energy use patterns of embryos from different *Sebastes* species—even after allowing for differences in methods and the high degree of variability in the compositional data. For example, the early stage quillback rockfish embryos studied here had lower lipid (~6.7%) and protein (~14.1%) wet tissue concentrations than those found by Eldridge et al. (2002) for late vitellogenic eggs and early embryos of yellowtail rockfish (*S. flavidus*) (~12.8% and ~21.0%, respectively). Quillback rockfish embryos had lower energy density on a dry mass basis (~24.3 kJ/g) compared with the yellowtail rockfish embryos (~27.1 kJ/g), but because of their larger dry mass, the embryos of quillback rockfish had much greater total energy per individual (3.40 J) than those of the yellowtail rockfish (~1.06 J).

The patterns of decline in lipid and protein in quillback rockfish differed somewhat from those reported by MacFarlane and Norton (1999) for yellowtail rockfish. They found that lipid as a proportion of wet mass declined 68% and protein decreased by 77%, whereas we found that lipid declined 51% and protein declined 41%. The smaller decreases in lipid and protein concentration we found may be an artifact of the different ranges of development observed (i.e., our study did not include data from unfertilized oocytes or the earliest stage-1 embryos, when protein and lipid levels were likely higher). The slightly greater decreases in protein concentration than in lipid concentration reported for yellowtail rockfish—opposite to the pattern we found with quillback rockfish—illustrates the high degree of variability among rockfish species. The results of MacFarlane and Norton (1999) for shortbelly rockfish (*S. jordani*) followed a pattern similar to ours, with lipid decreasing by 68% and protein by 55%, indicating greater conservation of protein by shortbelly rockfish

Table 5

Contributions of individual fatty acids (FAs) to total FA mass loss during quillback rockfish (*Sebastes maliger*) embryogenesis based on comparison of average FA masses for four early embryonic (stages 2–3) and four hatched larval (stage 10) samples. Each sample was a composite of hundreds of larvae from the same parent (n=8 maternal females). Results are ranked by mass loss in nanograms (ng), and grouped by degree of saturation (SFA=saturated fatty acid; MUFA=monounsaturated fatty acid; PUFA=polyunsaturated fatty acid). High variability (low precision), as indicated by coefficients of variation >10%, was found in duplicate samples for 18:1n11 (32.1%), 24:1n9 (21.2%) and 24:0 (11.3%). *=trace (≤1 ng).

Fatty acid	Mass (ng) per embryo ±1 SD	Mass (ng) per larva ±1 SD	Mass loss (ng)	% of total FA mass loss
SFA				
16:0	3250 ±481	2010 ±410	1240	13.5
14:0	660 ±111	300 ±41	360	3.9
18:0	605 ±87	536 ±119	69	0.8
15:0	113 ±9	49 ±13	64	0.7
17:0	73 ±9	37 ±6	36	0.4
20:0	11 ±1	9 ±1	2	<0.1
22:0	*	*	*	<0.1
24:0	*	*	*	<0.1
All SFAs	4710	2940	1770	19.4
MUFA				
18:1n9 *cis* and *trans*	3450 ±509	2230 ±576	1220	13.4
18:1n7	1260 ±180	731 ±148	529	5.8
16:1n7	1510 ±222	1180 ±340	330	3.6
20:1n11	269 ±100	86 ±44	183	2.0
20:1n9	255 ±42	128 ±16	127	1.4
18:1n11	115 ±35	41 ±53	74	0.8
22:1n11	80 ±36	21 ±10	59	0.7
22:1n9	24 ±5	12 ±1	12	0.1
24:1n9	64 ±9	53 ±13	11	0.1
14:1n5	10 ±2	8 ±3	2	<0.1
All MUFAs	7040	4490	2550	27.9
PUFA				
22:6n3	5950 ±959	3850 ±846	2100	23.0
20:5n3	4200 ±832	2240 ±454	1960	21.3
22:5n3	806 ±223	522 ±123	284	3.1
18:2n6	299 ±38	131 ±37	168	1.8
20:4n6	735 ±73	612 ±90	123	1.3
18:3n3	154 ±24	54 ±24	100	1.1
20:3n3	63 ±39	17 ±5	46	0.5
20:2n6	61 ±17	25 ±7	36	0.4
18:3n6	20 ±1	10 ±3	10	0.1
20:3n6	9 ±2	6 ±2	3	<0.1
22:2n6	3 ±1	*	*	<0.1
All PUFAs	12300	7470	4830	52.7

and quillback rockfish, both of which had lower initial concentrations of protein on a wet mass basis than yellowtail rockfish. From a purely energetic perspective, embryos of all three of these rockfish species show a greater decline in energy available as lipid than as protein.

The energy density of early-stage quillback rockfish embryos (5.24 J/mg) was similar to the typical value for marine spawning species of 6.0 J/mg reported by Kamler (1992). Changes in the energy density of wet tissue mass were largely a reflection of changes in the percent moisture; whereas changes in the dry tissue composition contributed less. Energy density on a dry mass basis was similar to the value for fish eggs of 23.48 J/mg reported by Wootton (1979) as an average across many species. This is not surprising, given that interspecific variation in the energy density of fish eggs is relatively low (Kamler, 1992), compared with the range of egg sizes and total energy contents.

The distinction between viviparous and ovoviviparous is a consideration in interpreting mass loss and energy data in our study because it hinges on whether the em-

bryos developing inside the mothers' bodies are supplied with maternal nutrients (viviparous), or rely entirely on their yolk sacs (ovoviviparous). Quillback rockfish have been described as viviparous (MacFarlane and Norton, 1999), and ovoviviparous (Matala et al., 2004). Previous research using radiocarbon-labeled amino acids found that embryos of black rockfish (*S. melanops*) took up nutrients from intraovarian fluid, but only at very late stages of development—presumably after they had hatched and their mouths and digestive systems were sufficiently functional (Yoklavich and Boehlert, 1991). MacFarlane and Bowers (1995) also found evidence of matrotrophy (postfertilization maternal nutrient provisioning) occurring in yellowtail rockfish because a radio-labeled phospholipid was transferred from mothers to embryos before their mouths opened, and the amount increased as they developed. Reviews of these and other studies have thus supported viviparity in rockfish (e.g., Parker et al., 2000). The reduction in dry tissue mass seen among the quillback rockfish embryos in our study was lower than the 25% to 55% range of dry mass losses typically seen in strict lecithotropes (MacFarlane and Bowers, 1995), which rely entirely on nutrients provided to the egg before fertilization, suggesting that quillback rockfish are also partly matrotrophic. The degree to which nutrition is obtained from the yolk rather than from maternal intraovarian fluids is unclear for quillback rockfish; therefore it is important to view data regarding mass loss and energy use given here as minimums.

It is likely that maternal traits (e.g., the size and age of the female parent) influence the biochemical compositions of rockfish embryos and larvae (Sogard et al., 2008). This introduces the possibility of maternal effects confounding the relationship between developmental stage and body composition (e.g., if our samples were biased towards larger females yielding the earlier stages of embryos). However, it is likely that developmental processes accounted for most of the differences that we found between early-stage embryos and hatched larvae. Developmental stage showed a much stronger relationship to lipid concentration (r^2=0.87) than did maternal length (r^2=0.39). Maternal length was only weakly correlated with developmental stage (r^2=0.26), and this correlation was largely driven by the presence of one large fish with stage 10 larvae. Removing this fish and its larvae resulted in virtually no relationship between maternal length and developmental stage (r^2=.15). This highlights one of the conclusions that can be drawn from our data: developmental stage should be accounted for when investigating maternal effects among wild caught fish with progeny at various stages.

If quillback rockfish preferentially use lipid as an energy source over protein, it would be useful to investigate how various maternal traits influence the relative rates of lipid and protein loss in embryos. For example, do embryos from older, larger, or fatter parents have greater lipid reserves, and do they exhibit lower rates of protein loss?

Why not simply use size or total energy content as indicators of viability? Such an approach is indicated by our finding that changes in total energy content per larva largely reflected changes in dry mass from early to late stages, rather than changes in the proportions of lipid and protein. In addition, there is great variability among species in the size and energy content of eggs and embryos—the early stage quillback rockfish embryos in our study were on average more than 2.6 times heavier on a dry mass basis than yellowtail rockfish embryos (Eldridge et al., 2002). Greater larval size may also confer advantages through reduced predation and increased range of feeding opportunities, and was probably the force driving the uptake of water during early development that we observed. However, various studies have found no relationship between egg size and offspring viability (reviewed in Kamler, 1992). Straightforward interpretation of the relationship of egg or embryo size and total energy content to larval viability is confounded by findings suggesting that larvae from smaller eggs often use yolk energy for growth more efficiently than those from larger eggs, and may undergo compensatory growth in later development (reviewed in Kamler, 1992). Even under conditions of food scarcity, where larger larvae may be expected to be at an advantage, results have been inconsistent; for example, larval length did not appear related to starvation resistance of black rockfish larvae (Berkeley et al., 2004).

Oil globule volume

Given the importance of lipid as an energy source for developing quillback rockfish embryos, the strong correlation of OGV with total lipid we found suggests that OGV may serve as an indicator of energetic status. Some maternal trait, such as age (e.g., Berkeley et al., 2004), may strongly influence OGV and be responsible for the variability. Investigating changes in the lipid class components (e.g., TAG and polar lipids) of the oil globules, as well as whole embryos, could provide information useful for better understanding the relationship of the oil globules to condition. The strength of the relationship between OGV and larval survival should also be investigated experimentally with quillback rockfish larvae. Using OGV as an indicator of energetic status represents a potentially large savings in resources required, compared with analytical chemistry techniques.

Fatty acid profile

The major FA components of the lipids in quillback rockfish embryos and larvae were generally similar to those reported elsewhere for many species of adult fish (reviewed in Tocher, 2003): predominantly the n-3 PUFAs 22:6n-3 and 20:5n-3; 20:4n-6 as the main n-6 PUFA; large quantities of the MUFA 18:1n-9; and 16:0 and 18:0 as the main SFAs. Previous researchers have also reported high levels of n-3 PUFAs in marine fish eggs (e.g., Tocher & Sargent, 1984); however, there can be marked interspecific differences in the precise order

of FA abundances. For example, in contrast to the quillback rockfish embryos studied here, which showed the n-3 PUFAs 22:6n-3 and 20:5n-3 in greatest abundance, Tveiten et al. (2004) reported that of 16 FAs they investigated in embryos of the spotted wolffish (*Anarhichas minor*), 18:1n-9 was predominant.

Caution must be used when attempting to apply condition indices based on FA amounts or proportions derived from other species. As lipids are broken down for use during development, the resulting FAs may be conserved as structural components of new tissues or metabolic compounds, modified into new FAs, or consumed as energy sources, and the timing and extent to which specific FAs are used varies considerably among species (reviewed in Tocher, 2003). In some marine fish, FAs appear to be utilized in a non-selective fashion (e.g., in order of their abundance) while in others, some FAs have been preferentially retained. For example, retention of 20:4n-6 was found to occur in Murray cod (*Maccullochella peelii peelii*) and trout cod (*Maccullochella macquariensis*; Gunasekera et al., 1999), Senegalese sole (*Solea senegalensis*; Mourente and Vazquez, 1996), and spotted wolffish (*Anarhichas minor*; Tveiten et al., 2004); this PUFA was also used less rapidly than the total lipid for the rockfish embryos in this study. Greater retention of 20:5n-3 has been reported in Atlantic halibut (*Hippoglossus hippoglossus*; Ronnestad et al., 1995), but this did not occur for quillback rockfish here. Tveiten et al. (2004) found that spotted wolffish embryos had lower ratios of 20:4n-6 to 20:5n-3 than those generally deemed necessary for survival in other species. In spotted wolffish embryos, the proportion of 16:0 increased, while 18:1n-9 decreased (Tveiten et al., 2004); for quillback rockfish, these FAs were used at the same rate as total FAs. This suggests that species differences must be considered in any assessment of the FA composition of developing fish.

Saturated fatty acids and monounsaturated fatty acids

The SFAs 16:0 and 18:0, and MUFAs that can be derived from them (e.g., 16:1n-7, 18:1n-9), are unlikely candidates for use as indicators of quillback rockfish nutritional or energetic status due to their relatively high abundances and the ability of all organisms to biosynthesize them. Any deficiencies in these FAs could be readily inferred from low total lipid levels.

The MUFAs with high percentage mass losses were generally present in very low amounts and likely were not of high metabolic importance. For example, the MUFA 22:1n-11, which is likely derived from calanoid copepods and transferred up through higher trophic levels in marine food chains (Saito and Kotani, 2000), was found to have the greatest rate of decrease in mass during larval development. However, its small initial mass and general absence from structural lipids in fish (Tocher, 2003) makes it likely to serve only as a minor energy source for developing quillback rockfish embryos.

Polyunsaturated fatty acids

The finding that 20:4n-6, which was the most abundant n-6 PUFA, was largely conserved seems consistent with its role as an important metabolic end product rather than a general energy source. As a precursor to the eicosanoids, a physiologically active and diverse group of hormone-like compounds, 20:4n-6 is believed to play a significant role in a variety of functions, including inducement of spawning, intercellular signaling, stress tolerance, immune response, inflammatory response, blood clotting, and is likely essential to normal growth and development (reviewed in Bell & Sargent, 2003; Tocher 2003). Several aquaculture studies have indicated that supplementing broodstock diets with 20:4n-6, within optimal concentration ranges or ratios to other FAs, results in improved egg and larval quality for a variety of marine fish species (reviewed in Bell & Sargent, 2003). Many marine fish seem to need 20:4n-6 in their diets and are unable to manufacture it from precursors (Mourente and Tocher, 1993; reviewed in Bell & Sargent, 2003); the levels of 20:4n-6 in embryos therefore likely reflect the quality of maternal provisioning. While measuring the relative abundance of 20:4n-6 may be useful in assessing condition of quillback rockfish embryos, further investigation is needed to determine what levels of 20:4n-6 may be considered deficient, and what specific effects may arise from that deficiency.

The PUFAs 20:5n-3 and 22:6n-3 were the most abundant FAs measured in quillback rockfish embryos and preparturition larvae, and decreased at approximately the same rate as total lipids. While 20:5n-3 and 22:6n-3 are important metabolic end products, they can also be consumed as major energy sources during the early life history of many marine fishes (reviewed in Tocher, 2003). Due to their abundance and role as energy sources, the amounts of 20:5n-3 and 22:6n-3 in quillback rockfish embryos are reflected in total lipid levels, and would not be informative as additional indicators of condition.

The remaining PUFAs were used more quickly than the total lipid, were generally not very abundant, and are likely of limited importance. For example, 18:3n-3, an essential fatty acid derived from marine plants, can serve as a precursor to both 20:5n-3 and 22:6n-3 in some organisms, following a metabolic pathway that is similar across widely varying taxa (reviewed in Tocher, 2003). However, the high abundances of 20:5n-3 and 22:6n-3, in combination with the relatively low levels of 18:3n-3 (<1% total FA mass), suggest that they were being synthesized from 18:3n-3 to supplement the maternally-provisioned amounts, it was only to a minor degree. Other research suggests that marine fish are largely incapable of synthesizing 20:5n-3 and 22:6n-3 from 18:3n-3 and they obtain these essential fatty acids from their diets (Tocher, 2003), in which case the embryos are likely using 18:3n-3 as a relatively small energy source. Similarly, 18:2n-6 may be of limited importance, as marine fish have limited ability to convert it to the metabolically-important PUFA 20:4n-6,

and it was present at relatively low levels in quillback rockfish embryos.

Although both lipid and protein are consumed during quillback rockfish embryogenesis, lipid is used more rapidly and contributes a greater portion of the total energy expended. Lipid is typically the most variable dry mass component of fish eggs, showing significant differences between populations and within a population over time; additionally, lipid concentration has been used as an indicator of larval viability for several species (reviewed in Kamler, 1992). Given the importance of lipid as an energy source, the strong relationship between OGV and lipid levels confirms the utility of OGV as an indicator of differences in condition of quillback rockfish embryos and preparturition larvae. Differences in FA profiles of early embryos and preparturition larvae indicate FAs are depleted at different rates during embryogenesis. More rapidly used FAs may contribute more to lipid energy use or serve as precursors in the synthesis of other FAs, while conserved FAs likely are incorporated into tissues or hormone-like compounds. The conservation of 20:4n-6, the most abundant n-6 PUFA, indicates that this essential fatty acid may well reflect the quality of maternal provisioning. The high degree of interspecific variability in body composition and energy use patterns among rockfish illustrates the need for data gathered from the species of interest, in order to make the most accurate models of energy use and most appropriate indicators of condition.

Acknowledgments

We thank R. Heintz for advice on study methodology and data analysis, M. Larsen for generating the fatty acid data, and R. Bradshaw for generating the protein, moisture, and ash content data. We also thank J. Maselko for developing the computer code for creating the Aitchison distance matrix and ANOSIM statistical analysis, C. Lunsford for assisting with field sampling, and J. Heifetz and L. Schaufler for providing helpful commentary and edits on earlier drafts.

Literature cited

Aitchison, J.
1992. On criteria for measures of compositional difference. Math. Geol. 24:365–379.

Bell, J. G., and J. R. Sargent.
2003. Arachidonic acid in aquaculture feeds: current status and future opportunities. Aquacult. 218:491–499.

Berkeley, S. A., C. Chapman, and S. M. Sogard.
2004. Maternal age as a determinant of larval growth and survival in a marine fish, *Sebastes melanops*. Ecology 85(5):1258–1264.

Brett, J. R.
1995. Energetics. *In* Physiological ecology of Pacific salmon (Groot, C., Margolis, L., and W.C. Clarke, eds.), p. 1–68. UBC Press, Vancouver, Canada.

Christie, W. W.
2003. Lipid analysis: Isolation, separation, identification and structural analysis of lipids, 416 p. Oily Press, Bridgwater, U.K.

Clarke, K. R., and R. M. Warwick.
1994. Change in marine communities: An approach to statistical analysis and interpretation, 144p. Plymouth Marine Laboratory, Plymouth, U.K.

Craig, J. F., M. J. Kenley, and J. F. Talling.
1978. Comparative estimations of the energy content of fish tissue from bomb calorimetry, wet oxidation and proximate analysis. Freshw. Biol. 8:585–590.

Eldridge, M. B., E. C. Norton, B. M. Jarvis, and R. B. MacFarlane.
2002. Energetics of early development in the viviparous yellowtail rockfish. J. Fish Biol. 61:1122–1134.

Gunasekera, R. M., S. S. De Silva, and B. A. Ingram.
1999. Early ontogeny-related changes of the fatty acid composition in the percichthyid fishes trout cod, *Maccullochella macquariensis* and Murray cod, *Maccullochella pelii peelii*. Aquat. Living Resour. 12:219–227.

Horwitz, W., ed.
2002. Official methods of analysis, 17th ed. AOAC (Association of Analytical Communities) International, Gaithersburg, MD.

Kamler, E.
1992. Early life history of fish, an energetics approach. 267 p. Chapman and Hall, London.

Lee, S. M.
2001. Review of the lipid and essential fatty acid requirements of rockfish (*Sebastes schlegeli*). Aquacult. Res. 32(s1):8–17.

MacFarlane, R. B., and M. J. Bowers.
1995. Matrotrophic viviparity in the yellowtail rockfish *Sebastes flavidus*. J. Exp. Biol. 198:1197–206.

MacFarlane, R. B., and E. C. Norton.
1999. Nutritional dynamics during embryonic development in the viviparous genus *Sebastes* and their application to the assessment of reproductive success. Fish. Bull. 97:273–281.

Matala, A. P., A. K. Gray, J. Heifetz, and A. J. Gharrett.
2004. Population structure of Alaskan shortraker rockfish, *Sebastes borealis*, inferred from microsatellite variation. Environ. Biol. Fishes 69:201–210.

Mourente, G., and D. R. Tocher.
1993. Incorporation and metabolism of ^{14}C-labeled polyunsaturated fatty acids in wild-caught juveniles of golden grey mullet, *Liza aurata*, in vivo. Fish Physiol. Biochem. 12(2):119–130.

Mourente, G., and R. Vazquez.
1996. Changes in the content of total lipid, lipid classes and fatty acids of developing eggs and unfed larvae of the Senegal sole, *Solea senegalensis* Kaup. Fish Physiol. Biochem. 15(3):221–235.

Norton, E. C., R. B. MacFarlane, and M. S. Mohr.
2001. Lipid class dynamics during development in early life stages of shortbelly rockfish and their application to condition assessment. J. Fish. Biol. 58:1010–1024.

Parker, S. J., S. A. Berkeley, J. T. Golden, D. R. Gunderson, J. Heifetz, M. A. Hixon, R. Larson, B. M. Leaman, M. S. Love, J. A. Musick, V. M. O'Connell, S. Ralston, H. J. Weeks, and M. M. Yoklavich.
2000. Management of Pacific rockfish. Fisheries 25(3): 22–30.

Ralston, S., and D. F. Howard
1995. On the development of year-class strength and cohort

variability in two northern California rockfishes. Fish. Bull. 93:710–720.

Ronnestad, I., R. N. Finn, I. Lein, and O. Lie.
1995. Compartmental changes in the contents of total lipid, lipid classes and their associated fatty acids in developing yolk-sac larvae of Atlantic halibut, *Hippoglossus hippoglossus* (L.). Aquacult. Nutr. 1:119–130.

Saito, H. and Y. Kotani.
2000. Lipids of four boreal species of calanoid copepods: origin of monoene fats of marine animals at higher trophic levels in the grazing food chain in the subarctic ocean ecosystem. Mar. Chem. 7:69–82.

Sogard, M. S., S. A. Berkeley, and R. Fisher.
2008. Maternal effects in rockfishes *Sebastes* spp.: a comparison among species. Mar. Ecol. Prog. Ser. 360:227–236.

Tocher, D. R.
2003. Metabolism and functions of lipids and fatty acids in teleost fish. Rev. Fish. Sci. 11(2):107–184.

Tocher, D. R., and J. R. Sargent
1984. Analyses of lipids and fatty acids in rope roes of some Northwest European marine fish. Lipids 19(7):492–499.

Tveiten, H., M. Jobling, and I. Andreassen.
2004. Influence of egg lipids and fatty acids on egg viability, and their utilization during embryonic development of spotted wolf-fish, *Anarhichas minor* Olafsen. Aquacult. Res. 35(2):152–161.

Watanabe, T.
1982. Lipid nutrition in fish. Comp. Biochem. Physiol. B 73(1):3–15.

Wootton, R. J.
1979. Energy costs of egg production and environmental determinants of fecundity in teleost fishes. Symp. Zool. Soc. Lond. 44:133–159.

Yamada, J., and M. Kusakari.
1991. Staging and the time course of embryonic development in kurosai, *Sebastes schlegeli*. Environ. Biol. Fishes 30:103–110.

Yoklavich, M., and G. W. Boehlert.
1991. Uptake and utilization of ^{14}C-glycine by embryos of *Sebastes melanops*. Environ. Biol. Fishes 30:147–153.

Evidence of the selection of tidal streams by northern rock sole (*Lepidopsetta polyxystra*) for transport in the eastern Bering Sea

Daniel G. Nichol (contact author)

David A. Somerton

E-mail address for contact author: dan.nichol@noaa.gov

Alaska Fisheries Science Center
National Marine Fisheries Service, NOAA
7600 Sand Point Way NE
Seattle, Washington 98115

Abstract—Depth data from archival tags on northern rock sole (*Lepidopsetta polyxystra*) were examined to assess whether fish used tidal currents to aid horizontal migration. Two northern rock sole, out of 115 released with archival tags in the eastern Bering Sea, were recovered 314 and 667 days after release. Both fish made periodic excursions away from the bottom during mostly nighttime hours, but also during particular phases of the tide cycle. One fish that was captured and released in an area of rotary currents made vertical excursions that were correlated with tidal current direction. To test the hypothesis that the fish made vertical excursions to use tidal currents to aid migration, a hypothetical migratory path was calculated using a tide model to predict the current direction and speed during periods when the fish was off the bottom. This migration included limited movements from July through December, followed by a 200-km southern migration from January through February, then a return northward in March and April. The successful application of tidal current information to predict a horizontal migratory path not only provides evidence of selective tidal stream transport but indicates that vertical excursions were conducted primarily to assist horizontal migration.

Manuscript submitted 29 July 2008.
Manuscript accepted 19 December 2008.
Fish. Bull. 107:221–234 (2009).

The views and opinions expressed or implied in this article are those of the author and do not necessarily reflect the position of the National Marine Fisheries Service, NOAA.

Northern rock sole (*Lepidopsetta polyxystra*) in the eastern Bering Sea off Alaska reportedly migrate from summer feeding grounds to deeper spawning grounds in winter (Shubnikov and Lisovenko, 1964; Fadeev, 1965). Although migration routes are poorly understood, at least some individuals are thought to migrate long distances between summer and winter grounds. Shubnikov and Lisovenko (1964) suggested that some northern rock sole migrate from Unimak Island in the Aleutian Islands to areas northeast of the Pribilof Islands between April and July, covering a distance of more than 500 km. As a means to understand better how this migration occurs, we focus here on one potential mechanism that northern rock sole use, that is, the opportunistic or exclusive use of selective tidal stream transport.

Selective tidal stream transport is a mechanism by which aquatic animals can assist their horizontal migration by actively changing their vertical position in the water column, timed to coincide with tidal currents flowing in a preferred direction. Selective tidal stream transport has been documented for a variety of aquatic animals (Forward and Tankersley, 2001; Gibson, 2003) and has been extensively documented in the North Sea for European plaice (*Pleuronectes platessa*) (Kuipers, 1973; Rijnsdorp and van Stralen, 1985; Metcalfe et al., 1990; Fox et al., 2006; Metcalfe et al., 2006). Even before the use of electronic fish tags, it was recognized that some flatfish species selectively leave the bottom during periods of a preferred tidal current direction (De Veen, 1967; Harden Jones et al., 1979). More recent work with archival tag data, used in combination with tide data (e.g., Hunter et al., 2004b), has highlighted the importance of both tide and diurnal factors in flatfish migration. For plaice and other flatfish species, the vertical movements (i.e., selective tidal stream transport) vary diurnally; most excursions are made away from bottom during the night (De Veen, 1967; Cadrin and Westwood, 2004; Hunter et al., 2004b; Walsh and Morgan, 2004). Juvenile flatfishes (Champalbert et al., 1992; Burrows, 1994), including northern rock sole (Hurst and Duffy, 2005), also show some preference for nighttime activity.

When flatfishes use selective tidal stream transport, the timing of vertical excursions away from the bottom can be combined with predictions of tidal current velocity to construct hypothetical migration trajectories (Arnold and Holford, 1995). For this estimation to be successful, vertical excursions need to be accurately identified and all directed horizontal movement must be restricted to those off-bottom periods. For species known to use tidal currents, selective tidal stream transport may not be used in all habitats because the strength or direction of the currents may be unsuitable for migration. For example, when European plaice inhabit areas of weak tidal currents in the North Sea, they migrate horizontally, staying near the seafloor where there is

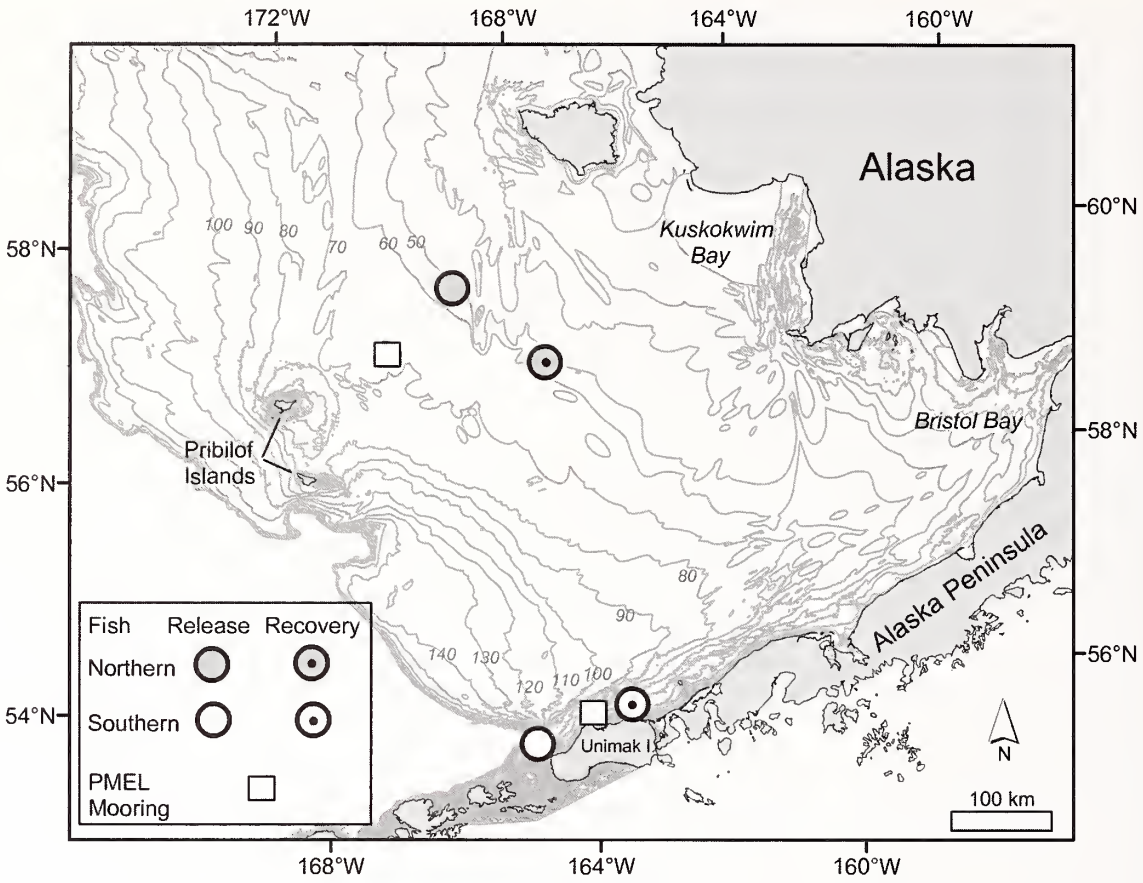

Figure 1

Map of release and capture locations for two female northern rock sole (*Lepidopsetta polyxystra*) tagged with archival tags in the eastern Bering Sea off Alaska in 2003. The locations of the Pacific Marine Environmental Laboratory (PMEL) subsurface moorings where tidal current velocity data (speed and direction) were collected are also shown. Gray lines with numbers indicate the bathymetric contours (in m) in the area.

no tidal assistance (Hunter et al., 2004a; Metcalfe et al., 2006). In addition to accurately determining periods when a fish is off-bottom, successful selective tidal stream transport modeling also requires the ability to accurately predict tidal currents.

Tidal currents over most of the eastern Bering Sea shelf have characteristics that offer fish a mechanism that assists horizontal movement. Such currents range from rotary motion on the central continental shelf (e.g., east of Pribilof Islands) to bidirectional motion along the Alaska Peninsula (Kowalik, 1999; Pearson et al., 1981), and a strong semidiurnal component everywhere which offers fish two opportunities within a 24-h period to use currents to migrate in a particular direction. Near-bottom tidal current velocities over much of the eastern Bering Sea shelf average approximately 20 cm/s and peak to over 50 cm/s, which if used for transport, could provide a significant increase in migration velocity. Moreover, the rotary nature of the currents offers an intriguing mechanism for transport because it can provide a means of transport in any direction a fish chooses.

Here, we examine depth and time data from archival tags attached to two northern rock sole to determine whether vertical excursions are related to diel and tidal influences, and whether a simple model of selective tidal stream transport can be used to construct a hypothetical horizontal migration path that is consistent with the observed tag release and recovery locations

Methods

Tagging

Two northern rock sole were recovered from among 115 released with attached electronic data storage tags in the eastern Bering Sea between 4 June and 26 July 2003. Release locations were approximately 200 km northeast of St. Paul Island in the Pribilof Islands (northern fish) and 18 km northwest of Unimak Island (southern fish) (Fig. 1). Fish were initially captured with a bottom trawl, tagged, and released during the course of the annual eastern Bering Sea bottom trawl survey (Acuna and

Lauth, 2008). The two recovered fish, both captured by commercial trawlers, were a 34-cm-total-length (TL) (at release) female at liberty for 314 days (northern fish) and a 40-cm-TL (at release) female at liberty for 667 days (southern fish). Both fish were assumed to be mature because they were larger than the reported mean size at maturity of 32.8 cm (Stark and Somerton, 2002).

The fish were tagged with Lotek wireless LTD-1100 (St. John's, NF, Canada) data storage tags. Tags were attached to the eyed-side, just below the anterior end of the dorsal fin with a 0.5-mm diameter stainless-steel wire. The wire was inserted through two points on the tag, through the epaxial musculature above the pectoral fin, and affixed on the blind side of the fish by using oval plastic backing. The two wire ends were fastened on the outside of the backing with a crimped connector sleeve.

Tag data, including depth (pressure) and temperature, were recorded at 0.5-h or 1-h time intervals, totaling 12,015 and 16,346 data pairs for the northern and southern fish, respectively. Two sampling intervals were used because, as a memory management function of the tags, the frequency of recordings decreased with the time at liberty. Depth had a resolution of 0.58 m when fish remained at depths less than 150 m, and 1.2 m if the fish exceeded 150 m; temperature had an accuracy of ±0.3°C. The northern tag recorded for the entire 314 days the fish was at liberty, whereas the southern tag recorded for 620 of 667 days at liberty before the battery died.

Tide prediction

Tidal height and current speed and direction were estimated at the midpoint location between fish release and recovery (northern fish: 58°18′N, 167°02′W; southern fish: 54°55′N, 164°31′W) for each depth measurement using the OTIS Tidal Inversion Software (Oregon State University, Corvallis, OR) which was created with solutions specifically for the eastern Bering Sea (Egbert et al., 1994; Egbert and Erofeeva, 2002). To test the accuracy of the tide model, speed and direction were also estimated at the site of an oceanographic mooring maintained by the Pacific Marine Environmental Laboratory (NOAA, Seattle, WA) near each fish (Fig. 1) and compared to the measured bottom current data. The northern mooring was located approximately 118 km west of the northern fish location and collected data from October 2004 to April 2005; the southern mooring was located approximately 66 km north of the southern fish location and collected data from March 1995 to September 1995. Each data set consisted of hourly current velocity vectors (u=east-west component, v=north-south component) over a period of 193 days.

Identification of vertical excursions

Time intervals during which the fish were off bottom were identified as follows. Measured tag depths were first corrected for tide height variation by subtracting the tide height predicted by the tide model. Because along-slope movements can be confused with off-bottom movements, the difference in bathymetric complexity between northern and southern tag release locations dictated differences in the subsequent analysis.

For the northern fish, distance off bottom was calculated as bottom depth minus tag depth where bottom depth was estimated in two stages. First, daily bottom depth was chosen as the maximum tag depth during each 24-h period, on the assumption that northern rock sole contact the bottom at least once a day. Second, bottom depths for each 0.5-h or 1-h recording were estimated by linearly interpolating between the times of daily maxima (proc Expand; SAS, vers. 8.02, SAS Inst., Inc., Cary, NC). Times of vertical excursions were identified as those when the off-bottom distance exceeded 2 m. Discrete excursions away from the bottom were defined as groups of successive off-bottom time recordings.

For the southern fish, which resided in steeper, more rugged terrain, distance off bottom was calculated similarly by using 6-h rather than 24-h time windows. In addition, during times when horizontal movements appeared to be occurring in steep terrain, off-bottom distance was calculated by using estimates of bottom depth for still more frequent intervals, assuming that bottom depth was identical to tag depth during each tag recording if tidal fluctuations were obvious in the original tag depth data (i.e., not corrected for tide). The assumption is that the fish was on bottom when tidal fluctuations were recognized. The southern fish was considered off bottom when off-bottom distances exceeded 3 m. Following the criteria used for the northern fish, each 0.5-h or 1-h depth value was designated as either on or off bottom, and discrete excursions were identified. Analyses of excursions for the southern fish were limited to summary statistics because of the difficulty in accurately identifying off-bottom periods (see *Discussion* section).

Diel and tidal influence on vertical excursions

To determine whether the likelihood of excursions differed between day and night, each 0.5-h or 1-h record collected by a tag was first designated as daytime or nighttime based on the predicted times of sunrise and sunset at the midpoint location between fish release and recovery. Daily sunrise and sunset times were calculated by using an algorithm obtained from the U.S. Naval Observatory, Astronomical Applications Department (Washington, DC). The percentage of off-bottom time recordings occurring during the day and night were then calculated for each fish, and the timing and duration of excursions were plotted with respect to day and night.

To determine if vertical excursions of the northern fish were selectively made with respect to tidal current direction, patterns in tidal current direction were examined using compass plots (function Compass (x,y); Matlab, vers. 7.5.0.342, The MathWorks, Inc., Natick, MA); plots of current direction during hours when the fish was off bottom were compared with plots of all

the available current directions. In addition, the significance of current speed and direction in determining whether the northern fish was off bottom was tested using Generalized Additive Modeling (GAM; Venables and Ripley, 1994). This was done by modeling off-bottom status (coded 0 for on bottom and 1 for off bottom) as a binomial response to a smooth function of current speed and direction, with significance based on analysis of deviance. The test was conducted independently for each month that the fish was at liberty, excluding daytime hours when fish remained on the bottom (see *Results* section).

Selective tidal transport model

To determine if the selective use of tidal currents by northern rock sole was an important component of their seasonal horizontal migrations, we developed a selective tidal stream transport model similar in its basic design to that discussed in Arnold and Holford (1995). Assuming that all horizontal movement occurred during off-bottom periods, we constructed a migration path as follows. Starting from the release location, the fish was assumed to drift at the current speed predicted for each off-bottom time and in the mean current direction during each vertical excursion. In addition, the fish was allowed to swim at a specified speed, also in the mean current direction during each vertical excursion. The specified fish swimming speed was held constant over the entire path, but because the true swimming speed was unknown, this speed was iteratively varied until the distance between the final path location and the actual capture location was minimized. Thus, for each 0.5-h or 1-h recording time starting with the release location, latitude and longitude positions were advanced by using the combined drift and swimming speed and mean current direction for each excursion. Tag locations along the selective tidal stream transport path were converted to latitude and longitude positions using great circle formulae.

To verify the accuracy of the predicted migration path, the predicted depth at each location along the path was plotted against the bottom depth (maximum 24-h depth) measured by the tag. Path depths were predicted with inverse distance-weighted surface interpolation (ArcMap 9.2 with Spatial Analyst Extension, ESRI, Redlands, CA) using National Imagery and Mapping Agency (NIMA) depth sounding data for the eastern Bering Sea continental shelf.

Results

Depth data and vertical excursions

The archival tag depth data contained relatively high frequency variation from three sources. First, vertical excursions away from the bottom were identifiable by sharp decreases in tag depth (Fig. 2). Second, tidal height fluctuations were evident in the tag depth record (Fig. 2A inset), an indication that fish were settled on the bottom. Third, rapid changes in depth resulted from horizontal movements along steep bottom gradients.

The identification of vertical excursions was clearer for the northern fish than for the southern fish. The northern fish inhabited areas of relatively flat bottom where estimated tag bottom depths ranged from 48 to 74 m; therefore rapid depth changes clearly reflected vertical excursions away from the bottom. The southern fish, by comparison, inhabited an area of complex bathymetric contours where bottom depths collected from tags ranged from 9 to 161 m. Movements along a steep bottom gradient were evident for the southern fish, particularly during April 2004 when fish depth increased and decreased more than 100 m within a 24-h period (Fig. 2B). Because of this complexity, there were occasions when it was unclear whether changes in tag depth resulted from a vertical excursion or a quick movement along a bottom gradient. For this reason, not all vertical excursions were identifiable for this fish. More gradual movements across bottom gradients were observed for both fish, and most often coincided with periods of vertical excursions, indicating that the excursions were related to the horizontal movement of the fish. In a few cases with the southern fish, however, movements across bottom gradients occurred in the absence of vertical excursions (Fig. 2B inset).

The frequency, duration, and distance of vertical excursions away from the bottom were similar for the two fish. A total of 78 distinct excursions away from the bottom were identified for the northern fish during a period of 314 days, and 154 excursions were identified for the southern fish during a period of 620 days (Table 1). These excursions were relatively rare, accounting from 2.0% (southern fish) to 2.6% (northern fish) of the time at liberty. Average excursion durations were 2.6 hours (northern fish) and 2.1 hours (southern fish); average excursion extent (i.e., maximum distance off bottom) was 14 m with a maximum of 64 m (Table 1). The frequency of vertical excursions varied seasonally; most excursions occurred from winter to spring for the northern fish and during fall and spring for the southern fish. Excursions were infrequent during summer months (Fig. 2).

The timing of vertical excursions was related to both diel and tidal factors. For the northern fish, 90% of the excursions occurred at night, whereas for the southern fish, 85% occurred at night (although not all vertical excursions could be identified with certainty). Both fish underwent vertical excursions that sometimes occurred over a series of consecutive nights (Fig. 3). In addition to being limited to nighttime, vertical excursions occurred during particular stages of the tide cycle. For example, during the beginning of September 2003, the southern fish made consecutive nightly excursions, but only before the dominant low tide (Fig. 3B). Examination of tidal current directions (northern fish only), revealed the fish did not indiscriminately choose nighttime periods, but made nightly vertical excursions only when tidal currents were in certain directions. For ex-

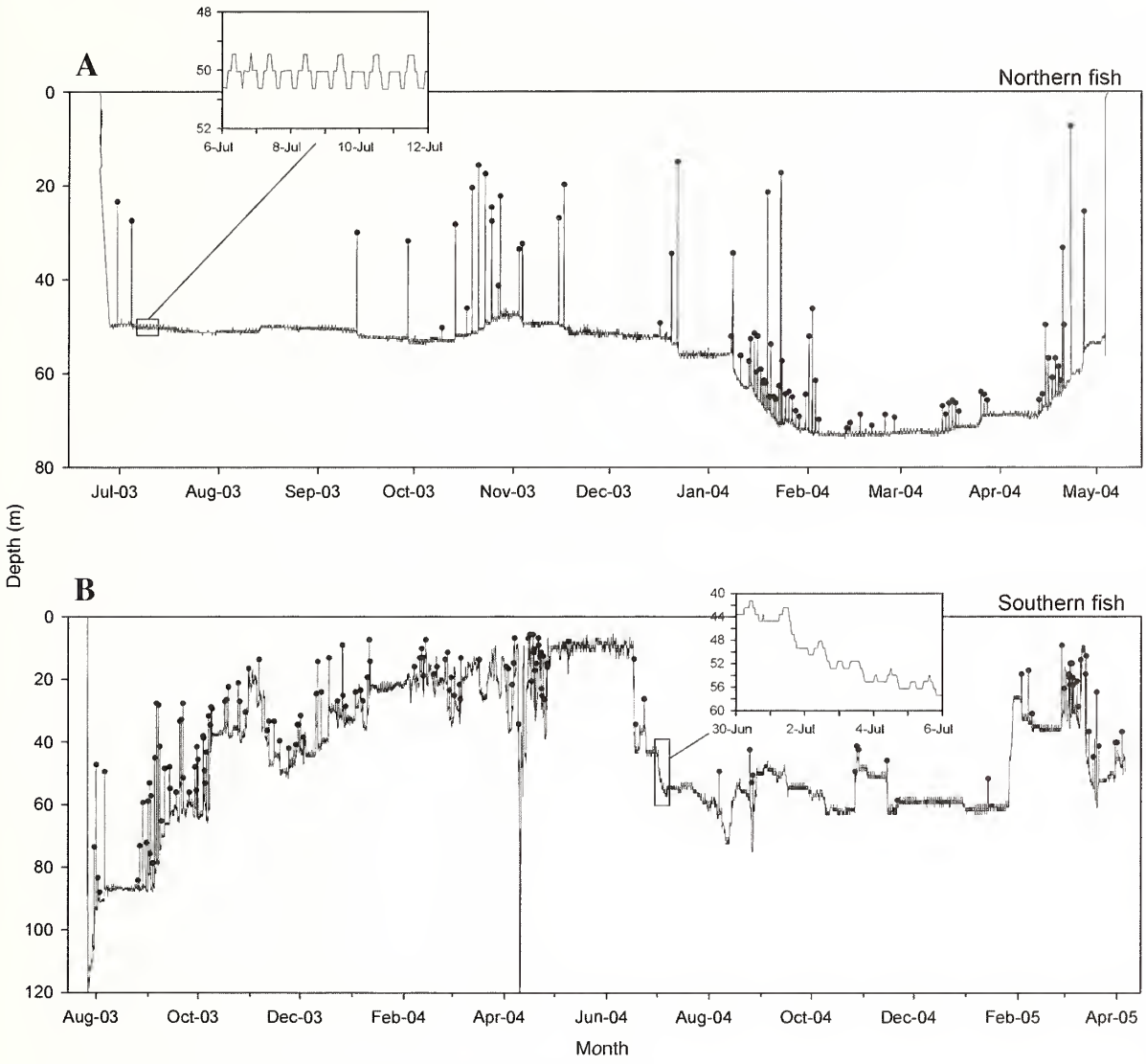

Figure 2

Depth records from two archival tags, each recovered from a female northern rock sole (*Lepidopsetta polyxystra*) at liberty in the eastern Bering Sea between 2003 and 2005. Vertical excursions are identified for the northern (**A**) and southern (**B**) fish, and dots indicate the peak of each excursion. Inset figures show tidal fluctuations in the depth data that indicated fish were on the bottom.

ample in January, when the northern fish made vertical excursions with greatest frequency, it did so when tidal currents were southerly directed, yet the prevailing nighttime tidal currents were directed toward the west and northeast (Fig. 4). During months with frequent excursions, the probability of being off-bottom was not significantly related to current speed but was highly significantly related to current direction (Table 2; GAM (generalized additive modeling) test). Considering the rotary nature of the tidal current where the northern fish resided, the timing of vertical excursion was selective, as opposed to random, with respect to tidal current direction. This selection was particularly evident during January when nighttime periods were sufficiently long to allow for two separate southerly directed currents in a single night. Coincident to these duel nightly southern currents, the fish sometimes made two separate nightly vertical excursions (Fig. 3A).

Migration path

The predicted migration path based on selective tidal stream transport for the northern fish extended for 503 km and ended 0.26 km from the reported capture

Table 1

Excursion duration and distance away from the bottom for two northern rock sole (*Lepidopsetta polyxystra*) released with archival tags and recaptured in the eastern Bering Sea between 2003 and 2005. Minimum durations were limited to the collection frequencies of the tags which were 0.5 hour and 1.0 hour, respectively, for the northern and southern fish. Mean distances were weighted by the sampling frequency for the tags. Numbers in parentheses indicate the average maximum distance off bottom among excursions. Not all excursions could be identified with certainty for the southern fish because of the variable bathymetric terrain in the area where the southern fish resided.

	Duration away from bottom (h)			Distance away from bottom (m)				
	Min.	Max.	Mean	Min.	Max.	Mean	Identified excursions	Time recordings
Northern fish	0.5	6.5	2.6	2.2	54.2	10.4 (13.8)	78	316
Southern fish	1.0	7.0	2.1	3.0	63.7	12.2 (13.4)	154	332

Table 2

Significance of tidal current direction and speed on the probability of a northern rock sole (*Lepidopsetta polyxystra*) being off the bottom. Data are from one fish tagged in the more northerly area of the eastern Bering Sea shelf. Generalized additive modeling (GAM) with a binomial error term (0=on bottom, 1=off bottom) was used to test probabilities for each month, during nighttime. n = the total number of timed tag depth recordings per month. Number in parentheses indicates the number of recordings when the fish was away from the bottom. Months of fewer than 10 nighttime off-bottom observations are excluded.

	Chi-square		*P*-value		
Month	Direction	Speed	Direction	Speed	n
Oct. 03	15.0	1.3	0.0018	0.7310	855 (28)
Nov. 03	9.2	8.6	0.0236	0.0329	969 (12)
Dec. 03	10.9	2.7	0.0106	0.4057	1079 (12)
Jan. 04	75.9	2.0	<0.0001	0.5364	1041 (126)
Feb. 04	40.7	3.4	<0.0001	0.3313	587 (36)
Mar. 04	14.5	2.8	0.0022	0.3991	373 (22)
Apr. 04	17.6	4.8	0.0005	0.1794	288 (39)

location (Fig. 5). A seasonal migration is apparent in this path. After its release in July, the fish remained in the general vicinity of the release location for about 5 months, then abruptly in January and early February 2004, it migrated south approximately 200 km (straight line) from the release location to the southern most point of the path. In March and April, the fish nearly reversed direction and migrated to the north where it was recaptured. During the migration, the fish traveled an average of 6.4 km and maximum of 17.3 km per vertical excursion. The swimming speed which minimized the distance between the final migration path position and the reported capture location was 47 cm/s or 1.4 body lengths per second (BL/s) for the 34-cm fish.

The bottom depths predicted at the locations along the migration path were very similar to the bottom depths (maximum depth within each 24-h period) measured by the archival tag (Fig. 6) and had a mean absolute difference of only 2.5 m, thus corroborating the predicted migration path. The maximum depth during this migration occurred at the beginning of March when the fish abruptly changed its migration direction from the south to the northeast.

Although a migration path for the southern fish could not be formulated, depth data from the archival tag (Fig. 2B), indicated that the fish must have remained along the Alaska Peninsula and did not migrate west toward the continental slope, or into the central Bering Sea shelf. Because predicted bottom depths gradually decreased from 90 m to 10 m over the first 10 months at liberty, the fish could not have migrated toward the slope. In addition, abrupt changes in bottom depth such as the 10-m to 40-m increase from 16 through 17 June 2004 (Fig. 2B), indicated that the fish remained in an area of relatively steep bathymetry—an area that does not exist on the central shelf.

Accuracy of tidal current prediction

Overall, current direction was more accurately predicted at the northern mooring site, where direction errors were less than 40 degrees during periods of the

most frequently observed current speeds (10–40 cm/s; Fig. 7A). By comparison, errors of over 40 degrees were common at the southern mooring site, particularly when current speeds were less than 20 cm/s (Fig. 7B). Model prediction of current direction improved with increasing observed current speed at both northern and southern mooring sites (Fig. 7). Model estimates of current speed at the northern mooring displayed progressive underestimation of the observed speed with increasing speed (Fig. 8A). When the observed current speeds were 33 cm/s, for example, the model underestimated these speeds by an average of 10 cm/s. At the southern mooring, observed speeds were underestimated at slow speeds and overestimated at faster speeds (Fig. 8B).

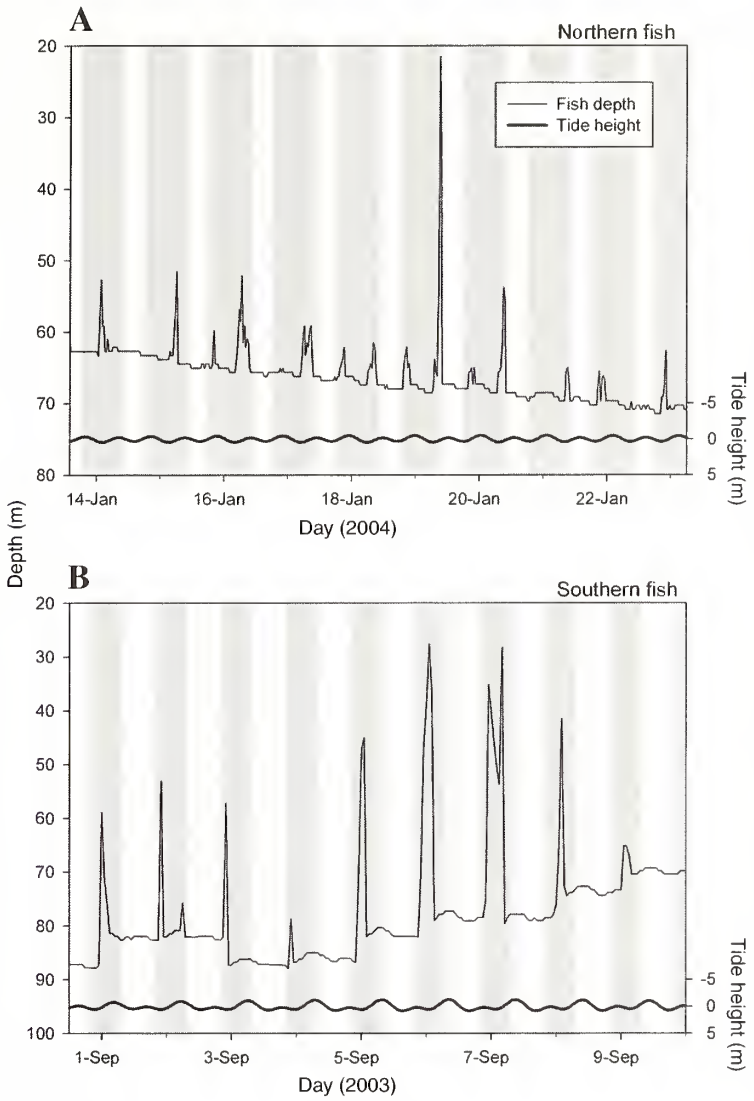

Figure 3

Consecutive nightly vertical excursions (shown as peaks) recorded for two female northern rock sole (*Lepidopsetta polyxystra*) tagged with archival tags in the eastern Bering Sea. Examples for both northern (**A**) southern fish (**B**) are presented. Nighttime periods are shaded. Model estimates of tide height (heavy line) at a position midway between fish release and recovery positions are provided to highlight the tidal fluctuation recorded by the tag and show that the timing of vertical excursions is related to tidal factors in addition to diel factors.

Discussion

Archival tag data from two northern rock sole released and recaptured in the eastern Bering Sea provide evidence that selective tidal stream transport can be used to aid horizontal migration. Vertical excursions, although infrequent, were correlated to both diel and tidal factors. Not only did both fish undergo vertical excursions during mostly nighttime hours, the northern fish did so during select periods of the tidal cycle when tidal currents were moving in a particular direction. The significance of current direction as a determinate of vertical movement for the northern fish indicated that the fish did not randomly leave the bottom, but did so only when the current was moving in a specific direction. The successful application of tidal current information to predict a migration path for the northern fish validates that at least some northern rock sole use tidal currents for transport, and also may indicate that their vertical excursions are conducted primarily for the purpose of horizontal migration.

Our attempt to predict a migration path for the southern fish was unsuccessful for several reasons. First, the identification of vertical excursions was less certain because of the variable bathymetric contours in the area. Second, model estimates of current direction were considerably less accurate when compared to the measured current direction at the location of the southern fish than for the location of the northern fish. Finally, the assumption for the model was that all horizontal movements occurred only during periods when the fish left the bottom; however, for the southern fish there was evidence of additional horizontal movement. Gradual decreases in fish depth sometimes occurred during periods in which tidal fluctuations could be recognized in the depth record, indicating that the fish migrated to some extent while it remained on or close to the seafloor. With no way to account for these movements in the model, we were unable to accurately calculate the projection of the path.

The estimated average swim speed of 1.4 BL/s (47 cm/s) that minimized the distance between the final

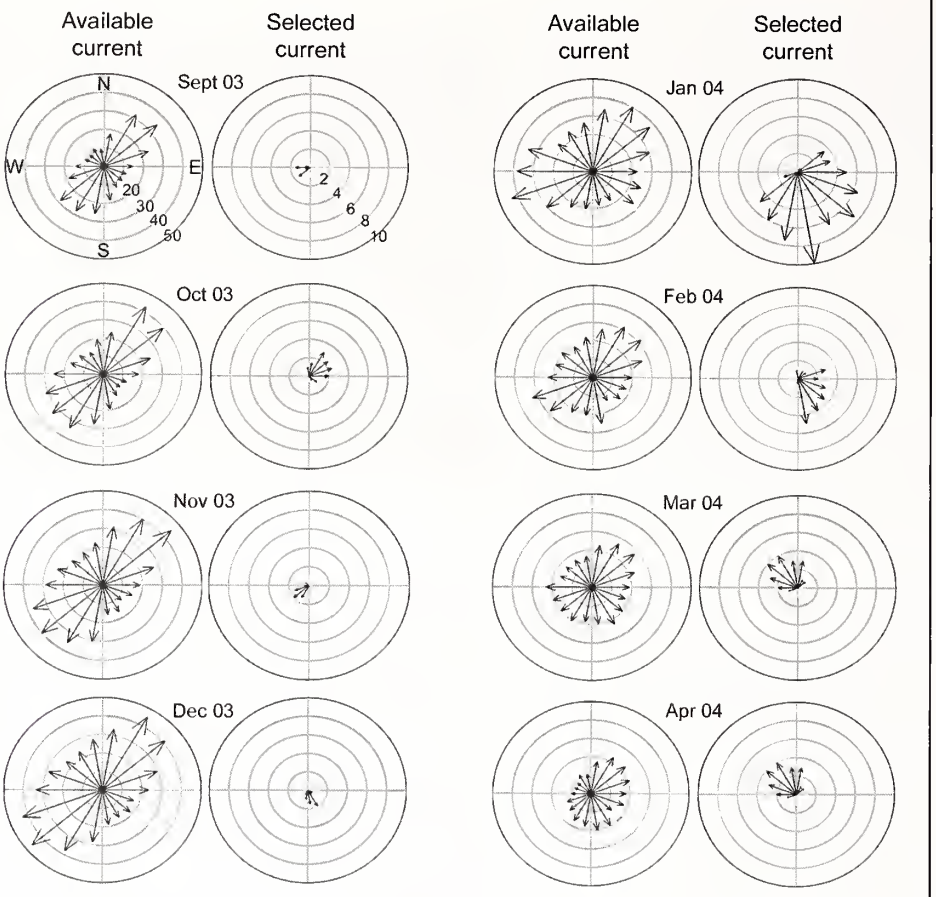

Figure 4

Monthly plots from September 2003 through April 2004 of predicted near-bottom tidal current directions for periods when a female northern rock sole (*Lepidopsetta polyxystra*) (the northern fish) underwent nightly vertical excursions (selected current), compared to all the available nightly near-bottom tidal current directions (available current). Arrow directions indicate the direction of the current and arrow lengths indicate the total number of hours spent in each direction. The available current is scaled from 0 to 50 hours (see upper leftmost diagram) and the selected current is scaled from 0 to 10 hours

migration path position and the recovery position is considerably higher than values of 0.6 BL/s reported for European plaice and Japanese flounder (*Paralichthys olivaceus*) during tidally assisted migration (Kawabe et al., 2004; Metcalfe et al., 1990). We offer several explanations. First, estimates of current speed in the model were lower than actual current speeds, a bias that would inflate our estimated swimming speed. Second, the northern fish may have been capable of maintaining a more consistent direction; that is, more aligned to the destination of the migration than the current directions. We assumed the fish traveled in the average direction of the current during each excursion event. However, if the fish had a predetermined destination and the ability to navigate, it may have actively deviated slightly from the average current direction. More efficient overall swimming directions would have reduced the overall distance traveled, and again would have resulted in lower swimming speeds necessary to complete the migration path. Finally, some vertical excursions may not have been identified because of the frequency of collection of archival tag data (0.5 hour or 1 hour), or the fish may have migrated toward its destination without undergoing vertical excursions (e.g., it swam while near the bottom). Evidence of this type of movement was clear for the southern fish, which appeared to use tidal currents, but its horizontal migration was not limited to periods of vertical excursions. The northern fish may also have migrated without undergoing vertical excursions, but because the bathymetric terrain was fairly flat on the central eastern Bering Sea shelf, such movements could not be detected.

Although we demonstrate the preference for nighttime vertical activity for only two adult northern rock

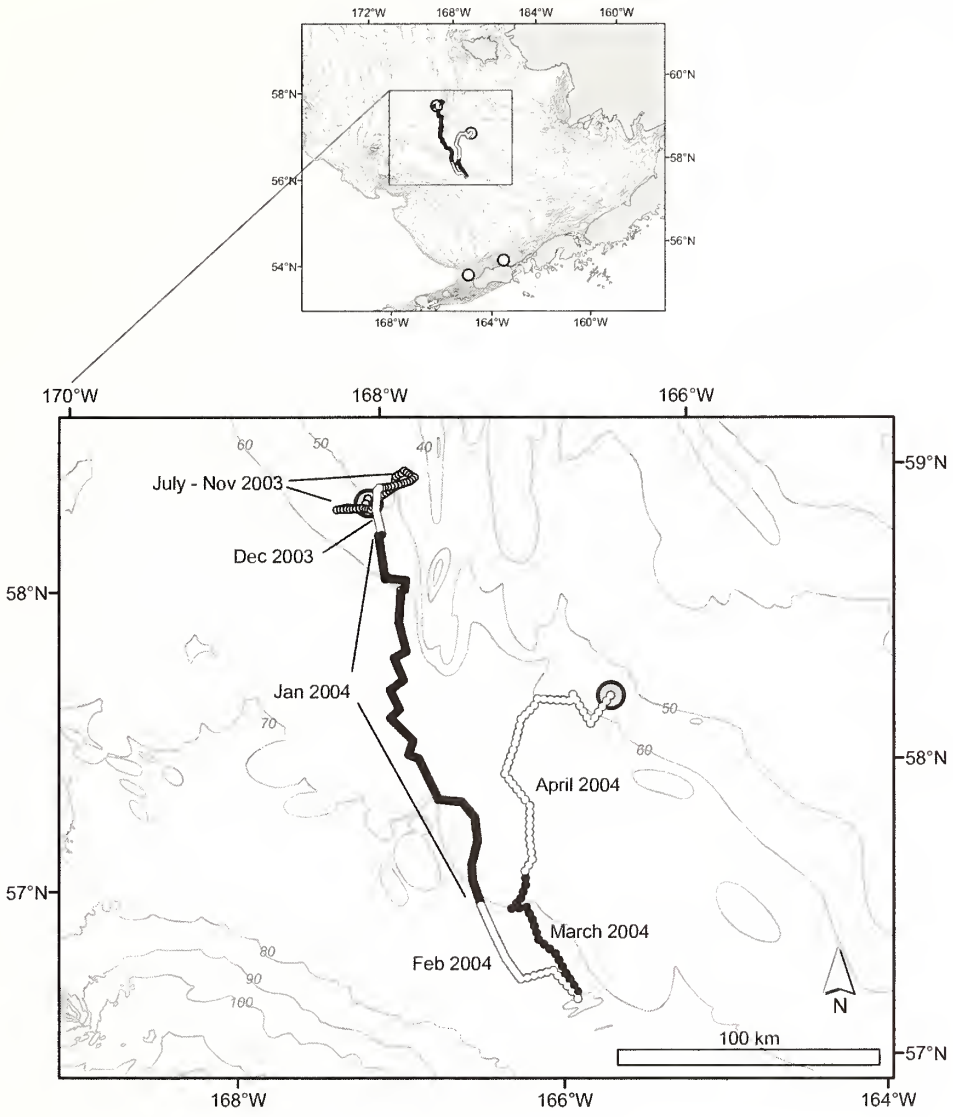

Figure 5

Migration path of one female northern rock sole (*Lepidopsetta polyxystra*), tagged and recaptured in the eastern Bering Sea, released in 2003 and captured in 2004. The migration path is based on current velocity vectors predicted during periods when the northern fish underwent excursions away from the bottom. Circles identify the release and recovery positions. Gray lines with numbers indicate the bathymetric contours (m). Months are indicated by the alternating black and white paths.

sole, this behavior is common among various flatfish species and juvenile northern rock sole. Nighttime vertical excursions have been reported for a variety of flatfishes from postlarval through adult stages (e.g., De Veen, 1967; Weinstein et al., 1980; Cadrin and Westwood, 2004; Hunter et al., 2004). Nighttime periods are thought to offer flatfishes a reduced risk of predation by visual predators (Burrows, 1994). In laboratory experiments, the swimming activity of juvenile northern rock sole (20–40 mm TL) away from the bottom occurred most often during nighttime (Hurst and Duffy, 2005). This activity involved vertical excursions to the surface, followed by horizontal swimming and gliding. It follows that, like adult northern rock sole, juveniles undergo vertical excursions away from the seafloor for the purpose of horizontal migration. Considering northern rock sole juveniles inhabit areas with tidal influence, it follows that they also use tidal currents for transport. Although it is unlikely that small juveniles migrate extensive distances, as some adults do, juveniles may use tidal current for short-term migrations as a mechanism to locate better feeding grounds within nursery areas (Hurst and Duffy, 2005). We believe that at least some adult northern rock sole employ this

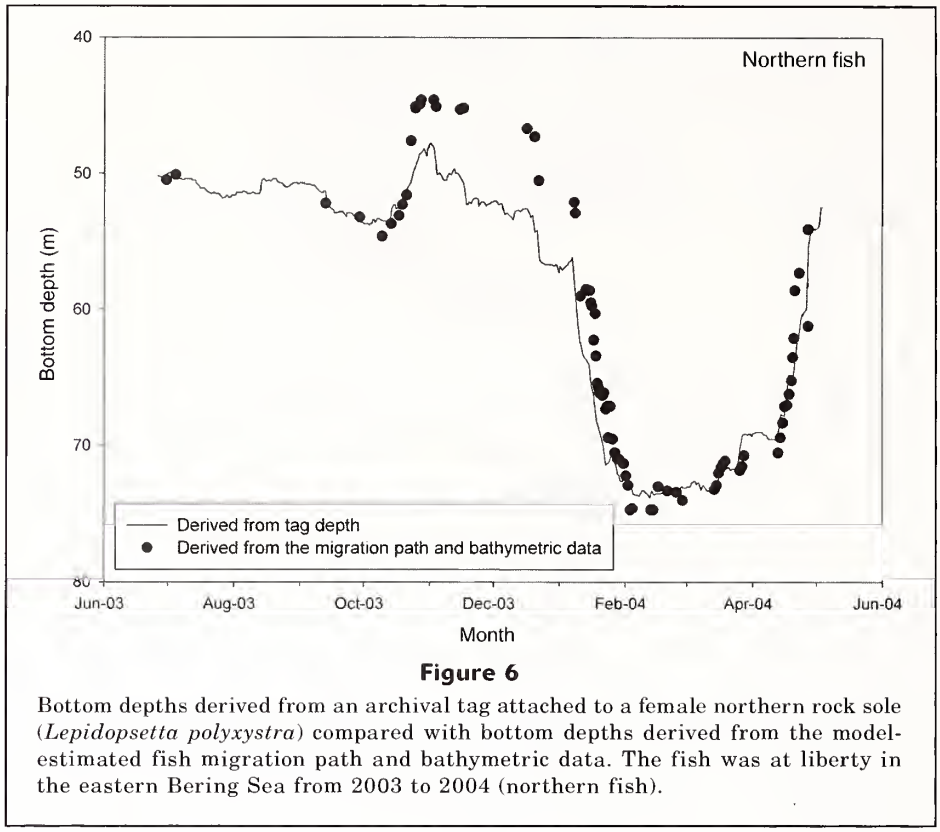

Figure 6

Bottom depths derived from an archival tag attached to a female northern rock sole (*Lepidopsetta polyxystra*) compared with bottom depths derived from the model-estimated fish migration path and bathymetric data. The fish was at liberty in the eastern Bering Sea from 2003 to 2004 (northern fish).

feeding strategy, albeit on a larger spatial scale. The so called "feeding months" for northern rock sole in the eastern Bering Sea reportedly occur during summer when they disperse across the shelf after aggregating for spawning during winter and spring (Fadeev, 1965; Shubnikov and Lisovenko, 1964). This feeding period may well be represented by the first five months that the northern fish was at liberty (July–November), during which migration was less frequent and not in a consistent direction.

As suggested by the migration path presented here, at least some adult northern rock sole undergo vertical excursions for the purpose of tidally assisted horizontal migration, as opposed to vertical movements into the water column for feeding or spawning. Both juvenile and adult northern rock sole feed during daylight hours, but rarely during the night (Corcobado Oñate, 1991; Hurst et al., 2007) when off-bottom swimming occurs. Unlike other eastern Bering Sea flatfish species such as arrowtooth flounder (*Atheresthes stomias*), which feed high in the water column (Yang, 1995), northern rock sole feed close to the bottom. Northern rock sole feed almost exclusively on benthic invertebrates, such as polychaete worms and other marine worms (Corcobado Oñate, 1991; Lang et al., 1995; McConnaughey and Smith, 2000). In addition, northern rock sole likely do not leave the bottom to spawn because, along with their congener, southern rock sole (*L. bilineata*), they are the only northeast Pacific flatfishes to spawn demersal adhesive eggs (Matarese et al. 1989; Stark and Somerton, 2002).

If most northern rock sole prefer to undergo vertical excursions during the night, winter offers greater opportunity to travel in a preferred direction because of the increased hours of darkness. For the northern fish, vertical excursions were most frequent during January, when it travelled in a southerly direction. Southerly directed tidal currents were sometimes available at two different periods within a single night because of the semidiurnal nature of the tides (e.g., a full clockwise rotation of tidal currents every 12 hours). Hunter et al. (2004b) noted similar nocturnal behavior for European plaice in the North Sea during winter when two "transporting tides" sometimes occurred within a night because of the longer periods of darkness lasting up to 15 hours.

The northern rock sole vertical movements examined here appear shorter in both duration and extent (Table 1) in comparison with other flatfish for which vertical behavior has been studied, with the exception of yellowtail flounder (*Limanda ferruginea*) whose excursions average 1.5 hours and 6 m off bottom (Cadrin and Moser, 2006). Some European plaice (*P. platessa*) in the North Sea reportedly spend from 6 hours to 12 hours a night swimming in midwater during winter months (Hunter et al., 2004b). Common sole (*Solea solea*) in the North Sea are thought to use the upper half of the water column for selective tidal stream transport during which

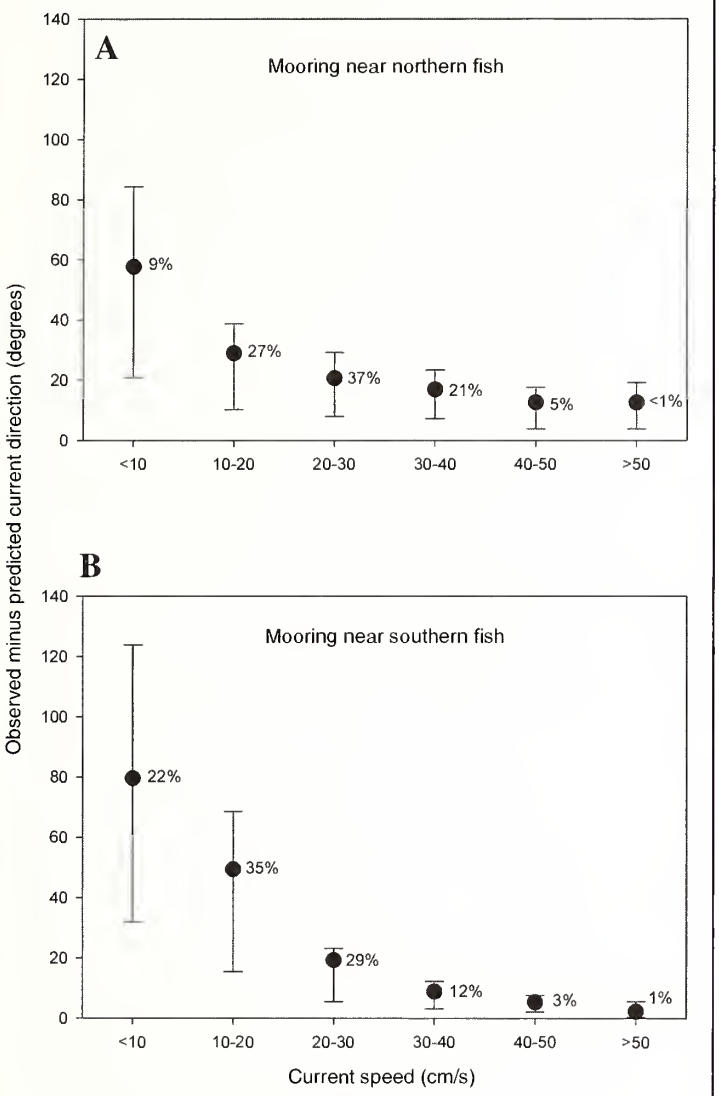

Figure 7

Angle difference between observed and predicted (model) near-bottom tidal current directions at the mooring site near the northern fish (**A**) and at the mooring site near the southern fish (**B**) in the eastern Bering Sea, plotted at different observed current speeds. The *y*-axis is expressed as the mean absolute value of the angle difference between observed and predicted current directions (in degrees). Error bars indicate 25th and 75th percentiles. Percentages next to the means (circles) indicate the percentage of time that each grouping of observed current speed represented during the 193 days of collection.

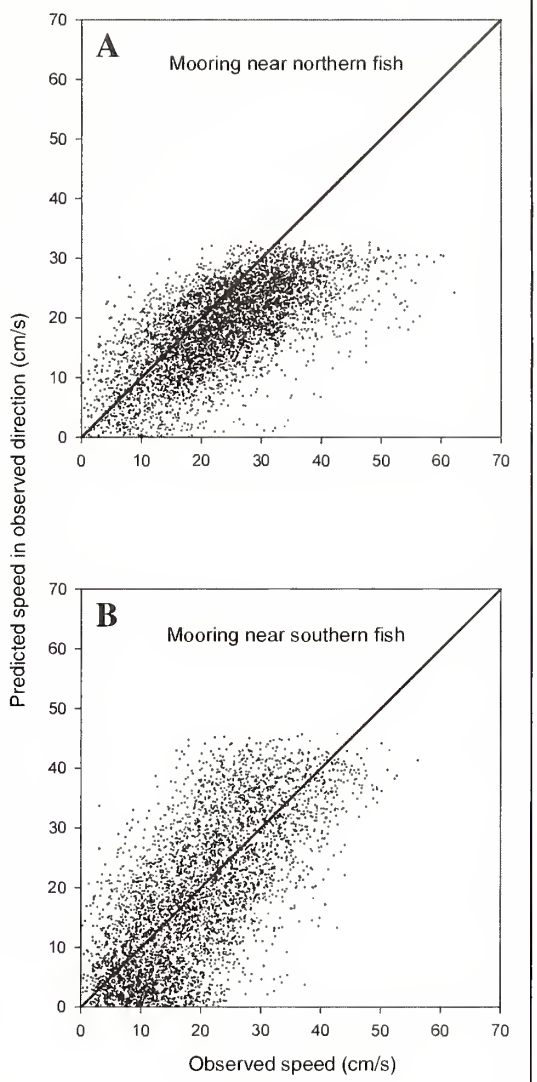

Figure 8

Comparison of observed and predicted (model) near-bottom tidal current speeds at the northern (**A**) and southern (**B**) mooring sites in the eastern Bering Sea. Predicted speed is presented as the component of the model speed projected in the observed direction, $MS_0\cos(\theta)$, where MS_0 = the model-predicted speed in the observed direction, and θ = the angle difference between observed and predicted current directions. The line indicates a 1:1 ratio. Model estimates of speed do not include residual (e.g., baroclinic) effects that may have been present in observed current speeds.

they frequently approach the surface (De Veen, 1967; Greer Walker et al., 1980). By comparison, the northern rock sole examined here only occasionally approached the surface; most vertical excursions occurred in the bottom half of the water column. Even during periods of active migration (e.g., January; northern fish), vertical excursions averaged only 2.6 hours in duration and were a maximum extent of 11.6 m away from the bottom. These vertical excursions could be of interest to fishery managers if they affect fish availability to bottom trawl surveys (Hunter et al., 2004b). However, the northern rock sole excursions were particularly infrequent during summer daylight hours when the bottom trawl surveys of the eastern Bering Sea are

conducted (Acuna and Lauth, 2008). From the data on the two fish examined here, northern rock sole remain on the bottom 99.8% of the time during summer (June and July) daylight hours.

Although we could not predict a migration path for the southern fish, it was apparent that the migration pattern differed between the two fish. The northern fish clearly used tidal currents to facilitate a southern migration to deeper water during winter and a migration back north during spring. These movements are consistent with the seasonal spawning and post-spawning migrations suggested by Fadeev (1965) and Shubnikov and Lisovenko (1964). As with some European plaice, which migrate south to warmer waters for spawning (Hunter et al., 2004a), northern rock sole that reside on the northern part of the eastern Bering Sea shelf during summer (i.e., the northern fish) may require a migration to more southern or deeper waters to reach temperatures suitable for spawning. Adult rock sole (likely *L. polyxystra*) from the western Bering Sea also undergo a migration to deeper water in winter, and do so presumably to avoid temperatures below 0°C (Shvetsov, 1979). Temperatures experienced by both fish decreased during winter months but stabilized to about 2°C in February and March. Had the northern fish stayed in the vicinity of its release, it would have experienced bottom temperatures below 0°C in February, as recorded by instruments at the northern oceanographic mooring site. The southern fish also underwent nighttime vertical excursions that were tidal in nature, but unlike the northern fish, there was no indication of a spawning migration; excursion frequency did not increase before the known spawning season (winter–spring), and depth records indicated no repeatable pattern from one winter (2004) to the next (2005). It is logical to assume that the extent of migrations is dependent on the proximity of feeding and spawning locations. Thus, the northern fish may require a directed seasonal migration to reach a viable spawning location, whereas the southern fish can remain resident if suitable feeding and spawning locations are within close proximity.

If the northern fish migrated south for the purpose of spawning, the southern extent of the migration route may have been a spawning location. We can infer from the spatial distribution of the fishery for roe of northern rock sole—a fishery that operates in the eastern Bering Sea during February and March just before the spawning season (Stark and Somerton, 2002; Wilderbuer and Nichol, 2007)—that spawning aggregations occur over a wide area of the central and outer continental shelf extending from Unimak Island to west of the Pribilof Islands. This distribution overlaps with the southern point of the migration path.

The eastern Bering Sea shelf offers a multitude of possibilities for tidally assisted transport, and the distribution range that individuals seasonally inhabit may partly depend on the nature of the tidal currents. Based on tidal current ellipses for the M_2 tidal constituent in the eastern Bering Sea, tidal currents are rotary in nature over the majority the shelf area south of latitude 60°N but become more bidirectional (i.e., 60- and 240-degrees) close to the Alaska Peninsula and into Bristol Bay (Pearson et al., 1981; Kowalik, 1999). Because the northern fish inhabited the central part of the eastern Bering Sea continental shelf, opportunities for selective tidal stream transport were available in all directions, thus enabling a round-trip migration. By comparison, the southern fish resided along the Alaska Peninsula; therefore opportunities for selective tidal stream transport were limited to northeasterly and southwesterly directions. Fish that undergo migrations in northeasterly and southwesterly directions could use selective tidal stream transport over much of the eastern Bering Sea shelf. Adult yellowfin sole (*Limanda aspera*), for example, are known to migrate annually in a northeasterly direction more than 500 km from winter grounds west and southeast of the Pribilof Islands to nearshore summer spawning grounds in Kuskokwim and Bristol bays (Wakabayashi, 1989). Given the extent of this migration and the availability of tidal currents, it is reasonable to assume that yellowfin sole also use selective tidal stream transport.

Results presented here provide the first known evidence of selective tidal stream transport among aquatic animals in the eastern Bering Sea. Among larval flatfish in the eastern Bering Sea, including northern rock sole, passive forms of transport involving wind-driven surface currents and geostrophic flow have been shown to contribute to their horizontal distribution and likelihood of survival (Wilderbuer et al., 2002; Lanksbury et al., 2007). The contribution of more active forms of transport such as selective tidal stream transport may become evident as more is learned about the vertical migration behavior of larvae. Evidence that larval northern rock sole as small as 8 mm can regulate their depth in the water column (Lanksbury et al., 2007) indicates that selective tidal stream transport is a possibility. As we learn about how adult, juvenile, and larval fishes use tidal currents for migration, the need becomes evident for more accurate tide-prediction models that can be used for modeling fish migration. Such models should become available in the near future with the completion of a baroclinic tide model of the eastern Bering Sea.

Acknowledgments

We thank D. Kachel and P. Stabeno for providing tidal information at Pacific Marine Environmental Laboratory (PMEL) mooring sites, and for providing insight concerning tides in the eastern Bering Sea. A. Greig, S. Kotwicki, and J. Benson provided technical support on use of ArcView and circular trigonometry. T. Wilderbuer and J. Gauvin provided productive discussion concerning flatfish spawning and migration. Finally, K. Baily, T. Hurst, T. Wilderbuer, J. Lee, S. Cadrin, and three anonymous reviewers improved the manuscript with insightful suggestions.

Literature cited

Acuna, E., and R. R. Lauth.
2008. Results of the 2007 eastern Bering Sea continental shelf bottom trawl survey of groundfish and invertebrate resources. NOAA Tech Memo. NMFS-AFSC-181, 195 p.

Arnold, G. P., and B. H. Holford.
1995. A computer simulation model for predicting rates and scales of movement of demersal fish on the European continental shelf. ICES J. Mar. Sci. 52:981–990.

Burrows, M. T.
1994. Foraging time strategy of small juvenile plaice: a laboratory study of diel and tidal behavior patterns with *Artemia* prey and shrimp predators. Mar. Ecol. Prog. Ser. 115:31–39.

Cadrin, S. X., and J. Moser.
2006. Partitioning on-bottom and off-bottom behavior: a case study with yellowtail flounder off New England. ICES CM 2006/Q:14.

Cadrin, S. X., and A. Westwood.
2004. The use of electronic tags to study fish movement: a case study with yellowtail flounder off New England. ICES CM 2004/K:81.

Champalbert, G., C. Macquart-Moulin, G. Patriti, and L. Le Direach-Boursier.
1992. Light control of vertical movements of larvae and juvenile sole (*Solea solea* L.). Mar. Behav. Physiol. 19:263–283.

Corcobado Oñate, E.
1991. Food and daily ration of the rock sole *Lepidopsetta bilineata* (Pleuronectidae) in the eastern Bering Sea. Mar. Biol. 108:185–191.

De Veen, J. F.
1967. On the phenomenon of Soles (*Solea solea* L.) swimming at the surface. J. Cons. Cons. Int. Explor. Mer 31:207–236.

Egbert, G. D., A. F. Bennett, and M. G. G. Foreman.
1994. TOPEX/Poseidon tides estimated using a global inverse model. J. Geophys. Res. 99:24,821–24,852.

Egbert, G. D., and S. Y. Erofeeva.
2002. Efficient inverse modeling of barotropic ocean tides. J. Atmos. Ocean. Tech. 19:183–204.

Fadeev, N. S.
1965. Comparative outline of the biology of flatfishes in the southeastern part of the Bering Sea and condition of their resources. Translated by Isr. Prog. Sci. Trans., 1968. *In* Soviet fisheries investigations in the northeast Pacific, part 4 (P. A. Moiseev, ed.), p. 112–129. [Available from U.S. Dep. Commer., Natl. Tech. Inf. Serv., Springfield, VA, as TT 67-51206.]

Forward, R. B., and R. A. Tankersley.
2001. Selective tidal-stream transport of marine animals. Oceanogr. Mar. Biol. Annu. Rev. 39:305–353.

Fox, C. J., P. McCloghrie, E. F. Young, and D. M. Nash.
2006. The importance of individual behavior for successful settlement of juvenile plaice (*Pleuronectes platessa* L.): a modeling and field study in the eastern Irish Sea. Fish. Oceanogr. 15:301–313.

Gibson, R. N.
2003. Go with the flow: tidal migration in marine animals. Hydrobiologia 503:153–161.

Greer Walker, M., J. D. Riley, and L. Emerson.
1980. On the movement of sole (*Solea solea*) and dogfish (*Scyliorhinus canicula*) tracked off the east Anglian coast. Neth. J. Sea Res. 14:66–77.

Harden Jones, F. R., G. P. Arnold, M. Greer Walker, and P. Scholes.
1979. Selective tidal stream transport and migration of plaice (*Pleuronectes platessa* L.) in the southern North Sea. J. Cons. CIEM 38:331–337.

Hunter, E., J. D. Metcalfe, G. P. Arnold, and J. D. Reynolds.
2004a. Impacts of migratory behavior on population structure in North Sea plaice. J. Aquat. Ecol. 73:377–385.

Hunter, E., J. D. Metcalfe, C. M. O'Brien, G. P. Arnold, and J. D. Reynolds.
2004b. Vertical activity patterns of free-swimming adult plaice in the southern North Sea. Mar. Ecol. Prog. Ser. 279:261–273.

Hurst, T. P., and T. A. Duffy.
2005. Activity patterns in northern rock sole are mediated by temperature and feeding history. J. Exp. Mar. Biol. 325:201–213.

Hurst, T. P., C. H. Ryer, J. M. Ramsey, and S. A. Haines.
2007. Divergent foraging strategies of three co-occurring north Pacific flatfishes. Mar. Biol. 151:1087–1098.

Kawabe, R., Y. Naito, K. Sato, K. Miyashita, and N. Yamashita.
2004. Direct measurement of swimming speed, tailbeat, and body angle of Japanese flounder (*Paralichthys olivaceus*). ICES J. Mar. Sci. 61:1080–1087.

Kowalik, Z.
1999. Bering Sea tides. *In* Dynamics of the Bering Sea (T. R. Loughlin and K. Ohtani, eds.), p. 93–127. Univ. Alaska Sea Grant Press., AK-SG-99-03, Fairbanks, AK.

Kuipers, B.
1973. On the tidal migration of young plaice (*Pleuronectes platessa*) in the Wadden Sea. Neth. J. Sea Res. 6:376–388.

Lang, G. M., P. A. Livingston, and B. S. Miller.
1995. Food habits of three congeneric flatfishes: Yellowfin sole (*Pleuronectes asper*), rock sole (*P. bilineatus*), and Alaska plaice (*P. quadrituberculatus*) in the eastern Bering Sea. *In* Proceedings of the international symposium on North Pacific flatfish, p. 225–245. Univ. Alaska Sea Grant Press, Fairbanks, AK.

Lanksbury, J. A., J. T. Duffy-Anderson, K. L. Mier, M. S. Busby, and P. J. Stabeno.
2007. Distribution and transport patterns of northern rock sole, *Lepidopsetta polyxystra*, larvae in the southeastern Bering Sea. Prog. Oceanogr. 72:39–62.

Matarese, A. C., A. W. Kendall, D. M. Blood, and B. M. Vinter.
1989. Laboratory guide to the early life history stages of northeast Pacific fishes. NOAA Tech. Rep. NMFS 80, 652 p.

McConnaughey, R. A., and K. R. Smith.
2000. Associations between flatfish abundance and surficial sediments in the eastern Bering Sea. Can. J. Fish. Aquat. Sci. 57:2410–2419.

Metcalfe, J. D., G. P. Arnold, and P. W. Webb.
1990. The energetics of selective tidal stream transport: an analysis for plaice tracked in the southern North Sea. J. Mar. Biol. Assoc., U.K. 70:149–162.

Metcalfe, J. D., E. Hunter, and A. A. Buckley.
2006. The migratory behavior of North Sea plaice: Currents, clocks and clues. Mar. Freshw. Behav. Physiol. 39:25–36.

Pearson, C. A., H. O. Mofjeld, and R. B. Tripp.
1981. Tides of the eastern Bering Sea shelf. *In* The eastern Bering Sea shelf: oceanography and resources

(D. W. Hood, and J. A. Calder, eds.), vol. 1, p. 111–130. Office of Marine Pollution Assessment, NOAA, Univ. Washington Press, Seattle, WA.

Rijnsdorp, A. D., and M. van Stralen.
1985. Selective tidal transport of North Sea plaice larvae *Pleuronectes platessa* in coastal nursery areas. Trans. Am. Fish. Soc. 114:461–470.

Shubnikov, D. A., and L. A. Lisovenko.
1964. Data on the biology of rock sole of the southeastern Bering Sea. Translated by Isr. Prog. Sci. Trans., 1968. *In* Soviet fisheries investigations in the northeast Pacific, part 2 (P. A. Moiseev, ed.), p. 220–226. [Available from U.S. Dep. Commer., Natl. Tech. Inf. Serv., Springfield, VA, as TT 67-51204.]

Shvetsov, F. G.
1979. Distribution and migrations of the rock sole, *Lepidopsetta bilineata bilineata*, in the region of the Okhotsk Sea coast of Paramushir and Shumshu Islands. J. Icthyol./Vopr. Ikhtiol. 18:56–62.

Stark, J. W., and D. A. Somerton.
2002. Maturation, spawning and growth of rock soles off Kodiak in the Gulf of Alaska. J. Fish. Biol. 61:417–431.

Venables W. N., and B. D. Ripley.
1994. Modern applied statistics with S-plus. Springer, New York, 462 p.

Wakabayashi, K.
1989. Studies on the fishery biology of yellowfin sole in the eastern Bering Sea. [In Jpn., Engl. summ.] Bull. Far Seas Fish. Res. Lab. 26:21–152.

Walsh, S. J., and M. J. Morgan.
2004. Observations of natural behavior of yellowtail flounder derived from data storage tags. ICES J. Mar. Sci. 61:1151–1156.

Weinstein, M. P., S. L. Weiss, R. G. Hodson, and L. R. Gerry.
1980. Retention of three taxa of postlarval fishes in an intensively flushed tidal estuary, Cape Fear River, North Carolina. Fish. Bull. 78:419–435.

Wilderbuer, T. K., A. B. Hollowed, W. J. Ingraham Jr., P. D. Spencer, M. E. Conners, N. A. Bond, and G. E. Walters.
2002. Flatfish recruitment response to decadal climatic variability and ocean conditions in the eastern Bering Sea. Prog. Oceangr. 55:235–247.

Wilderbuer, T. K., and D. G. Nichol.
2007. Northern rock sole. *In* Stock assessment and fishery evaluation report for the groundfish resources of the Bering Sea/Aleutian Islands region, chapter 7, p. 627–686. [Available from North Pacific Fishery Management Council, 605 West 4th Ave, Suite 306, Anchorage, AK 99501.]

Yang, M.
1995. Food habits and diet overlap of arrowtooth flounder (*Atheresthes stomias*) and Pacific halibut (*Hippoglossus stenolepis*) in the Gulf of Alaska. *In* Proceedings of the international flatfish symposium; October 1994, Anchorage, Alaska, p. 205–223.

Abstract—Horseshoe crabs (*Limulus polyphemus)* are valued by many stakeholders, including the commercial fishing industry, biomedical companies, and environmental interest groups. We designed a study to test the accuracy of the conversion factors that were used by NOAA Fisheries and state agencies to estimate horseshoe crab landings before mandatory reporting that began in 1998. Our results indicate that the NOAA Fisheries conversion factor consistently overestimates the weight of male horseshoe crabs, particularly those from New England populations. Because of the inaccuracy of this and other conversion factors, states are now mandated to report the number (not biomass) and sex of landed horseshoe crabs. However, accurate estimates of biomass are still necessary for use in prediction models that are being developed to better manage the horseshoe crab fishery. We recommend that managers use the conversion factors presented in this study to convert current landing data from numbers to biomass of harvested horseshoe crabs for future assessments.

Prosomal-width-to-weight relationships in American horseshoe crabs (*Limulus polyphemus*): examining conversion factors used to estimate landings

Larissa J. Graham (contact author)[1]

Mark L. Botton[2]

David Hata[1]

Robert E. Loveland[3]

Brian R. Murphy[1]

Email address for contact author: Ljg85@cornell.edu

[1] Department of Fisheries and Wildlife Sciences
Virginia Polytechnic Institute and State University
100 Cheatham Hall
Blacksburg, Virginia 24061
Present address for contact author: New York Sea Grant
Stony Brook University
146 Suffolk Hall
Stony Brook, New York 11794-5002

[2] Department of Natural Sciences
Fordham University, College at Lincoln Center
113 West 60th Street
New York, New York 10023

[3] Department of Ecology, Evolution, and Natural Resources
Cook College, Rutgers University
New Brunswick, New Jersey 08901

Manuscript submitted 11 June 2008.
Manuscript accepted 14 January 2009.
Fish. Bull. 107:235–243 (2009).

Horseshoe crabs (*Limulus polyphemus*) are considered a multiple-use resource. They are valued by many stakeholders, including the commercial fishing industry, biomedical companies, and environmental interest groups (Berkson and Shuster, 1999). Horseshoe crabs are commercially harvested and sold as bait for whelk (*Busycon* spp. and *Busycotypus* spp.) and American eel (*Anguilla rostrata*) fisheries. This species is also gathered for biomedical companies because its copper-containing blood is used to create a pharmaceutical product, *Limulus* amoebocyte lysate (LAL) that is used to detect pathogenic endotoxins on medical devices and in injectable drugs (Novitsky, 1984; Mikkelsen, 1988; Levin et al., 2003). The mortality associated with the handling and bleeding of horseshoe crabs is minimized (i.e., 8–20% [Rudloe, 1983; Kurz and James-Pirri, 2002; Walls and Berkson, 2003; Hurton and Berkson, 2004]) because the animals are required to be returned to the water within 72 hours. Horseshoe crabs are ecologically important because their eggs serve as a food source for migrating shorebirds most notably in Delaware Bay (Tsipoura and Burger, 1999; Botton et al., 2003; Karpanty et al., 2006; Haramis et al., 2007).

In 1998, a fishery management plan was developed for the horseshoe crab. However, before this plan, most states did not require the mandatory reporting of harvested horseshoe crabs. NOAA Fisheries collected commercial landing data by state, year, and gear type, but these data were incomplete and disjunct. To estimate reference period (or a basis for reductions in landing data), the Horseshoe Crab Technical Committee asked state agencies to provide their best estimate of the number of horseshoe crabs harvested before 1998. These numbers were converted to pounds using various conversion factors. The number of horseshoe

crabs harvested in Delaware and Virginia waters were converted to biomass using conversion factors derived from fishery-independent and fishery-dependent data (i.e., Delaware: 1.05 kg/male, 2.32 kg/female, 1.69 kg/combined catch; Virginia: 1.8 kg/horseshoe crab or 2.27 kg/horseshoe crab depending on the composition of the catch). The landing data from all other states were converted to pounds using a NOAA Fisheries conversion factor (i.e., 1.21 kg/horseshoe crab). These data have since been used to generate estimates of total landings, to set state-by-state quotas, and to manage the stock (Fig. 1).

Once the horseshoe crab fishery management plan was initiated, all landings were required to be reported by sex, harvest method, and the number and pounds of harvested horseshoe crabs. However, many fishermen reported their catch in numbers of harvested horseshoe crabs, and state agencies used conversion factors to convert harvests from numbers to pounds. Because of the uncertainty in these conversion factors and resulting biomass estimates, state agencies are no longer required to report the pounds of horseshoe crabs landed. The Atlantic States Marine Fisheries Commission (ASMFC) and state agencies now assess and manage stocks using only the number of horseshoe crabs (not pounds) harvested.

ASMFC currently uses trend analysis to manage horseshoe crab populations, but numerous prediction models are being developed for future, more accurate management. For some of these models, landing data are required to be reported in pounds, not numbers. Because all state landings are currently reported by numbers of landed horseshoe crabs, conversion factors need to be derived to estimate pounds of landed horseshoe crabs. The availability of accurate conversion factors will serve as a factor in choosing an appropriate model to better manage horseshoe crab populations.

The objective of our study was to derive prosomal-width-to-weight equations to calculate alternative sex-specific conversion factors based on the average width of horseshoe crabs from each state. We also tested the NOAA Fisheries conversion factor by comparing the observed total biomass of horseshoe crabs to the total biomass that was estimated with the conversion factor.

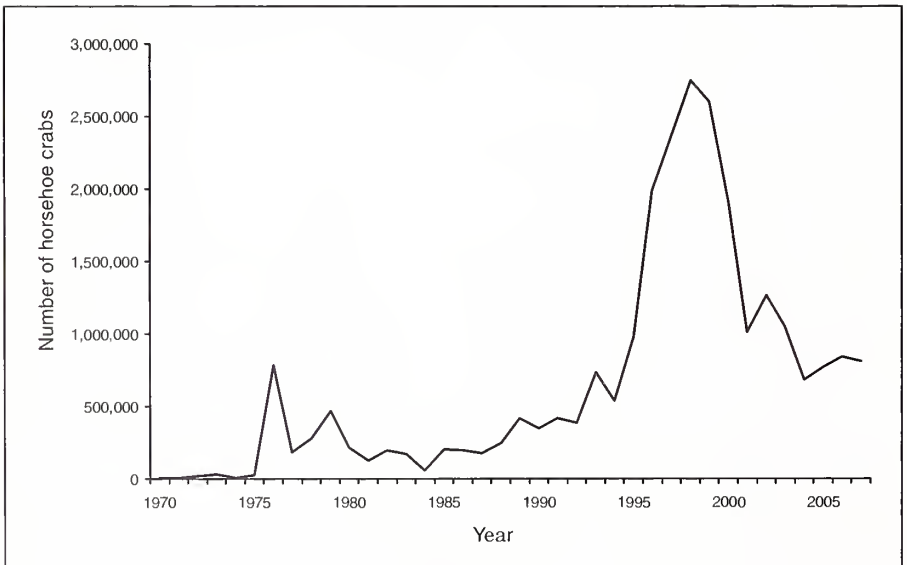

Figure 1

Commercial horseshoe crab (*Limulus polyphemus*) landings between 1970 and 2007. Landings before 1998 were reported in pounds of horseshoe crabs and were converted to numbers of horseshoe crabs using various conversion factors.

Materials and methods

Data collection

Data were collected during three spawning surveys in the Mid-Atlantic (i.e., Delaware Bay, NJ, sampled in 1997 and 2000 [n=379]; Raritan Bay, NJ, sampled in 1988 [n=297]) and southern New England (i.e., Great Bay, NH, sampled in 1988 [n=131]) and from the Delaware commercial fishery (i.e., Delaware Bay, DE, sampled in 1999, 2003, and 2004 [n=348]) (Fig. 2). The sex, prosomal width (PW; to the nearest 1 mm), and weight (to the nearest 10 g) were recorded from a sample of individuals that were collected from the vicinity of each breeding beach. During spawning surveys, animals were collected as either mated pairs (a male coupled to a female) or as unpaired (or satellite males) because previous studies (Botton and Loveland, 1989) have shown that there is no significant size difference between unattached males within a population. The majority of the samples collected from the commercial fishery were harvested by hand during spawning events. All samples were mature individuals because only mature horseshoe crabs visit beaches during spawning events.

Measurements also were recorded for horseshoe crabs in coastal waters (i.e., within 12 nautical miles from shore) between New York and Virginia (Fig. 2). In September, October, and November of 2005 and 2006, 743 individuals were collected and measured during the Horseshoe Crab Research Center (HCRC) trawl survey (for methods see Hata and Berkson, 2004). In June of 2006, an additional 182 horseshoe crabs were sampled aboard a commercial trawl vessel harvesting crabs for a biomedical company off the coast of Ocean City, Maryland. Trawling gear, specifically a flounder net, was used to collect all horseshoe

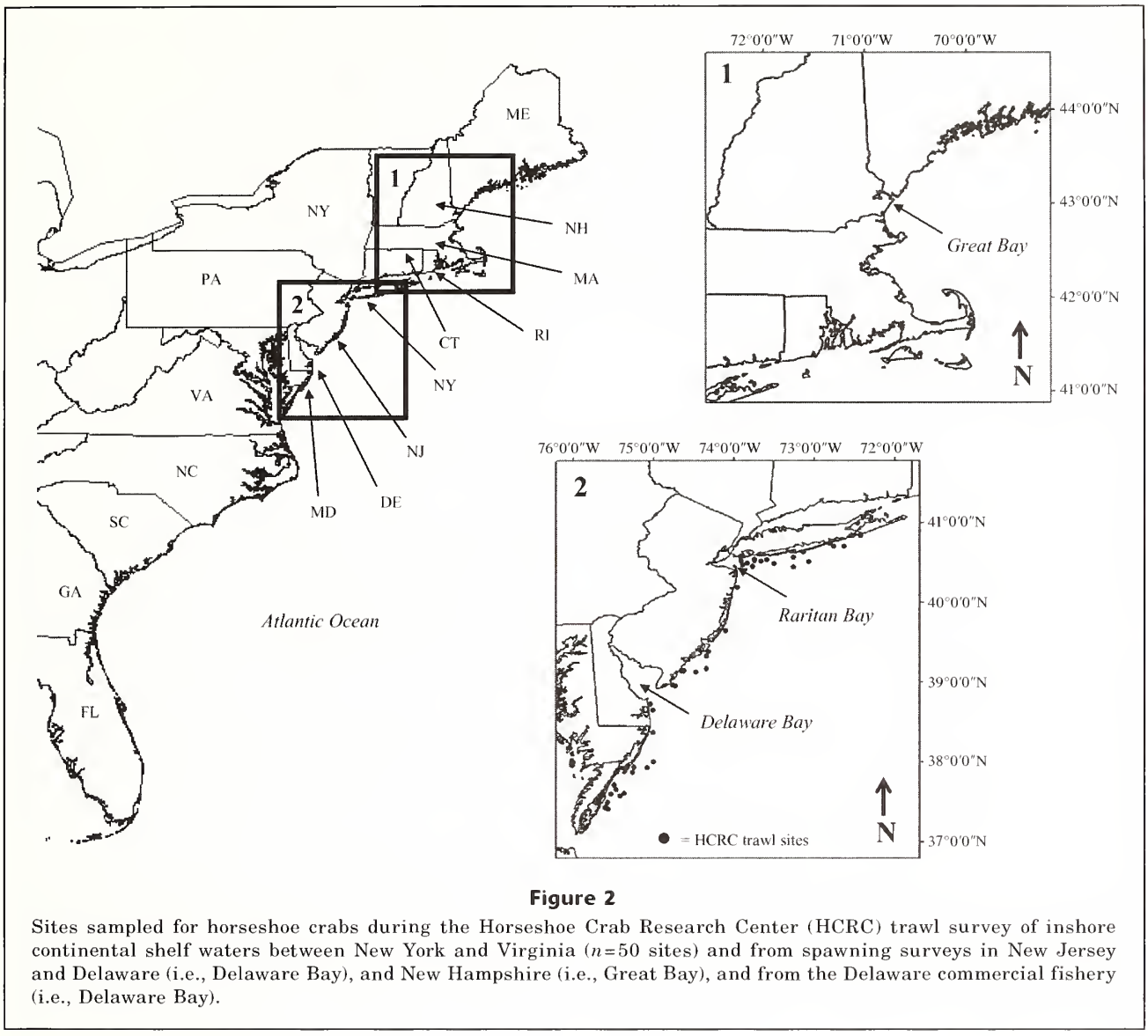

Figure 2

Sites sampled for horseshoe crabs during the Horseshoe Crab Research Center (HCRC) trawl survey of inshore continental shelf waters between New York and Virginia (n=50 sites) and from spawning surveys in New Jersey and Delaware (i.e., Delaware Bay), and New Hampshire (i.e., Great Bay), and from the Delaware commercial fishery (i.e., Delaware Bay).

crabs. The ground gear on the flounder net was modified with a Texas sweep, which has a chain line instead of a footrope, to effectively sample horseshoe crabs (Hata and Berkson, 2003; Hata and Berkson, 2004). We recorded prosomal width (to the nearest 1 mm), weight (to the nearest 10 g), sex, and maturity stage for all or a subsample of horseshoe crabs at each site. Maturity stage was classified into two groups: immature and mature. Male horseshoe crabs without modified pedipalps (claspers) were considered immature and those with modified pedipalps were considered mature (Hata and Berkson, 2004). Females with mating scars (i.e., indentations and abrasions on the dorsal surface of the opisthosoma resulting from the attached male) were categorized as mature. Maturity stage in newly molted females is not morphologically distinct, therefore some individuals had to be probed with an awl for evidence of eggs and determine the stage of maturity (Leschen et al., 2006). Females with eggs were categorized as mature (Hata and Berkson, 2004).

Prosomal-width-to-weight relationship

We log-transformed the PW and weight measurements collected during the HCRC trawl survey and used a general linear model (PROC GLM, SAS, vers. 9.1, SAS Inst., Inc., Cary, NC) to test for significant differences in the PW, weight, and PW–weight relationship between sexes and maturity stages. The P-value of each family of comparisons was adjusted using a Bonferroni correction to protect the experimental-wise error rate.

We combined all data (i.e., three spawning surveys, Delaware commercial fishery, HCRC trawl survey) to develop PW–weight regression equations for each group (i.e., mature males, mature females, immature males,

and immature females) of horseshoe crabs using the form

$$\log_e(Wt) = \log_e(PW) \cdot a + \log_e(b), \quad (1)$$

where Wt = weight of a horseshoe crab (kg);
PW = prosomal width (mm);
a = slope; and
b = y-intercept (PROC REG, SAS).

We could not develop equations for each group of horseshoe crabs by state because of the small sample size collected from some states.

Testing current and developing alternative conversion factors

The predictive accuracy of the NOAA Fisheries conversion factor was tested using data collected from four data sets: the three spawning surveys and the Delaware commercial fishery. We calculated total biomass for each sample using the NOAA Fisheries conversion factor and then compared it to the total observed biomass for each sample.

We used various data sets (i.e., three spawning surveys, the Delaware commercial fishery, the HCRC trawl survey, unpublished data) and previously published studies to generate the average PW and weight for male and female horseshoe crabs from each state (Table 1). For some states, the average weight of horseshoe crabs was not available, and therefore we used the PW–weight equations that were derived from this study to estimate the average weight of horseshoe crabs based on an average measured prosomal width. For states where average weight data were available, we compared the observed weight to the estimated weight (i.e., using PW–weight equation) to determine the accuracy of the PW–weight equations.

Results

Prosomal-width-to-weight relationship

The average weight differs between male and female horseshoe crabs. Mature female horseshoe crabs were significantly larger (i.e., prosomal width; df=1, 346; F=1488.03; P<0.0001) and heavier (df=1, 346; F=2245.72; P<0.0001) than mature male horseshoe crabs. The weight of horseshoe crabs was significantly different among sex and maturity stages (df=7, 924; F=6.86; P=0.0090; Table 2). Significant differences did not occur in the PW–weight relationship of mature male and mature female horseshoe crabs (df=3, 577; F=2.19; P=0.1396; Table 2); however, when comparing only horseshoe crabs of overlapping size ranges (PW=181–292 mm; weight=0.88–3.14 kg), the PW–weight relationship of mature female horseshoe crabs was significantly different than that of mature males (df=3, 626; F=8.21; P=0.0043).

Separate PW–weight equations were developed for all females, mature females, immature females, all males, mature males, and immature males (Table 3). The derived PW–weight equations were used to estimate an average weight of horseshoe crabs from each state based on the observed prosomal width (Table 1). However, we used only the PW–weight equation derived for mature horseshoe crabs (i.e., one for mature males and one for mature females) to estimate weight because the PW–weight relationship was significantly different between sexes of mature horseshoe crabs, and the commercial fishery is directed only at mature horseshoe crabs. The estimated average weight of both male and female horseshoe crabs with the derived PW–weight equations was relatively accurate compared to the observed average weight for each state (Table 1).

Testing current and developing alternative conversion factors

The conversion factor used by NOAA Fisheries (i.e., 1.21 kg/horseshoe crab) consistently overestimated the total weight of horseshoe crabs collected during spawning surveys and from the Delaware commercial fishery (Table 4). For female horseshoe crabs from Mid-Atlantic populations (i.e., Delaware Bay and Raritan Bay), this conversion factor provided a relatively close estimate of total weight. However, when estimating the total weight of male horseshoe crabs, the NOAA Fisheries conversion factor overestimated total weight. The weight of horseshoe crabs from the New England population (i.e., Great Bay) was overestimated to the greatest degree, by more than 70% for both males and females.

The average weight of a horseshoe crab also varies by location. Horseshoe crabs between Rhode Island and South Carolina are larger and heavier than horseshoe crabs from Maine, New Hampshire, Massachusetts, and Florida; and the conversion factors that have been used by most states reflect the differences in size and weight among states (Table 1). For those states where a single conversion factor has been used in the past to estimate the weight for both male and female horseshoe crabs (i.e., Maine, Rhode Island, Virginia, North Carolina, South Carolina, and Florida), the weight of at least one sex, in most cases the weight of female horseshoe crabs (Table 4) has been predicted inaccurately. Most states in the Mid-Atlantic have derived two conversion factors (i.e., one for each sex) that are relatively close to the average weight of mature horseshoe crabs collected within that area (Table 1).

Discussion

Female horseshoe crabs are much larger than male horseshoe crabs; therefore separate conversion factors should be used for each sex. Our results indicate that horseshoe crabs exhibit considerable sexual size dimorphism with mature female horseshoe crabs being significantly larger and heavier than males. Males in any

Table 1

Sample size, mean, and range of the prosomal width (PW) and weight (Wt) of mature horseshoe crabs (*Limulus polyphemus*) sampled along the Atlantic coast of the United States. Samples were collected during the Horseshoe Crab Research Center trawl survey, from the commercial fishery, or during spawning surveys, unless otherwise noted. The conversion factors (CF) that were previously used by each state to convert landing data are also listed (an asterisk indicates areas where the NOAA Fisheries conversion factor is used). The weight of each sample was also estimated (Est. Wt) using the PW-weight equations derived in this study.

State (specific location)	*n* (PW)	*n* (Wt)	Mean PW in mm (range)	Previously used CF (kg)	Mean Wt in kg (range)	Est. Wt (kg)
Males						
Maine (Medomak River)[1]	17	—	158 (139–182)	1.21*	—	0.47
Maine (Damariscotta River)[1]	14	—	144 (129–163)	1.21*	—	0.35
Maine (Casco Bay)[1]	4	—	140 (129–146)	1.21*	—	0.33
New Hampshire (Great Bay)	199	199	127 (108–159)	0.25	0.23 (0.14–0.44)	0.24
New Hampshire (Great Bay)[1]	11	—	136 (121–152)	0.25	—	0.30
Massachusetts (Plum Island Sound)[1]	552	—	118 (97–140)	—	—	0.20
Massachusetts (Barnstable Harbor)[1]	32	—	166 (123–212)	—	—	0.54
Massachusetts (Monomoy National Wildlife Refuge, Cape Cod)[2]	909	—	188 (135–287)	—	—	0.78
Massachusetts (Pleasant Bay)[1]	288	—	168 (137–222)	—	—	0.56
Massachusetts (Pleasant Bay, Cape Cod)[2]	1775	—	179 (120–235)	—	—	0.67
Massachusetts (Nauset Estuary, Cape Cod)[2]	433	—	175 (134–249)	—	—	0.63
Massachusetts (Cape Cod Bay, Cape Cod)[2]	2942	—	174 (119–250)	—	—	0.62
Rhode Island (Narragansett Bay)[1]	54	—	186 (159–224)	1.87	—	0.76
Connecticut (Milford, New Haven and Norwalk)[3]	1760	72	195 (100–300)	—	1.06 (0.6–1.9)	0.87
New York (Inshore continental shelf)	121	121	205 (174–231)	—	0.95 (0.38–1.40)	1.01
New Jersey (Delaware Bay)	211	211	207 (160–254)	1.05	1.12 (0.51–2.04)	1.04
New Jersey (Raritan Bay)	195	195	202 (167–243)	1.05	0.99 (0.51–1.73)	0.97
New Jersey (Raritan Bay)[1]	102	—	186 (159–224)	1.05	—	0.76
New Jersey (Inshore continental shelf)	58	58	210 (177–244)	1.05	1.08 (0.62–1.76)	1.08
Delaware (Delaware Bay)[4]	87	87	207 (175–245)	1.05	1.03 (0.61–1.53)	1.04
Delaware (Inshore continental shelf)	25	25	205 (176–225)	1.05	0.92 (0.56–1.22)	1.01
Maryland (Chesapeake Bay)[1]	142	—	179 (142–229)	0.96	—	0.67
Maryland (Inshore continental shelf)	57	57	217 (184–239)	0.96	1.14 (0.68–1.88)	1.20
Virginia (Inshore continental shelf)	58	58	207 (172–292)	0.91	1.01 (0.62–3.14)	1.04
Mid-Atlantic (New York to Virginia; Inshore continental shelf)	319	319	209 (172–292)	1.21*	1.02 (0.88–3.94)	1.07
North Carolina (Beaufort Inlet)[1]	13	—	232 (218–251)	1.36	—	1.46
South Carolina (St. Helena Sound)[1]	1	—	240	2.49	—	1.61
Florida (Bald Point and Ochlockonee)[1]	24	—	174 (154–201)	0.45	—	0.62
Florida (Sarasota Bay)[1]	122	—	141 (121–176)	0.45	—	0.33

continued

Table 1 (continued)

State (specific location)	*n* (PW)	*n* (Wt)	Mean PW in mm (range)	Previously used CF (kg)	Mean Wt in kg (range)	Est. Wt (kg)
Females						
Maine (Medomak River)[1]	15	—	201 (180–219)	1.21*	—	1.23
Maine (Damariscotta River)[1]	11	—	180 (161–202)	1.21*	—	0.92
Maine (Casco Bay)[1]	5	—	191 (172–208)	1.21*	—	1.07
New Hampshire (Great Bay)	12	12	154 (140–178)	0.80	0.61 (0.33–0.88)	0.61
New Hampshire (Great Bay)[1]	20	—	179 (154–209)	0.80	—	0.90
Massachusetts (Plum Island Sound)[1]	538	—	155 (126–199)	—	—	0.62
Massachusetts (Barnstable Harbor)[1]	13	—	214 (175–238)	—	—	1.45
Massachusetts (Monomoy National Wildlife Refuge, Cape Cod)[2]	477	—	242 (186–304)	—	—	2.01
Massachusetts (Pleasant Bay)[1]	115	—	220 (186–272)	—	—	1.56
Massachusetts (Pleasant Bay, Cape Cod)[2]	298	—	229 (170–295)	—	—	1.73
Massachusetts (Nauset Estuary, Cape Cod)[2]	256	—	234 (185–292)	—	—	1.83
Massachusetts (Cape Cod Bay, Cape Cod)[2]	759	—	227 (161–285)	—	—	1.69
Rhode Island (Narragansett Bay)[1]	288	—	240 (201–300)	1.87	—	1.96
Connecticut (Milford, New Haven and Norwalk)[3]	1145	71	249 (150–370)	—	2.56 (1.6–3.9)	2.16
New York (Inshore continental shelf)	136	136	262 (219–321)	—	2.53 (1.40–3.94)	2.47
New Jersey (Delaware Bay)	168	168	264 (220–314)	2.32	2.66 (1.02–4.25)	2.53
New Jersey (Raritan Bay)	102	102	254 (207–311)	2.32	2.27 (1.39–3.83)	2.28
New Jersey (Raritan Bay)[1]	56	—	291 (243–351)	2.32	—	3.27
New Jersey (Inshore continental shelf)	41	41	269 (220–304)	2.32	2.66 (1.56–3.84)	2.65
Delaware (Delaware Bay)[4]	261	261	267 (225–325)	2.32	2.42 (1.48–4.40)	2.60
Delaware (Inshore continental shelf)	3	3	251 (225–272)	2.32	2.23 (1.50–2.64)	2.21
Maryland (Chesapeake Bay)[1]	62	—	291 (243–351)	2.25	—	3.27
Maryland (Inshore continental shelf)	30	30	270 (218–320)	2.25	2.73 (1.46–3.90)	2.68
Virginia (Inshore continental shelf)	40	40	260 (181–306)	0.91	2.35 (0.88–3.82)	2.42
Mid-Atlantic (New York to Virginia; Inshore continental shelf)	259	259	264 (181–321)	1.21*	2.55 (0.38–3.14)	2.53
North Carolina (Beaufort Inlet)[1]	4	—	329 (321–340)	1.36	—	4.52
South Carolina (St. Helena Sound)[1]	3	—	325 (308–335)	2.49	—	4.38
Florida (Bald Point and Ochlockonee)[1]	17	—	231 (208–272)	0.45	—	1.77

[1] Shuster (1979).
[2] James-Pirri et al. (2005).
[3] J. Mattei and M. Beekey. Unpubl. data. 2006. Sacred Heart University, 5151 Park Ave., Fairfield, CT 06825.
[4] S. Michels. Unpubl. data. 1999, 2003, 2004. Delaware Fish and Wildlife, P.O. Box 330, Little Creek, DE 19961.

Table 2

General linear model *F*-values and *P*-values for horseshoe crabs (*Limulus polyphemus*) that were collected during the Horseshoe Crab Research Center trawl survey which sampled inshore continental shelf waters between New York and Virginia. Values are listed for all horseshoe crabs combined, immature and mature females, immature and mature males, mature females and males, and immature females and males. The prosomal-width(PW)-to-weight relationship was analyzed for various combinations of sex and maturity stage (*Mat*). Significant interactions, after Bonferroni adjustment, are indicated by an asterisk.

	All data (df=7, 924; n=925)		Mature females vs. Immature females (df=3, 481;n=482)		Mature males vs. Immature males (df=3, 442; n=443)		Immature females vs. Immature males (df=3, 346; n=347)		Mature females vs. Mature males (df=3, 577; n=578)	
Variable	*F*	*P*	*F*	*P*	*F*	*P*	*F*	*P*	*F*	*P*
PW	3770.45	<0.0001*	2490.51	< 0.0001*	1456.77	<0.0001*	2849.41	<0.0001*	2056.93	<0.0001*
Sex	0.00	0.9866	—	—	—	—	6.17	0.0135*	3.46	0.0635
Mat	0.20	0.6582	1.46	0.2271	5.61	0.0183	—	—	—	—
PW×*Sex*	1.16	0.2815	—	—	—	—	6.76	0.0097*	2.19	0.1396
PW×*Mat*	1.59	0.2075	0.98	0.3234	5.51	0.0194	—	—	—	—
Sex×*Mat*	6.86	0.0090*	—	—	—	—	—	—	—	—
PW×*Sex*×*Mat*	6.18	0.0131	—	—	—	—	—	—	—	—

Table 3

The number of individuals sampled (n), coefficient values (a, b), standard errors for coefficients (SE[a], SE[b]), and correlation coefficient (r^2) of the relationship between prosomal width and weight for horseshoe crabs (*Limulus polyphemus*), $\log_e(Wt)=\log_e(PW\times a)+\log_e(b)$. Samples were collected during the Horseshoe Crab Research Center trawl survey (i.e., inshore continental shelf waters between New York and Virginia), spawning surveys (i.e., New Jersey, Delaware, New Hampshire), and the commercial fishery (i.e., Delaware). All regressions are significant.

	n	a	b	SE(a)	SE(b)	r^2
Female (all)	1025	2.98	–15.71	0.02	0.10	0.96
Females (mature)	802	2.65	–13.85	0.04	0.21	0.86
Females (immature)	223	2.85	–15.10	0.05	0.23	0.95
Males (all)	1055	2.89	–15.39	0.02	0.12	0.94
Males (mature)	931	2.97	–15.80	0.02	0.13	0.94
Males (immature)	124	2.58	–13.81	0.10	0.50	0.85

population average about 80% of the prosomal width of the females (Shuster, 1979) and mature females are significantly heavier than mature males because of their larger size and added weight associated with numerous eggs within their prosomas (Leschen et al., 2006). Therefore, it is inappropriate to use the same conversion factor for both sexes.

Conversion factors should also vary by state, to take into account the larger size and greater weight of horseshoe crabs in Mid-Atlantic states. Horseshoe crabs from the middle Atlantic region are significantly larger than animals from Cape Cod Bay to Maine and those from the Gulf of Mexico (Shuster, 1979). Morphometrics (Shuster, 1979; Riska, 1981), survey data on the distribution of horseshoe crabs along the continental shelf (Botton and Ropes, 1987), and population genetic studies (King et al., 2005) strongly indicate that there are geographically distinct breeding populations throughout the range. Some intermingling of populations occurs along the middle Atlantic coast, especially from New Jersey to Virginia (Swan, 2005), where much of the trawl-based fishery has been located. Because of this geographic variation, it is inappropriate to use the same conversion factor for horseshoe crabs from all states.

The conversion factor that was used by NOAA Fisheries (i.e., 1.21 kg per horseshoe crab) to estimate reference period landing data does not accurately estimate total biomass. From our results, it seems that reference period landing data were overestimated, especially in cases where the fishery could have been male-biased. The effects of this inaccurate conversion factor could have been further magnified in areas where the average size and weight of horseshoe crabs is much smaller than that for Mid-Atlantic states, notably embayments from the northern (Cape Cod to Maine) and southern (Gulf of Mexico) parts of the distribtuion range of this

Table 4

The aggregate observed weight and estimated weight using the NOAA Fisheries conversion factor (i.e., 1.21 kg per animal) of horseshoe crabs (*Limulus polyphemus*) collected during spawning surveys. The percent that the NOAA Fisheries conversion factor overestimates weight is also listed.

Location	Sex	Aggregate observed weight (kg)	Aggregate estimated weight (kg)	Percent weight overestimated
New Jersey (Delaware Bay)	Female (n=168)	446	448	0.3
	Male (n=211)	237	563	58
	Total (n=379)	683	1011	32
New Jersey (Raritan Bay)	Female (n=102)	231	272	15
	Male (n=195)	192	521	63
	Total (n=297)	424	793	47
Delaware (Delaware Bay)[1]	Female (n=261)	631	697	9
	Male (n=87)	90	232	61
	Total (n=348)	721	929	22
New Hampshire (Great Bay)	Female (n=12)	7	31	77
	Male (n=119)	28	309	91
	Total (n=131)	35	341	90

[1] S. Michels. Unpubl. data. 1999, 2003, 2004. Delaware Fish and Wildlife, P.O. Box 330, Little Creek, DE 19961.

species. According to our analyses, a New England harvest, composed of mostly male horseshoe crabs, would be the worst-case scenario for overestimating landings data when measured in pounds.

To more accurately estimate reference period landings, biomass should be recalculated using state-specific conversion factors for each sex. However, determining the male-to-female ratios from landing data may be a challenge. Before 1998, participants in the fishery were not required to record the ratio of males to females among landed horseshoe crabs. It has been suggested that eel bait fishermen prefer to harvest females, because of a chemical attractant associated with the eggs (Ferrari and Targett, 2003). In contrast, both male and female horseshoe crabs were used, as available, for the whelk fishery. Unfortunately, no data are available on the percentage of horseshoe crabs landed as bait for eels versus whelks, from which one might be able to deduce the sex ratio in the early commercial catches.

Future estimates of the biomass of harvested horseshoe crabs should incorporate the sex and location of horseshoe crab harvests. Use of geographically-appropriate conversion factors for each sex would provide an accurate estimate of biomass despite the differing regulations among states. Some states have already derived their own sex-specific conversion factors, and most seem to provide an accurate representation of the average weight for male and female horseshoe crabs. States that have used one conversion factor to estimate the weight of both female and male horseshoe crabs (i.e., Maine, Rhode Island, Virginia, South Carolina, and Florida) either underestimate the weight of female horseshoe crabs or overestimate the weight of male horseshoe crabs. Although state agencies are no longer required to report landings in number and pounds, the conversion factors that have already been derived by state agencies may serve as a useful tool for accurately converting data to be used in prediction models. For states that have not developed accurate conversion factors, the PW–weight equations derived from this study can be used to develop conversion factors based on the average width of male and female horseshoe crabs from that area. Besides providing a more accurate estimate of biomass, use of state-specific and sex-specific conversion factors is feasible for management purposes because states are already required to report the location, sex, and number of horseshoe crabs harvested.

At present, only very limited size and weight data are available for horseshoe crabs from North Carolina through northern Florida. Our PW–weight relationships for both sexes are very robust across a wide range of sizes, but could be further improved by the inclusion of horseshoe crab populations from this part of their range.

Conclusion

It is important to provide accurate biomass estimates of harvest data for future management purposes and, therefore, accurate conversion factors should be developed. From the results of this study, it seems that the most practical approach to estimating landing data is to use state-specific conversion factors, one for females and one for males, based on the average weight of horseshoe crabs from that area. Researchers should continue

to collect data on the average PW of female and male horseshoe crabs to fine tune these conversion factors. The PW–equations derived from this study can be used to estimate weight based on an average prosomal width. In this way, the accuracy of these conversion factors could be improved, thereby providing better data for future management assessments.

Acknowledgments

We sincerely thank S. Michels, M. Beekey, and J. Mattei for generously providing unpublished data on horseshoe crab populations from Delaware and Connecticut (listed in Table 1), and B. Spear for his contributions to this manuscript. J. Brust, R. Burgess, L. DeLancey, S. Doctor, S. Gerhart, L. Gillingham, P. Himchak, A. Leschen, C. McBane, T. Moore, M. Oates, S. Olszewski, and P. Thayer provided valuable information about state conversion factors. We also thank M. Davis, M. Duncan, R. Leaf, B. Ray, and A. Villamagna for their assistance with data analyses, manuscript reviews, and discussion of research ideas.

Literature cited

Berkson, J. and C. N. Shuster.
1999. The horseshoe crab: the battle for a true multiple-use resource. Fisheries 24:6–10.

Botton, M. L., B. A. Harrington, N. Tsipoura, and D. Mizrahi.
2003. Synchronies in migration: Shorebirds, horseshoe crabs, and Delaware Bay. *In* The American horseshoe crab (C. N. Shuster Jr., R. B. Barlow, and H. J. Brockmann, eds.), p. 5–32. Harvard Press, Cambridge, MA.

Botton, M. L., and R. E. Loveland.
1989. Reproductive risk: high mortality associated with spawning by horseshoe crabs (*Limulus polyphemus*) in Delaware Bay, USA. Mar. Biol. 101:143–151.

Botton, M. L., and J. W. Ropes.
1987. Populations of horseshoe crabs, *Limulus polyphemus*, on the northwestern Atlantic continental shelf. Fish. Bull. 85:805–812.

Ferrari, K. M., and N. M. Targett.
2003. Chemical attractants in horseshoe crab, *Limulus polyphemus*, eggs: The potential for an artificial bait. J. Chem. Ecol. 29:477–496.

Haramis, G. M., W. A. Link, P. C. Osenton, D. B. Carter, R. G. Weber, N. A. Clark, M. A. Teece, and D. S. Mizrahi.
2007. Stable isotope and pen feeding trial studies confirm value of horseshoe crab eggs to spring migrant shorebirds in Delaware Bay. J. Avian Biol. 37:367–376.

Hata, D., and J. Berkson.
2003. Abundance of horseshoe crabs (*Limulus polyphemus*) in the Delaware Bay area. Fish. Bull. 101:933–938.
2004. Factors affecting horseshoe crab *Limulus polyphemus* trawl survey design. Trans. Am. Fish. Soc. 133:292–299.

Hurton, L., and J. Berkson.
2004. Potential causes of mortality for horseshoe crabs (*Limulus polyphemus*) during the biomedical bleeding process. Fish. Bull. 104:293–298.

James-Pirri, M. J., K. Tuxbury, S. Marino, and S. Koch.
2005. Spawning densities, egg densities, size structure, and movement patterns of spawning horseshoe crabs, *Limulus polyphemus,* within four coastal embayments on Cape Cod, Massachusetts. Estuaries 20:296–313.

Karpanty, S. M., J. D. Fraser, J. Berkson, L. J. Niles, A. Dey, and E. P. Smith.
2006. Horseshoe crab eggs determine red knot distribution in Delaware Bay. J. Wildl. Manag. 70:1704–1710.

King, T. L., M. S. Eackles, A. P. Spidle, and H. J. Brockmann.
2005. Regional differentiation and sex-based dispersal among populations of horseshoe crabs *Limulus polyphemus*. Trans. Am. Fish. Soc. 134:441–465.

Kurz, W., and M. J. James-Pirri.
2002. The impact of biomedical bleeding on horseshoe crab, *Limulus polyphemus*, movement patterns on Cape Cod, Massachusetts. Mar. Freshw. Behav. Physiol. 35:261–268.

Leschen, A. S., S. P. Grady, and I. Valiela.
2006. Fecundity and spawning of the Atlantic horseshoe crab, *Limulus polyphemus*, in Pleasant Bay, Cape Cod. Mar. Ecol. 27:54–65.

Levin, J., H. D. Hochstein, and T. J. Novitsky.
2003. Clotting cells and *Limulus* amoebocyte lysate: an amazing analytical tool. *In* The American horseshoe crab (C. N. Shuster, R. B. Barlow, H. J. Brockmann, eds.), p. 310–340. Harvard Univ. Press, Cambridge, MA.

Mikkelsen, T.
1988. The secret in the blue blood. Science Press, Beijing, China.

Novitsky, T. J.
1984. Discovery to commercialization: the blood of the horseshoe crab. Oceanus 27:13–18.

Riska, B.
1981. Morphological variation in the horseshoe crab *Limulus polyphemus*. Evolution 35:647–658.

Rudloe, A.
1983. The effect of heavy bleeding on mortality of the horseshoe crab, *Limulus polyphemus*, in the natural environment. J. Invertebr. Pathol. 42:167–176.

Shuster, C. N. Jr.
1979. Distribution of the American horseshoe "crab," *Limulus polyphemus* (L.). *In* Biomedical applications of the horseshoe crab (Limulidae) (E. Cohen, ed.), p. 3–26. Alan R. Liss Inc., New York.

Swan, B. L.
2005. Migrations of adult horseshoe crabs, *Limulus polyphemus*, in the Middle Atlantic Bight: a 17-year tagging study. Estuaries and Coasts 28:28–40.

Tsipoura N., and J. Burger.
1999. Shorebird diet during spring migration stopover on Delaware Bay. Condor 101:635–644.

Walls, E. A., and J. Berkson.
2003. Effects of blood extraction on horseshoe crabs (*Limulus polyphemus*). Fish. Bull. 101:457–459.

Population structure of chum salmon (*Oncorhynchus keta*) across the Pacific Rim, determined from microsatellite analysis

Terry D. Beacham (contact author)
John R. Candy
Khai D. Le
Michael Wetklo

Email address for contact author: Terry.Beacham@dfo-mpo.gc.ca

Fisheries and Oceans Canada,
Pacific Biological Station,
3190 Hammond Bay Road
Nanaimo, B. C., Canada V9T 6N7

Abstract—The Pacific Rim population structure of chum salmon (*Oncorhynchus keta*) was examined with a survey of microsatellite variation to describe the distribution of genetic variation and to evaluate whether chum salmon may have originated from two or more glacial refuges following dispersal to newly available habitat after glacial retreat. Variation at 14 microsatellite loci was surveyed for over 53,000 chum salmon sampled from over 380 localities ranging from Korea through Washington State. An index of genetic differentiation, F_{ST}, over all populations and loci was 0.033, with individual locus values ranging from 0.009 to 0.104. The most genetically diverse chum salmon were observed from Asia, particularly Japan, whereas chum salmon from the Skeena River and Queen Charlotte Islands in northern British Columbia and those from Washington State displayed the fewest number of alleles compared with chum salmon in other regions. Differentiation in chum salmon allele frequencies among regions and populations within regions was approximately 18 times greater than that of annual variation within populations. A regional structuring of populations was the general pattern observed, with chum salmon spawning in different tributaries within a major river drainage or spawning in smaller rivers in a geographic area generally more similar to each other than to populations in different major river drainages or geographic areas. Population structure of chum salmon on a Pacific Rim basis supports the concept of a minimum of two refuges, northern and southern, during the last glaciation, but four possible refuges fit better the observed distribution of genetic variation. The distribution of microsatellite variation of chum salmon on a Pacific Rim basis likely reflects the origins of salmon radiating from refuges after the last glaciation period.

Manuscript submitted 28 August 2008.
Manuscript accepted 22 January 2009.
Fish. Bull. 107:244–260 (2009).

Delineation of phylogenetically and adaptively distinct groups in the distribution of chum salmon around the Pacific Rim may lead to conservation of genetic diversity through an understanding of the origin and the evolutionary processes promoting and maintaining genetic differentiation. An evaluation of genetic variation in describing the population structure of salmonids, is a key component in the elucidation of management units or conservation units in a species and can be applied to manage fisheries exploiting specific stocks of salmon. Several methods of surveying genetic variation have been used to investigate regional and Pacific Rim variation in chum salmon (*Oncorhynchus keta* Walbaum). Allozymes have been used for a number of years to describe chum salmon population differentiation and structure (Okazaki, 1982a; Kijima and Fujio, 1982; Wilmot et al., 1994; Efremov, 2001; Salmenkova et al., 2007). Variation in mitochondrial (mt) DNA has also been investigated (Park et al., 1993; Sato et al., 2001, 2004), as has minisatellite variation (Taylor et al., 1994; Beacham, 1996). Non-mtDNA single nucleotide polymorphisms have been examined (Smith and Seeb, 2008), as have microsatellites (Chen et al. 2005; Beacham et al. 2008a, 2008b, 2008c, 2009). Microsatellites are useful for evaluating fine-scale population structure in salmonids (Banks et al., 2000), and for investigating population structure around the Pacific Rim (Beacham et al., 2006a, 2006b).

Chum salmon display one of the widest spawning distributions of Pacific salmon. In Asia, chum salmon are distributed from Korea and Japan in the south to the Arctic Ocean coast of Russia in the north; in North America, the distribution has historically ranged from California in the south to the Beaufort Sea coast in the north, and as far east as the Mackenzie River in the Arctic (Salo, 1991). After fry emerge from the gravel nest in the spring or are released from hatcheries, they generally move directly to marine residence, first to estuaries, and later in the year to nearshore and offshore waters. Most individuals reside three to five years in the marine environment and then undertake spawning migrations generally to their natal river beds.

Chum salmon were likely fairly widely distributed along the Pacific Rim before the last major glaciation (McPhail and Lindsey, 1970). The advent of glaciation restricted the distribution of chum salmon to some major and perhaps minor refuges. Existing chum salmon population structure has been associated with colonization events following the last glaciation (Seeb and Crane, 1999). Modern populations were thought to have originated largely from a Bering Sea refuge in the north and a Columbia River refuge in the south (McPhail and Lindsey, 1970). In Asia,

local refuges may also have been present in the Kamchatka region (Varnavskaya et al., 1994), and in British Columbia, on the Queen Charlotte Islands and perhaps on coastal islands in the central coast region (Warner et al., 1982; Wood, 1995). Seeb and Crane (1999) indicated that existing populations from the Alaska Peninsula south to Washington may have derived primarily from the southern refuge, whereas Asian and western Alaskan populations may have derived from a northern refuge. Microsatellite variation can be used to examine relationships between existing Pacific Rim population structure and proposed patterns of dispersal from glacial refuges.

In the current study, we evaluated chum salmon dispersal pathways from glacial refugia after glacial retreat. In addition, we examined regional differentiation in allelic frequencies and levels of allelic diversity to evaluate whether local enhancement activities have had any effect on genetic diversity or population structure. These objectives were accomplished by analyzing variation at 14 microsatellite loci to evaluate relationships among Pacific Rim populations of chum salmon. The distribution of genetic diversity among regions, populations, and sampling years was estimated in the study.

Materials and methods

More than 53,000 chum salmon from 381 populations from Korea, Japan, Russia, Alaska, Canada, and Washington were analyed from 59 geographic regions (Table 1, Fig. 1), with the specific populations and sample sizes outlined by Beacham et al.[1] Tissue samples were collected from mature chum salmon, preserved in 95% ethanol, and analyzed at the Molecular Genetics Laboratory at the Pacific Biological Station (Fisheries and Oceans Canada, Nanaimo, BC). DNA was extracted from the tissue samples using a variety of methods, including a chelex resin protocol outlined by Small et al. (1998), a Qiagen 96-well Dneasy® procedure (Mississauga, Ontario), or a Promega Wizard SV96 Genomic DNA Purification system (Promega, Madison, WI). Once DNA was extracted, surveys of variation at 14 microsatellite loci were conducted: *Ots3* (Banks et al., 1999), *Oke3* (Buchholz et al., 2001), *Oki2* (Smith et al., 1998), *Oki100* (Beacham et al., 2008a), *Omm1070* (Rexroad et al., 2001), *Omy1011* (Spies et al., 2005), *One101, One102, One104, One111,* and *One114* (Olsen et al., 2000), *Ots103* (Nelson and Beacham, 1999), *Ssa419* (Cairney et al., 2000), and *OtsG68* (Williamson et al., 2002).

In general, polymerase chain reaction (PCR) DNA amplifications were conducted using DNA Engine Cycler Tetrad2 (BioRad, Hercules, CA) in 6μL volumes consisting of 0.15 units of Taq polymerase, 1 μL of extracted DNA, 1× PCR Hotstar buffer (Qiagen, Mississauga, Ontario, Canada), 60 μM each nucleotide, 0.40 μM of each primer, and deionized water. The thermal cycling profile involved one cycle of 15 minutes at 95°C, followed by 30–40 cycles of 20 seconds at 94°C, 30 to 60 seconds at 47–65°C and 30 to 60 seconds at 68–72°C (depending on the locus). Specific PCR conditions for a particular locus could vary from this general summary as outlined by Beacham et al. (in press). PCR fragments were initially size fractionated in denaturing polyacrylamide gels using an ABI 377 automated DNA sequencer (Applied Biosystems, Foster City, CA), and genotypes were scored by Genotyper 2.5 software (Applied Biosystems, Foster City, CA) using an internal lane sizing standard. Later in the study, microsatellites were size fractionated in an ABI 3730 capillary DNA sequencer (Applied Biosystems, Foster City, CA), and genotypes were scored by GeneMapper software 3.0 (Applied Biosystems, Foster City, CA) using an internal lane sizing standard. Allele identification between the two sequencers were standardized by analyzing approximately 600 individuals on both platforms and converting the sizing in the gel-based data set to match that obtained from the capillary-based set.

Data analysis

All annual samples available for a location were combined to estimate population allele frequencies, as was recommended by Waples (1990). Each population at each locus was tested for departure from Hardy-Weinberg equilibrium by using the computer software Genetic Data Analysis (GDA) (Univ. of Connecticut, Storrs, CT). Critical significance levels for simultaneous tests were evaluated using sequential Bonferroni adjustment (Rice 1989). Weir and Cockerham's (1984) F_{ST} estimates for each locus over all populations were calculated with FSTAT version 2.9.3.2 (Goudet, 1995). The significance of the multilocus F_{ST} value over all samples was determined by jackknifing the F_{ST} value over loci. The 59 geographic regions outlined in Table 1 were combined into 15 larger regional groups as outlined in Table 3 in order to display mean pairwise F_{ST} values between regions, but the two additional continental reporting groups (Asia, North America) incorporated in Table 3 were not used in the analysis of regional F_{ST} variation. Cavalli-Sforza and Edwards (CSE) (1967) chord distance was used to estimate genetic distances among all populations. An unrooted neighbor-joining tree based upon CSE was generated using NJPLOT (Perriere and Gouy, 1996). Bootstrap support (by sampling loci) for the major nodes in the tree was evaluated with the CONSENSE program in PHYLIP software, based upon 1000 replicate trees (Felsenstein, 1993). FSTAT was used to measure the "allelic richness" (allelic diversity standardized to a sample size of 911 fish) for each regional group of populations evaluated. The distribution of genetic variation in chum salmon was evaluated among regions, among populations within regions, and among sampling years within populations. In order to

[1] Beacham, T. D., J. R. Candy, S. Urawa, S. Sato, N. V. Varnavskaya, K. D. Le, and M. Wetklo. 2008. Microsatellite stock identification of chum salmon on a Pacific Rim basis and a comparison with single nucleotide polymorphisms (SNPs). Manuscript in review.

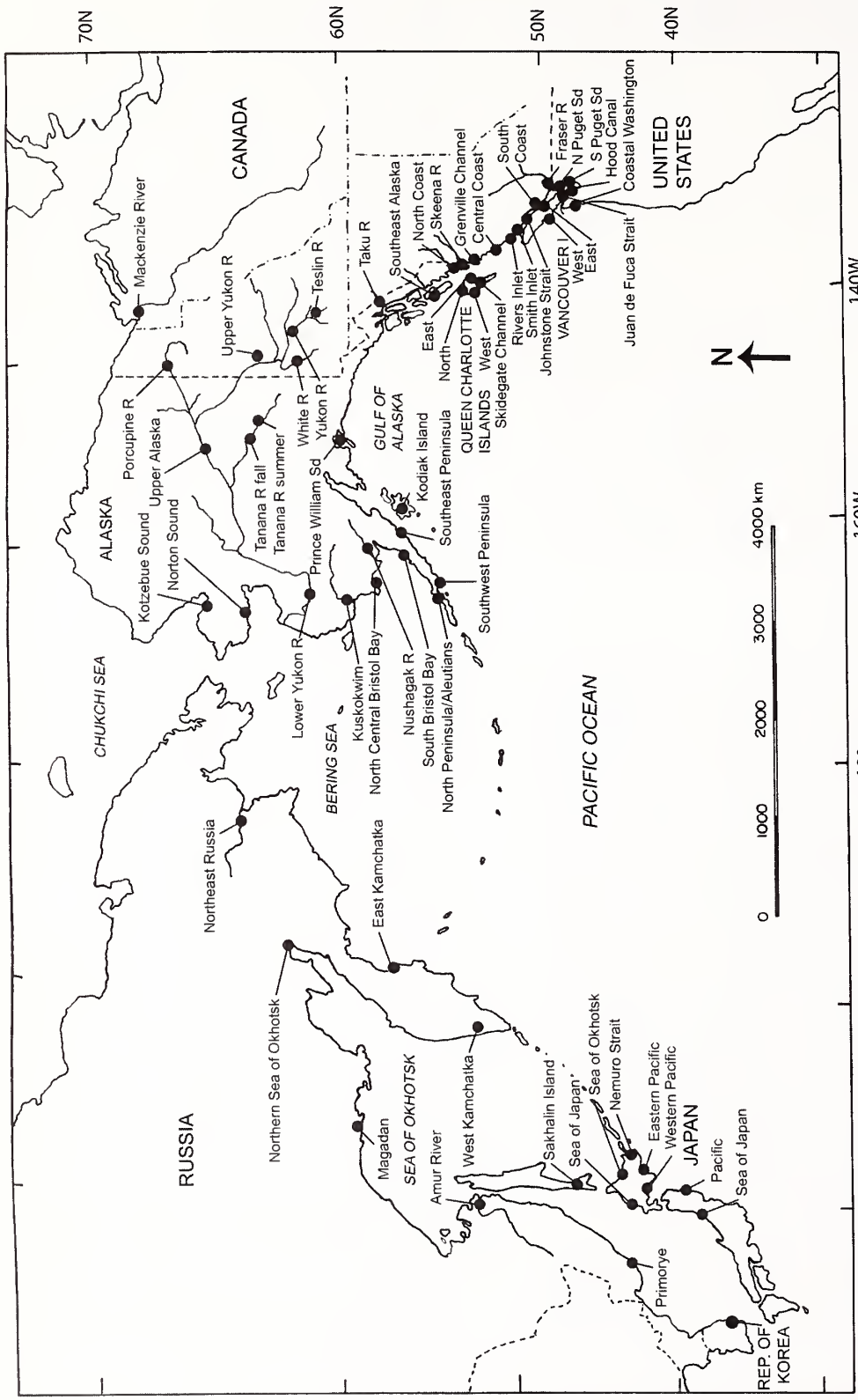

Figure 1

Map of the Pacific Rim indicating the general geographic regions where chum salmon (*Oncorhynchus keta*) from 381 populations were surveyed. The regions are listed in Table 1.

Table 1

Summary of the number of sampling sites or populations of chum salmon (*Oncorhynchus keta*) within each geographic region listed in Figure 1. A complete listing of the populations is outlined by Beacham et al.[1] in their Appendix Table 1. *n* is the number of populations sampled within regions. The range of population sample sizes within regions is given in parentheses.

Geographic area	Reporting region	*n*	Mean population sample size
Korea	Korea	1	100 (100–100)
Japan	Honshu Island, Sea of Japan Coast	5	106 (80–160)
	Hokkaido Island, Sea of Japan Coast	3	147 (60–280)
	Hokkaido Island, Sea of Okhotsk Coast	5	108 (50–160)
	Hokkaido Island, Nemuro Strait	2	95 (80–110)
	Hokkaido Island, eastern Pacific Coast	2	105 (80–130)
	Hokkaido Island, western Pacific Coast	4	120 (80–160)
	Honshu Island, Pacific Coast	5	68 (19–80)
Russia	Primorye	3	34 (17–49)
	Amur River	1	338 (338–338)
	Sakhalin Island	4	76 (49–149)
	Magadan	5	89 (55–120)
	Northern Sea of Okhotsk	2	60 (43–76)
	West Kamchatka	8	116 (40–249)
	East Kamchatka	9	58 (39–128)
	Northeast Russia	2	87 (79–94)
Arctic Canada	Mackenzie River	1	33 (33–33)
Yukon River	Lower river summer run (United States)	11	185 (92–347)
	Tanana River summer run (United States)	2	211 (185–236)
	Tanana River fall run (United States)	3	160 (80–241)
	Upper Alaska (United States)	4	149 (73–229)
	Porcupine River (Canada)	2	463 (329–597)
	White River (Canada)	3	207 (62–486)
	Mainstem Yukon River (Canada)	4	144 (83–175)
	Teslin River (Canada)	1	143 (143–143)
	Upper Yukon River early fall (Canada)	1	120 (120–120)
Western Alaska	Kotzebue Sound	6	155 (45–374)
	Norton Sound	10	278 (50–474)
	Kuskokwim River and bay	6	94 (68–171)
	Nushagak River	2	78 (74–82)
	North Central Bristol Bay	4	77 (64–92)
	South Bristol Bay	4	83 (57–97)
	North Peninsula and Aleutians	3	122 (93–179)
Central Alaska	Southwest Peninsula	4	83 (70–104)
	Southeast Peninsula	3	91 (87–94)
	Kodiak Island	3	89 (71–100)
	Prince William Sound	4	98 (92–100)
Southeast Alaska	Southeast Alaska	14	119 (50–333)
Queen Charlotte Islands	West Coast	11	209 (42–393)
	North Coast	4	132 (80–221)
	East Coast	11	161 (17–376)
	Skidegate Channel	8	181 (79–232)

Continued

Table 1 (continued)

Geographic area	Reporting region	*n*	Mean population sample size
Northern British Columbia	Taku River	5	34 (12–65)
	North Coast	18	117 (28–242)
	Skeena River	13	95 (12–182)
	Grenville Channel	6	122 (40–242)
	Central Coast	52	190 (13–419)
	Rivers Inlet	8	79 (40–153)
	Smith Inlet	2	363 (226–499)
Southern British Columbia	Johnstone Strait	13	134 (20–409)
	South Coast	14	137 (15–344)
	Vancouver Island east coast	9	227 (167–285)
	Vancouver Island west coast	10	133 (43–243)
	Fraser River	23	151 (24–427)
Washington	North Puget Sound	7	85 (50–100)
	South Puget Sound	3	100 (100–100)
	Hood Canal	2	95 (88–102)
	Strait of Juan de Fuca	2	100 (100–100)
	Coast of Washington	4	91 (61–106)

maintain a balanced design, regions included in the analysis required two or more populations each with two or more years of samples available. Regions were distributed around the Pacific Rim and were a subset of the 59 geographic regions outlined in Table 1 and Figure 1. The specific populations included from each region are in shown parentheses: West Kamchatka (Hairusova, Vorovskaya), Western Alaska (Snake, Eldorado), Yukon River summer run (Gisasa, Tozitna), Southeast Alaska (DIPAC hatchery, Disappearance), Queen Charlotte Islands west coast (Clapp Basin, Mace), Queen Charlotte Islands east coast (Lagoon, Pallant), Northern British Columbia (Ensheshese, Kateen), Grenville Channel (Markle, Wilson), British Columbia central coast (Bullock Channel, Quaal, Salmon), Smith Inlet (Walkum, Nekite), Johnstone Strait (Viner Sound, Nimpkish), Vancouver Island east coast (Big Qualicum, Cowichan), and Fraser River (Inch, Stave). Estimation of variance components of river drainage or region differentiation, among populations within drainages or regions, and among years within populations was determined with Genetic Data Analysis.

Results

Variation within populations

Substantial variation was observed in the number of alleles at the 14 microsatellite loci surveyed in the study. The fewest number of alleles was observed at *Oke3* (26 alleles), and the greatest number of alleles observed at *One111* (149 alleles) (Table 2). Lower heterozygosity was observed at loci with fewer than 40 alleles. The genotypic frequencies at each locus conformed to those expected under Hardy-Weinberg equilibrium (HWE).

The number of alleles observed displayed considerable variation across regional groups of chum salmon. Asian chum salmon were considerably more diverse than those in North America, with Asian populations displaying the greatest number of alleles at all 14 loci examined (P=0.0001) (Table 3). With sample sizes standardized to 911 fish per region, Japanese chum salmon were the most genetically diverse set of populations examined with 581 alleles observed, greater than in all other regional groups of populations. The least diverse groups of populations were observed in the Queen Charlotte Islands, the Skeena River, the east coast of Vancouver Island, and Washington State, with an average of 414 alleles observed in chum salmon from these regions. Japanese chum salmon displayed 40% more alleles and Russian chum salmon 35% more alleles than did chum salmon from the four regions of lower genetic diversity. The greatest difference in diversity was observed at locus *One111,* with the greatest number of observed alleles, and Asian chum salmon displayed 80% more alleles than did chum salmon from the four regions of lower genetic diversity. Even with *One111* removed from the analysis, Asian chum salmon were still more diverse than chum salmon in all regions in North America (P=0.0002).

Distribution of genetic variance

Gene diversity analysis of the 14 loci surveyed was used to evaluate the distribution of genetic variation

Table 2

Number of alleles per locus, an index of gentic differentiation F_{ST} (SD in parentheses), expected heterozygosity (H_e), observed heterozygosity (H_o), and percent significant Hardy-Weinberg equilibrium (HWE) test for 14 microsatellites (n=381 tests) among 381 chum salmon (*Oncorhynchus keta*) populations.

Locus	Number of alleles	F_{ST}	H_e	H_o	HWE
1 *Oke3*	26	0.104 (0.005)	0.67	0.65	3.7
2 *Oki100*	31	0.039 (0.002)	0.83	0.83	0.3
3 *Ots3*	31	0.097 (0.005)	0.76	0.75	4.7
4 *Oki2*	42	0.062 (0.005)	0.86	0.85	0.8
5 *Omy1011*	44	0.027 (0.001)	0.90	0.89	0.3
6 *One104*	48	0.027 (0.001)	0.93	0.92	1.6
7 *Ots103*	54	0.019 (0.001)	0.94	0.93	1.1
8 *Ssa419*	54	0.028 (0.001)	0.84	0.83	0.5
9 *One101*	56	0.058 (0.002)	0.87	0.86	1.6
10 *Omm1070*	60	0.009 (0.000)	0.95	0.94	1.3
11 *One114*	60	0.017 (0.001)	0.92	0.91	1.6
12 *One102*	69	0.011 (0.001)	0.92	0.90	2.1
13 *OtsG68*	69	0.017 (0.001)	0.95	0.94	1.8
14 *One111*	149	0.036 (0.003)	0.94	0.93	3.9
Total		0.033 (0.007)	0.88	0.87	

Table 3

Mean number of alleles observed per locus at 14 microsatellite loci for chum salmon (*Oncorhynchus keta*) from 15 geographic areas standardized to a sample size of 911 fish per geographic area. Geographic areas, listed in Table 1, were: Japan (includes Korea), Russia, Western Alaska (WAK), Yukon River (includes Arctic Canada), Central Alaska (CAK), Southeast Alaska (SeAK), Queen Charlotte Islands (QCI), northern British Columbia (NBC), Skeena River, Central Coast British Columbia (CBC) (includes Grenville Channel, Rivers Inlet, and Smith Inlet), Southern British Columbia (includes Johnstone Strait), east coast Vancouver Island (ECVI), west coast Vancouver Island (WCVI), Fraser River, Washington (Wash), and North America (NA).

Area	*Oke 3*	*Oki 100*	*Oki 2*	*Omm 1070*	*Omy 1011*	*One 101*	*One 102*	*One 104*	*One 111*	*One 114*	*Ots 3*	*Ots 103*	*Ots G68*	*Ssa 419*	Total
Japan	16.6	25.0	23.8	51.0	39.5	37.8	42.3	37.4	122.0	34.5	25.8	46.8	53.1	25.2	580.8
Russia	14.9	27.1	18.9	45.1	31.3	40.2	28.4	34.4	130.2	40.6	22.4	47.6	51.2	26.6	558.9
Total Asia	15.8	26.1	21.4	48.1	35.4	39.0	35.4	35.9	126.1	37.6	24.1	47.2	52.2	25.9	569.9
WAK	9.9	24.2	18.2	37.2	28.1	33.0	21.7	27.7	110.7	39.9	19.2	40.4	41.7	17.9	469.8
Yukon R.	12.9	22.8	20.5	37.7	28.6	35.9	28.2	29.3	112.1	35.0	21.2	38.1	41.3	16.7	480.3
CAK	9.7	25.2	20.0	36.3	25.7	29.5	27.0	30.6	106.4	35.4	18.9	39.7	40.6	20.2	465.2
SeAK	8.6	21.6	20.4	40.9	24.3	37.6	28.9	28.5	94.7	35.5	18.6	43.3	43.1	22.8	468.8
QCI	11.8	17.2	20.8	38.3	21.1	36.6	29.1	28.5	69.7	26.1	18.1	39.7	44.0	23.1	424.1
NBC	14.5	19.2	20.3	40.4	26.5	41.0	31.3	31.3	102.0	31.1	18.2	42.5	45.8	25.2	489.3
Skeena R.	7.5	15.8	18.0	37.3	22.7	35.9	25.9	28.0	65.3	25.2	16.1	37.5	42.0	17.7	394.9
CBC	13.9	19.3	20.2	41.7	26.2	39.0	31.4	28.6	93.8	33.7	21.4	42.1	45.2	22.7	479.2
SBC	16.2	17.9	20.2	38.8	26.0	40.6	28.8	33.0	76.1	31.2	22.0	39.1	44.8	20.5	455.2
ECVI	8.0	15.7	23.0	39.8	21.8	37.0	24.9	25.9	73.9	27.0	19.6	36.9	44.9	19.0	417.4
WCVI	11.0	17.8	25.8	35.9	24.7	39.8	28.2	29.8	74.6	31.7	22.4	39.0	47.4	16.8	444.9
Fraser R.	13.0	20.8	18.1	42.2	25.0	38.8	23.4	31.1	89.6	34.3	20.6	38.7	56.0	15.4	467.0
Washington	10.5	17.6	18.0	38.8	18.8	36.3	26.6	29.0	71.0	34.0	15.8	40.5	45.5	15.6	418.0
Total NA	11.3	19.6	20.3	38.9	24.6	37.0	27.3	29.3	87.7	32.3	18.2	39.8	44.8	19.5	451.8

Table 4

Hierarchical gene-diversity analysis of 27 populations of chum salmon (*Oncorhynchus keta*) within 13 regions for 14 microsatellite loci. Regions had a Pacific Rim distribution, and the time difference between the earliest and latest samples included for specific populations ranged from 1 to 21 years. Ratio is the sum of the variance components of among populations within regions and among regions divided by the variance component among years within populations. * $P<0.05$ ** $P<0.01$.

Locus	Within populations	Among years within populations	Among populations within regions	Among regions	Ratio
Oke3	0.9204	0.0004	0.0056**	0.0736**	198.0
Oki100	0.9673	0.0008	0.0070**	0.0249**	39.9
Ots3	0.9254	0.0018*	0.0044**	0.0685**	40.5
Oki2	0.9625	0.0065**	0.0044*	0.0266**	4.8
Omy1011	0.9783	0.0016	0.0013	0.0187**	12.5
One104	0.9783	0.0004	0.0030**	0.0183**	53.3
Ots103	0.9837	0.0007	0.0029**	0.0126**	22.1
Ssa419	0.9785	0.0018*	0.0054**	0.0143**	10.9
One101	0.9635	0.0015	0.0088**	0.0262**	23.3
Omm1070	0.9918	0.0011	0.0031**	0.0040*	6.5
One114	0.9881	0.0009	0.0042**	0.0068*	12.2
One102	0.9941	0.0008	0.0018	0.0033*	6.4
OtsG68	0.9854	0.0015	0.0036**	0.0095**	8.7
One111	0.9727	0.0016*	0.0030	0.0227**	16.1
Total	0.9722	0.0015	0.0041**	0.0222**	17.5

among regions, among populations within regions, and among years within populations. Within populations, the time difference between the earliest and latest samples included in the analysis ranged from 21 years (1986–2007) for Disappearance Creek (Southeast Alaska), 18 years (1986–2004) for Lagoon Creek (Queen Charlotte Islands), 16 years (1989–2005) for Nekite River in Smith Inlet, 15 years (1988–2003) for Gisasa River (Lower Yukon River), down to 1–3 year differences for populations in a number of regions. For 13 regions ranging from west Kamchatka to the Fraser River, the amount of variation within populations ranged from 92% (*Oke3*) to 99% (*Omm1070*), with the average for an individual locus 97% (Table 4). Variation among the 13 regions included in the analysis accounted for 2.2% of total observed variation. Variation among populations within regions accounted for 0.4% of observed variation, with differences among regions over five times greater than differences among populations within regions. The variation among sampling years within populations was the smallest source of variation observed, accounting for 0.2% of all variation. Differentiation among regions and populations within regions was approximately 18 times greater than that of annual variation within populations. For the time intervals surveyed in our study, annual variation in microsatellite allele frequencies was relatively minor compared with differences among populations within regions and among regions on a geographically diverse scale of distribution of the populations analyzed.

Population structure

Significant genetic differentiation was observed among chum salmon populations sampled in the different geographic regions surveyed. The F_{ST} value over all populations and loci was 0.033, with individual locus values ranging from 0.009 (*Omm1070*) to 0.104 (*Oke3*) (Table 2). Chum salmon from Japan and the Yukon River were among the most distinct regional groups of stocks included in the survey (Table 5). Greatest genetic differentiation (greatest difference in F_{ST} values) was observed in comparisons between Japanese, Russian, western Alaskan, and Yukon River chum salmon compared with those in other regions in North America to the south and east. In Asia, chum salmon from Japan were generally distinct from those in Russia. In North America, significant regional differentiation was generally observed, with chum salmon in more northern regions distinct from those in more southern regions.

Two major lineages of chum salmon populations were identified in the cluster analysis. The first lineage included all populations sampled from Korea, Japan, Russia, the Mackenzie River, Kotzebue Sound, Norton Sound, the Yukon River, and northern and central Bristol Bay. Populations from southern Bristol Bay were intermediate between the two major lineages, and all populations from the Alaska Peninsula south and east to Washington State were identified as the second major lineage (Fig. 2). Within the first lineage, all Asian populations were distinct from all North American

Table 5

Mean pairwise F_{ST} values averaged over 14 microsatellite loci from 15 regional groups of chum salmon (*Oncorhynchus keta*) outlined in Table 3 that were sampled at 381 locations across the Pacific Rim. Comparisons were conducted between individual populations in each region. Values in bold are the diagonal, and are comparisons among populations within each region. F_{ST} values are listed below the diagonal, with standard deviations above the diagonal. Some of the reporting regions listed in Table 1 were combined as indicated in Table 3 in order to facilitate the analysis. RC is region code, and codes are as follows: 1) Japan, 2) Russia, 3) Western Alaska, 4) Yukon River, 5) Central Alaska, 6) Southeast Alaska, 7) Queen Charlotte Islands, 8) Northern British Columbia, 9) Skeena River, 10) Central British Columbia, 11) Southern mainland British Columbia, 12) West coast Vancouver Island, 13) East coast Vancouver Island, 14) Fraser River, 15) Washington.

	1	2	3	4	5	6	7	8	9	10	11	12	13	14	15
1	**0.019**	0.009	0.014	0.023	0.015	0.007	0.008	0.009	0.009	0.009	0.008	0.007	0.008	0.011	0.011
2	0.026	**0.017**	0.013	0.018	0.016	0.011	0.010	0.011	0.012	0.011	0.011	0.010	0.010	0.011	0.014
3	0.028	0.024	**0.012**	0.018	0.018	0.011	0.011	0.011	0.012	0.011	0.009	0.010	0.011	0.015	0.013
4	0.053	0.054	0.031	**0.018**	0.020	0.013	0.014	0.014	0.019	0.014	0.015	0.013	0.017	0.022	0.016
5	0.042	0.032	0.037	0.064	**0.027**	0.014	0.016	0.015	0.019	0.016	0.014	0.015	0.013	0.011	0.015
6	0.042	0.029	0.035	0.062	0.024	**0.007**	0.006	0.005	0.016	0.006	0.007	0.005	0.011	0.006	0.009
7	0.050	0.039	0.043	0.068	0.034	0.015	**0.012**	0.007	0.017	0.007	0.007	0.005	0.014	0.008	0.010
8	0.044	0.031	0.037	0.063	0.026	0.008	0.015	**0.008**	0.017	0.007	0.009	0.007	0.013	0.009	0.012
9	0.053	0.041	0.046	0.066	0.035	0.019	0.025	0.019	**0.014**	0.017	0.014	0.012	0.017	0.015	0.017
10	0.043	0.031	0.037	0.062	0.030	0.011	0.014	0.010	0.020	**0.008**	0.007	0.005	0.013	0.008	0.009
11	0.046	0.033	0.040	0.068	0.039	0.022	0.025	0.021	0.030	0.018	**0.014**	0.007	0.019	0.012	0.012
12	0.044	0.034	0.038	0.062	0.038	0.019	0.018	0.019	0.026	0.017	0.016	**0.008**	0.016	0.009	0.010
13	0.043	0.032	0.034	0.060	0.039	0.026	0.031	0.026	0.035	0.025	0.019	0.022	**0.022**	0.018	0.011
14	0.041	0.028	0.035	0.063	0.037	0.025	0.030	0.026	0.033	0.024	0.018	0.021	0.020	**0.013**	0.015
15	0.051	0.039	0.047	0.076	0.045	0.028	0.033	0.029	0.035	0.025	0.022	0.023	0.028	0.022	**0.022**

populations. Within the Asian portion of the lineage, Japanese, Korean, and Russian Primorye populations were distinct from other Asian populations. In the second lineage, populations from Washington and southern British Columbia were among the most distinct group of populations, along with populations from the Queen Charlotte Islands in northern British Columbia.

Chum salmon spawning in tributaries of different major river drainages generally clustered together in the analysis. For example, Fraser River populations clustered together in 39% of dendrograms evaluated, Skeena River populations clustered together in 97% of dendrograms evaluated, and Taku River populations clustered together in 96% of dendrograms evaluated (Fig. 2). The one exception was the Yukon River, where lower river summer-run populations did not form distinct clusters unique from neighboring populations in the Kuskokwim River and the Nushagak River.

A very distinct regional cluster of populations was observed in the Asian populations, with Korean, Japanese, and populations from the Primorye region in Russia clustering together in 100% of dendrograms evaluated. Within that cluster, populations from Primorye clustered together in 67% of dendrograms evaluated, indicative of genetic differentiation between populations from that region and those in Japan and Korea. Within Japan, a general regional structuring of populations was observed, with populations from the Pacific coast of Honshu Island forming a distinct group (92% of dendrograms evaluated), as did populations from the Nemuro Strait (89% of dendrograms) and the eastern Pacific coast of Hokkaido Island (50% of dendrograms). Within Russia, Magadan region populations clustered together in 41% of dendrograms evaluated, as did populations from the northern Sea of Okhotsk (100% of dendrograms). Although populations from east coast of Kamchatka and west coast of Kamchatka generally clustered as two distinct regional groups, the groupings were not strongly supported by the bootstrap analysis. Populations from northeast Russia were distinct from those in other regions, with the possible exception of the Utka River population from west Kamchatka.

In North America, some level of regional structuring of populations was observed in both Kotzebue Sound and Norton Sound (Fig. 2). Within the Yukon River drainage, there was clear separation between summer-run populations in the lower and mid- portions of the drainage and fall-run populations in the upper portion of the drainage. For the fall-run, populations in the White River in the Yukon Territory were quite distinct, clustering together in 100% of dendrograms evaluated. Similarly, fall-run populations in the Tanana River (upper portion of Yukon River drainage in Alaska) clustered together in 74% of the dendrograms evaluated, and summer-run populations in the Tanana River drainage clustered together in 96% of dendrograms. Summer-run populations in the lower Yukon River drainage did not cluster exclusively with each

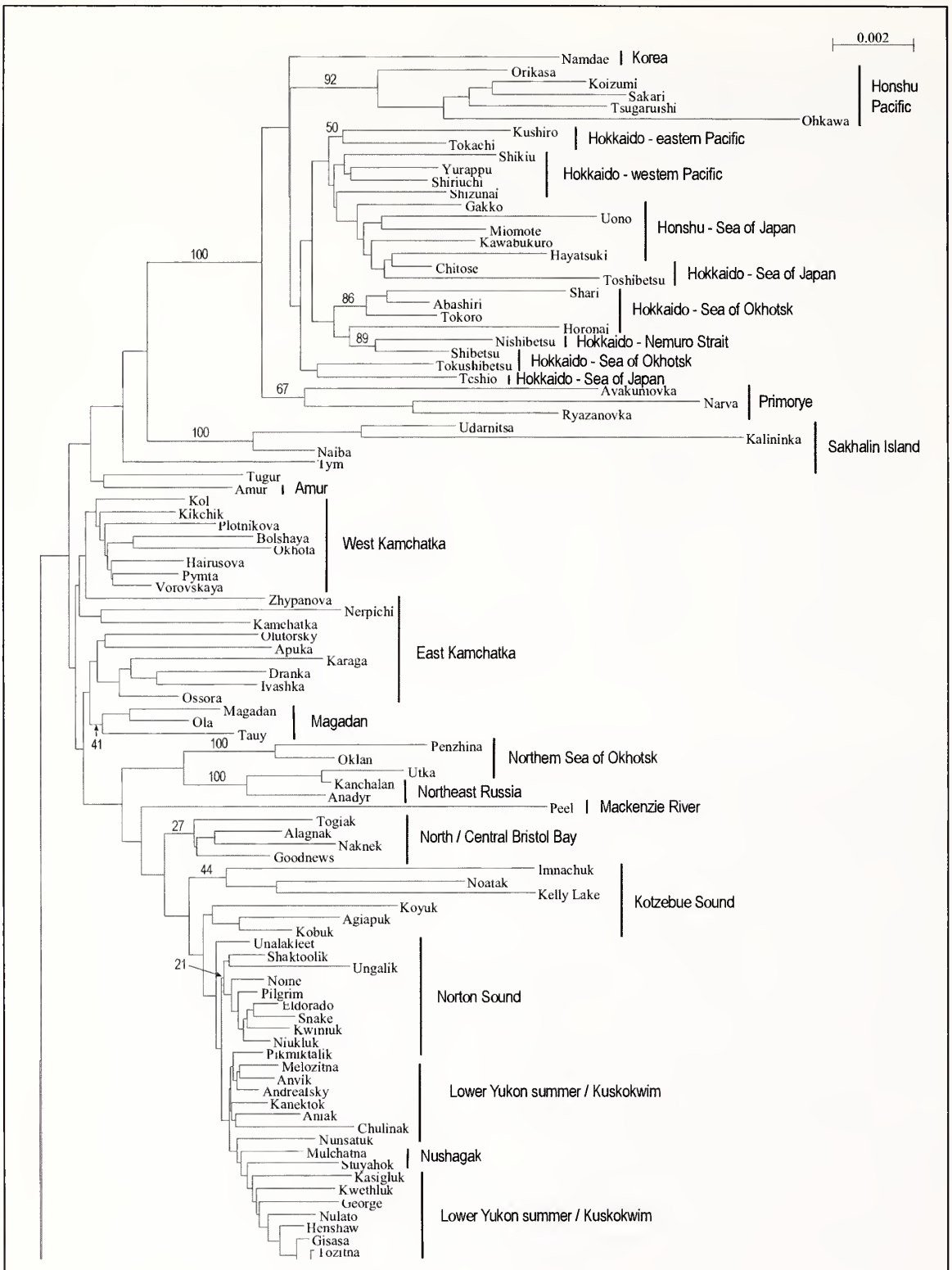

Figure 2

Neighbour-joining dendrogram of Cavalli-Sforza and Edwards (1967) chord distance for 381 Pacific Rim populations of chum salmon (*Oncorhynchus keta*) surveyed at 14 microsatellite loci. Bootstrap values at major tree nodes indicate the percentage of 1000 trees where populations beyond the node clustered together.

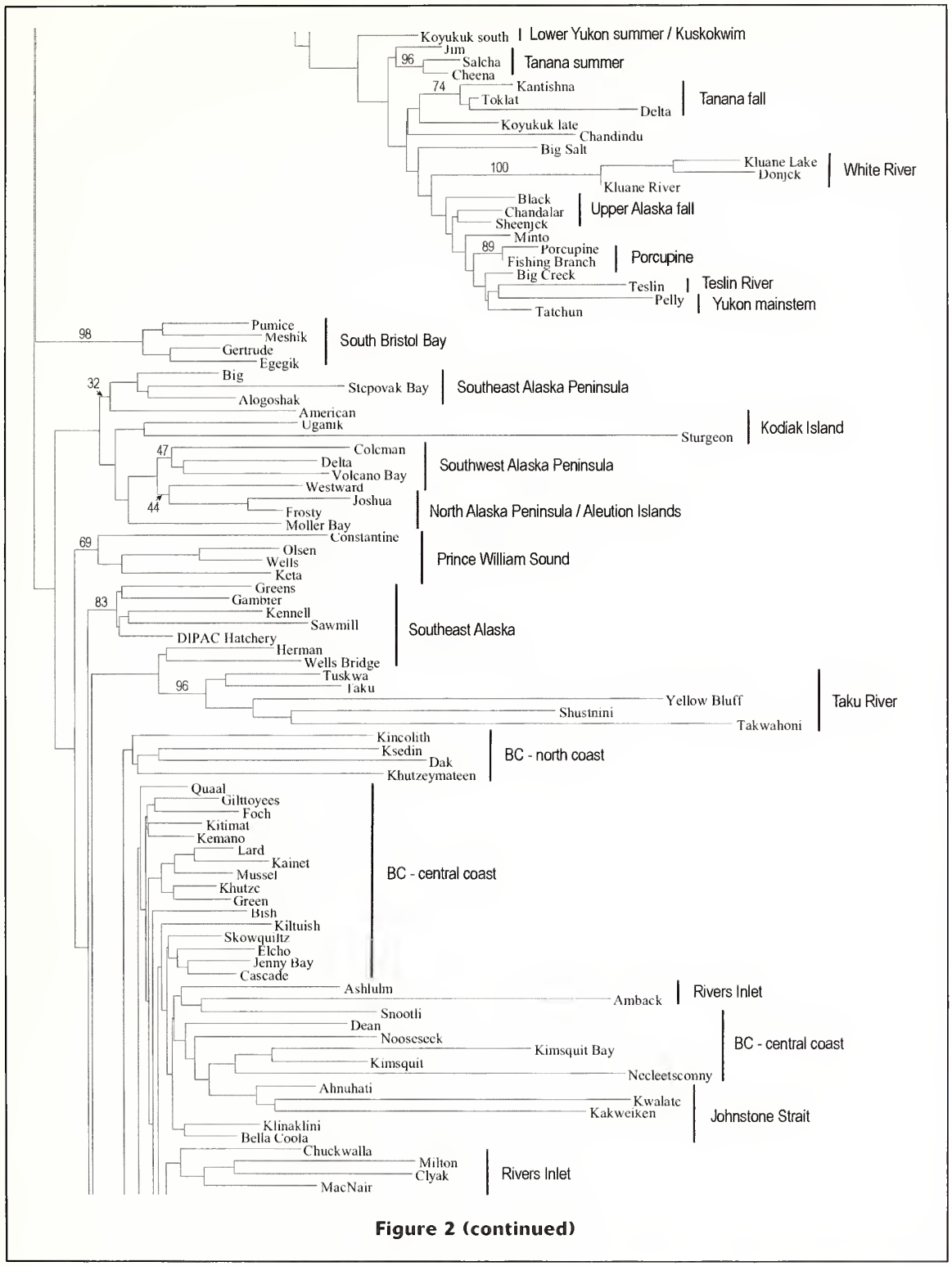

Figure 2 (continued)

other, including populations from the Kuskokwim River in western Alaska and Nushagak River from northern Bristol Bay in the dendrogram cluster.

Geographically-based regional clustering was observed in the populations surveyed south and east of northern Bristol Bay. Populations from southern Bristol Bay formed a distinct cluster in 98% of dendrograms evaluated, with bootstrap support observed for populations from the western south coast of the Alaska Peninsula, eastern south coast of the Alaska Peninsula, Kodiak

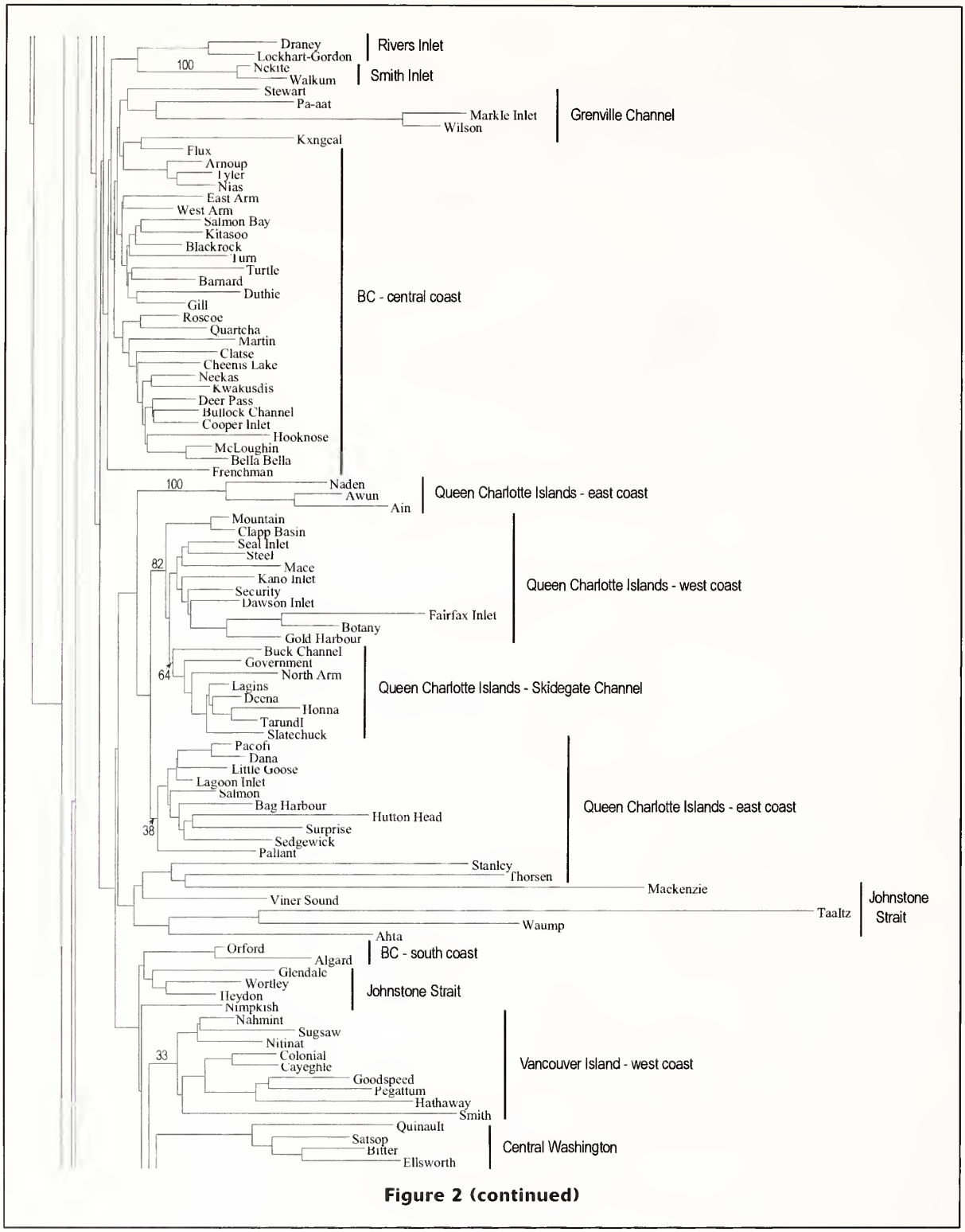

Figure 2 (continued)

Island, and Prince William Sound. Populations from northern southeast Alaska formed a distinct cluster in the analysis, but populations from southern southeast Alaska were less distinct than those in the northern portion of the region. Some clusters in the dendrogram included populations from both southern southeast Alaska and northern British Columbia (Fig. 2).

In British Columbia (BC), four geographically based regional groups of populations were observed in the Queen Charlotte Islands (QCI). North coast QCI popu-

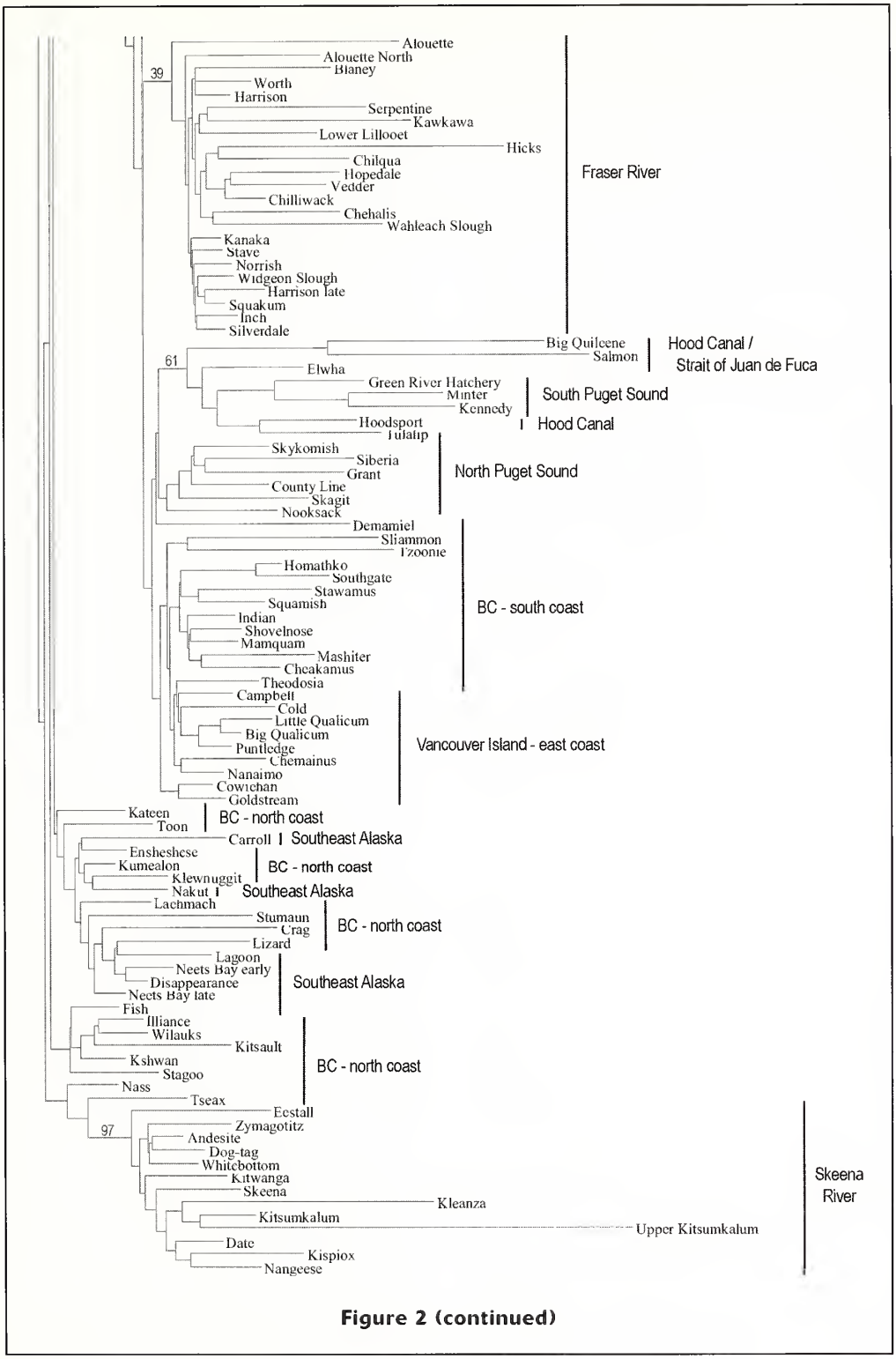

Figure 2 (continued)

lations were the most distinct clustering together in 100% of dendrograms evaluated. Regional populations were also observed along the east and west coasts of the QCI. Populations adjacent to Skidegate Channel, the body of water separating the major QCI components of Graham Island (north) and Moresby Island (south), clustered together with 64% bootstrap support. On the northern mainland, populations north of the Skeena River mouth were distinct from those south of the Skeena River. North of the Skeena River, there

were not distinct clusters observed between northern coastal British Columbia populations and those from southeast Alaska. Populations immediately south of the Skeena River in the Grenville Channel area clustered separately from those further south in the central coastal region of British Columbia. Yet farther south, populations from Rivers Inlet and Smith Inlet clustered together in geographically based groups, and this result was confirmed by 100% boostrap support observed for Smith Inlet populations (Fig. 2).

In southern BC, five geographically based groups of populations were revealed. East coast and west coast of Vancouver Island populations were regionally separate from each other, and also from other regional populations in southern BC. On the mainland, Johnstone Strait populations were separate from those in southern coastal areas, and the demarcation point between the two groups is Bute Inlet, at the northeast limit of the Strait of Georgia. Fraser River populations were distinct from other regional groups in southern BC.

In Washington, regional structuring of chum populations was observed. The most distinct regional group comprised populations from the outer Pacific coast, with populations clustering together with 100% bootstrap support. In more inside waters, populations from north Puget Sound were generally distinct from those in south Puget Sound, Hood Canal, and the Strait of Juan de Fuca. South Puget Sound populations were distinct from those in Hood Canal and the Strait of Juan de Fuca.

Discussion

The survey of microsatellite variation included an examination of variation at 14 loci encompassing approximately 800 alleles, with 26 to 149 alleles recognized per locus. The number of fish surveyed per population ranged from 12 to 597 individuals (Beacham et al.[1]). With a variable number of individuals surveyed per population, there was a potential for sampling error in estimated allele frequencies and in obscuring genetic relationships among related populations, particularly if sample sizes were small for some populations in a lineage. For example, for the Primorye populations from Russia, population sample sizes ranged from 17 to 49 individuals, and it was possible that estimates of genetic distances among populations were not determined satisfactorily for populations of smaller sample size, particularly for those loci with larger numbers of alleles. However, Kalinowski (2005) reported that loci with larger numbers of alleles (higher mutation rates) produced estimates of genetic distance with lower coefficients of variation than loci with fewer numbers of alleles, without requiring larger sample sizes from each population. Population structuring based upon geographic differences were observed for populations from Primorye, and all populations clustered together in 67% of dendrograms evaluated. Therefore, it seems likely that variation in the number of individuals surveyed within a population in our study did not generally result in misidentification of genetic relationships among populations.

Size homoplasy of microsatellite alleles may have some effect on the estimate of genetic differentiation observed among populations. Inferences about the genetic relationships of populations surveyed in our study were dependent upon accurate determination of population allele frequencies. Microsatellite alleles differ in size, but alleles of the same size at a locus in geographically disparate populations may not have the same origin as a result of size homoplasy. Convergent mutations in different lineages may produce alleles of the same size, with the result that there may be greater differentiation among lineages than revealed by analysis of size variation. However, with approximately 800 alleles observed across all loci in the study, the large amount of variation present at these loci largely compensates for size homoplasy (Estoup et al., 2002).

In this study, population allele frequencies were estimated by combining all samples collected over time for a population, regardless of the length of time that occurred between samples. In practice, the maximum length of time between samples for a population was 21 years, and up to six annual samples were combined for a population. Analysis of the distribution of genetic variation indicated that differentiation among regions and populations within regions was approximately 18 times greater than that of annual variation within populations, indicating that pooling of annual samples over time is a practical approach to estimate population allele frequencies. Relative stability of microsatellite allele frequencies over time is not unique to chum salmon; similar relative stability has been reported for sockeye salmon (*O. nerka*) (Beacham et al., 2006a) and Chinook salmon (*O. tshawytscha*) (Beacham et al., 2006b).

Surveys of genetically based population structure in chum salmon were initially conducted with allozymes. Okazaki (1982b), in a study evaluating allozyme variation in Asian and North American populations, concluded that there were 11 geographically based regional groups of populations across the Pacific Rim. The regional groups consisted of adjacent river populations that were genetically similar within one region. Many allozyme-based studies of regional population structure were subsequently reported. For example, Winans et al. (1994) provided additional details concerning population structure of Asian populations, Wilmot et al. (1994) compared population structure of chum salmon from western Alaska and northeast Russia, Kondzela et al. (1994) compared population structure of chum salmon from southeast Alaska and northern British Columbia, Beacham et al.(1987) evaluated population structure of chum salmon in British Columbia, and Phelps et al. (1994) evaluated population structure in the Pacific Northwest. Seeb and Crane (1999) again investigated chum salmon population structure throughout the Pacific Rim by examining variation at 40 allozymes, and reported that two major lineages of populations were observed. The northern lineage occurred in areas north of the Alaska Peninsula and into Russia and Japan,

whereas the southern lineage was observed in the Alaska Peninsula, Kodiak Island, and areas to the south and east. The two lineages were reported to overlap in the northern Alaska Peninsula.

Development of DNA-level markers provided additional markers for genetic evaluation of population structure of chum salmon, and surveys of mitochondrial DNA variation have been reported. Differentiation among Russian populations has been reported (Ginatulina, 1992; Brykov, 2003; Polyakova et al., 2006), as well as in Japanese populations (Sato et al., 2001). In an analysis of mtDNA variation across the Pacific Rim, Sato et al. (2004) reported that there were three major lineages of chum salmon, with populations from Japan, Russia, and North America comprising three distinct regional groups. Chum salmon from Japan were observed to be the most distinct, with less divergence between populations from Russia and western Alaska.

Minisatellite variation was used by Taylor et al. (1994) and Beacham (1996) to survey variation in 42 chum salmon populations across the Pacific Rim. Three regional groups of populations showed that those from Japan were the most distinct, followed by a second (less distinct) group comprising Russian and Yukon River populations, and a third group comprising southeast Alaska and British Columbia populations.

Microsatellites have been used to evaluate chum salmon population differentiation and structure on a local and regional basis (Chen et al., 2005; Beacham et al., 2008a, 2008b, 2008c, in press). In those studies, as in the previous allozyme-based studies, regional groups of populations were observed, with the regional groups consisting of adjacent river populations or local populations that were genetically similar within one region. The results from the current study were remarkably similar to the results of the allozyme-based study reported by Seeb and Crane (1999), with populations from Korea, Japan, Russia, Kotzebue Sound, Norton Sound, the Yukon River, and northern Bristol Bay determined to be in one major lineage. Populations from southern Bristol Bay and the northern Alaska Peninsula were intermediate, and populations on the south side of the Alaska Peninsula, Kodiak Island, and areas to the south and east to Washington State were determined to be in a second major lineage.

Successful transplantation of salmon within the range of a species has the potential to alter genetic population structure. Population structure of chum salmon has been influenced to some degree by transplantations within its range. For example, due to frequent transplantations associated with hatcheries, most Japanese populations have received some level of transplantation of non-natal fish. Although initial studies indicated that the effect of transplantations were minimal in Japanese populations (Okazaki, 1982a), more recent work has shown that some current run-timing variation in populations may be a result of transplantations. Beacham et al. (2008b) reported that allozyme monitoring indicated that successful introduction and establishment of broodstock from the Chitose River on the Sea of Japan coast of Hokkaido Island to the Gakko River on the Sea of Japan coast of Honshu Island accounts for observed temporal differentiation in the existing Gakko River population. Transplantations have also occurred in Russian and North American populations, but there is little evidence for a demonstrable change in population structure as a result of transplantations.

Although most production of Japanese chum salmon is currently derived from hatcheries, there is little evidence that hatchery production has resulted in reduced genetic variation of the populations, in relation to chum salmon in other portions of the range. Initially, Kaeriyama (1999) indicated that, on the basis of allozymes, Japanese populations were less variable than Russian wild populations. In our study, on the basis of 14 microsatellites, we found no evidence that Japanese chum salmon populations were less genetically variable than Russian or North American chum salmon. In fact, the opposite result was observed, with higher levels of genetic variation observed in Japanese populations compared with chum salmon from other regions across the Pacific Rim.

Population structure of chum salmon across the Pacific Rim was demonstrated to have a regional basis. A regionally based population structure is generally required for genetic stock identification estimation because an important assumption is that the portion of the mixed-stock sample derived from unsampled populations is allocated to sampled populations from the same region. This assumption reduces the cost and complexity of developing a baseline for stock composition analysis. Chum salmon population structure thus meets the important condition that unsampled populations contributing to mixed fishery samples will likely be allocated to sampled populations in the same region.

Populations in the major river drainages surveyed all clustered together within a drainage, with the exception of the Yukon River, where lower river summer-run populations clustered with populations from the Kuskokwim River in western Alaska and the Nushagak River in northern Bristol Bay. Similar results were also reported in the allozyme survey conducted by Seeb and Crane (1999), who suggested that genetic exchange may have occurred between the Kuskokwim and Nushagak rivers during the last glaciation because both rivers were headwaters to a Bering Sea Land Bridge river that drained into the Bering Sea (Hopkins, 1967; Lindsay and McPhail, 1986). The ancient mouth of the Yukon River was farther south than at present (Hopkins, 1967; Knebel and Creager, 1973), increasing the probability of genetic exchange among ancestral populations of the Yukon, Kuskokwim, and Nushagak rivers.

Chum salmon likely had a different pattern of dispersal from refuges after the last glaciation ended in the Pleistocene Era some 10,000 years ago than did either sockeye salmon or Chinook salmon. For example, evaluation of genetic diversity in Asian and North American populations of sockeye salmon and Chinook salmon have indicated that there were similar levels of genetic diversity between populations from these

two continents (Beacham et al., 2006a, 2006b). This is in marked contrast to the pattern observed in chum salmon, with Asian chum salmon displaying significantly greater genetic diversity than that observed in chum salmon populations in North America. Surveys of mtDNA variation have also indicated that Japanese populations have the highest genetic diversity among Pacific Rim chum salmon (Sato et al., 2004). Chum salmon in Asia display a wider geographic distribution than either sockeye salmon or Chinook salmon, with most populations of these two species restricted to a Russian distribution, whereas chum salmon range as far south as South Korea. The distinctive nature of Korean, Japanese, and Primorye chum salmon, coupled with the higher diversity observed in Asian populations, indicates an Asian refuge from which chum salmon dispersed after the retreat of glaciers during the Pleistocene, either on the southern Asian mainland or the islands of Japan. The fact that Asian chum salmon display more genetic diversity than North American chum salmon reflects either that either higher population sizes were present in this refuge, allowing more genetic variation to be retained, or that dispersal from this refuge preceded those in North America, allowing more time for genetic mutations to accumulate. The concept of a glacial refuge near Japan was also suggested by Taylor et al. (1994).

In North America, the observed population structure of chum salmon would support the concept at a minimum of a Bering Sea refuge in the north (unglaciated areas of western Alaska or Russia) and a Columbia River refuge in the south (unglaciated area west of the Continental Divide) as suggested by McPhail and Lindsey (1970). Present day populations in Korea, Japan, and Primorye may be derived from the southern Asian (Japanese) refuge, populations from the Amur River through to southern Bristol Bay may be derived from the northern Bering refuge, and populations from the Alaska Peninsula to Washington may have been derived from the southern refuge. In British Columbia, an additional refuge may also have been present on the Queen Charlotte Islands (Warner et al., 1982). Queen Charlotte Islands chum salmon populations were distinct and also displayed lower genetic variation, very similar to sockeye salmon populations from the region (Beacham et al., 2006a). Wood (1995) suggested that sockeye salmon population structure on the central coast region of British Columbia was consistent with colonization from two different refugia, and therefore it is possible that present day populations in British Columbia are derived from chum salmon originating from a Queen Charlotte Islands refuge and that other portions of the coast were colonized by chum salmon that originated from a southern refuge.

Acknowledgments

A very substantial effort was undertaken to obtain samples from chum salmon sampled in this study. In North America, starting from the south, we thank J. B. Shaklee, various staff of Fisheries and Oceans Canada (DFO) for baseline sample collection, as well as First Nations staff, R. L. Wilmot, L. W. Seeb, S. Johnston, P. Milligan, J. Wenburg, and A. J. Gharrett. For Asia, samples were provided by V. V. Efremov, N. V. Varnakskaya, G. Winans, S. Urawa, S. Sato, and J. Park. L. Fitzpatrick drafted the map. C. Wallace assisted in the analysis. Funding for the study was provided by Fisheries and Oceans, Canada.

Literature cited

Banks, M. A., M. S. Blouin, B. A. Baldwin, V. K. Rashbrook, H. A. Fitzgerald, S. M. Blankenship, and D. Hedgecock.
1999. Isolation and inheritance of novel microsatellites in chinook salmon (*Oncorhynchus tshawytscha*). J. Hered. 90:281–288.

Banks, M. A., V. K. Rashbrook, M. J. Calavetta, C. A. Dean, and D. Hedgecock.
2000. Analysis of microsatellite DNA resolves genetic structure and diversity of chinook salmon (*Oncorhynchus tshawytscha*) in California's Central Valley. Can. J. Fish. Aquat. Sci. 57:915–927.

Beacham, T. D.
1996. The use of minisatellite DNA variation for stock identification of chum salmon, *Oncorhynchus keta*. Fish. Bull. 94:611–627.

Beacham, T. D., A. P. Gould, R. E. Withler, C. B. Murray, and L. W. Barner.
1987. Biochemical genetic survey and stock identification of chum salmon (*Oncorhynchus keta*) in British Columbia. Can. J. Fish. Aquat. Sci. 44:1702–1713.

Beacham, T. D., K. D. Le, M. Wetklo, B. McIntosh, T. Ming, and K. M. Miller.
In press. Population structure and stock identification of chum salmon from western Alaska determined with microsatellite and major histocompatibility complex variation. *In* Pacific salmon: ecology and management of western Alaska's populations (C. C. Krueger, and C. E. Zimmerman, eds.). Am. Fish. Soc., Symp., Bethesda, MD.

Beacham, T. D., S. Urawa, K. D. Le, and M. Wetklo.
2008b. Population structure and stock identification of chum salmon from Japan determined with microsatellite DNA variation. Fish. Sci. 74:983–994.

Beacham, T. D., B. Spilsted, K. D. Le, and M. Wetklo.
2008c. Population structure and stock identification of chum salmon *Oncorhynchus keta* from British Columbia determined with microsatellite DNA variation. Can. J. Zool. 86:1002–1014.

Beacham, T. D., B. McIntosh, C. MacConnachie, K. M. Miller, R. E. Withler, and N. V. Varnavskaya.
2006a. Pacific Rim population structure of sockeye salmon as determined from microsatellite analysis. Trans. Am. Fish. Soc. 135:174–187.

Beacham, K. L. Jonsen, J. Supernault, M. Wetklo, L. Deng, and N. Varnavskaya.
2006b. Pacific Rim population structure of Chinook salmon as determined from microsatellite variation. Trans. Am. Fish. Soc. 135:1604–1621.

Beacham, T. D., N. V. Varnavskaya, K. D. Le, and M. Wetklo.
2008a. Determination of population structure and stock identification of chum salmon (*Oncorhynchus keta*) in

Russia determined with microsatellites. Fish. Bull. 106:245–256.

Brykov, V. A., N. E. Poliakova, and A. V. Prokhorova.
2003. Phylogenic and geographic analysis of chum salmon *Oncorhynchus keta* (Walbaum) in Asian populations based on mitochondrial DNA variation. Russ. J. Genet. 39:61–67.

Buchholz, W. G., S. J. Miller, and W. J. Spearman.
2001. Isolation and characterization of chum salmon microsatellite loci and use across species. Anim. Genet. 32:160–165.

Cairney, M., J. B. Taggart, and B. Hoyheim.
2000. Characterization of microsatellite and minisatellite loci in Atlantic salmon (*Salmo salar* L.) and cross-species amplification in other salmonids. Mol. Ecol. 9:2175–2178.

Cavalli-Sforza, L. L., and A. W. F. Edwards.
1967. Phylogenetic analysis: models and estimation procedures. Am. J. Hum. Genet. 19:233–257.

Chen, J.-P., D.-J. Sun, C.-Z. Dong, B. Liang, W.-H.Wu, and S.-Y. Zhang.
2005. Genetic analysis of four wild chum salmon *Oncorhynchus keta* populations in China based on microsatellite markers. Environ. Biol. Fishes 73:181–188.

Efremov, V. V.
2001. Genetic variation and differentiation of populations of chum salmon *Oncorhynchus keta* (Walbaum) from Southern Russian Far East. Russ. J. Genet. 37:283–289.

Estoup, A., P. Jarne, and J. M. Cornuet.
2002. Homoplasy and mutation model at microsatellite loci and their consequences for population genetics analysis. Mol. Ecol. 11:1591–1604.

Felsenstein J.
1993. PHYLIP: Phylogeny Inference Package. Univ. Washington, Seattle, WA.

Ginatulina, L. K.
1992. Genetic differentiation among chum salmon, *Oncorhynchus keta* (Walbaum), from Primorye and Sakhalin. J. Fish Biol. 40:33–38.

Goudet, J.
1995. FSTAT (version 1.2): A program for IBM PC compatibles to calculate Weir and Cockerham's (1984) estimators of F-statistics. J. Hered. 86:485–486.

Hopkins, D. M.
1967. The Cenozoic history of Beringia-a synthesis. *In* The Bering land bridge. (D. M. Hopkins, ed.) p. 451–484. Stanford Univ. Press, Stanford, CA.

Kaeriyama M.
1999. Hatchery programmes and stock management of salmonid populations in Japan. *In* Stock enhancement and sea ranching (B. R. Howell, E. Moksness, and T. Svasand, eds.). p.153–167. Blackwell Science, Oxford, U.K.

Kalinowski, S. T.
2005. Do polymorphic loci require large sample sizes to estimate genetic distances? Heredity 94:33–36.

Kijima A, and Y. Fujio.
1982. Correlation between geographic distance and genetic distance in populations. Bull. Jap. Soc. Sci. Fish. 48:1703–1709.

Knebel, H. J., and J. S. Creager.
1973. Yukon River: evidence for extensive migration during the Holocene transgression. Science 179:1230–1232.

Kondzela, C. M., C. M. Guthrie, S. L. Hawkins, C. D. Russell, J. H. Helle, and A. J. Gharrett.
1994. Genetic relationships among chum salmon populations in southeast Alaska and northern British Columbia. Can. J. Fish. Aquat. Sci. (suppl. 1):50–64.

Lindsey, C. C., and J. D. McPhail.
1986. Zoogeograpy of fishes of the Yukon and Mackenzie basins. *In* The zoogeography of North American freshwater fishes (C. H. Hocutt and E. O. Wiley, eds.) p. 639–674. Wiley, New York.

McPhail, J. D., and C. C. Lindsey.
1970. Freshwater fishes of northwestern Canada and Alaska. Bull. Fish. Res. Board Can. 173:1–381.

Nelson, R. J., and T. D. Beacham.
1999. Isolation and cross species amplification of microsatellite loci useful for study of Pacific salmon. Anim. Genet. 30:228–229.

Okazaki, T.
1982a. Geographical distribution of allelic variation of enzymes in chum salmon *Oncorhynchus keta*, river populations of Japan and the effects of transplantation. Bull. Jap. Soc. Sci. Fish. 48:1525–1535.

Okazaki, T.
1982b. Genetic study on population structure in chum salmon (*Oncorhynchus keta*). Bull. Far Seas Fish. Res. Lab. 19:25–116.

Olsen, J. B., S. L. Wilson, E. J. Kretschmer, K. C. Jones, and J. E. Seeb.
2000. Characterization of 14 tetranucleotide microsatellite loci derived from sockeye salmon. Mol. Ecol. 9:2185–2187.

Park, L. K, M. A. Brainard, D. A. Dightman, and G. A. Winans.
1993. Low levels of intraspecific variation in the mitochondrial DNA of chum salmon (*Oncorhynchus keta*). Mol. Mar. Biol. Biotech. 2:362–370.

Perriere, G., and M. Gouy.
1996. WWW-query: An on-line retrieval system for biological sequence banks. Biochimie 78:364–369.

Phelps, S. R., L. L. LeClair, S. Young, and H. L. Blankenship.
1994. Genetic diversity patterns of chum salmon in the Pacific Northwest. Can. J. Fish. Aquat. Sci. (suppl. 1):65–83.

Polyakova, N. E., A. V. Semina, and V. A. Brykov.
2006. The variability in chum salmon *Oncorhynchus keta* (Walbaum) mitochondrial DNA and its connection with the paleogeological events in the northwest Pacific. Russ. J. Genet. 42:1164–1171.

Rexroad, C. E., R. L. Coleman, A. M. Martin, W. K. Hershberger, and J. Killefer.
2001. Thirty-five polymorphic microsatellite markers for rainbow trout (*Oncorhynchus mykiss*). Anim. Genet. 32:317–319.

Rice, W. R.
1989. Analyzing tables of statistical tests. Evolution 43:223–225.

Salo, E. O.
1991. Life history of chum salmon (*Oncorhynchus keta*). *In* Life history of Pacific salmon (C. Groot and L. Margolis, eds.), p. 231–309. UBC Press, Vancouver, BC.

Salmenkova, E. A., V. T. Omelchenko, D. V. Politov, K. I. Afanasyev, and G. A. Rubtsova.
2007. Genetic diversity of northern Okhotsk Sea coast populations of chum salmon with natural and artificial reproduction. Biologiya Morya 33:299–308.

Sato, S., J. Ando, H. Ando, S. Urawa, A. Urano, and S. Abe.
2001. Genetic variation among Japanese populations of chum salmon inferred from the nucleotide sequences of the mitochondrial DNA control region. Zool. Sci. (Tokyo) 18: 99–106.

Sato, S., H. Kojima, J. Ando, H. Ando, R. L. Wilmot, L. W. Seeb, V. Efremov, L. LeClair, W. Buchholz, D.-H. Jin, S. Urawa, M. Kaeriyama, A. Urano, and S. Abe.
2004. Genetic population structure of chum salmon in the Pacific Rim inferred from mitochondrial DNA sequence variation. Environ. Biol. Fishes 69:37–50.

Seeb, L. W., and P. A. Crane.
1999. High genetic heterogeneity in chum salmon in Western Alaska, the contact zone between northern and southern lineages. Trans. Am. Fish. Soc. 128:58–87.

Small, M. P., T. D. Beacham, R. E. Withler, and R. J. Nelson.
1998. Discriminating coho salmon (*Oncorhynchus kisutch*) populations within the Fraser River, British Columbia using microsatellite DNA markers. Mol. Ecol. 7:141–155.

Smith, C. T., B. F. Koop, and R. J. Nelson.
1998. Isolation and characterization of coho salmon (*Oncorhynchus kisutch*) microsatellites and their use in other salmonids. Mol. Ecol. 7:1613–1621.

Smith, C. T., and L. W. Seeb.
2008. Number of alleles as a predictor of the relative assignment accuracy of short tandem repeat (STR) and single-nucleotide-polymorphism (SNP) baselines for chum salmon. Trans. Am. Fish. Soc. 137:751–762.

Spies, I. B., D. J. Brasier, P. T. L. O'Reilly, T. R. Seamons, and P. Bentzen.
2005. Development and characterization of novel tetra-, tri-, and dinucleotide microsatellite markers in rainbow trout (*Oncorhynchus mykiss*). Mol. Ecol. Notes 5:278–281.

Taylor, E. B., T. D. Beacham, and M. Kaeriyama.
1994. Population structure and identification of North Pacific Ocean chum salmon (*Oncorhynchus keta*) revealed by an analysis of minisatellite DNA variation. Can. J. Fish. Aquat. Sci. 51:1430–1442.

Varnavskaya, N. V., C. C. Wood, and R. J. Everett.
1994a. Genetic variation in sockeye salmon (*Oncorhynchus nerka*) populations of Asia and North America. Can. J. Fish. Aquat. Sci. 51(suppl. 1):132–146.

Waples, R. S.
1990. Temporal changes of allele frequency in Pacific salmon populations: implications for mixed-stock fishery analysis. Can. J. Fish. Aquat. Sci. 47:968–976.

Warner, B. C., R. W. Mathews, and J. J. Clague.
1982. Ice-free conditions on the Queen Charlotte Islands, British Columbia, at the height of the late Wisconsin glaciation. Science 218:675–677.

Weir, B.S., and C. C. Cockerham.
1984. Estimating F-statistics for the analysis of population structure. Evolution 38:1358–1370.

Williamson, K. S., J. F. Cordes, and B. P. May.
2002. Characterization of microsatellite loci in chinook salmon (*Oncorhynchus tshawytscha*) and cross-species amplification in other salmonids. Mol. Ecol. Notes 2:17–19.

Wilmot, R. L., R. J. Everett, W. J. Spearman, R. Baccus, N. V. Varnavskaya, and S. V. Putivkin.
1994. Genetic stock structure of Western Alaska chum salmon and a comparison with Russian Far East stocks. Can. J. Fish. Aquat. Sci. 51 (suppl. 1):84–94.

Winans, G. A., P. B. Aebersold, S. Urawa, and N. V. Varnavskaya.
1994. Determining continent of origin of chum salmon (*Oncorhynchus keta*) using genetic identification techniques: status of allozyme baseline in Asia. Can. J. Fish. Aquat. Sci. 51(suppl. 1):95–113.

Wood, C. C.
1995. Life history variation and population structure in sockeye salmon. Am. Fish. Soc. Symp. 17:195–216.

Corrigendum

Fishery Bulletin 105(3), p. 404.

Stark, James W.

Geographic and seasonal variations in maturation and growth of female Pacific cod (*Gadus macrocephalus*) in the Gulf of Alaska and Bering Sea

Page 404. The x-axis scale in Figure 5 should read as follows:

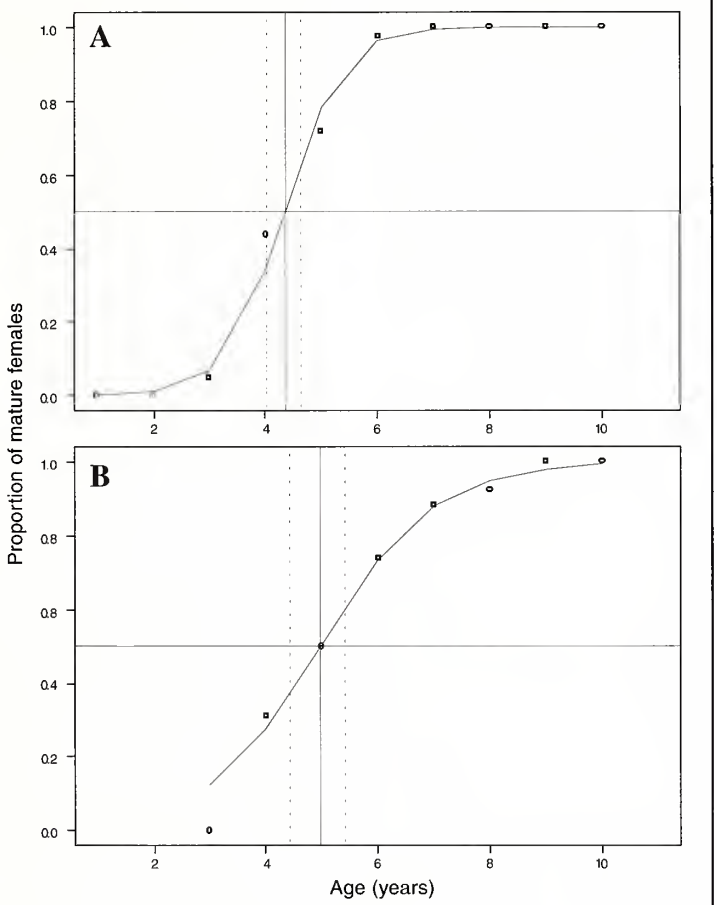

Figure 5

The proportion of mature female Pacific cod (*Gadus macrocephalus*) by age in (**A**) the Gulf of Alaska, based on the January 1999 and 2004 (n=154) collection and in (**B**) the Bering Sea, based on the February 2003 (n=129) collection. The mean age at 50% maturity=4.4 (A) and 4.9 years (B), and the 95% confidence intervals are represented by the parallel dotted lines.

Fishery Bulletin

Guidelines for authors

Manuscript Preparation

Contributions published in *Fishery Bulletin* describe original research in marine fishery science, fishery engineering and economics, as well as the areas of marine environmental and ecological sciences (including modeling). Preference will be given to manuscripts that examine processes and underlying patterns. Descriptive reports, surveys, and observational papers may occasionally be published but should appeal to an audience outside the locale in which the study was conducted. Although all contributions are subject to peer review, responsibility for the contents of papers rests upon the authors and not on the editor or publisher. *Submission of an article implies that the article is original and is not being considered for publication elsewhere.* **Articles** may range from relatively short contributions (10–15 typed, double-spaced pages, tables and figures not included) to extensive contributions (20–30 typed pages). Manuscripts must be written in English; authors whose native language is not English are strongly advised to have their manuscripts checked by English-speaking colleagues before submission.

Title page should include authors' full names and mailing addresses and the senior author's telephone, fax number, and e-mail address, and a list of key words to describe the contents of the manuscript. **Abstract** should be limited to 200 words (one-half typed page), state the main scope of the research, and emphasize the author's conclusions and relevant findings. Do not review the methods of the study or list the contents of the paper. Because abstracts are circulated by abstracting agencies, it is important that they represent the research clearly and concisely. **Text** must be typed in 12 point Times New Roman font throughout. A brief introduction should convey the broad significance of the paper; the remainder of the paper should be divided into the following sections: **Materials and methods, Results, Discussion** (or **Conclusions**), and **Acknowledgments**. Headings within each section must be short, reflect a logical sequence, and follow the rules of multiple subdivision (i.e., there can be no subdivision without at least two items). The entire text should be intelligible to interdisciplinary readers; therefore, all acronyms, abbreviations, and technical terms should be written out in full the first time they are mentioned. Include FAO common names for species in the list of keywords and in the introduction. Regional common names may be used throughout the rest of the text if they are different from FAO common names which can be found at http://www.fishbase.org/search.html. Follow the U.S. Government Printing Office Style Manual (1984 ed.) and the CBE Style Manual (6th ed.) for editorial style; for fish nomenclature follow the most current issue of the American Fisheries Society's Common and Scientific Names of Fishes from the United States and Canada. Dates should be written as follows: 11 November 2000. Measurements should be expressed in metric units, e.g., 58 metric tons (t); if other units of measurement are used, please make this fact explicit to the reader. Write out the numbers zero through nine unless they form part of measurement units (e.g., nine fish but 9 mm). Refrain from using the shorthand slash (/), an ambiguous symbol, in the general text

Literature cited comprises published works and those accepted for publication in peer-reviewed literature (in press). Follow the name and year system for citation format in the "Literature cited" section (that is say, citations should be listed alphabetically by the authors' last names, and then by year if there is more than one citation with the same authorship). If there is a sequence of citations in the text, list chronologically: (Smith, 1932; Green, 1947; Smith and Jones, 1985). Abbreviations of serials should conform to abbreviations given in the Serial Sources for the BIOSIS Previews Database. Authors are responsible for the accuracy and completeness of all citations. Literature citation format: Author (last name, followed by first-name initials). Year. Title of report or manuscript. Abbreviated title of the series to which it belongs. Always include number of pages. Cite all software and special equipment or chemical solutions used in the study, not in a footnote but within parentheses in the text (e.g., SAS, vers. 6.03, SAS Inst., Inc., Cary, NC).

Tables are often overused in scientific papers; it is seldom necessary or even desirable to present all the data associated with a study. Tables should not be excessive in size and must be cited in numerical order in the text. Headings should be short but ample enough to allow the table to be intelligible on its own. All unusual symbols must be explained in the table legend. Other incidental comments may be footnoted with italic numeral footnote markers. Use asterisks to indicate probability in statistical data. Do not type table legends on a separate page; place them above the table data. *Do not submit tables in photo mode.*

- Zeros should precede all decimal points for values less than one.
- Sample size, n, should be italicized.
- Capitalize the first letter of the first word in all labels within figures.
- Do not use overly large font sizes in maps and for units of measurements along axes in figures.
- Do not use bold fonts or bold lines in figures.
- Do not place outline rules around graphs.
- Do not use horizontal lines through graphs to indicate measurement units.
- Use a comma in numbers of five digits or more (e.g. 13,000 but 3000).
- Maps require a North arrow and degrees latitude-longitude (e.g., 170°E).

Figures include line illustrations, photographs (or slides), and computer-generated graphs and must be cited in numerical order in the text. Graphics should aid in the comprehension of the text, but they should be limited to presenting patterns rather than raw data. Figures should not exceed one figure for every four pages of text. Figures must be labeled with author's name and number of the figure. Avoid placing labels vertically (except of y axis). Figure legends should explain all symbols and abbreviations and should be double-spaced on a separate page at the end of the manuscript. Please note that we do not print graphs in color.

Failure to follow these guidelines and failure to correspond with editors in a timely manner will delay publication of a manuscript.

Copyright law does not apply to *Fishery Bulletin*, which falls within the public domain. However, if an author reproduces any part of an article from *Fishery Bulletin* in his or her work, reference to source is considered correct form (e.g., Source: Fish. Bull 97:105).

Submission

The Scientific Editorial Office encourages authors to submit their manuscripts as a *single* PDF (preferred) or Word (zipped) document by e-mail to Fishery.Bulletin@noaa.gov. Please use the subject heading, "Fishery Bulletin manuscript submission". *Do not* send encrypted files. For further details on electronic submission, please contact the Scientific Editorial Office directly (see address below). Or you may send your manuscript on a compact disc in one of the above formats along with four printed copies (one original plus three copies [stapled]) to the Scientific Editor, at the address shown below.

Richard D. Brodeur, Ph.D.
Scientific Editor, *Fishery Bulletin*
Northwest Fisheries Science Center
2030 S. Marine Science Dr.
Newport, Oregon 97365-5296

Once the manuscript has been accepted for publication, you will be asked to submit a final electronic copy of your manuscript. When requested, the text and tables should be submitted in Word or Word Rich Text Format. Figures should be sent as PDF files, Windows metafiles, tiff files, or EPS files. Send a copy of figures in the original software if conversion to any of these formats yields a degraded version.

Questions? If you have questions regarding these guidelines, please contact the Managing Editor, Sharyn Matriotti, at

Sharyn.Matriotti@noaa.gov

Questions regarding manuscripts under review should be addressed to Richard Brodeur, Scientific Editor, at Rick.Brodeur@noaa.gov.

Fishery Bulletin

Subscription form

Superintendent of Documents **Publications** Order Form

*5178

☐ YES, please send me the following publications:

____ Subscriptions to *Fishery Bulletin*
for $36.00 per year ($50.40 foreign)

The total cost of my order is $ _____ . Prices include regular domestic postage and handling and are subject to change.

_____
(Company or Personal Name) (Please type or print)

_____
(Additional address/attention line)

_____
(Street address)

_____
(City, State, ZIP Code)

_____
(Daytime phone including area code)

_____
(Purchase Order No.)

Charge your order. IT'S EASY!

VISA

MasterCard

Please Choose Method of Payment:

☐ Check Payable to the Superintendent of Documents
☐ GPO Deposit Account ☐☐☐☐☐☐–☐
☐ VISA or MasterCard Account
☐☐☐☐☐☐☐☐☐☐☐☐☐☐☐☐
☐☐☐☐ (Credit card expiration date)

To fax your orders (202) 512-2250

_____
(Authorizing Signature)

Mail To: Superintendent of Documents
P.O. Box 371954, Pittsburgh, PA 15250-7954

Thank you for your order!

Also available online at http://bookstore.gpo.gov/collections/fishery-bulletin